AD-A048 385 DAVID W TAYLOR NAVAL SHIP RESEARCH AND DEVELOPMENT CE--ETC F/G 13/10
EXPERIMENTAL UNSTEADY AND TIME AVERAGE LOADS ON THE BLADES OF T--ETC(U)
DEC 77 S D JESSUP, R J BOSWELL, J J NELKA

UNCLASSIFIED DTNSRDC-77-0110 NL

1 OF 4
AD
A048385

AD A048385

REPORT 77-0119

DAVID W. TAYLOR NAVAL SH
RESEARCH AND DEVELOPMENT C

Bethesda, Md. 20084

9 Final rept.,

6

EXPERIMENTAL UNSTEADY AND TIME AVERA
BLADES OF THE CP PROPELLER ON A M
DD-963 CLASS DESTROYER FOR SIMULA
OF OPERATION .

by

10 Stuart D. Jessup,
Robert J. Boswell
John J. Nelka

APPROVED FOR PUBLIC RELEASE: DISTRIBUTION

16 S0379SL

17 S0379SL01

SHIP PERFORMANCE DEPARTME
RESEARCH AND DEVELOPMENT R

December 1977

AD No.
DDC FILE COPY

387 682

635 08N

UNCLASSIFIED

SECURITY CLASSIFICATION OF THIS PAGE (When Data Entered)

REPORT DOCUMENTATION PAGE		READ INSTRUCTIONS BEFORE COMPLETING FORM
1. REPORT NUMBER 77-0110	2. GOVT ACCESSION NO.	3. RECIPIENT'S CATALOG NUMBER
4. TITLE (and Subtitle) Experimental Unsteady and Time Average Loads of the CP Propeller on a Model of the DD963 Class Destroyer for Simulated Modes of Operation		5. TYPE OF REPORT & PERIOD COVERED Final
		6. PERFORMING ORG. REPORT NUMBER 77-0110
7. AUTHOR(s) Stuart D. Jessup Robert J. Boswell John J. Nelka		8. CONTRACT OR GRANT NUMBER(s)
9. PERFORMING ORGANIZATION NAME AND ADDRESS David W. Taylor Naval Ship Research and Development Center Bethesda, Maryland 20084		10. PROGRAM ELEMENT, PROJECT, TASK AREA & WORK UNIT NUMBERS Task Area S0379-SL001 Task 19977 Work Unit No. 1544-296
11. CONTROLLING OFFICE NAME AND ADDRESS Naval Sea Systems Command (0331G) Energy Conversion & Explosive Devices Division Washington, D.C. 20362		12. REPORT DATE December 1977
		13. NUMBER OF PAGES 310
14. MONITORING AGENCY NAME & ADDRESS(if different from Controlling Office) Naval Ship Engineering Center (6148) Propeller, Shafting & Bearing Branch Washington, D.C. 20362		15. SECURITY CLASS. (of this report) Unclassified
		15a. DECLASSIFICATION/DOWNGRADING SCHEDULE

16. DISTRIBUTION STATEMENT (of this Report)

Approved for public release: Distribution Unlimited

17. DISTRIBUTION STATEMENT (of the abstract entered in Block 20, if different from Report)

18. SUPPLEMENTARY NOTES

19. KEY WORDS (Continue on reverse side if necessary and identify by block number)

Marine Propeller
Controllable-Pitch Propeller
Loads
Propulsion
Model Experiments
Propeller Research
Unsteady Loads
DD963 Class Destroyer

20. ABSTRACT (Continue on reverse side if necessary and identify by block number)

Experiments are described in which the mean and unsteady loads were measured on a single blade of a model of the controllable-pitch propeller on the DD-963 Class Destroyer. The experiments were conducted behind a model of the DD-963 hull under steady ahead operation, hull pitching motions, and simulated acceleration maneuvers. The experimental techniques are outlined and the dynamometer and data analysis system described.

The results show that all significant loads except radial force are predominantly of hydrodynamic origin. The circumferential variation of all

DD FORM 1 JAN 73 1473 EDITION OF 1 NOV 65 IS OBSOLETE
S/N 0102-014-6601

UNCLASSIFIED

SECURITY CLASSIFICATION OF THIS PAGE (When Data Entered)

measured components of blade loading is primarily a once-per-revolution variation, with the variation following approximately the variation of the tangential wake velocity.

For sinusoidal pitching of the hull with maximum pitch angle of 1.85 degrees and a simulated full scale frequency of 0.16 hertz, the peak-to-peak circumferential variation of measured forces and moments increased by approximately 50 percent over the values without hull pitching.

For simulated operation during an acceleration maneuver, the circumferential variation of measured forces and moments varied approximately as the product of ship speed and propeller rotational speed. At no time during the simulated acceleration maneuvers were the circumferential variations of loads as large as during full power steady ahead operation.

For steady ahead operation, circumferential variation of loading determined from the model experiments agreed fairly well with full-scale data, but was substantially larger than the theoretically calculated values.

For all conditions evaluated, the results follow close to previously reported results of similar experiments on a model of the FF-1088.

TABLE OF CONTENTS

LIST OF FIGURES

Page

LIST OF TABLES

NOTATION

	Expanded area, $Z\int_{r_h}^{R} c\,dr$
A_O	Propeller disk area, $\pi D^2/4$
A_r	Fourier cosine coefficient of radial component of wake velocity
A_t	Velocity cosine coefficient of tangential component of wake velocity
A_x	Fourier cosine coefficient of longitudinal component of wake velocity
B_r	Fourier sine coefficient of radial component of wake velocity
B_t	Fourier sine coefficient of tangential component of wake velocity
B_x	Fourier sine coefficient of longitudinal component of wake velocity
C_A	Correlation allowance
$C_{i,j}$	Elements of calibration matrix
C_{Th}	Thrust loading coefficient, $T/((\rho/2)V_A{}^2 A_O))$
c	Blade section chord length
D	Propeller diameter
F_n	Froude number
$(F)_n$	nth harmonic amplitude of F
$F_{x,y,z}$	Force components on blade in x,y,z directions
f_M	Camber of propeller blade section
J	Advance coefficient, $J=V_A/nD$
J_T	Effective advance coefficient based on thrust identity
J_Q	Effective advance coefficient based on torque identity
J_V	Ship speed advance coefficient, $J=V/nD$
$K_{F_{x,y,z}}$	Force coefficient, $F_{x,y,z}/(\rho n^2 D^4)$

$K_{M_{x,y,z}}$	Moment coefficient, $M_{x,y,z}/(\rho n^2 D^5)$
K_Q	Torque coefficient, $Q/(\rho n^2 D^5)$
K_{SC}	Centrifugal blade spindle torque coefficient, $M_{Z_C}/(\rho_P n^2 D^5)$
K_T	Thrust coefficient, $T/(\rho n^2 D^4)$
$M_{x,y,z}$	Moment components about x,y,z axes from loading on one blade
$(M)_n$	nth harmonic amplitude of M
n	Propeller revolutions per unit time
P	Propeller blade section pitch
Q	Time average propeller torque arising from loading on all blades, $-Z\overline{M}_x$
R	Radius of propeller
R_n	Reynolds number, $c_{0.7}V_R{}^*/\nu$
r	Radial coordinate from propeller axis
r_{Fx_H}	Radial center of hydrodynamic component of axial force, $M_{y_H}/(F_{x_H})$
r_{Fy_H}	Radial center of hydrodynamic component of transverse force, $M_{x_H}/(F_{y_H})$
S	Skew back of propeller blade section measured from the spindle axis to the midchord point of the blade section, positive towards trailing edge
T	Time average thrust of propeller, positive foward, $Z\overline{F}_x$
t	Maximum thickness of propeller blade section
V	Model speed
V_A	Propeller speed of advance
$V_R{}^*$	Vector sum of speed of advance and rotational velocity at the 0.7 radius, $(V_A{}^2 + (0.7\pi nD)^2)^{1/2}$
$V_r(r, \theta_W)$	Radial component of wake velocity, positive towards hub
$(V_r)_n$	nth harmonic amplitude of V_r

$V_t(r,\theta_W)$	Tangential component of wake velocity, positive clockwise looking upstream for starboard propeller (left hand rotation), positive counterclockwise looking upstream for port propeller (right hand rotation)
$(V_t)_n$	nth harmonic amplitude of V_t
$V_x(r,\theta_W)$	Longitudinal component of wake velocity, positive forward
$(V_x)_n$	nth harmonic amplitude of V_x
V_{VM}	Volume mean longitudinal velocity through propeller disk determined from wake survey
w_Q	Taylor wake fraction determined from torque identity
w_T	Taylor wake fraction determined from thrust identity
w_{VM}	Wake fraction determined from volume mean longitudinal velocity through propeller disk determined from a wake survey, $(V-V_{VM})/V$
x,y,z	Coordinate axes
Z	Number of blades
Z_R	Rake of propeller blade section measured from the propeller plane to the generator line, positive aft
β^*	Advance angle at 0.7 radius, $\tan^{-1}\left[V_x\ (r=0.07)/(0.7\pi n\ D)\right]$
ε	Blade strain
θ	Angular coordinate used to define location of blade and variation of loads, from vertical upward positive counterclockwise looking upstream for starboard propeller (left hand rotation), positive clockwise looking upstream for port propeller (right hand rotation), $\theta=-\theta_W$
θ_S	Skew angle measured from spindle axis to projection of blade section midchord into propeller plane, positive toward trailing edge
θ_W	Angular coordinate of wake velocity, from upward vertical, positive clockwise looking upstream for starboard propeller (left hand rotation), positive counterclockwise looking upstream for port propeller (right hand rotation), $\theta_W=-\theta$

λ	Ship to model linear scale ratio
ν	Kinematic viscosity of water
ρ	Mass density of water
ρ_P	Mass density of propeller blade
ϕ	Pitch angle of propeller blade section, $\tan^{-1}(P/(2\pi r))$
$(\phi_{F,M})_n$	nth harmonic phase angles of F,M based on a cosine series $(F,M)=(\overline{F},\overline{M}) + \sum_{n=1}^{N} (F,M)_n \cos(n\theta-(\phi_{F,M})_n)$
(ϕ_{Vr}^*)	nth harmonic phase angles of V_r based on a sine series, $V_r=(\overline{V}_r) + \sum_{n=1}^{N} (V_r)_n \sin(n\theta_W + (\phi_{Vr}^*)_n)$
(ϕ_{Vt}^*)	nth harmonic phase angles of V_t based on a sine series, $V_t=(\overline{V}_t) + \sum_{n=1}^{N} (V_t)_n \sin(n\theta_W + (\phi_{Vt}^*)_n)$
(ϕ_{Vx}^*)	nth harmonic phase angles of V_x based on a sine series, $(V_x)=(\overline{V}_x) + \sum_{n=1}^{N} (V_x)_n \sin(n\theta_W + (\phi_{Vx}^*)_n)$
ψ	Pitch angle of hull

Subscripts:

A	Applied values of loads
c	Arising from centrifugal loading
CW	Value in calm water
g	Arising from gravitational loading
H	Arising from hydrodynamic loading
h	Value of hub radius
I	Indicated values of loads before calibration matrix is applied
M	Model value
MAX	Maximum value at any blade angular position
MIN	Minimum value at any blade angular position

n	Value of nth harmonic
p	Port propeller
PEAK	Peak value including variation of both time-average value per revolution and variation with blade angular position
S	Ship value
SP	Value at self-propulsion point
s	Starboard propeller
T	Total loading from hydrodynamic, centrifugal, and gravitational components
x,y,z	Component in x,y,z direction
0.3	Value at r=0.3R
0.4	Value at r=0.4R
0.7	Value at r=0.7R

Superscripts:

–	Time average value per revolution
~	Unsteady value
•	Rate of change with time

ABSTRACT

Experiments are described in which the mean and unsteady loads were measured on a single blade of a model of the controllable-pitch propeller on the DD-963 Class Destroyer. The experiments were conducted behind a model of the DD-963 hull under steady ahead operation, hull pitching motions, and simulated acceleration maneuvers. The experimental techniques are outlined and the dynamometer and data analysis system described.

The results show that all significant loads except radial force are predominantly of hydrodynamic origin. The circumferential variation of all measured components of blade loading is primarily a once-per-revolution variation, with the variation following approximately the variation of the tangential wake velocity.

For sinusoidal pitching of the hull with maximum pitch angle of 1.85 degrees and a simulated full scale frequency of 0.16 hertz, the peak-to-peak circumferential variation of measured forces and moments increased by approximately 50 percent over the values without hull pitching.

For simulated operation during an acceleration maneuver, the circumferential variation of measured forces and moments varied approximately as the product of ship speed and propeller rotational speed. At no time during the simulated acceleration maneuvers were the circumferential variations of loads as large as during full power steady ahead operation.

For steady ahead operation, circumferential variation of loading determined from the model experiments agreed fairly well with full-scale data, but was substantially larger than the theoretically calculated values.

For all conditions evaluated, the results follow close to previously reported results of similar experiments on a model of the FF-1088.

ADMINISTRATIVE INFORMATION

The work reported herein was funded by the Naval Sea Systems Command (NAVSEA 033), Task Area S0379-SL001, Task 19977. The work was performed under David W. Taylor Naval Ship Research and Development Center (DTNSRDC) Work Unit No. 1544-296.

The English system of units was used in the original calculations presented in this report. Therefore, all data are presented in the English units. However, the International System (SI) of metric units are shown in the text in parentheses following the English units.

INTRODUCTION

Major naval ships powered with marine gas turbines and using controllable-pitch (CP) propellers for thrust reversal are currently being added to the Fleet. Ships with CP propellers include the DD-963 Class, the FFG-7 Class, and the DDG-47 Class.

Accordingly, the Navy has been conducting a research and development (R&D) program to establish the technology for producing reliable CP propellers with delivered power in the range of 35,000 to 40,000 horsepower (26,000 to 30,000 kW).[1] As part of this program, CP propellers were installed on the U.S.S. PATTERSON (FF-1061) and U.S.S. BARBEY (FF-1088) with delivered power of 35,000 horsepower (26,100 kW). These installations were intended to demonstrate that CP propellers in this range of power had adequate reliability for application to ships with gas turbine prime movers.

Because of the structural failure of the crank rings to which the blades of the CP propeller on the FF-1088 were bolted, R&D efforts were intensified. The program undertaken at DTNSRDC included:

1. Blade Loading of CP Propellers
   a. Model measurement and theoretical prediction of blade loading on CP propellers.
   b. Model and full-scale wake measurements and theoretical predictions of wake.
   c. Full-scale measurements of forces, pressures, and strains in CP propeller components.
2. Structural Design of CP Propeller Blade Attachments.
3. Development of Materials for CP Propeller Systems.

The current report presents the results of work conducted under Section 1a of the CP Propeller Research and Development Program, i.e., model

---

[1] Angelo, J.J. et al, "U.S. Navy Controllable Pitch Propeller Programs," presented at a Joint Session of the Chesapeake Section of the Society of Naval Architects and Marine Engineers and the Flagship Section of the American Society of Naval Engineers, Bethesda, Maryland (19 April 1977).

measurement and theoretical prediction of blade loading of CP propellers. Work under the other sections of this program will be reported separately.

The present report presents experimental results obtained on a model of the CP propeller on the DD-963 Class Destroyer. The results of similar experiments on a model of the FF-1088 were reported in Reference 2.

BACKGROUND

Extreme care must be taken to design the blades and pitch-changing mechanisms of high power CP propellers so that they possess adequate strength including consideration of yield and fatigue stresses. This requires an accurate estimate of the maximum time-average and alternating loads under all operating conditions. High time-average and alternating loads occur at steady full-power ahead conditions and during high-speed maneuvers including full-power crash astern, full-power crash ahead, and full-power turns. In addition, the influence of the seaway may substantially increase the time-average and alternating loads. At present there appears to be no confirmed technique whereby the pertinent loads can be predicted to the desired accuracy. Schwanecke and Wereldsma[3] reviewed the factors affecting blade loading for propellers in general, and Rusetskiy[4] and Hawdon et al,[5] discussed some of the factors peculiar to blade loading of CP propellers.

[2]Boswell, R.J. et al, "Experimental Determination of Mean and Unsteady Loads on a Model CP Propeller Blade for Various Simulated Modes of Ship Operation," The Eleventh Symposium on Naval Hydrodynamics sponsored Jointly by the Office of Naval Research and University College London, Mechanical Engineering Publications Limited, London and New York, pp 789-823, 832-834, (April 1976); also "Experimental Unsteady and Mean Loads on a CP Propeller Blade of the FF-1088 for Simulated Modes of Operation," David Taylor Naval Ship Research and Development Center Report 76-0125, October 1976.

[3]Schwanecke, H. and R. Wereldsma, "Strength of Propellers Considering Steady and Unsteady Shaft and Blade Forces, Stationary and Nonstationary Environmental Conditions," Proceedings of the Thirteenth International Towing Tank Conference, Report of the Propeller Committee, Appendix 2b, Vol. 2, pp 495-526 (1972).

[4]Rusetskiy, A.A., "Hydrodynamics of Controllable Pitch Propellers," Shipbuilding Publishing House, Leningrad (1968).

[5]Hawdon, L. et al, "The Analysis of Controllable-Pitch Propeller Characteristics at Off-Design Conditions," Transactions of the Institute of Marine Engineers, Vol. 88, Series A, Part 4, pp 162-184 (1976).

Near the self-propulsion point in calm water, the time-average loads can probably be calculated with reasonable accuracy. However, even at these conditions, the variation of loads with blade angular position apparently cannot be calculated with high accuracy. Various techniques, including quasi-steady procedures, stripwise unstead procedures, and methods based on unsteady lifting surface theory, have been proposed for calculating the unsteady loading arising from the circumferential variation in the inflow velocity.[6-12] However, all of these procedures require knowledge of the flow patterns (wake profile) in the propeller disk. In current practice, the wake profile is measured in the plane of the propeller behind the model hull with the propeller removed. For high-speed displacement ships of the type under consideration in this report, these results are usually extrapolated to full scale without making allowance for

---

[6] Kerwin, J.E., "The Development of Numerical Methods for the Computation of Unsteady Propeller Forces," Presented to the Symposium on Hydrodynamics of Ship and Off-Shore Propulsion Systems, Oslo, Norway (March 1977).

[7] *Ito*, T. et al, "Calculation of Unsteady Propeller Forces by Lifting Surface Theory," Presented to the Symposium on Hydrodynamics of Ship and Off-Shore Propulsion Systems, Oslo, Norway (March 1977).

[8] Roddy, R.F., "A New Method for the Calculation of Unsteady Forces on a Marine Propeller," Presented to the Chesapeake Section of the Society of Naval Architects and Marine Engineers, Washington, D.C. (February 1977).

[9] van Gent, W., "Unsteady Lifting Surface Theory for Ships Screws: Derivation and Numerical Treatment of Integral Equations," Journal of Ship Research, Vol. 19, No. 4, pp 243-253 (December 1975).

[10] Schwanecke, H., "Comparative Calculations on Unsteady Propeller Blade Forces," Proceedings of the Fourteenth International Towing Tank Conference, Report of Propeller Committee, Appendix A, Vol. 3, pp 357-397 (1975).

[11] Breslin, J.P., "Propeller Excitation Theory," Proceedings of the Thirteenth International Towing Tank Conference, Report of the Propeller Committee, Appendix 2c, Vol. 2, pp 527-540 (1972).

[12] Boswell, R.J. and M.L. Miller, "Unsteady Propeller Loading - Measurement, Correlation with Theory, and Parametric Study," Naval Ship Research and Development Center Report 2625 (October 1968).

(1) the change in Reynolds number and the corresponding reduction in relative boundary layer thickness and (2) the effect of the propeller suction on the boundary layer and thereby the wake pattern in propeller disk. Although these two factors may be important for full-form ships such as cargo ships, they are probably not important for high-speed transom stern ships of the type under consideration in this report.

Existing measurements which give information on unsteady blade loading include:

1. Measurements of strain on the blades of the model propellers or full-scale propellers. However, some calculations and assumptions are required to convert measured strains into loads. Published data of this type have been summarized by Meyne.[13]

2. Measurement of bearing (shaft) forces and moments on model propellers operating in wakes generated by model hulls or wire grid screens. However, these experiments give information on only some components of blade loading and on only those harmonics of shaft rotational speed corresponding to $nZ-1$, nZ, and $nZ+1$, where n is an integer and Z is the number of blades. Measurements of this nature have been conducted by many investigators, as summarized by Breslin[11] and Wereldsma.[14]

3. Measurements of forces and moments on individual blades of model propellers operating in wakes generated by model hulls or wire grid screens. Measurements behind model hulls have been made by Huse[15] and Blaurock,[16] measurements behind screens have been made by Hawdon et al,[5]

---

[13] Meyne, K., "Propeller Manufacture - Propeller Materials - Propeller Strength," International Shipbuilding Progress, Vol. 22, No. 247, pp 77-102 (March 1975).

[14] Wereldsma, R., "Comparative Tests on Vibratory Propeller Forces," Proceedings of the Thirteenth International Towing Tank Conference, Report of the Propeller Committee, Appendix 2a, Vol. 2, pp 482-494 (1972).

[15] Huse, E., "An Experimental Investigation of the Dynamic Forces and Moments on One Blade of a Ship Propeller," Proceedings of the Symposium on Testing Techniques in Ship Cavitation Research, The Norwegian Ship Model Experimental Tank, Trondheim, Norway, Publication No. 99, Vol II, pp 19-188 (December 1967).

[16] Blaurock, J., "Propeller Blade Loading in Nonuniform Flow," The Society of Naval Architects and Marine Engineers, Propellers 75 Technical and Research Symposium S-4, Paper No. 4, pp 4/1-4/17 (February 1976).

and Raestad,[17] measurements in inclined flow have been made by Albrecht and Suhrbier,[18] Bednarzik,[19] and Raestad,[17] and measurements on partially submerged propellers have been made by Dobay.[20]

Experiments in wakes generated by screens are advantageous for evaluating the ability of a procedure to calculate the loading for a given wake since for this case, the propeller apparently does not influence the wake pattern. Although some good correlation has apparently been obtained between analytical predictions and unsteady bearing forces measured behind wire grid screens,[11, 12] correlation has been rather inconsistent between analytically predicted unsteady blade loads, or resulting strains, and measured blade loads, or strains.[14, 21]

The mechanism by which the seaway influences the mean and unsteady blade loads is complex. Factors include the increased mean propeller loading due to increased hull resistance and the increased unsteady loading resulting from the influence of the free surface and modification of the flow pattern into the propeller disk. This flow pattern is influenced by (1) direct trochoidal velocities from the ocean waves, (2) relative velocities of the propeller due to ship motions, and (3) modification of the hull wake pattern due to the seaway and ship motions. Procedures for calculating the loads in a seaway are much less refined than for steady

---

[17] Raestad, A.E., "Hydrodynamic Propeller Loading in the Behind Condition," det Norske Veritas Research Department Report 74-31-M (1974).

[18] Albrecht, K. and K.R. Suhrbier, "Investigation of the Fluctuating Blade Forces of a Cavitating Propeller in Oblique Flow," International Shipbuilding Progress, Vol. 22, No. 248, pp 132-147 (April 1975).

[19] Bednarzik, R., "Untersuchung uber die Belastungsschwankungen am Einzelflugel schrag angestromter Propeller," Schiffbauforschung, Vol. 8, No. 1/2, pp 57-80 (1969).

[20] Dobay, G.F., "Time-Dependent Blade-Load Measurements on a Screw-Propeller," Presented to the Sixteenth American Towing Tank Conference, Instituto De Pesquisas Techologicas, Marinha Do Brasil (August 1971).

[21] Wereldsma, R., "Last Remarks on the Comparative Model Tests on Vibratory Propeller Forces," Proceedings of the Fourteenth International Towing Tank Conference, Report of the Propeller Committee, Appendix 7, Vol. 3, pp 421-426 (1975).

operation in calm water. Tasaki[22] gives a good review of the mechanisms and procedures for predicting the effect of the seaway on bearing forces which, in principle, also apply to unsteady loading on an individual blade. Keil et al,[23] and Watanabe et al,[24] present strain measurements on the blades of full-scale propellers in both calm and rough seas.

Apparently no rational analytical procedures are available for accurately calculating the time-average loads per revolution or the unsteady loads including variation with blade angular position during crash-ahead or crash-astern maneuvers. These loads may depend on many factors including the time rate of change of propeller pitch $\dot{p}$ (for CP propellers), time rate of change of rotational speed $\dot{n}$, time rate of change of ship speed $\dot{V}$, propeller blade-section stall, cavitation, ventilation, flow separation from the hull, and large interactions between the propeller and the hull. Some of these factors are discussed and considered by Hawdon et al.[5]

For turns, the factors affecting the time-average loads per revolution and the unsteady loads are somewhat the same as those affecting the loads under crash-ahead and crash-astern conditions except that for turns, there is a relatively large drift angle of the flow into the propeller. This drift angle tends to increase the circumferential nonuniformity of the flow into the propeller, thereby increasing the unsteady loading. However, this circumferential nonuniformity of the inflow tends to be offset by the lower values of ship speed and propeller rotational speed in turns compared to steady ahead operation.

Prior to the present R&D investigation, no experimental measurements existed to the authors' knowledge which showed the time-average loads and

---

[22]Tasaki, R., "Propulsion Factors and Fluctuating Propeller Loads in Waves," Proceedings of the Fourteenth International Towing Tank Conference, Report of Seakeeping Committee, Appendix 7, Vol. 4, pp 224-236 (1975).

[23]Keil, H.G. et al, "Stresses in the Blades of a Cargo Ship Propeller," Journal of Hydronautics, Vol. 6, No. 1, pp 2-7 (January 1972).

[24]Watanabe, K. et al, "Propeller Stress Measurements on the Container Ship HAKONE MARU," Shipbuilding Research Association of Japan, Vol. 3, No. 3, pp 41-51 (1973).

circumferential variation of loads with blade angular position on CP propellers behind a hull under a wide range of operating conditions. An experimental program was therefore undertaken to measure the six components of loading (Figure 1)* on model CP propellers operating behind model hulls. The initial experiments were conducted on a single-screw ship, namely, a model of the FF-1088. These results were reported previously.[2] The second set of experiments were conducted on a twin-screw ship, namely, a model of the DD-963 Class. These results are presented in the current report.

For the DD-963 Class, the experimental conditions included (1) steady-ahead operation near the self-propulsion point, (2) steady-ahead operation near the self-propulsion point with forced dynamic pitching of the model hull, and (3) simulated acceleration operation.

Results for the steady ahead operation were correlated with predictions based on unsteady lifting surface theory as developed by Tsakonas et al,[25] and with the quasi-steady method of McCarthy,[26] and with strains measured on the full-scale propeller.

Blade loading measurements were made on the propeller on the starboard shaft since this shaft had a larger rake angle than the port shaft. The propellers used in these experiments were DTNSRDC propellers 4660 (right hand rotation on port shaft) and 4661 (left hand rotation on starboard shaft), which were made of aluminum; see Figure 2 and Table 1.** The hull of the DD-963 Class was represented by DTNSRDC model hull 5265-1B; see Figure 3.

---

*Figures are presented following the section on acknowledgments.

**The tables are presented following the figures.

[25]Tsakonas, S. et al, "An Exact Linear Lifting Surface Theory for Marine Propeller in a Nonuniform Flow Field," Journal of Ship Research, Vol. 17, No. 4, pp 196-207 (December 1974).

[26]McCarthy, J.H., "On the Calculation of Thrust and Torque Fluctuations of Propellers in Nonuniform Wake Flow," David Taylor Model Basin Report 1533 (October 1961).

EXPERIMENTAL TECHNIQUE

FACILITY AND DYNAMOMETRY

All experiments were conducted on DTNSRDC Carriage I using basically the same dynamometry and hardware as previously described in Reference 2.

The port propeller, on which blade loads were not measured was driven from inside the model hull as would be the case in a self propulsion experiment. The propeller rotational speed, which could be controlled independently of the starboard propeller, was measured via a toothed-pickup and recorded on a digital voltmeter. The time-averaged thrust and torque were measured for selected runs by a transmission dynamometer.

The starboard propeller, on which blade loads were measured, was located in its proper position relative to the model hull but was isolated from the hull and driven from downstream (see Figure 4). This downstream drive system was necessary in order to obtain the required characteristics of the system for measuring unsteady loading. The general criteria for the design of an unsteady force measuring system are:

1. The support structure of the force measuring system should be soft mounted and possess a large mass to eliminate transmission of extraneous vibration to the system.

2. The natural frequency of the system should be well above the highest frequency of the quantities to be measured (to avoid phase shift and amplification of the signal).

3. The system response in the force magnitude range should be sufficiently large to be measurable (sensitivity).

4. The system should be free of interaction, that is, each measuring element should respond only to that force or moment which it is intended to measure.

These four major aims are not complementary. The high natural frequency requires a stiff, rigid system whereas high sensitivity requires an elastic, soft system. The necessary compromise results in some interaction between the force-measuring elements.

Criterion 1 dictated that a massive flywheel be used, and Criterion 2 dictated that this flywheel be connected to the sensing elements (located inside the propeller hub) by a short thick shaft. Therefore, because

of the geometry of the hull and shafting of the configuration under evaluation, it was not feasible to achieve both these criteria with an upstream drive system from inside the model hull. Criteria 1 and 2 controlled the minimum allowable beam and draft of the downstream body and the maximum allowable clearance from the bow of the downstream body to the propeller. Although the downstream body may exert some influence on the flow into the propeller, that location was considered necessary in order to meet these measuring criteria. The influence of the downstream body on the flow into the propeller is discussed in the section on experimental results.

The drive and mounting system was basically the same as that used in the DTNSRDC BASS dynamometer which has been described by Brandau.[27] Utilized from this dynamometer were the propeller (tail) shaft, drive shaft with flywheel, belt-type (quiet) transmission, and sliprings. Power to rotate the propeller was supplied by a d-c permanent-magnet servomotor capable of delivering up to 33 foot-pounds (45 N-m) of torque. The electrical power to this motor was delivered through a precision solid-state motor controller so that the shaft revolution rate could be controlled very accurately and held over the wide range of propeller torque loadings required for some of the experimental conditions. Mounted on the propeller shaft was a digital encoder that generated electrical pulses as a function of shaft angular position. Two types of pulses were generated: a single pulse per revolution and a multipulse per revolution (90 equally spaced pulses for the current experiment). The single pulse was syncronized with the reference line of the instrumented propeller blade. The pulses generated by this encoder are accurate to within 0.01 degree.

The downstream body which housed the drive system was basically that used by Dobay[20] but modified to allow deeper submergence and an inclined shaft angle. Both the body housing (the drive system was soft mounted to this body) and the model hull were rigidly attached to a pitch-heave

---

[27] Brandau, J.H., "Static and Dynamic Calibration of Propeller Model Fluctuating Force Balances," David Taylor Model Basin Report 2350 (March 1967); also Technologia Naval, Vol. 1, pp 48-74 (January 1968).

oscillator which, in turn, was rigidly mounted on the towing carriage. This arrangement enabled the model hull and the drive system to be dynamically pitched together while maintaining independent support from one another.

The sensing elements were flexures to which were bonded high-sensitivity, semiconductor strain-gage bridges. The design of these flexures has been described by Dobay.[20] There were three flexures, each of which measured two components of blade loading. Flexure 1 measured components F_x and M_y, Flexure 2 measured components F_y and M_x, and Flexure 3 measured components F_z and M_z (Figures 1, 5, and 6). An arrangement of three separate flexures rather than one to measure all components of blade loading was adopted because it appeared to result in higher natural frequencies (Criterion 1), higher sensitivities (Criterion 3), and lower interactions (Criterion 4), than would have resulted had a single flexure been used.

The flexures were mounted inside a propeller hub which was specifically designed for these experiments (Figure 6). Only one flexure could be mounted at a time, because of space limitations, and this necessitated duplicate runs, as discussed later in the section on experimental conditions and procedures.

The strain-gage bridges were excited by a common d.c. voltage source, transmitted through the sliprings on the propeller shaft. The constant-current excitation used by Dobay[20] was not employed in the present experiment because it appeared to be too sensitive to temperature.

The voltage output from the flexures (due to blade loading) was transmitted through the sliprings to individual amplifiers (NEFF 119-121). These amplifiers utilized field effect transistors to produce an extremely high input-impedance (100 megohms, minimum). This high impedance essentially eliminated slipring noise to the amplifier. The voltage signals were transferred across the sliprings in the presence of only a small amount of noise-producing current. The amplifiers used here had zero-phase shift qualities in the d.c. to 20 kilohertz range. They were chopper-stabilized to enable both the steady and unsteady signals to be recorded simultaneously. This signal-conditioning system was essentially the same as that used by Dobay.[20]

The signals were then digitized and analyzed by using a Model 70 Interdata Digital Computer, and then stored in digital form on a nine-track magnetic tape. The on-line analysis of the data is discussed in the section on data acquisition and analysis.

CALIBRATION

Prior to the experiment, each flexure was statically calibrated in air to establish flexure sensitivities, interactions, and linearity over the loading range of interest. These calibrations were conducted with the flexures mounted in a calibration stand, with the flexure electrical cables connected through the flywheel and drive assembly as in the experiment. Each flexure was subjected to independently controlled forces in the axial, transverse, and radial directions (i.e., F_x, F_y, and F_z, respectively) and to independently controlled moments about the axial, transverse, and radial directions (i.e., M_x, M_y, and M_z, respectively); see Figure 1.

The static calibration showed that all flexures had a linear response over the load range of interest. Table 2 shows the interaction matrix. These calibrations indicated that all flexures had good sensitivity except F_z whose sensitivity was slightly lower than desirable. The interactions were small except for the effect of M_z on F_z. The inferior characteristics of the F_z flexure is not considered a serious shortcoming since F_z arises primarily from centrifugal loading and can be analytically calculated. In addition, no significant variation of F_z with blade angular position was anticipated. Flexure 3, which measured F_z and M_z, was further evaluated by correlation of air-spin experiments with analytically calculated results, as discussed later. The interactions were taken into consideration during data analysis.

The flexures used in this experiment had been dynamically calibrated by Dobay[20] to determine the frequency range over which unsteady forces and moments could be reliably measured. In this procedure, an electromagnetic shaker in air was used to apply a relatively constant, maximum amplitude, variable-frequency force or moment-excitation in all six-component directions to all six flexure elements. The force or moment amplitude imposed by the shaker was monitored through an extremely

light-weight, strain-gaged single flexure element. The measured lowest natural frequencies of the three flexures in air were as follows:

	Frequency (hertz)	Mode
Flexure 1	550	M_x
Flexure 2	450	M_y
Flexure 3	282	M_z

The measured amplification factor (ratio of output amplitude to input amplitude) and phase shift for all three flexures was as follows:

Frequency Range (hertz)	0 to 60	60 to 120
Phase Shift (degrees)	0 to 0.05	0.05 to 0.15
Amplification Factor	1.00	1.00 to 1.05

In the previous experiment[2] the natural frequency of the flexures was found to be reduced by 55 percent when submerged with blades attached. As a result, it was concluded that the flexures had a "true" dynamic response up to at least the third harmonic and no greater than a five percent amplification up to the sixth harmonic. Because the blades used on the present experiment were lighter and smaller than those used on the previous experiment, it was assumed that the natural frequency of the flexures would be reduced to a lesser extent when submerged with blades, so that the dynamic amplification would be less. This assumption was supported by the increase in frequency of the extraneous signals appearing in the unfiltered experimental data as discussed in the experimental results section.

The propeller shaft drive and soft-mount support system were dynamnamically loaded in the vertical, longitudinal, and transverse directions to obtain the lowest natural frequencies of the system. The natural frequencies of the system in air were found to be:

Mode	Natural Frequency (hertz)
Vertical bending	12.2
Horizontal bending	6.0
Axial	4.6

The support system had a low resonant range; however, the softmount system was specifically designed to prevent towing-carriage

oscillation (with the resonance at 100 to 200 hertz) from being transmitted to the blade flexures. Based on the measured resonance, it is concluded that the soft-mount system should successfully meet this objective. Although some resonances were close to the propeller rotational speed for some experimental conditions, it was considered more desirable to isolate the system from towing-carriage vibration.

EXPERIMENTAL CONDITIONS AND PROCEDURES

Experiments were conducted at several conditions including steady-ahead operation, simulated pitching of the hull, and simulated acceleration. All conditions were run with the model hull rigidly attached to its support, with no freedom to sink or trim, and with essentially equal rotational speed on the port and starboard propellers.

The steady-ahead condition is defined in Tables 3 and 4. The simulated full scale ship speed and propeller rotational speed for this condition were determined from model self-propulsion data* at simulated displacement of 7,800 tons (7,920 tonnes) including corrections for wind drag at zero true wind and a three-percent margin on effective power with $C_A = 0.0005$.

The trim and draft at this speed were obtained from Reference 28. These had been determined by setting the specified still water trim (even keel) and draft (19.5 feet (6.40 m) full-scale equivalent), attaching the model to the carriage so that it was free to trim and sink, running at the specified speed, and locking the model at this equilibrium trim and draft. The equilibrium sinkage was 0.5 feet (15.4 cm) at the bow and 3.0 feet (98.4 cm) at the stern.

Runs simulating hull pitching were conducted at the same conditions as the steady-ahead run, except that the hull pitch was varied. Two types of runs were conducted: (1) quasi-steady simulation in which the hull pitch angle ψ was set at various fixed positions, and (2) unsteady

---

*DTNSRDC experiments 21 and 22 on Model 5265-1B.

[28] Day, W.G., "The Effect of Speed on the Wake in Way of the Propeller Plane for the DD-963 Class Destroyer Represented by Model 5265-1B," David Taylor Naval Ship Research and Development Center Report SPD-311-37 (July 1975).

simulation in which ψ was varied sinusoidally with time. For the quasi-steady simulation, runs were conducted at five different values of ψ, from 1.85 degrees bow up from the calm water equilibrium $\psi(\psi=\psi_{CW})$ to 1.85 degrees, bow down from ψ_{CW} (Tables 3 and 4). For the unsteady pitch simulation, the value of ψ was varied sinusoidally about ψ_{CW} with an amplitude of 1.85 degrees and a frequency of 0.8 hertz.* The selected scaled amplitude and frequency were within the predicted response characteristics of the DD-963. All runs were conducted in calm water; therefore, the response of the hull to the seaway was simulated but the seaway was not simulated.

Acceleration runs were conducted based on analytical dynamic simulation studies of the DD-963.[29] The experimental conditions followed run 7501061 of Reference 29, which was an acceleration from 8.7 knots to full power (see Tables 3 and 4 and Figure 7). Trim and displacement were fixed at the values corresponding to the self-propulsion condition (Condition 1 of Table 3). Two types of runs were conducted: (1) quasi-steady runs in which all quantities including model speed V, rotational speed n, and propeller pitch P were held constant ($\dot{V}=\dot{n}=\dot{P}=0$), and (2) unsteady runs in which V was varied with time but n and P were held constant ($\dot{V}>0$, $\dot{n}=\dot{P}=0$). For the quasi-steady simulation, runs were conducted at five different combinations of V, n, and P. The conditions for each run represent the conditions at one instant of time during a "true" acceleration in which V, n, and P vary with time. Thus, one "true" acceleration run is represented by five steady runs which do not simulate the time rate of change of V, n, and P. For the unsteady simulation, runs were conducted at the same five combinations of fixed n and P as used for the quasi-steady simulation, and V was varied with time (the same variation was used for each run) representing an acceleration of the model hull (Figure 7). For each of these runs, data are of interest only near that value of V which occurred concurrently with the fixed values of n and P during the "true"

---

*Full scale equivalent frequency is 0.16 hertz.

[29] Rubis, C.J. and T.R. Harper, "Propulsion Dynamics Simulation of the DD-963 Class Destroyer," Propulsion Dynamics, Inc., Report 74R1B (January 1975).

acceleration ($\dot{V}>0$, $\dot{n}\neq0$, $\dot{P}\neq0$). Thus, one "true" acceleration run is represented by five runs which simulate the proper time rate of change of V but not the proper time rate of change of n and P. The quasi-steady and unsteady acceleration simulations were for the same conditions, the only difference being that $\dot{V}=0$ for the quasi-steady simulation whereas $\dot{V}>0$ for the unsteady simulation. In general, P varies with time during a "true" acceleration run; however, for the acceleration run under simulation here, P was constant throughout the portion of the run simulated.

For the unsteady acceleration runs, the carriage speed was manually varied with time in a carefully controlled manner. This was achieved with the aid of an inked pen on a two-dimensional Cartesian plotter. In one direction, the pen was controlled so that it moved linearly with time, and in the orthogonal direction, it was controlled so that it varied with the instantaneous carriage speed. When an acceleration maneuver was to be executed, the switch moving the pen with time was turned on and the carriage operator manually varied the carriage speed so that the inked pen followed a prescribed velocity versus time curve.

As discussed earlier, each of the three load-sensing flexures measured only two components of blade loading. Therefore, each of the experimental conditions described in Table 3 was run with each of the three blade loading flexures.

The blade pitch was set by using a Sheffield Cordax 300 measuring machine. In order to change either the blade pitch or the flexure, the propeller had to be removed from the drive system.

Air-spin experiments were conducted with all three flexures over a range of rotational speeds in order to isolate the effects of centrifugal and gravitational loading from hydrodynamic loading. Supplemental experiments were conducted to assess the influence of the downstream dynamometer boat on the flow in the propeller plane. These supplemental experiments consisted of wake surveys in the propeller plane at the self-propulsion point (Condition 1 in Table 3) with and without the downstream body, but without the propeller. These wake surveys yielded a direct measure of the change in the velocity distribution through the propeller

disk attributable to the downstream body. The details of these wake surveys will be reported in a future DTNSRDC report.*

DATA ACQUISITION AND ANALYSIS

Data were collected, stored, and analyzed on-line by using a Model 70 Interdata Digital Computer. A special-purpose computer program was written with options for analyzing each of the three basic types of runs: (1) steady ahead, (2) dynamic hull pitching, and (3) unsteady acceleration. These types of runs have already been discussed in detail.

The program allowed the propeller blade force and moment data to be sampled and stored on magnetic tape as a function of shaft position. Sampling was triggered by external pulses generated by a Baldwin Digital Encoder mounted on the propeller shaft, as discussed earlier. Pulses were generated as a function of shaft angular position; hence, the sampling of blade force and moment data was related to shaft position. There were two outputs from the shaft encoder; a single pulse per revolution and multipulse (90 pulses per revolution for the current experiments).

When the experimental condition was achieved, the computer operator initiated the data collection cycle. The program "waited" until the single pulse occurred; when the single pulse occurred, the computer again "waited" for the occurrence of the first following pulse of the 90 pulses; data were then sampled for all channels through an analog-to-digital converter and stored in computer memory. This process was repeated for 180 pulses, or two shaft revolutions. At the same time, the program "read" two frequency counters into core memory which measured model velocity V and propeller rotational speed n. The values of V and n were measured by counting the pulses from geared wheels attached to the towing carriage drive system and to the propeller shaft, respectively. The values of V and n were averaged over two shaft revolutions. Thus, there was an average V and n corresponding to each pair of two consecutive revolutions.

After two revolutions of data were sampled and stored in core memory, the data were transmitted from core to a nine-track digital tape recorder. The transfer time was small and no pulses were missed during the transfer.

---

*These wake surveys were conducted by R.F. Roddy, DTNSRDC Code 1524.

The data collection cycle proceeded continuously until the operator disengaged the computer. The sampling procedure was the same for all types of experimental conditions, and at the completion of an experimental run, all data were stored on magnetic tape and were available for analysis immediately or at any later time. For the analysis, the computer operator selected the appropriate option of the program depending on the type of run, i.e., (1) steady ahead, (2) dynamic hull pitching, or (3) unsteady acceleration.

The appropriate calibration factors were stored in the computer and considered in the analysis. However, since only two of the six components of blade loading were measured during a given run, the interactions between the various loading components could not be considered during the on-line analysis. The interactions were taken into account later after measurements were completed with all three flexures for a given condition.

For the steady ahead condition, blade force and moment data at each 4-degree increment of blade angular position were averaged over the number of cycles recorded (usually over more than 200 cycles). Spurious data not related to shaft position are averaged out by this method. An harmonic analysis was then performed on the average wave forms of the blade loading components. This gave the amplitude and phase of the first 16 harmonics.

For the dynamic pitch runs, the hull pitch angle varied sinusoidally with a frequency of 0.8 hertz. A position potentiometer translated bow vertical displacement into hull pitch angle, and this was read into the computer in the same manner as blade loading components. During dynamic pitching, the shaft rotated independent of the pitch oscillator. During a single propeller revolution, 90 pitch positions were measured. Thus, to correlate pitch angle position and revolution, an average pitch must be taken over each revolution.

Fourteen dynamic pitch angle positions were selected for analysis. These were characterized by pitch angle ψ and the sign of the time rate of change of pitch angle $\dot{\psi}$. The computer calculated the average ψ and sign of $\dot{\psi}$ corresponding to each propeller revolution. Based on these calculated average values of ψ and sign of $\dot{\psi}$, each propeller revolution was either placed in a suitable hull-pitch angle category or discarded if its average ψ fell outside the tolerance band of all the 14 specified values

of ψ. Several passes down the towing tank were required in order to obtain a sufficient number of samples. After all the data had been sorted based on ψ, sign of $\dot{\psi}$, and tolerance, the cycles for each combination of ψ, and sign of $\dot{\psi}$ were analyzed in exactly the same manner as the data for the steady-ahead condition at fixed ψ.

For unsteady-acceleration runs, the model speed V varied with time t. During an acceleration run, data, including a measure of V, were sampled and stored in the same manner as for the steady-ahead runs.

Five values of V were specified for analysis. For each acceleration run and for each specified V, the computer selected the propeller revolution which had the average value of measured V nearest to the specified V. However, because only one revolution at each specified velocity was obtained for a single acceleration run, each such run was repeated five times. This yielded five revolutions at each specified velocity. All the cycles for each specified V were then analyzed in exactly the same manner as the data for the steady-ahead conditions.

Thus, the on-line analysis system yielded average wave forms and harmonic analyses of the average wave forms for steady-ahead conditions, for specified conditions of ψ, sign of $\dot{\psi}$ during the dynamic pitch cycle, and for specified velocities V during the acceleration operation. However, these on-line results are preliminary because:

1. They do not consider the interactions between the various load components. These interactions were determined during the static calibration of the flexures.

2. They include the complete measured signals with no filtering. As discussed in the section on experimental results, some extraneous signals near the natural frequency of the flexure being used appeared to be superimposed on the signals generated by blade loading.

3. They include the effect of centrifugal and gravitational loading on the aluminum model propeller. The centrifugal and gravitational components of loading were measured separately during air-spin experiments, as discussed earlier.

4. They do not have any corrections for the influence of the dynamometer boat. These corrections are discussed later.

5. The bending moments were calculated about the radial location of the strain gages on the flexures, rather than about the shaft axis or some desired radius on the blade.

Final analyses were conducted after completion of the experiment to consider interactions, to filter out extraneous high frequency noise, to isolate hydrodynamic loading from centrifugal and gravitational loading, to correct for the dynamometer boat, and to resolve bending moments as desired. These analyses were conducted using a Control Data Corporation (CDC) 6700 Computer.

For each condition, the average wave form for each of the six loading components was multiplied by the inverse of the calibration matrix given in Table 2.

$$\begin{bmatrix} F_{xA} \\ M_{yA} \\ F_{yA} \\ M_{xA} \\ F_{zA} \\ M_{zA} \end{bmatrix} = \begin{bmatrix} F_{xI} \\ M_{yI} \\ F_{yI} \\ M_{xI} \\ F_{zI} \\ M_{zI} \end{bmatrix} \begin{bmatrix} C_{i,j} \end{bmatrix}^{-1}$$

This matrix multiplication was performed at 4-degree increments of blade angular position.

An harmonic analysis was then performed on the signals corrected for the interactions. Based on an harmonic analysis of the wake in the propeller plane,[30] it was judged that there should be no significant loading of hydrodynamic origin at frequencies above ten times shaft frequency. Therefore, the wave form was then reconstructed by using the first ten harmonics of shaft frequency. This reconstruction using only the first ten harmonics had the same effect as filtering out all frequencies above ten times shaft frequency.

---

[30] Cummings, D.E., "Numerical Prediction of Propeller Characteristics," Journal of Ship Research, Vol. 17, No. 1, pp 12-18 (March 1973)

Corrections were made to the mean values of the measured loading components to account for centrifugal loads and the influence of the dynamometer boat, and to the first harmonic of the measured loading components to account for gravitational loads. The derivation of these corrections is discussed later.

From the known values of the three measured force components and three measured moment components, the values of the bending moments about the shaft centerline and bending moments normal to the nose-tail line at the 0.3 and 0.4 radii were calculated. These bending moments were calculated at every 4 degrees of blade angular position, and harmonically analyzed. The wave form was reconstructed by using the first 10 harmonics of blade angular position, in exactly the same manner as was used for the other components of blade loading.

Plots of the data were generated by the CDC computer system using a Calcomp Plotter.

ACCURACY

During the experiments for steady operation, $\dot{V}=0$, and dynamic pitching, $\dot{\psi}\neq0$, where many revolutions of data were averaged during a single run, the standard deviations of speed V, rotational speed n, forces, and moments were computed, assuming the distribution in these variables at a given condition follows the normal probability distribution. For forces and moments, the standard deviation was calculated at every increment of blade angular position at which forces and moments were recorded. An error band around the data mean was then represented using the standard deviation multiplied by a factor dependent on the confidence level chosen. For the present analysis, the factor of 1.96 was selected which corresponds to a confidendence level of 95 percent. A confidence level of 95 percent indicates a confidence (or probability) that 95 percent of the data considered falls within the error band. For a given run the average error (95 percent confidence band) in model speed V was approximately ±0.005 foot per second (1.6 mm/s), while the error in rotational speed n was less than 0.001 revolution per second. The very low error in n resulted from the use of a precision solid-state motor controller as discussed in the section on facility and dynamometry.

For a given steady run ($\dot{V}=0$, $\psi\neq0$) the error (95 percent confidence band) in measured forces and moments, fluctuated from ±5 to ±10 percent of the mean signal, depending on the circumferential blade position. Figure 8 demonstrates the variation in error in one revolution of the uncorrected, raw F_x signal at the full power condition. This figure represents the general trend of all the force and moment components measured.

Besides the fluctuation in signals occurring in a given run, the overall accuracy of the data is dependent on the repeatability from one run to the next. An effort was made to set experimental conditions identically on repeat runs; however, the propeller rotational speed and model velocity were set by hand, so some variation was unavoidable. Table 5 demonstrates the variation in the measured experimental conditions and the raw data for the F_x component for 11 repeat runs. The variation in the mean force was ±4 percent over all the runs, but on a given day the variation averaged ±2 percent. The same trend can be observed in rotational speed, model velocity and the harmonic force components. This day-to-day variation could be due to different operators setting the experimental conditions, slight variations in the draft of the model, and variations in the gain of the sensing electronics. The variations shown for F_x are typical of all the measured force and moment components.

For all experimental conditions the rotational speed of the port and starboard propellers were intended to be equal. However, some exploratory runs were conducted to determine whether the mean or unsteady loads, which were measured on the starboard propeller, were influenced by the rotational speed of the port propeller. At a fixed value of rotational speed on the starboard propeller n_s, the rotational speed on the port propeller n_p was varied. The results showed that there was no measurable effect of n_p on the mean or unsteady loads in the region $0.95\ n_s \leq n_p \leq 1.05\ n_s$. For all runs for which data are presented, $0.99\ n_s \leq n_p \leq 1.01\ n_s$; therefore, the results presented are not measurably influenced by inaccuracies in n_p.

For the unsteady acceleration ($\dot{V}>0$), the average of the five values of V and n for which data are presented during the unsteady runs was generally within ±0.2 foot per second (6.5 cm/s) and ±0.2 revolution per second of the target values respectively.

For runs with fixed hull pitch angle ψ, ($\dot{\psi}$=0), the value of ψ could be controlled to within ±0.005 degree. For dynamic pitch runs $\dot{\psi}$±0, the selection of a propeller revolution at a specified ψ necessitated a tolerance of 0.1 degree to ψ; however, the average value of ψ for which data are presented during the unsteady runs was generally within 0.02 degree of the target ψ.

Considering all sources of error including deviations during a run and inaccuracies in setting conditions, the model scale forces and moments presented in this report are generally considered to be accurate to within (plus or minus) the following variations:

	$\overline{F}$		F_{MAX}		$\overline{M}$		M_{MAX}	
	lb	(N)	lb	(N)	in-lb	(N-m)	in-lb	(N-m)
Steady ahead $\dot{V}$=0,$\dot{\psi}$=0	0.1	(0.4)	0.2	(0.9)	0.2	(0.02)	0.4	(0.06)
Dynamic pitch $\dot{V}$=0,$\dot{\psi}$≠0	0.2	(0.9)	0.3	(1.3)	0.4	(0.04)	0.6	(0.07)
Acceleration $\dot{V}$>0,$\dot{\psi}$=0	0.3	(1.3)	0.4	(1.8)	0.6	(0.07)	0.8	(0.09)

The values are somewhat more accurate for the steady-ahead runs than for the time-dependent runs, because the experimental conditions could be controlled more precisely for the steady runs and the measured forces and moments were averaged over many more revolutions of the propeller. The time-average values per revolution (based on 90 samples per revelolution) are slightly more accurate than the maximum values (based on one sample per revolution) which took into account the variation with blade angular position. Further, the peak values may have been slightly influenced by the dynamic response of the flexures, as discussed in the section on calibration.

EXPERIMENTAL RESULTS

LOADING COMPONENTS

The basic loading components are shown in Figure 1. For a right-hand propeller the sign convention follows the conventional right-hand rule with a right-hand Cartesian coordinate system. For a left-hand propeller all the loads are the same, but for this case the sign convention follows a left-hand rule with a left-hand Cartesian coordinate system.

The sign conventions for both right-hand and left-hand propellers are shown in Figure 1. In all pertinent figures and tables throughout this report the blade loading components are listed in the following order:

1. Components measured by Flexure 1:

   a. F_x - axial force, or thrust per blade.

   b. M_y - bending moment about the axis normal to the shaft axis at r=0. This moment is generated primarily by the F_x component of force.

2. Components measured by Flexure 2:

   a. F_y - tangential force, or force normal to the propeller axis and the spindle axis.

   b. M_x - moment about the propeller axis, (r=0), or torque per blade. This moment is generated primarily by the F_y component of force.

3. Components measured by Flexure 3:

   a. F_z - radial force, or force parallel to the blade spindle axis.

   b. M_z - moment about the spindle axis, or spindle torque.

4. Supplemental components which were derived from the components listed above (not derived for all conditions).

   a. $M_{0.3} = F_x\ (r_{F_x}\ -0.3R) \cos \phi_{0.3} + F_y\ (r_{F_y}\ -0.3R) \sin \phi_{0.3}$ - bending moment applied on the spindle axis about the axis intersecting the spindle axis at r=0.3R and parallel to the expanded pitch line at r=0.3R. The $M_{0.3}$ vector as defined by the conventional right-hand rule for a right-hand propeller (left-hand rule for left-hand propeller) intersects the plane normal to the propeller axis at the angle $\phi_{0.3} = \tan^{-1}(P_{0.3}/0.3\ \pi D)$ and is directed so that a positive $M_{0.3}$ puts the face (pressure side) of the blade in tension.

   b. $M_{0.4} = F_x\ (0.97r_{F_x}\ -0.4R) \cos \phi_{0.4} + F_y\ (0.97r_{F_Y}\ -0.4R) \sin \phi_{0.4}$ - bending moment applied on the spindle axis about the axis intersecting the spindle axis at r=0.4R and parallel to the expanded pitch line at r=0.4R. The $M_{0.4}$ vector as defined by the conventional right-hand rule for a right-hand propeller (left-hand rule

for the left-hand propeller) intersects the plane normal to the propeller axis at the angle $\phi_{0.4} = \tan^{-1}(P_{0.4}/(0.4\pi D))$ and is directed so that a positive $M_{0.4}$ puts the face (pressure side) of the blade in tension. In calculating $M_{0.4}$ from the experimental values of the three measured forces and three measured moments, an adjustment was necessary to allow for the contribution of loading in the region $0.4R>r>r_h=0.3R$ where r_h is the hub radius. It was estimated that for all harmonics including the time average values, 3 percent of M_x and M_y was contributed by the loading in the region $0.4R>r>r_h$. These estimates were based on a refinement of the method of Cummings[30] for the time-average values, and the method of Tsakonas et al[25] for the unsteady values.

Hydrodynamic, centrifugal, and gravitational loads may contribute to each of these components of loading; however, for some components the centrifugal loads and/or gravitational loads are zero, as discussed in the section on centrifugal and gravitational loads.

Each component of loading is generally presented as a variation of the instantaneous value with blade angular position θ and as a Fourier series in blade angular position in the following form:

$$F,M(\theta) = (\bar{F},\bar{M}) + \sum_{n=1}^{N} (F,M)_n \cos\,(n\theta - (\phi_{F,M})_n)$$

where $\bar{F},\bar{M}$ = circumferential average value of F,M

$(F,M)_n$ = amplitude of the nth harmonic of F,M

θ = angular position about the propeller axis, positive counterclockwise from the vertical upward looking upstream for starboard propeller (left-hand rotation) positive clockwise looking upstream for port propeller (right-hand rotation)

$(\phi_{F,M})_n$ = phase angle of nth harmonic of F,M

where the reference line of the blade is the spindle axis; see Figure 2 and Table 1.

The components M_y and M_x are the most important for determination of the time-average and unsteady stresses in the hub mechanism of an actual

controllable pitch propeller. The components $M_{0.3}$ and $M_{0.4}$ are the most important for determination of the time-average and unsteady stresses in the blades of a propeller.

CENTRIFUGAL AND GRAVITATIONAL LOADS

The results of the air-spin experiments, corrected for interactions, are presented in Table 6. The time-average values arise from centrifugal force whereas the first harmonic arises from gravitational force. Therefore, the mean values should vary as n^2 where n is the propeller rotational speed, and the first harmonic should be independent of n.

For the mean values, which arise from centrifugal force, signficant nonzero values were obtained only for the F_y, F_z, M_y, and M_z components. Any realistic propeller would have nonzero values of centrifugal loading components $(\bar{F}_z)_c$ and $(\bar{M}_z)_c$.[31] Nonzero values of $(\bar{F}_y)_c$ and $(\bar{M}_y)c$ are produced by the nonzero values of skew and rake of the propeller evaluated. The components $(\bar{F}_x)_c$ and $(\bar{M}_x)_c$ should be zero for any geometry, however, a small value of $(\bar{F}_x)_c$ was measured. This small nonzero $(\bar{F}_x)_c$ probably arises from inaccuracies in the air-spin experiment and interaction matrix. For all components the experimentally determined mean value varies essentially as n^2. The experimental air-spin results were faired so that the values of the mean loading components used for separating hydrodynamic loads from total loads varied exactly as n^2.

For the first harmonic loads, which arise from acceleration due to gravity, nonzero values were obtained only for the F_y, M_x and F_z flexures. For $(M_x)_{1g}$ and $(F_y)_{1g}$ the phase angles are +96 degrees and -96 degrees, respectively; therefore the maximum and minimum values of these components occur when the blade is approximately horizontal. This would be expected from the geometry. The phase angle for $(F_x)_{1g}$ is -159 degrees; therefore

---

[31]Boswell, R.J., "A Method of Calculating the Spindle Torque of a Controllable-Pitch Propeller at Design Conditions," David Taylor Model Basin Report 1529 (August 1961).

maximum value occurs when the blade is nearly vertical downward (6 o'clock position). This is again as would be expected from geometry. The phase angles would not be expected to be precisely ± 90 degrees or 180 degrees since the propeller has 22 degrees of skew. The amplitudes of $(F_y)_{1g}$ and $(F_z)_{1g}$ each should be equal to the combined weight of the blade and that portion of the appropriate flexure at radii greater than the radius of the appropriate strain gage. The values of $(F_y)_{1g}$ and $(F_z)_{1g}$ were confirmed by weighing the blade and appropriate flexures. The values of $(M_y)_{1g}$ and $(M_z)_{1g}$ are essentially zero because the blade is skewed and raked so that mass of the blade is balanced about the spindle axis in both the plane containing the spindle axis and the propeller axis, and the plane normal to the propeller axis which contains the spindle axis (see Figure 2 and Table 1). The value of $(F_x)_{1g}$ is nearly zero since F_x is always in a nearly horizontal direction. For all components the experimentally determined amplitude and phase of the first harmonic were essentially independent of rotational speed n. The experimental air-spin results were faired so that values of the amplitude and phase of the first harmonic of the loading components used for separating hydrodynamic loads from total loads were constant, independent of n.

Approximate scaling parameters for centrifugal loads are $(F/\rho_p n^2 D^4)$ and $(M/\rho_p n^2 D^5)$, whereas appropriate scaling parameters for gravitational loads are $(F/\rho_p g D^3)$ and $(M/\rho_p g D^4)$. The model experiments presented in this report were conducted at full scale values of Froude number $F_n = (V/\sqrt{gL})$ and advance coefficient $J = (V/nD)$. Constant Froude number implies that

$$V \sim (gL)^{1/2} \sim (gD)^{1/2}$$

$$V^2 \sim gD$$

Constant advance coefficient implies that

$$V \sim nD$$

$$V^2 \sim n^2 D^2$$

Therefore,

$$g \sim n^2 D$$

$$\rho_p g D^3 \sim \rho_p n^2 D^4$$

$$\rho_p g D^4 \sim \rho_p n^2 D^5$$

Thus, for the results presented in this report gravitational loads and centrifugal loads scale the same. Furthermore, if proper allowance is made for the difference in density between the model propeller and the full scale propeller,* the gravitational and centrifugal loads scale the same as the hydrodynamic loads.

Therefore, in addition to the components of loading arising from hydrodynamic effects alone, for many experimental conditions the components of loading arising from the sum of hydrodynamic, centrifugal, and gravitational effects are presented. The components of loading arising from the sum of the hydrodynamic, centrifugal and gravitational effects are designated components of total loading. The centrifugal and gravitational loads presented are equivalent values for a nickel-aluminum-bronze propeller blade. These combined, or total, loading results are discussed in later sections.

The time-average centrifugal spindle torque results, $\overline{M}_{z_c}$ are compared in Figure 9 with calculated values using the method of Boswell.[31] Previous measurements of spindle torque by Boswell et all[32] and by Hawdon et al[5] have correlated well with values calculated by this procedure. The calculated value of $\overline{M}_{z_c}$ is 33 percent lower than the experimental value at design pitch (see Figure 9); however, this is within experimental accuracy. The largest measured value of $\overline{M}_{z_c}$ is 0.5 inch-pounds (0.07 N-m) as shown in Table 6 whereas the accuracy of this measurement is plus or minus 0.2 inch-pounds (0.02 N-m) as discussed in the section on accuracy. The large experimental inaccuracy as a percent of the measured $\overline{M}_{z_c}$ value results from a combination of (1) the small value of the measured $\overline{M}_{z_c}$, and (2) the inferior characteristics of flexure number 3, which measures

---

*The model propeller used in these experiments was made of aluminum, density ρ_p=5.44 lbf-s^2/ft^4 (2.80 g/cm^3). The full scale propeller on the DD-963 is made of nickel-aluminum-bronze, density ρ_p=14.48 lbf-s^2/ft^4 (7.46 g/cm^3).

[32]Boswell, R.J. et al, "Experimental Spindle Torque and Open-Water Performance of Two Skewed Controllable-Pitch Propellers," David Taylor Naval Ship Research and Development Center Report 4753 (December 1975).

F_z and M_z, relative to the other two flexures as discussed in the section on calibration.

INFLUENCE OF DYNAMOMETER BOAT

The results of the wake surveys with and without the downstream body (dynamomemter boat) are presented in Figure 10, and in Appendix A. These data indicate that the downstream body had only a small effect on the circumferential and radial variation in the flow and only a small effect on the harmonic content of the flow. However, they also indicate that the downstream body reduced the volume mean velocity through the propeller disk by approximately 12 percent; i.e., without the downstream body the volume mean wake $(1-w_{VM})=1.06$ and with the downstream body $(1-w_{VM})=0.93$. These results are, of course, without the propeller in place.

The change in effective velocity through the propeller due to the downstream body was deducted from thrust and torque identities between the mean thrust and torque measured during the blade loading experiments at the self propulsion point (Condition 1 in Table 3), and mean thrust and torque measured during a previous self propulsion model experiment.* These results, which include the effect of the propeller, indicate that the downstream body reduced the effective velocity through the propeller disk by approximately 5 percent; i.e., without the body, $(1-w_T)=1.02$ and $(1-w_Q)=1.00$, whereas, with the body, $(1-w_T)=0.97$ and $(1-w_Q)=0.95$.

The difference between the effect of the downstream body on volume mean wake and effective wake is probably due to a combination of the following:

1. The effect of the propeller action; $(1-w_T)$ and $(1-w_Q)$ include the effect of the propeller but $(1-w_{VM})$ does not.

2. Experimental inaccuracies; both methods for calculating the change in velocity are based on a small difference of two much larger nearly equal experimental results.

---

*DTNSRDC experiments 21 and 22 on Model 5265-1B, in which the mean thrust and torque was measured using transmission dynamometers mounted inside the model hull.

It is judged that the dominant cause of the discrepancy is the effect of the propeller.

Based on these results it was concluded that the downstream body reduced the mean velocity into the propeller by 5 percent at the self-propulsion condition. This is somewhat smaller than the 10 to 14 percent reduction in effective wake that was obtained in Reference 2 in which the same dynamometer boat was used behind a single screw model hull. It was assumed that the 5 percent reduction in the present experiment occurred at all conditions at which experiments were conducted. Therefore, after the effects of centrifugal force were subtracted from the measured loading components as discussed previously, the time-average value per revolution of each hydrodynamic loading component was corrected for the effect of the downstream body as follows: From the measured hydrodynamic blade thrust ($\overline{F}_{x_H}$) and hydrodynamic blade torque ($\overline{M}_{x_H}$), effective advance coefficients based on thrust identity (J_T) and torque identity (J_Q) were deduced from the open-water data (Figure 11). These values were multiplied by (1/0.95) to obtain corrected values of J_T and J_Q, i.e., without the downsteam body. The corrected values of $\overline{F}_{x_H}$ and $\overline{M}_{x_H}$ were then obtained from the open-water data at the corrected advance coefficients J_T and J_q, respectively. It was assumed that the downstream body did not affect the radial center of thrust $\overline{F}_{x_H}$ and tangential force $\overline{F}_{y_H}$. Therefore,

$$\overline{M}_{y_H} \text{ corrected} = (\overline{F}_{x_H} \text{ corrected}/\overline{F}_{x_H} \text{ measured})\ (\overline{M}_{y_H} \text{ measured})$$

$$\overline{F}_{y_H} \text{ corrected} = (\overline{M}_{x_H} \text{ corrected}/\overline{M}_{x_H} \text{ measured})\ (\overline{F}_{y_H} \text{ measured})$$

The spindle torque ($\overline{M}_{z_H}$) was corrected by the same procedure as used for $\overline{F}_{x_H}$ and $\overline{M}_{x_H}$, using unpublished hydrodynamic spindle torque data for the DD-963 propeller. No corrections were made to $\overline{F}_{z_H}$ for the effect of the downstream body; however, $\overline{F}_{z_H}$ is very small for all experimental conditions, as discussed later.

No correction for the effect of the downstream dynamometer boat was made to the measured circumferential variation of the loading components.

Calculations made by the methods of Tsakonas et al[25] and McCarthy[26] indicated that the influence of the downstream body alters the peak-to-peak circumferential variation of the loads by no more than 2 percent. However, these methods did not agree well with the experimental results, as discussed in the section on correlation with full-scale data and theory.

STEADY-AHEAD OPERATION

For operation near the self-propulsion point (Condition 1 in Table 3), Figure 12 presents the variation of the various components of total blade loading with blade angular position and Figure 13 presents the amplitude of the first 25 harmonics of the various components of total blade loading.

Based on the dynamic calibration, as discussed in the section on calibration, it was judged that for all loading components the data are valid for the first 10 harmonics. In addition, the wake data shows no significant amplitudes for harmonics greater than the tenth; see Appendix A. Therefore, all data and analysis except Figures 12 and 13 are based on reconstructed signals using the first 10 harmonics. The symbols shown in Figure 12 indicate unfiltered values determined from the experiment; each represents the average value at the indicated blade angular position for over 200 propeller revolutions. The variation in measured values at a given angular position is discussed in the section on accuracy; see Figure 8. The lines on Figure 12 are the signals reconstructed from the first 10 harmonics. Figure 12 indicates that the variation of the signals with blade angular position are adequately represented by the number of harmonics retained.

Figure 13 shows that there are no significant resonances for any of the loading components below the 23rd harmonic, which corresponds to (23)x(14.08)=324 hertz. This is higher than the lowest frequency resonance obtained in the results presented in Reference 2; i.e., 247 hertz. As discussed in the section on calibration, the higher frequency of the fundamental significant resonance obtained in the present experiment was anticipated because smaller and lighter blades were used in this experiment than were used in Reference 2.

The variation of all measured loading components with blade angular position for the self propulsion condition (Condition 1 in Table 3) is shown in Figures 14 and 15 for the hydrodynamic loads, and is shown in Figure 16 for the total (hydrodynamic, centrifugal and gravitational) loads. The amplitudes and phases of the harmonics of these loading components are presented in Figure 17 for the hydrodynamic loads and in Figure 18 for the total loads. Appendix B presents tabulated values of all the data in Figures 14 through 18, and Table 7 presents a summary showing the maximum value, minimum value and first harmonic of each loading component. The values for each loading component are presented as decimal fractions of the time-average value of the corresponding loading component. These time-average values for both hydrodynamic loads and total loads are presented in Table 8.

These data show that for hydrodynamic loading the variation of all loading components was predominantly a once-per-revolution variation. The extreme values for all loading components, except F_Z and M_Z, occurred near the angular position of the spingle axis, θ=124 and 304 degrees; i.e., 34 degrees beyond the horizontal. At these positions the blade tip is approximately 12 degrees beyond the horizontal. This suggests that the tangential component of the wake is the primary driving force; see Figure 10. The extreme values of F_Z and M_Z occur at up to 120 degrees after the extreme values of the other components. The reason for this variation in location of extreme values is not clear; however, it may be partially due to experimental inaccuracy with the F_Z-M_Z flexure as discussed in the section on calibration.

For total loading, the variation of all components with blade angular position follows basically the same pattern as for hydrodynamic loading. This occurs because the unsteady loading due to gravity, which is a pure first harmonic of blade angular position, is much smaller than that due to hydrodynamic force. Further for all components with a measurable gravitational load, except F_Z, the maximum value occurs near the angular position at which the spindle axis is horizontal; i.e., the gravitational load is nearly in phase or 180 degrees out of phase with the hydrodynamic load.

For hydrodynamic loading, F_{x_H} and M_{y_H} were the largest measured force and moment components; see Table 8. For these components the maximum values were approximately 1.43 times the time-average values, and the maximum value minus the minimum value (double amplitude) was approximately 0.91 times the time-average values; see Table 7. For F_{y_H} and $|M_{x_H}|$, the maximum values and range of values with blade angular position were slightly smaller fractions of the respective time-average values. For F_{z_H}, the maximum value and range of values with blade angular position were much greater fractions of its time-average. This large fractional variation in F_{z_H} occurs because $|\bar{F}_{z_H}|$ was very small. For $|M_{z_H}|$ the maximum value and range of values were 1.30 and 0.67, respectively, times the time-average value. The radial point of application of F_{x_H} varies from 0.68R to 0.73R, and the radial point of application of F_{y_H} varies from 0.67R to 0.79R.

The maximum values of F_x and M_y were approximately 1.41 times the time-average values, and the range of values were approximately 0.88 times the time-average values for combined hydrodynamic, centrifugal and gravitational loading components, or total loading components. These results are nearly the same as the hydrodynamic results since the centrifugal and gravitational loads are small for these components; see Tables 6 and 8.

The centrifugal and gravitational loads are a significant portion of the total loads for other loading components; for total loads $F_{y_{MAX}}/\bar{F}_y=1.14$ whereas for hydrodynamic loads $F_{y_{H,MAX}}/\bar{F}_{y_H}=1.40$. This large difference results from the combination of centrifugal force adding to the time-average hydrodynamic force and gravitational force substracting from the circumferential variation of hydrodynamic force. Similarly, for total loads $M_{x_{MAX}}/\bar{M}_x=1.26$ whereas for hydrodynamic loads $|M_{x_{H,MAX}}/\bar{M}_{x_H}|=1.34$. The centrifugal loading $\bar{F}_Z$ is two orders of magnitude larger than the time-average hydrodynamic loading, and for $\bar{M}_Z$, the centrifugal loading is almost as large as the time-average hydrodynamic loading; see Table 8.

The results presented here follow trends similar to those in Reference 2 for the FF-1088 which is a single screw transom stern configuration. The component M_y, which is the largest moment component for both cases, yields $M_{y_{MAX}}/\bar{M}_y=1.40$ for the present configuration (DD-963 Class) and $M_{y_{MAX}}/\bar{M}_y=1.38$ for Reference 2 (FF-1088). The maximum and minimum values occur at approximately the same angular position of the blade mid-chord at the 70 percent radius for the two configurations.

HULL PITCH

Figure 19 presents the variation of the peak values and time-average values per revolution of the various components of blade total (hydrodynamic, centrifugal and gravitation) loading* with hull pitch angle ψ for both quasi-steady simulation (time rate of change of hull pitch angle $\dot{\psi}=0$) and unsteady simulation ($\dot{\psi}\neq0$). These data show that for the quasi-steady simulation the time-average value per revolution of each loading component remains within 6 percent of its value corresponding to self-propulsion in calm water. The time-average value per revolution for the unsteady simulation, deviates by up to 12 percent from its value corresponding to self propulsion in calm water.

Data at each specified value of hull pitch angle ψ for the quasi-steady runs were recorded and averaged for a minimum of 200 propeller revolutions whereas data for the dynamic pitching runs at each specified ψ represented an average of from 10 to 35 propeller revolutions. As discussed earlier, the selection of a propeller revolution at a specified ψ during the dynamic pitch runs necessitated a tolerance of only 0.05 degree to ψ. Therefore, the differences between the results for the quasi-steady and unsteady simulations, including the time-average values per revolution, were significantly larger than any errors which may have arisen from inaccuracies in setting the experimental conditions.

For quasi-steady simulation, the absolute value of the time-average value per revolution of all loading components, except spindle torque M_z,

---

*No results are ahown for F_z since the F_z loading arises primarily from centrifugal effects, as discussed previously, which are independent of hull pitch.

were larger for the stern-up condition than for the stern-down condition; the largest value occurs at $(\psi-\psi_{CW})$=1.85 degrees or time=0.31 seconds in the reference of Figure 19. This suggests that the effective speed of advance of the propeller increases slightly for the stern-down condition and decreases slightly for the stern-up condition. This appears reasonable since for stern-up the propeller tends to be further into the boundary layer of the hull. However, the time-average value per revolution did not monotonically increase with increasing ψ for all components.

For dynamic simulation the largest absolute value of the time-average value per revolution of all loading components, except spindle torque M_Z, occurs at approximately 0.15 second after the condition $(\psi-\psi_{CW})=0$, $\dot{\psi}>0$, which is the reference for time t=0 in Figure 19. This indicates that the maximum time-average value during dynamic simulation occurs at a value of hull pitch angle ψ which occurs 0.16 second or 0.1 cycle, before the ψ at which the maximum time-average value occurs during quasi-steady simulation.

There was a significant difference between the peak values for the quasi-steady simulation and the unsteady simulation. For the quasi-steady simulation, the variation of the peak values with hull pitch angle ψ followed approximately the same trends as the variation of time-average values per revolution. These quasi-steady results indicated that for $\psi-\psi_{CW}$ up to 1.85 degrees, the maximum increase in the peak value of any loading component above the corresponding value for $\psi=\psi_{CW}$ was 5 percent. For the dynamic simulation, however, the maximum value of the peak loads increased as much as 23 percent above the corresponding value for steady ahead at a fixed hull pitch $\psi=\psi_{CW}$.

The dynamic simulation exhibited a dramatically different trend of peak load with ψ than was indicated by the quasi-steady simulation. For the dynamic simulation, the largest value of the peak loading, for all components except spindle torque M_Z, occurred at approximately time t=0.8 second in the hull pitch cycle shown in Figure 19. This corresponds to ψ=1.5 degrees stern down during the portion of the cycle in which the stern is moving down; i.e., $(\psi-\psi_{CW})$=-1.5 degrees, $\dot{\psi}<0$. For dynamic

simulation, the smallest value of peak loading occurred near $\psi=\psi_{CW}$ as the hull passed from the stern-down to the stern-up portion of the cycle; i.e., $(\psi-\psi_{CW})=0$, $\dot{\psi}>0$.

This difference in the unsteady loading between the quasi-steady and unsteady simulations may be due to an additional relative velocity component arising from the motion of the hull during dynamic pitching. As the hull passes through $\psi=\psi_{CW}$, the vertical velocity of the hull (and propeller) is a maximum. As the hull goes from stern up to stern down through $\psi=\psi_{CW}$, the upward velocity component relative to the propeller in the plane of the propeller tends to increase above the values at fixed hull pitch at $\psi=\psi_{CW}$. This tends to increase the amplitude of the first harmonic of the tangential velocity, and thereby increase the unsteady loading (and increase the peak loading). The maximum vertical velocity of the propeller for sinusoidal pitching with $(\psi_{MAX}-\psi_{CW})=1.85$ degrees and frequency=0.8 hertz is approximately 1.47 feet per second (0.448 m/s). This is equivalent to an additional tangential velocity ratio (V_t/V) of 0.133. For ψ fixed at $\psi=\psi_{CW}$, $((V_t)_1/V)=0.130$ (see Appendix A). Therefore,

$$\frac{((V_t)_1/V)_{MAX,\dot{\psi}\neq 0}}{((V_t)_1/V)_{\dot{\psi}=0,\psi=\psi_{CW}}} = \frac{0.130 + 0.133}{0.130} = 2.02^*$$

This maximum occurs at a model simulated time of approximately 0.2 second before the maximum measured loads. The measured increase in unsteady loads arising from dynamic pitching was somewhat smaller than this calculated increase in tangential velocity, for example:

$$\frac{F_{x_{MAX,\dot{\psi}\neq 0}} - \bar{F}_{x_{\psi=\psi_{CW}}}}{F_{x_{MAX,\dot{\psi}=0}} - \bar{F}_{x_{\psi=\psi_{CW}}}} = \frac{0.62}{0.44} = 1.41$$

*A numerical error was found in a similar calculation presented in Reference 2. With the numerical error corrected the results in Reference 2 are substantially the same as those presented here.

On the basis of two-dimensional quasi-steady theory, the increase unsteady loading should be approximately proportional to the increase in tangential velocity.*

The unsteady loading is important from consideration of fatigue of the propeller blades and hub mechanism. Since a ship may operate for an extended period in a seaway, the effect of the ship motions, such as dynamic hull pitching, on unsteady blade loads is significant. The difference between the peak load and the time-average load per revolution is a measure of the unsteady loading. With this difference as a measure of the unsteady loading, the quasi-steady simulation indicates that for hull pitch angles $\psi-\psi_{CW}$ up to 1.85 degrees, the unsteady loading for M_y, which is the largest moment component, increased by 8 percent above its corresponding value for $\psi=\psi_{CW}$. By contrast, the dynamic simulation showed the unsteady loading for the M_y component increased by 50 percent above its corresponding value for $\psi=\psi_{CW}$ without hull pitching. This indicates that the quasi-steady simulation is completely inadequate for estimating the effect of the seaway on unsteady loading. This also shows that the effect of the ship motions can dramatically increase the unsteady loading on the blades. Therefore, the effect of the ship motions due to operation in a seaway should be considered in any analysis of blade loading and in any fatigue analysis of the propeller blades or hub mechanism.

The results presented here for hull pitching generally agree with the same type of results presented in Reference 2 for a model of the FF-1088, which is a single screw transom stern configuration. For M_y, which is the largest measured moment component in both cases, the comparative results, presented as a fraction of the time-average value without hull pitching, are as follows:

---

*This simple analysis provides an upper bound to the dynamic pitching load, since the hull boundary above the propeller would tend to reduce the dynamic pitching induced upward tangential velocity relative to the propeller.

	DD-963 (Present Report)	FF-1088 (Reference 2)
Peak value, $\dot{\psi}\neq 0$	1.60	1.57
Peak value, $\dot{\psi}=0$	1.43	1.40
Peak value without pitching $\dot{\psi}=0$, $\psi=\psi_{CW}$	1.40	1.36
Maximum time-average value, $\dot{\psi}\neq 0$	1.10	1.03
Maximum time-average value, $\dot{\psi}=0$	1.05	1.04

The variation of the loading components with simulated time during the pitch cycle are also somewhat similar for these two configurations. The comparative results for M_y, presented as time in seconds following the point $\psi-\psi_{CW}=0$, $\dot{\psi}>0$ are as follows:

	DD-963 (Present Report)	FF-1088 (Reference 2)
Peak value, $\dot{\psi}\neq 0$	0.77	0.62
Peak value, $\dot{\psi}=0$	0.31	0.31
Maximum time-average values, $\dot{\psi}\neq 0$	0.20	0.72
Maximum time-average value, $\dot{\psi}=0$	0.31	0.31

ACCELERATION

The variation of all measured loading components with blade angular position for the quasi-steady simulated acceleration condition $\dot{V}=\dot{P}=\dot{n}=0$ (Conditions 7 through 11 in Table 3) is shown in Figures 20 and 21 for the hydrodynamic loads, and is shown in Figure 22 for the total (hydrodynamic, centrifugal, and gravitational) loads. The amplitudes and phases of the harmonics of these loading components are presented in Figure 23 for the hydrodynamic loads and in Figure 24 for the total loads. Appendix B presents tabulated values of the data in Figures 20 through 24. The values for each loading component are presented as decimal fractions of the time-average value of the corresponding loading component at the self propulsion condition (Condition 1 in Table 3). These average values for both hydrodynamic loads and total loads are presented in Table 8.

Figure 25 presents the Taylor wake fraction based on thrust $1-w_T$ and the Taylor wake fraction based on torque $1-w_Q$ as derived from the measured values of $\overline{F}_{x_H}$ and $\overline{M}_{x_H}$ and the open-water characteristics of the propeller (Figure 11). These data indicate that $(1-w_T)$ varies by only approximately 3 percent during the simulated acceleration. The value of $(1-w_Q)$ varies by only 1 percent for simulated time $t \geq 40$ seconds; however, the value of $(1-w_Q)$ varies substantially during the initial portion of the simulated acceleration ($t<40$ seconds).

Figures 20 and 22 show that for all measured hydrodynamic and total loading components, except F_{Z_H} which is small, the peak values, including variation with blade angular position occurred at the self propulsion condition. That is, for the acceleration condition simulated (see Figure 7 and Table 3), the propeller is not exposed to higher peak loads than those to which it is exposed during full-power steady-ahead operation.

In contrast to the peak loads, for most components the largest time-average loads per revolution occurred at the first experimental condition ($V=2.65$ knots, $n=10.21$ revolutions per second, $J=0.64$) during the simulated acceleration maneuver. The largest measured hydrodynamic force and moment components, F_{x_H} and M_{y_H}, yield $(\overline{F}_{x_{H,MAX}}/\overline{F}_{x_{H,SP}})=1.21$ and $(\overline{M}_{y_{H,MAX}}/\overline{M}_{y_{H,SP}})=$ 1.29, whereas for total loading $(\overline{F}_{x_{MAX}}/\overline{F}_{x_{SP}})=1.16$ and $(\overline{M}_{y_{MAX}}/\overline{M}_{y_{SP}})=1.21$. The conditions $(\overline{F}_{x_{H,MAX}}/\overline{F}_{x_{H,SP}}) > (\overline{F}_{x_{MAX}}/\overline{F}_{x_{SP}})$ and $(\overline{M}_{y_{H,MAX}}/\overline{M}_{y_{H,SP}}) >$ $(\overline{M}_{y_{MAX}}/\overline{M}_{y_{SP}})$ occur because the centrifugal and hydrodynamic components are additive for F_x and M_y (i.e., they have the same signs) and the hydrodynamic loads increase with decreasing rotational speed n, whereas the centrifugal loads decrease with decreasing n.

Higher time-average and peak loads than those shown in Figures 20 and 22 could, of course, be developed during acceleration maneuvers, depending on values of $\dot{v}$, $\dot{n}$, and $\dot{P}$.

Figure 21 shows the variation in the radial center of longitudinal force, $r_{F_{x_H}}$ and radial center of tangential force, $r_{F_{y_H}}$. These results show that the time-average radial centers of these force components vary

monotonically with advance coefficient over the range evaluated. As the advance coefficient based on thrust effective wake, $J_T=J_V(1-w_T)$ increases from 0.63 (at V=2.65 knots) to its design value of 1.14 (at V=6.52 knots), $\bar{r}_{F_{x_H}}$ decreases from 0.76R to 0.71R whereas $\bar{r}_{F_{y_H}}$ increases from 0.66R to 0.74R. This variation in $\bar{r}_{F_{x_H}}$ is the reason that $(\bar{F}_{x_{H,MAX}}/\bar{F}_{x_{H,SP}}) <$ $(\bar{M}_{y_{H,MAX}}/\bar{M}_{y_{H,SP}})$ as discussed in the preceeding paragraph.

For all loading components, the variation with blade angular position tended to be dominated by the first harmonic for all conditions throughout the simulated acceleration maneuver. For all conditions at which there was significant variation in loading with blade angular position, the maximum and minimum values for all components except F_z and M_z occurred for the blade spindle axis near θ=135 or 315 degrees (blade tip near θ=115 or 195 degrees). This suggests that the variation in loading with blade angular position is produced primarily by the circumferential variation of the tangential velocity in the propeller plane (see Figure 10). The angular variation of each loading component retained basically the same shape independent of speed and advance coefficient.

There was a dramatic reduction in the circumferential variation of all measured loading components with decreasing speed V and decreasing rotational speed n. Previous data have shown that for a given propeller in a given flow field, the circumferential variation in the hydrodynamic loading varies approximately as the product of ship speed V and rotational speed n; see Wereldsma.[33] Figure 26 presents results in a form which allows evaluation of how closely the measured unsteady loading varies with nV. The ordinate is the first harmonic of the components of hydrodynamic blade loading except F_{z_H}, which is very small, and the abscissa is nV. The data shown in Figure 26 indicate that the first harmonic of each of the presented hydrodynamic loading components is approximately proportional to nV.

---

[33]Wereldsma, R., "Tendencies of Marine Propeller Shaft Excitation," International Shipbuilding Progress, Vol. 19, No. 218, pp 328-332 (October 1972).

Figure 27 presents the variation of the time-average values per revolution and peak values of the various components of total blade loading for both quasi-steady simulated acceleration ($\dot{V}=\dot{n}=\dot{P}=0$) and unsteady simulated acceleration ($\dot{V}>0$, $\dot{n}=\dot{P}=0$).

There was only a small variation in the measured loading components between the quasi-steady simulated acceleration and the unsteady simulated acceleration. For all components except M_Z, the largest variation between the results from the two types of simulation expressed as a decimal fraction of the corresponding time-average value at the self-propulsion point was 0.05 for the peak values and 0.02 for the time-average value per revolution. The corresponding variations for M_Z were no greater than 0.06 for the peak values and 0.05 for the time-average value per revolution.

The variation in the results between the two types of simulation appeared to be essentially random. This suggests that these deviations are some measure of the experimental accuracy and do not represent any systematic trends arising from the difference in $\dot{V}$ between the two types of simulation.

Data for the quasi-steady simulation were recorded and averaged for a minimum of 200 propeller revolutions, whereas data presented for the unsteady runs represent an average of only five revolutions. Further, the steady experimental conditions which were set during the quasi-steady simulation allow the values of V and n to be controlled more precisely than during the unsteady runs; however, the average of the five values of V and n during the unsteady runs for which data are presented was generally within one percent of the target values.

The results presented in this section for a simulated acceleration maneuver follow trends similar to those in Reference 2 for a simulated crash-forward maneuver on a model of the FF-1088. Both sets of data show the following:

1. The values of $(1-w_T)$ and $(1-w_Q)$ do not vary substantially except during the initial stages of the acceleration or crash-forward maneuver.

2. The variation of all loading components with blade angular position was dominated by the first harmonic throughout the simulated maneuver.

3. The amplitude of the first harmonic of all loading components varied essentially as nV.

4. The acceleration of the hull did not have a significant effect on the loads; i.e., the loads for quasi-steady acceleration $\dot{V}=0$ and unsteady acceleration $\dot{V}>0$ were not significantly different.

The ratios of either the peak or time-average loads during the acceleration (or crash-forward) maneuver to the time-average loads at the self-propulsion point do not agree closely for the results in the present report (DD-963 Class) and Reference 2 (FF-1088). This difference is to be expected since these ratios are very sensitive to the value of $\dot{V}$, $\dot{n}$, and $\dot{P}$ for the simulated maneuvers, which are quite different for these two cases. The largest moment component for both cases M_y, gives $M_{y_{peak}}/\overline{M}_{y_{SP}} = 1.40$ from the present report and 1.51 from Reference 2. The results from the present report show $\overline{M}_{y_{MAX}}/\overline{M}_{y_{SP}} = 1.21$ whereas the results from Reference 2 yield $\overline{M}_{y_{MAX}}/\overline{M}_{y_{SP}} = 1.35$.

CORRELATION WITH FULL-SCALE DATA AND THEORY

For operation near the self-propulsion point (Condition 1 in Table 3), correlation was made between the model experimental loads obtained in the present investigation, bending moments deduced from strains measured on the corresponding full-scale propeller, and analytical calculations.

These comparisons were made for $M_{0.3}$ and $M_{0.4}$ which were calculated from the three measured forces and three measured moments. As discussed in the section on experimental results, $M_{0.3}$ is defined as the bending moment applied on the spindle axis about the axis intersecting the spindle axis at r=0.3R and parallel to the expanded pitch line at r=0.3R. The $M_{0.3}$ vector as defined by the conventional right-hand rule for a right-hand propeller (left-hand rule for a left-hand propeller) intersects the plane normal to the propeller axis at the angle $\phi_{0.3} = \tan^{-1}(P_{0.3}/(0.3\pi D))$ and is directed so that a positive $M_{0.3}$ puts the face (pressure side) of the blade in tension. The component $M_{0.4}$ is defined in a manner analogous to $M_{0.3}$, except it is referred to r=0.4R.

The full-scale data used for correlation are preliminary values of strains ε measured* at several chordwise stations at r=0.35R and r=0.45R on both sides of the blade on the DD-963 CP propeller. Both time-average strains per revolution and variation of strain with blade angular position were recorded during full-power stready-ahead operation. By interpolation, values of radial strain at the spindle axis at r=0.4R were obtained. Assuming that the variation in radial strain is proportional to the variation in total (hydrodynamic, centrifugal, and gravitational) bending moment; i.e., that $(\varepsilon_{r0.4_{MAX}}/\bar{\varepsilon}_{r0.4}) = (M_{0.4_{MAX}}/\bar{M}_{0.4})$, these full-scale data indicate that $(M_{0.4_{MAX}}/\bar{M}_{0.4}) = 1.48$. From the model data $(M_{0.3_{MAX}}/\bar{M}_{0.3}) = 1.43$ and $(M_{0.4_{MAX}}/\bar{M}_{0.4}) = 1.56$. A cursory evaluation of the variation of the full scale strain with blade angular position indicates that it follows trends similar to the bending moment determined from the model experiments. The correlation with full scale data presented here is preliminary; a more thorough correlation with the full scale data will be undertaken when analysis of the full scale data is complete.

Theoretical calculations of hydrodynamic loads were made by using the method of Tsakonas et al,[25,34] which is based on unsteady lifting-surface theory and the method of McCarthy,[26] a quasi-steady technique which utilizes the open-water characteristics of the propeller. Although the method of McCarthy is a simple quasi-steady technique, it was judged that this method should be suitable to the cases under consideration in this report because the dominant unsteady loading occurs at a low reduced frequency and the dominant first harmonic of the wake is in phase radially

---

*The full-scale measurements were conducted by personnel in DTNSRDC Code 1962 under the direction of G.P. Antonides. The results presented here are preliminary, and thorough analysis of the data is continuing. The details of this full-scale trial will be reported in a future DTNSRDC report.

[34]Tsakonas, S. et al, "Documentation of a Computer Program for the Pressure Distribution, Forces and Moments on Ship Propellers in Hull Wakes," (In Four Volumes), Stevens Institute of Technology, Davidson Laboratory Report SIT-DL-76-1863 (January 1976). Revised April 1977.

(see Figure 10 and Appendix A). These calculations were made for Condition 1 in Table 3 using the wake measured in the plane of the propeller both with and without the downstream dynamometer boat in place (Figure 10 and Appendix A), and with the mean velocity through the propeller determined from thrust identity used as the reference velocity.

The use of the speed of advance based on thrust effective wake, $V_A=V(1-w_T)$, as the reference speed in these calculations is consistent with the use of this velocity to correct the time-average loads for the effect of the dynamometer boat as discussed in the section on experimental results. Tsakonas et al[34] recommend using the ship speed as the reference velocity, which is equivalent to using $(1-w_T)=1.0$; however, this recommendation was not followed here because the flow does not pass through the propeller at the ship speed. To evaluate the sensitivity of the procedure of Tsaknoas et al,[25,34] to the reference speed, calculations were performed for the first harmonic using the thrust effective wake $(1-w_T)$ and the volume mean wake determined from the wake surveys $(1-w_{VM})$. These calculations showed the following:

Wake without dynamometer boat

$$\frac{M_{0.3_1} \text{ (using } (1-w_T) = 1.02)}{M_{0.3_1} \text{ (using } (1-w_{VM}) = 1.06)} = 0.99$$

$$\phi_{M0.3_1}(1-w_T) - \phi_{M0.3_1}(1-w_{VM}) = -0.3 \text{ degrees}$$

Wake with dynamometer boat

$$\frac{M_{0.3_1} \text{ (using } (1-w_T) = 0.97)}{M_{0.3_1} \text{ (using } (1-w_{VM}) = 0.93)} = 1.02$$

$$\phi_{M0.3_1}(1-w_T) - \phi_{M0.3_1}(1-w_{VM}) = 0.5 \text{ degrees}$$

Therefore, the calculated unsteady loads using the method of Tsakonas et al,[25,34] are not sensitive to the reference speed over the range of concern in the present case.

For the method of Tsakonas et al,[25,34] calculations were conducted for the first ten harmonics of the wake.* The "normal" components of wake harmonics, as required by this method, were defined as the wake harmonics normal to the chord line of the blade section at the local radius rather than normal to the advance angle at the local radius as recommended by Tsakonas et al.[34,35] With the wake harmonics resolved normal to the blade chord, this method apparently considers both the unsteady flow normal to the resultant inflow and an approximation to the unsteady flow parallel to the resultant inflow.

The quasi-steady calculations are based on the circumferential variation of the wakes measured at the 0.7 radial station. These calculations were made at 10-degree increments of blade angular position θ. It is assumed that the radial centers of the unsteady thrust and tangential force are at $r/R=0.70$ for all blade angular positions.

Figure 28 presents values of $M_{0.3_H}$ and $M_{0.4_H}$ with and without the downstream dynamometer boat, calculated with the methods of Tsakonas et al[25,34] and McCarthy.[26] Based on these calculated results it appears that the dynamometer boat does not have a significant influence on the circumferential variation of the blade loads.

Figures 29 and 30 present the variation with blade angular position and the first ten harmonics of $M_{0.3_H}$ and $M_{0.4_H}$ from the model experiments and analytical calculations. All data are nondimensionalized on the same quantity, i.e., the time-average bending moment determined from the model experiments and corrected for the downstream body as discussed in the section on experimental results. This comparison indicated that the experimental unsteady hydrodynamic bending moments were substantially higher than the calculated results. A typical comparison is as follows:

---

*These calculations were made by using the computer program developed by the Davidson Laboratory including refinements made through April 1977. None of the refinements made since December 1975 influence the calculated unsteady loads presented in this report. Therefore, this calculation procedure is the same as that used in Reference 2 for calculating the unsteady bending moments on the propeller on the FF-1088.

[35] Tsakonas, S. et al, "Correlation and Application of an Unsteady Flow Theory for Propeller Forces," Transactions of the Society of Naval Architects and Marine Engineers, Vol. 75, pp 158-193 (1967).

Prediction Method	$\dfrac{M_{0.3_{H,MAX}} - \overline{M}_{0.3_H}}{\overline{M}_{0.3_H}}$ (experiment)	$\dfrac{M_{0.4_{H,MAX}} - \overline{M}_{0.4_H}}{\overline{M}_{0.4_H}}$ (experiment)
Model Experiment	0.36	0.36
Quasi-Steady Procedure[26]	0.25	0.24
Unsteady Procedure[25]	0.20	0.19

For this typical comparison the experimental result is approximately 47 percent higher than the quasi-steady prediction and approximately 85 percent higher than the unsteady prediction.

The circumferential variations in the model experimental results of other components of blade loading F_{x_H}, F_{y_H}, M_{x_H}, and M_{y_H} were larger than the values calculated by the two indicated procedures by approximately the same ratio as shown for $M_{0.3_H}$ and $M_{0.4_H}$. These comparisons are not shown.

Previous investigators have compared experimental unsteady forces and moments on a single blade of various propellers in inclined flow with forces and moments calculated by a quasi-steady procedure similar to that described by McCarthy.[26] These experimental loads were obtained by direct measurement of unsteady forces and moments on a single blade (References 2, 3, 17, 18, and 19) or were deduced from measured steady transverse forces and moments along axes fixed relative to the flow, i.e., not rotating with the propeller (Reference 36). References 2, 3, 17, 18, 19, and 36 all show that for noncavitating conditions, the experimental unsteady blade loading was from 1.5 to 2.0 times as large as the values calculated by the quasi-steady method. This agrees with the results of the present investigation; see Figures 29 and 30.

---

[36] Gutsche, F., "The Study of Ships' Propellers in Oblique Flow," Defence Research Information Centre Translation No. 4306, Copyright Controller: Her Majesties Stationary Office, London, England, October 1975; English Translation of "Untersuchung von Schiffsschrauben in schrager Anstromung," Schiffbauforschung, Vol. 3, No. 3/4, pp 97-102 (1964).

Preliminary results from blade loading experiments[37] conducted in idealized flows indicate that:

1. The unsteady blade loads in either axial or tangential wakes are not influenced by the presence of a nearby boundary above the propeller.

2. In inclined flow without an upstream hull, the experimental unsteady loading near the design advance coefficient is nearly two times as large as that calculated by the method of Tsakonas et al,[25,34] and approximately 80 percent larger than that calculated by the method of McCarthy.[26]

3. In an axial wake with a dominant first harmonic of blade angular position which was generated by upstream wire grid screens with zero shaft angle, the unsteady loading near the design advance coefficient is within approximately 15 percent of the values calculated by the methods of Tsakonas et al,[25,34] and McCarthy.[26] This is in agreement with previous correlations with the method of Tsakonas et al for unsteady shaft (bearing) forces and moments for operation in axial wakes.[*,12]

These results indicate that the large discrepancy between the experimental and calculated unsteady bending moments presented in the current report appear to be due to the inability of the present theories to properly account for all important characteristics of the flow field for operation in inclined flow. All available procedures, including the unsteady theory of Tsakonas et al[25,34] and the quasi-steady procedure of McCarthy,[26] implicitly assumed that the propeller slipstream follows the propeller axis rather than the direction of the effective velocity into the propeller which is at an angle to the propeller axis in inclined flow. It is speculated that this failure to consider the true direction of the slipstream is the major factor in the analytical underprediction of the

---

*The results in Reference 12 were at substantially higher reduced frequency than the results in the present study; therefore, the quasi-steady procedure of McCarthy over-predicted the unsteady loads in Reference 12.

[37]Boswell, R.J. and S.D. Jessup, "Experimental Determination of Periodic Propeller Blade Loads in a Towing Tank," Presented to the 18th American Towing Tank Conference, U.S. Naval Academy, Annapolis, Maryland (August 1977).

unsteady blade loads in inclined flow. Numerical computations to check this hypothesis are planned.

SUMMARY AND CONCLUSIONS

Experiments were described in which the mean and unsteady loads, including hydrodynamic, centrifugal, and gravitational loads, were measured on a single blade of a model of a CP propeller on the DD-963 Class Destroyer. The experiments were conducted behind a model of the DD-963 hull under steady-ahead operation, hull pitching motions, and simulated acceleration maneuvers. The discussion of experimental techniques includes a description of the dynamometer and data analysis system. The results are summarized as follows:

1. For all significant loading components, except for radial force, the loads are predominantly of hydrodynamic origin.

2. The circumferential variations of all measured components of hydrodynamic and total blade loading are primarily a first harmonic, with maximum and minimum values occurring near the blade angular position which is 25 degrees past the position at which a radial line from the propeller axis to the tip is horizontal.

3. For steady-ahead operation:

    a. The maximum values and peak-to-peak circumferential variations for measured hydrodynamic forces and bending moments were up to approximately 1.43 and 0.91 of the time-average values, respectively.

    b. The maximum values and the peak-to-peak circumferential variations for measured total forces and bending moments were up to approximately 1.41 and 0.88 of the time-average values, respectively.

    c. The model results for circumferential variation of bending moments about the nose-tail lines of the 0.3 and 0.4 radii agreed fairly well with loads deduced from strain measurements on the full-scale propeller, but they were larger than theoretically calculated values.

4. For simulated hull pitching (maximum pitch angle of 1.85 degrees):

a. The maximum values of measured total forces and bending moments increased over the corresponding values without hull pitch by 5 percent for quasi-steady simulation and by 23 percent for unsteady simulation with model pitching frequency equal to 0.8 hertz (full scale equivalent frequency is 0.16 hertz).

b. The peak-to-peak circumferential variation of the measured total forces and bending moments increased over the corresponding values without hull pitch by approximately 5 percent for quasi-steady simulation and by approximately 50 percent for unsteady simulation with model pitching frequency equal to 0.8 hertz. Therefore, any quasi-steady simulation of ship motions is completely inadequate for estimating the effect of ship motions on unsteady propeller blade loading.

5. For the simulated acceleration maneuver:

a. The dominant first harmonic of the measured hydrodynamic forces and bending moments varied in a nearly linear manner with the product of ship speed and propeller rotational speed.

b. The acceleration of the hull did not have a significant effect on the measured loads. Therefore, propeller blade loading during an acceleration maneuver can be adequately estimated by quasi-steady experiments.

c. The maximum time-average values of measured forces and bending moments per revolution were in the range of 1.21 to 1.29 of the time-average values during full-power steady-ahead operation for hydrodynamic loads, and in the range 1.16 to 1.21 of the time-average values during full-power steady-ahead operation for total loads.

d. The simulated acceleration condition did not expose the propeller to higher peak loads than those to which it is exposed during full power steady-ahead operation. However, these loads are very sensitive to the maneuver simulated and substantially higher peak loads could be developed during other acceleration maneuvers.

e. Except for the initial portion of the simulated acceleration maneuver, the Taylor wake fractions were within three percent of their values at the self propulsion point.

All of the results presented here on a model of the DD-963 Class Destroyer follow close to previously reported results of similar experiments on a model of the FF-1088.

ACKNOWLEDGEMENTS

The authors are indebted to many members of the staff of the David W. Taylor Naval Ship Research and Development Center. Special appreciation is extended to Mr. George Gilbert for the design modifications of the experimental apparatus, to Mr. Michael Jeffers for development of the online data analysis system, to Mr. John Gordon for development of electronic and mechanical systems for the experiment, and to Mr. Jack Diskin for assistance in data analysis and analytical calculations.

APPENDIX A

DETAILS OF WAKES*

Tables 9 and 10 present the velocity component ratios and the harmonic content of the wakes in the plane of the propeller, both with and without the downstream dynamometer boat. The data at even radial stations were obtained by interpolation and extrapolation of the measured data as described in Reference 38.

---

*All data presented in Appendix A were obtained from wake surveys conducted by R.F. Roddy, DTNSRDC Code 1524. Further details of these wake surveys will be presented in a future DTNSRDC report.

[38] Cheng, H.M., "Analysis of Wake Survey of Ship Models - Computer Program AML Problem No. 840-219F," David Taylor Model Basin Report 1804, March 1964.

Preceding Page Blank - NOT FILMED

APPENDIX B

DETAILED EXPERIMENTAL RESULTS

Table 11 presents detailed experimental results, including variation with blade angular position and harmonic analyses, for steady-ahead operation at V=6.52 knots, n=14.08 rev/sec. The data in Table 11 are tabulated values of the data presented in Figures 12, 13, 14, 16, 17, and 18.

Tables 12 to 15 present detailed experimental results including variation with blade angular position and harmonic analyses, for the quasi-steady acceleration conditions. The data in Tables 12 to 15 are tabulated values of the data presented in Figures 20, 22, 23, and 24.

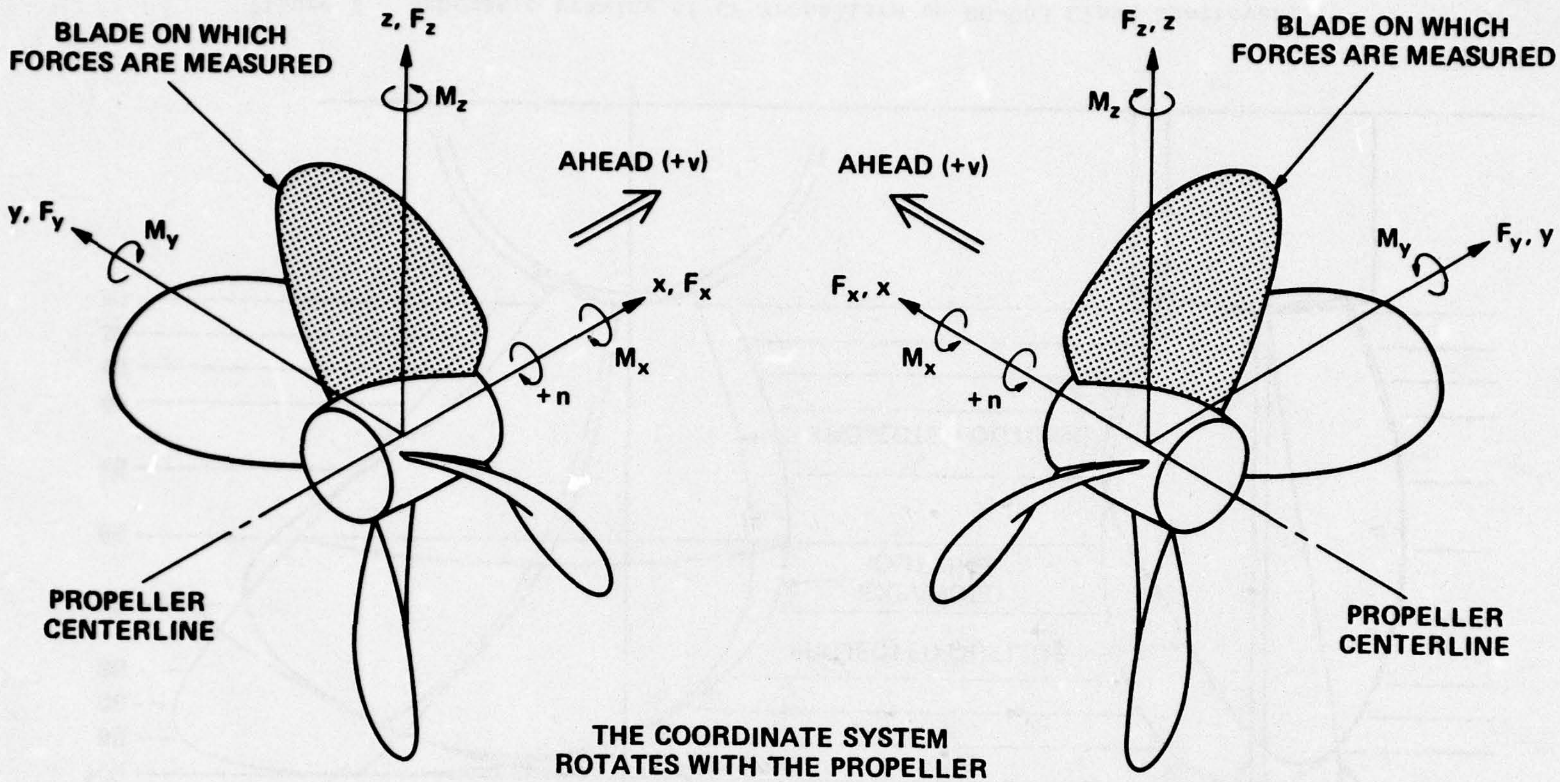

Figure 1a - Equivalent Coordinate System for Right Hand Propeller

Figure 1b - Coordinate System for Left Hand Propeller as Used in Experiment

Figure 1 - Components of Blade Loading

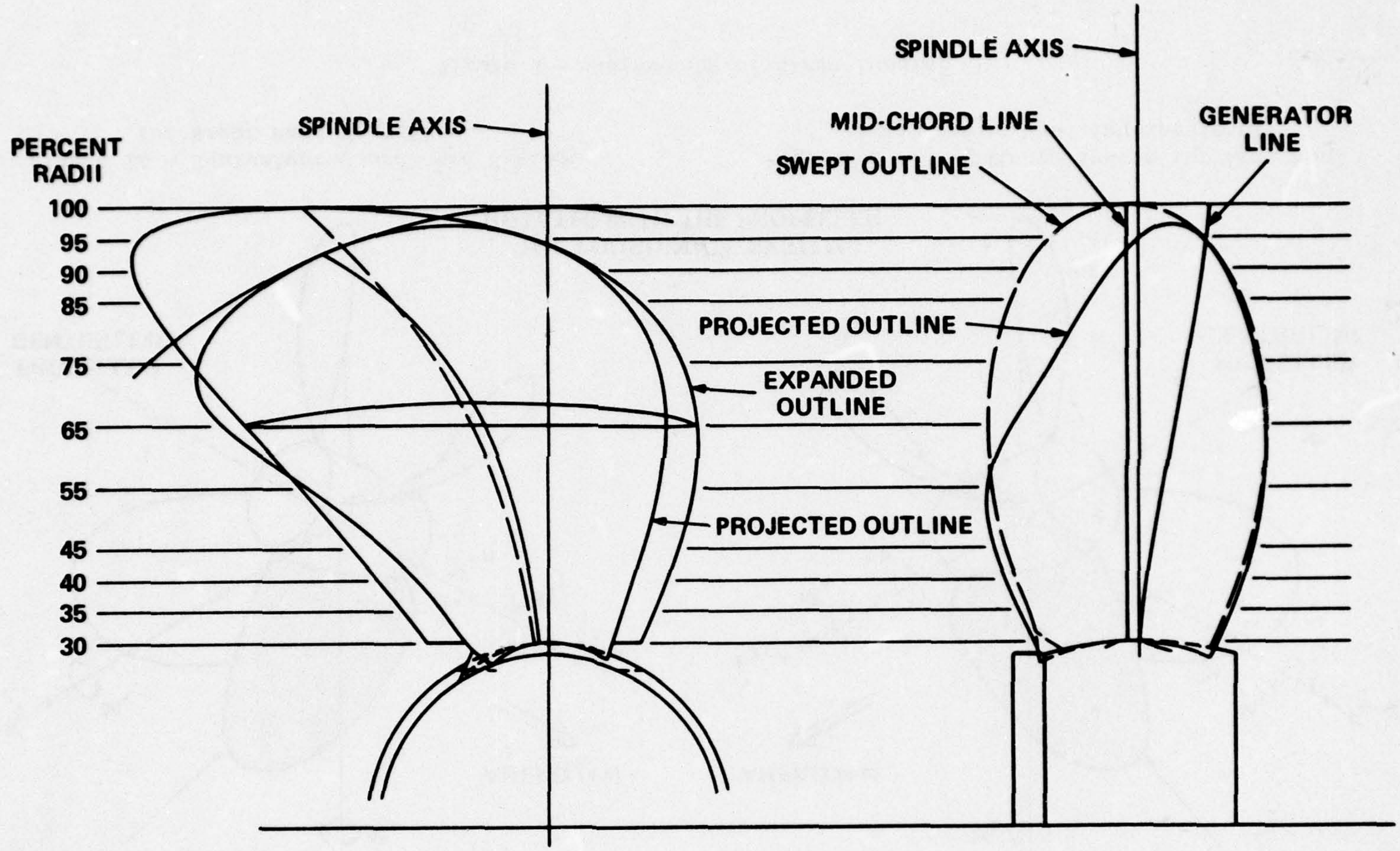

Figure 2 - Schematic Drawing of CP Propellers on DD-963 Class Destroyer; DTNSRDC Model Propellers 4660 and 4661

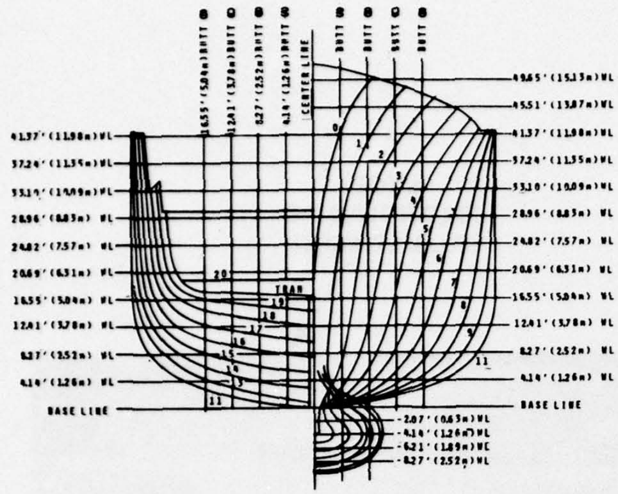

	SHIP	MODEL
LENGTH, AT LOAD WATERLINE	530.2 FEET	21.359 FEET
BEAM	55.0 FEET	2.216 FEET
DRAFT	19.5 FEET	0.786 FEET
TRIM	EVEN KEEL	EVEN KEEL
DISPLACEMENT	7800 TONS, S.W.	1111 POUNDS, F.W.
WETTED SURFACE	33150 SQUARE FEET	53.8 SQUARE FEET
PROPELLER DIAMETER	17.0 FEET	0.685 FEET

APPENDAGES: SHAFTS, MAIN STRUTS, INTERMEDIATE STRUTS, ℄ SKEG, BILGE KEELS, SONAR DOME

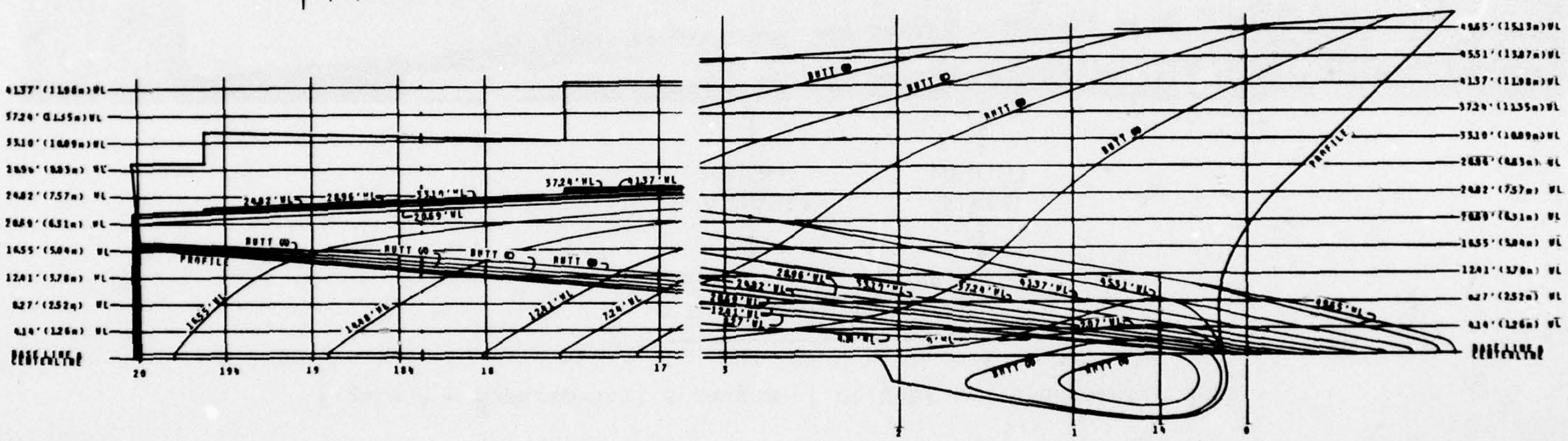

Figure 3 - Ship and Model Particulars

Figure 4 - Experimental Arrangement of Hull and Dynamometer Boat

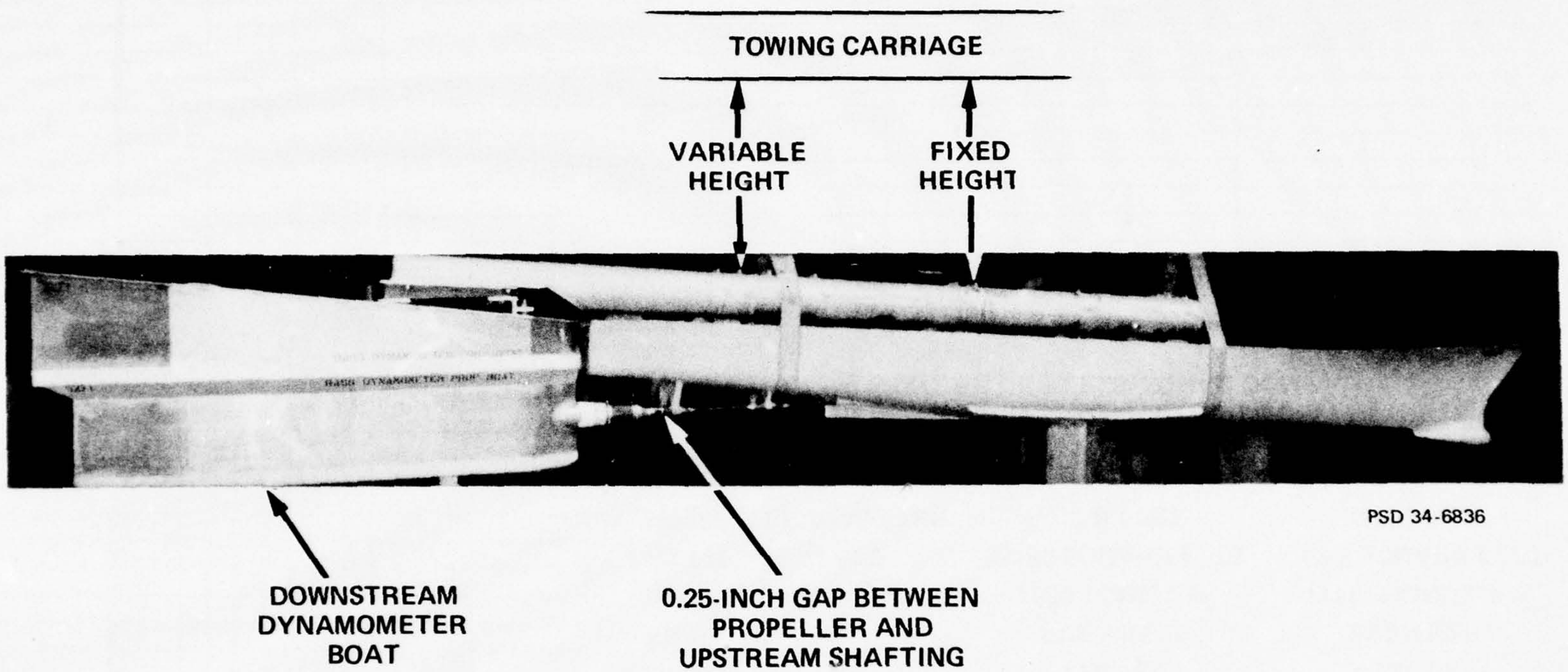

Figure 4a - Overall View

Figure 4 (Continued)

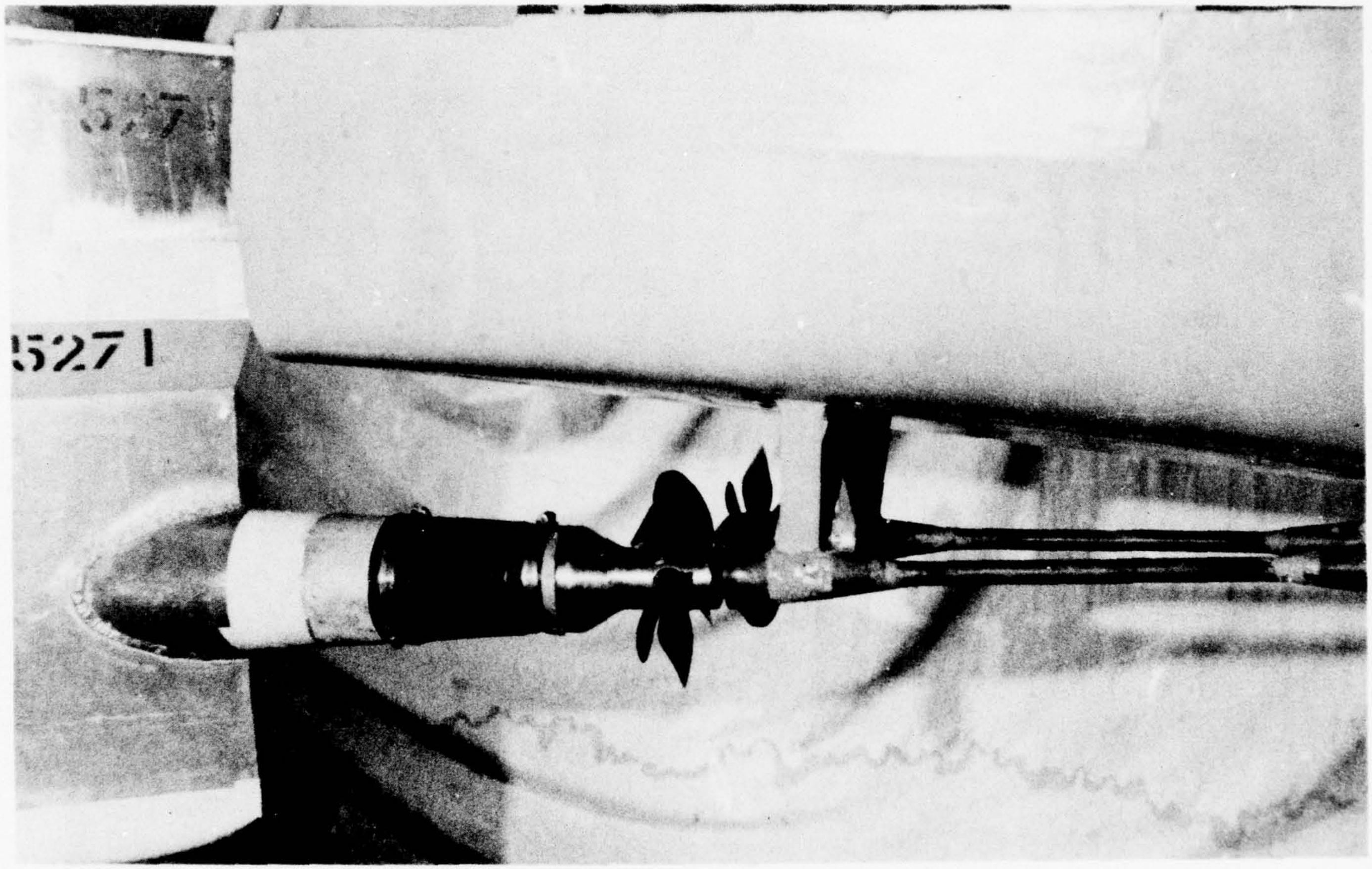

Figure 4b - Closeup of Propellers

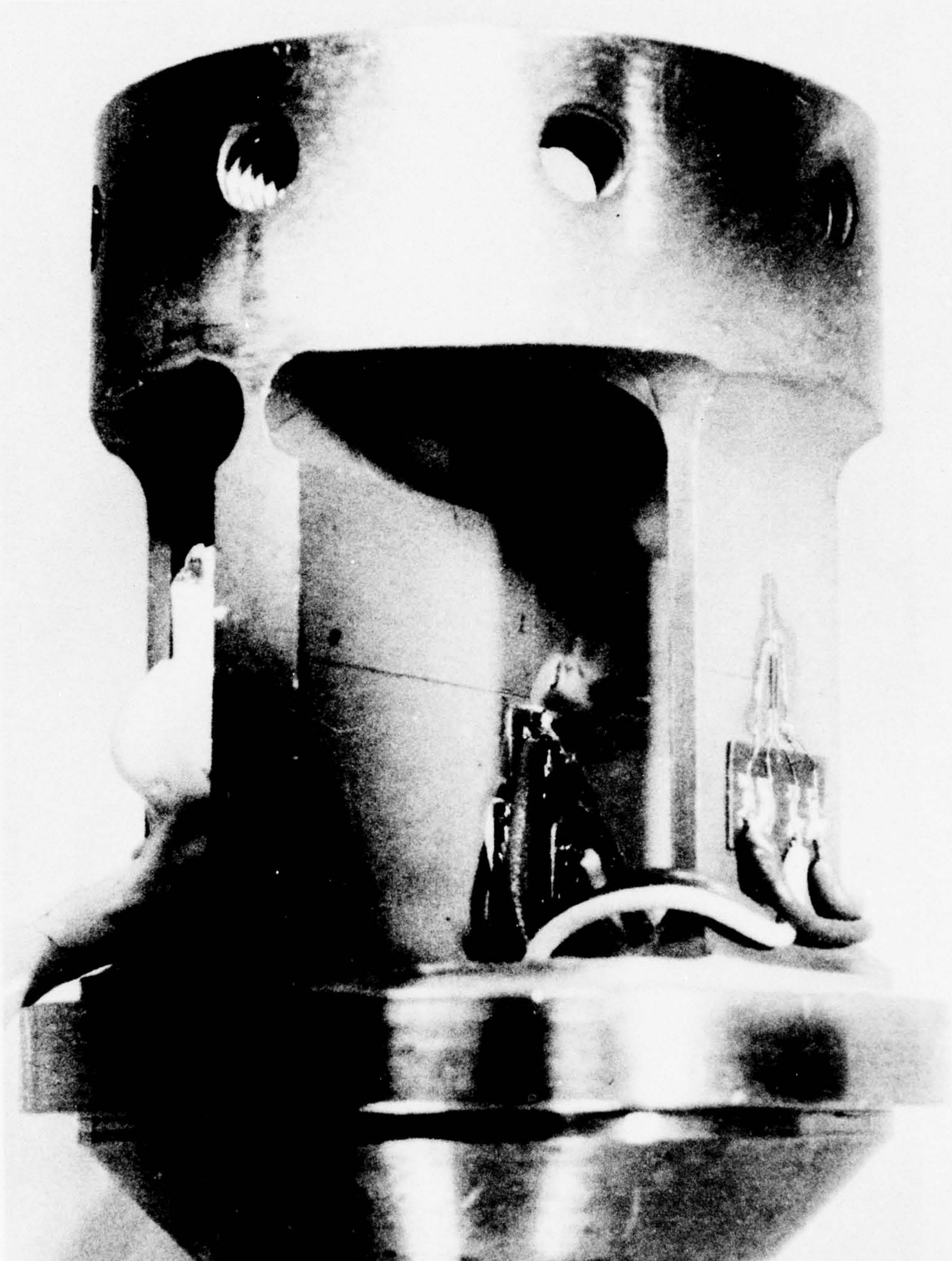

Figure 5 - Typical Strain-Gaged Flexure

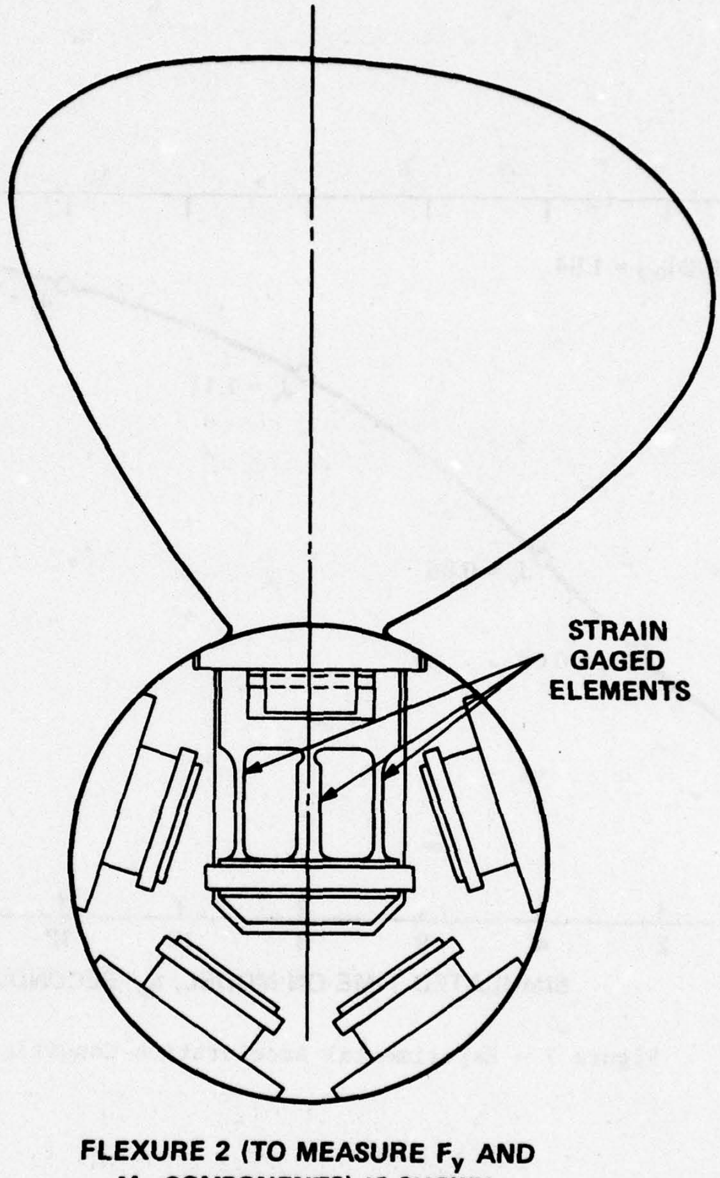

Figure 6 - Arrangement of Typical Flexure in Hub

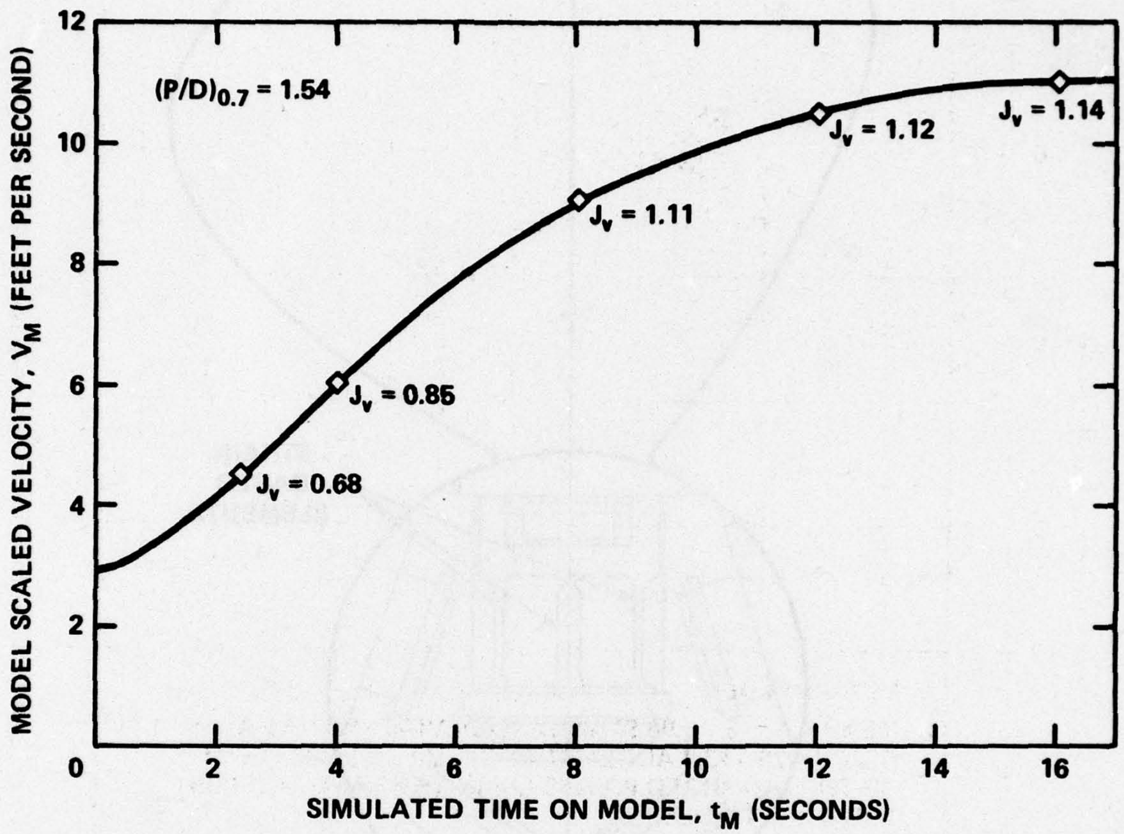

Figure 7 - Experimental Acceleration Conditions

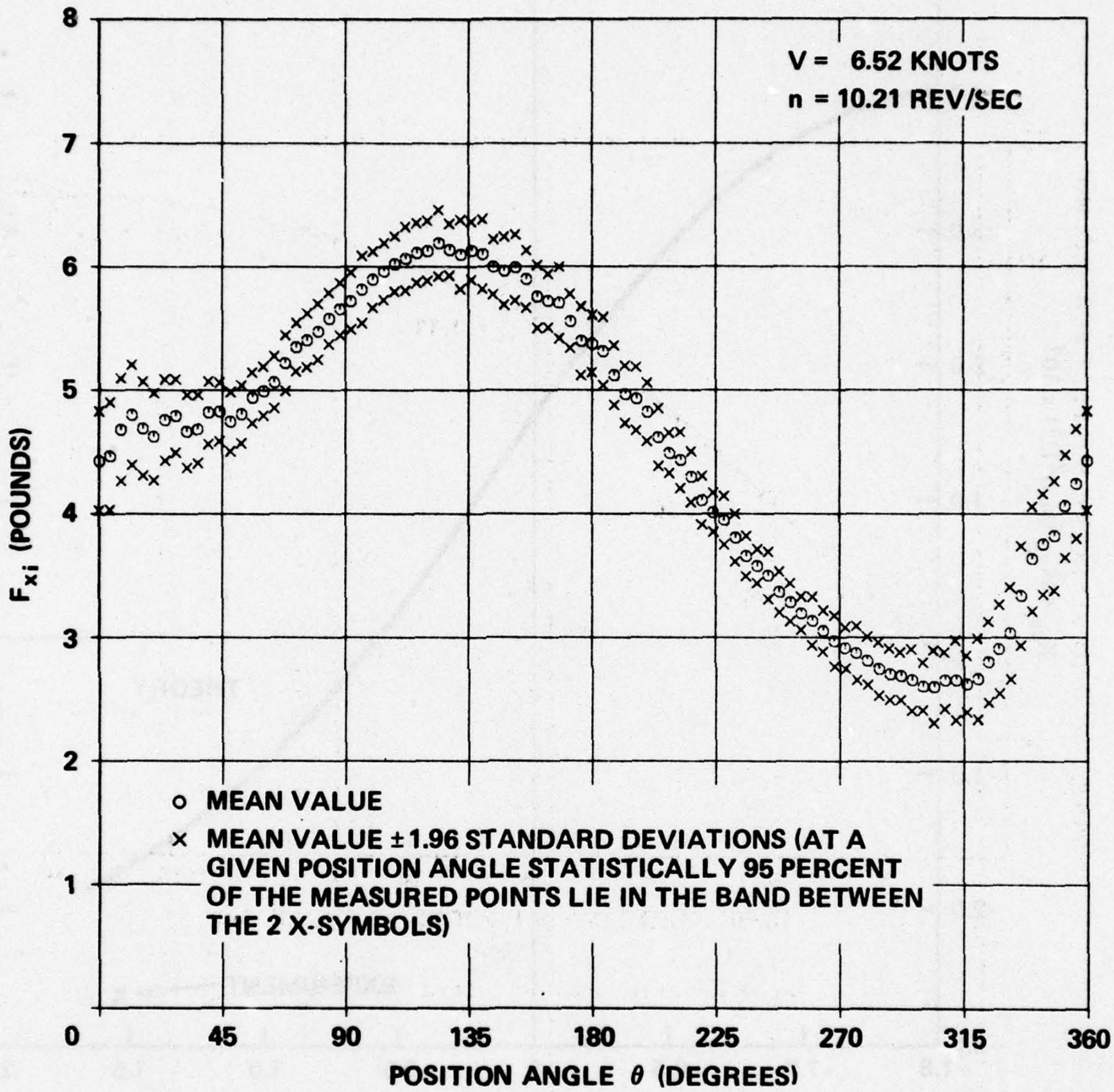

Figure 8 - Experimental Data Showing Plus and Minus Two Standard Deviations on Measured Values of F_x

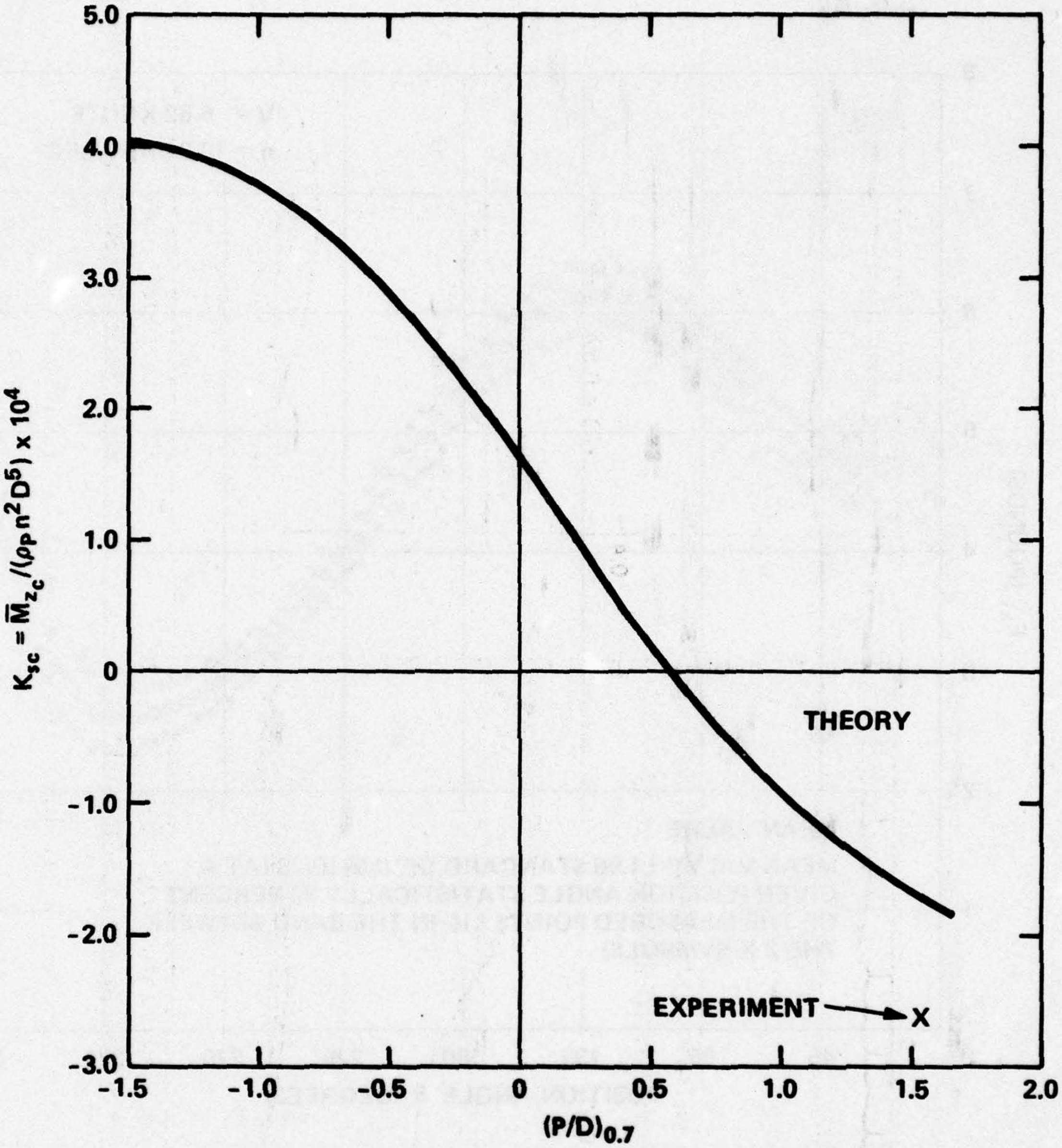

Figure 9 - Correlation of Theory and Experiment for Time Average Centrifugal Spindle Torque

Figure 10 - Distribution of Wake in Propeller Disk

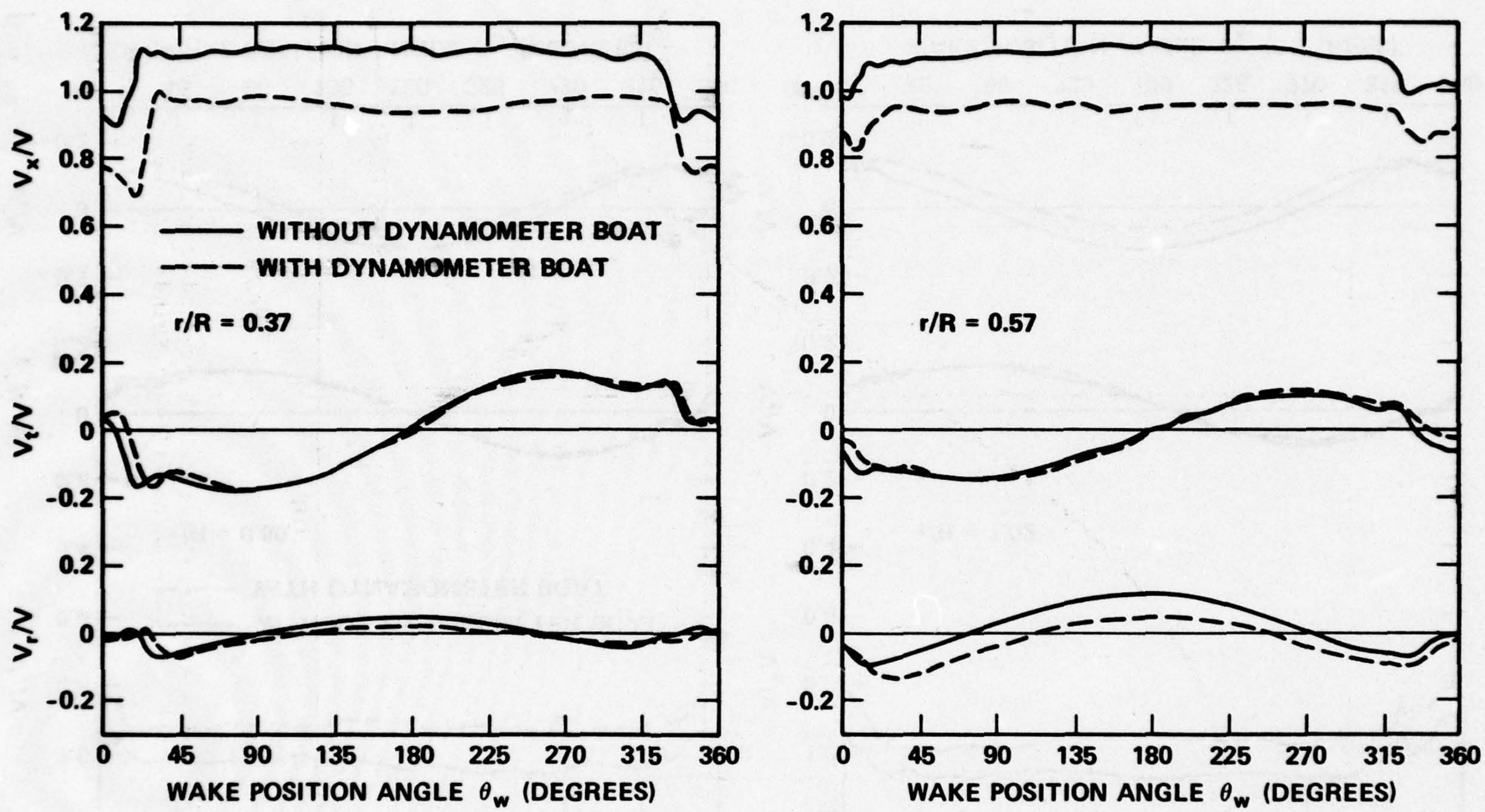

Figure 10a - Circumferential Distributions

Figure 10 (Continued)

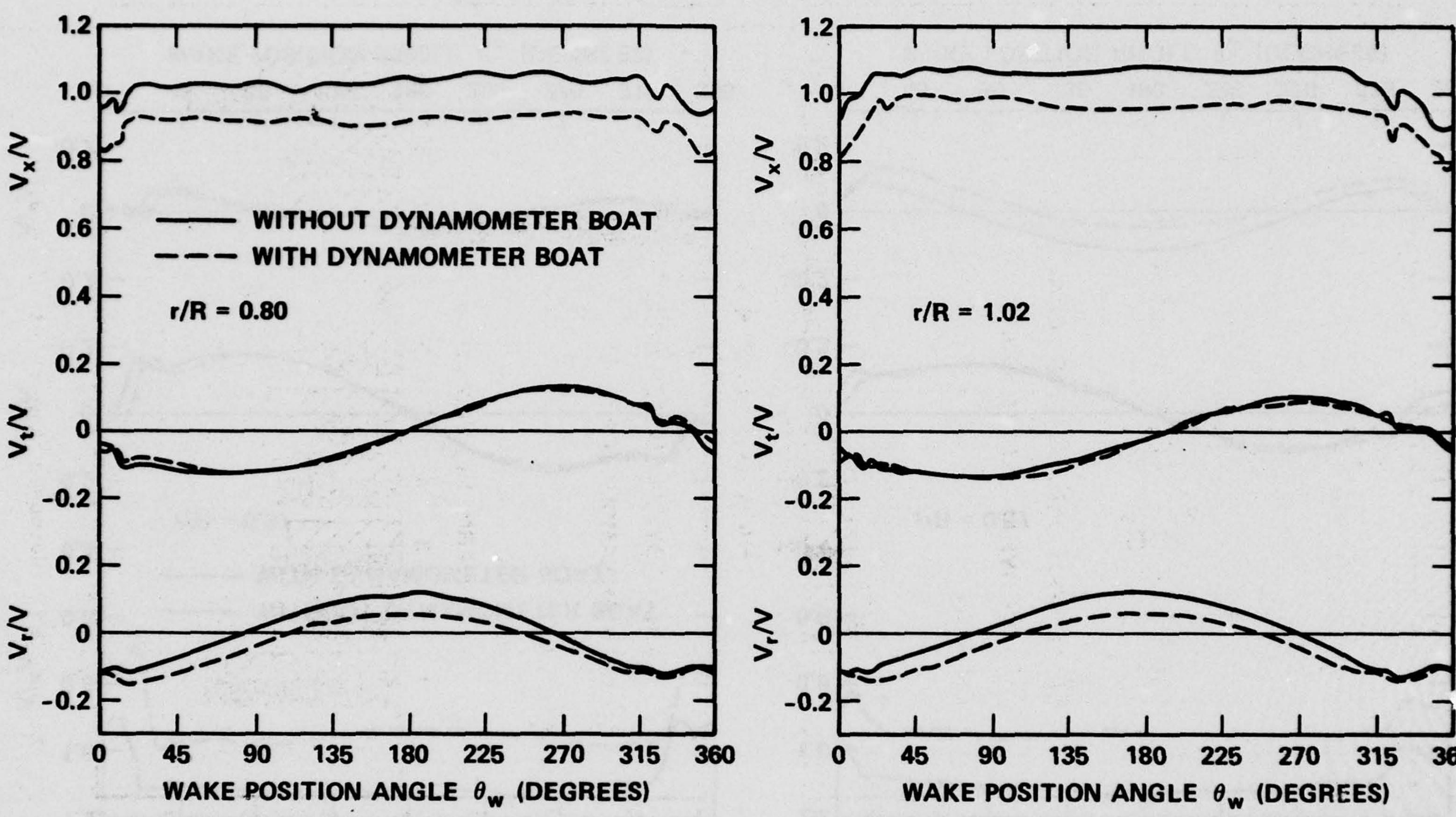

Figure 10a (Continued)

Figure 10 (Continued)

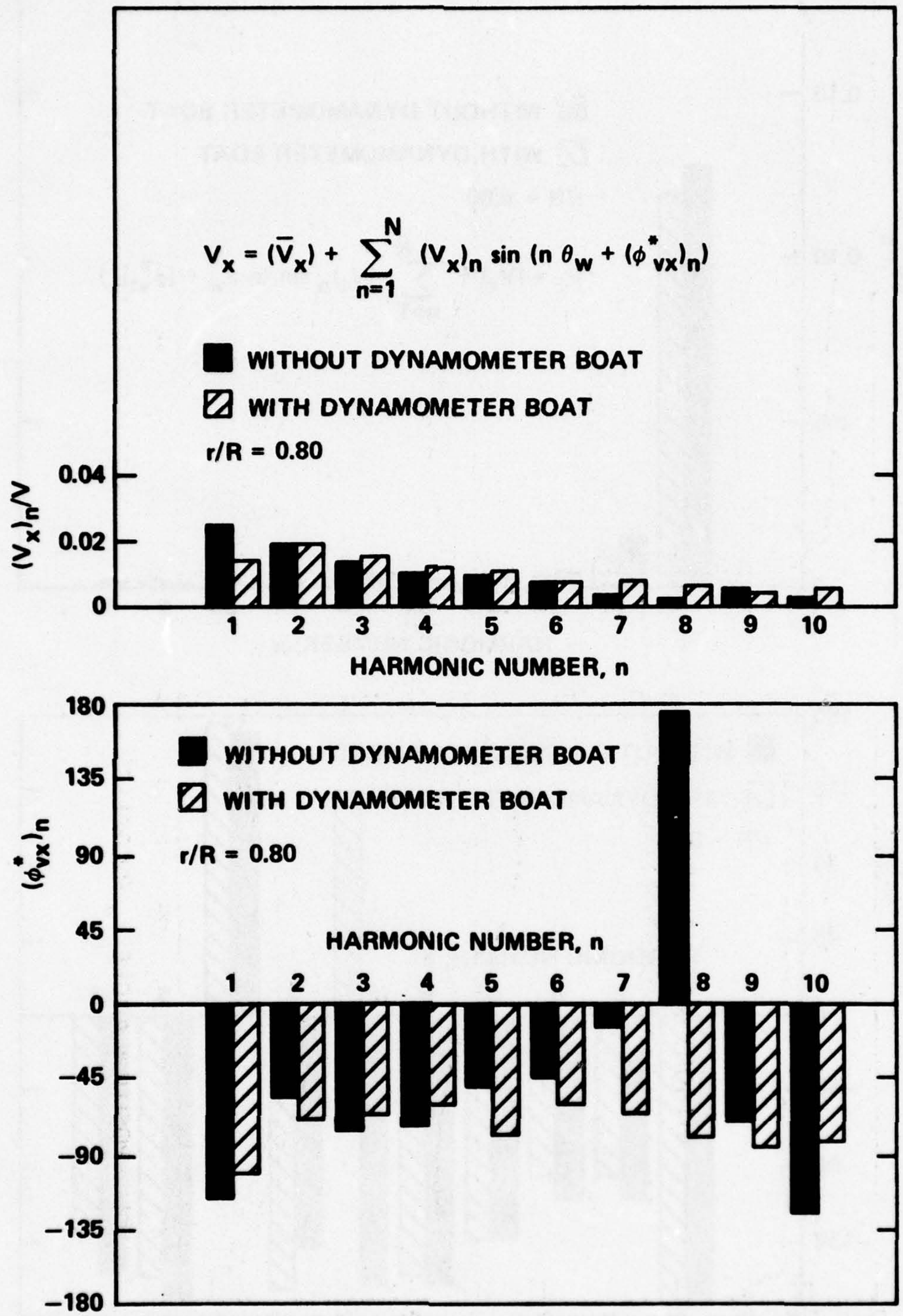

Figure 10b - Harmonic Content at r/R = 0.80

Figure 10 (Continued)

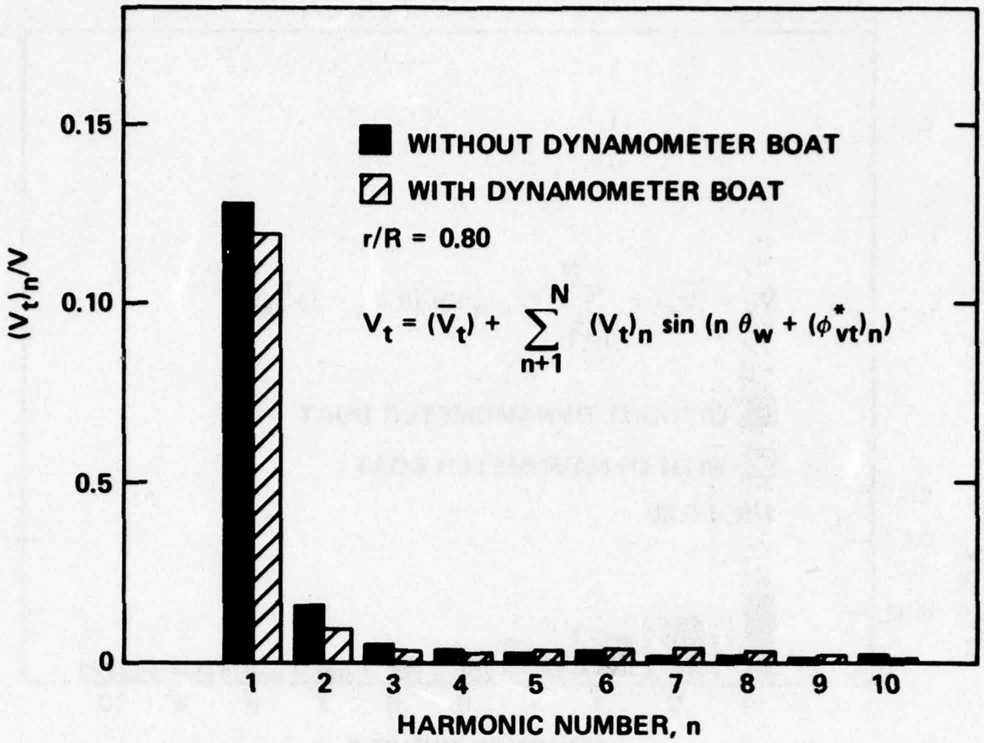

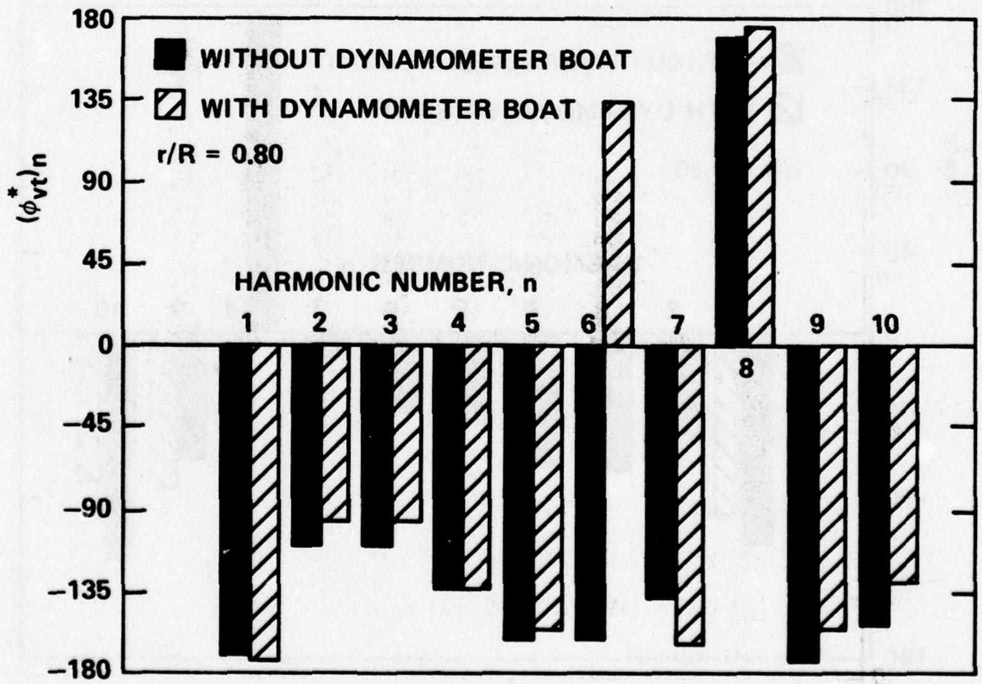

Figure 10b (Continued)

Figure 10 (Continued)

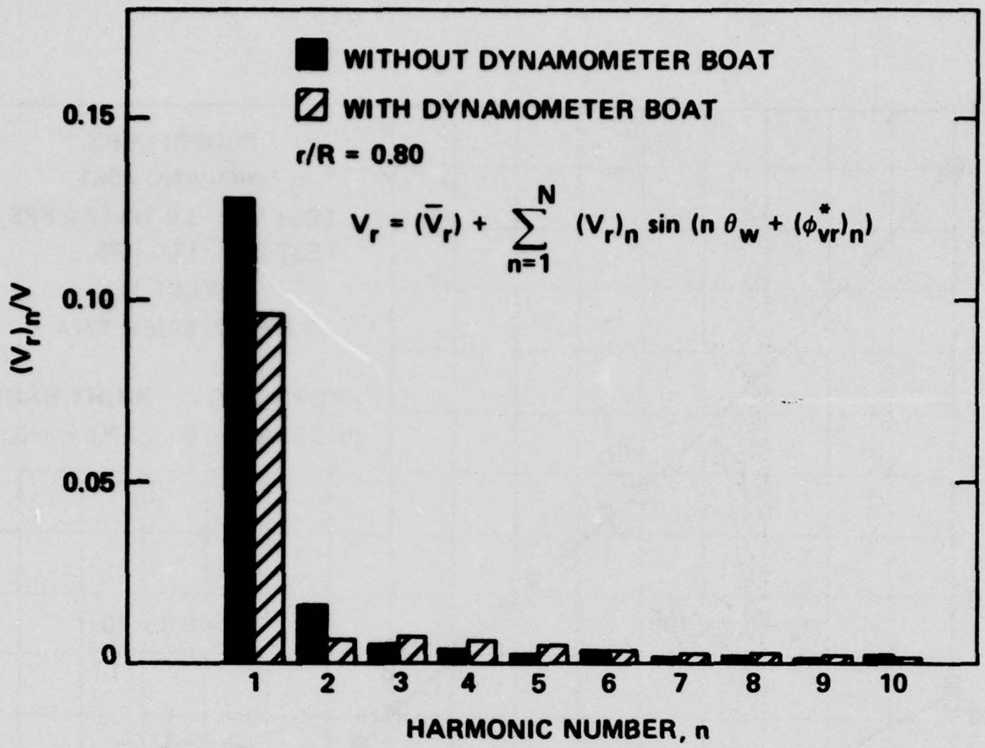

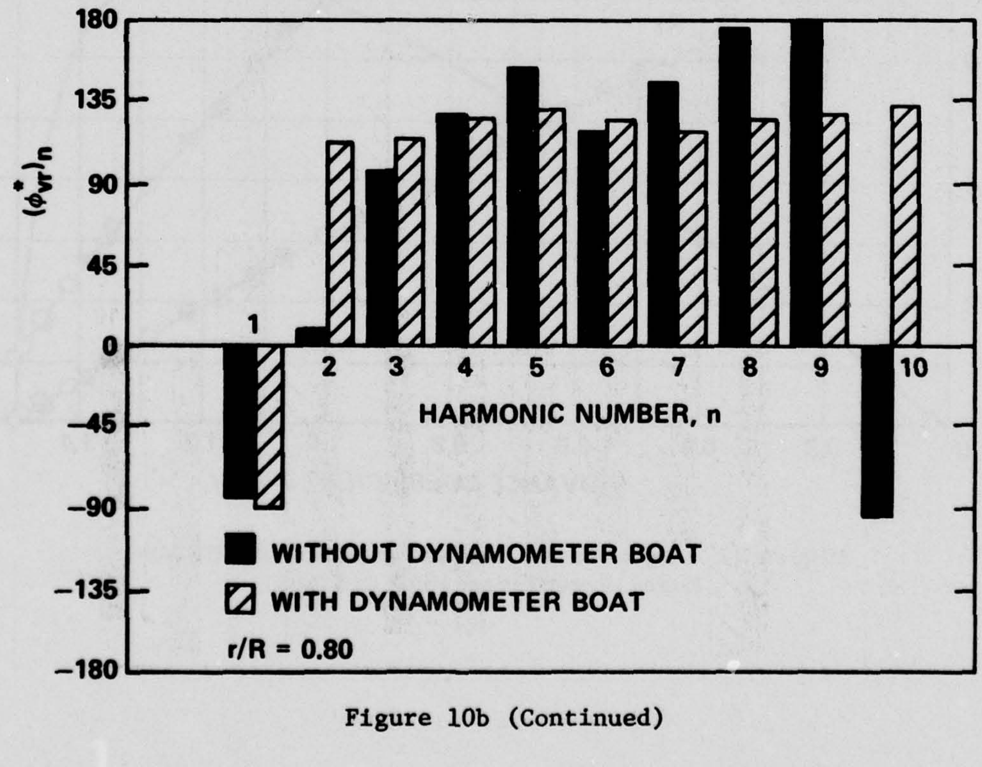

Figure 10b (Continued)

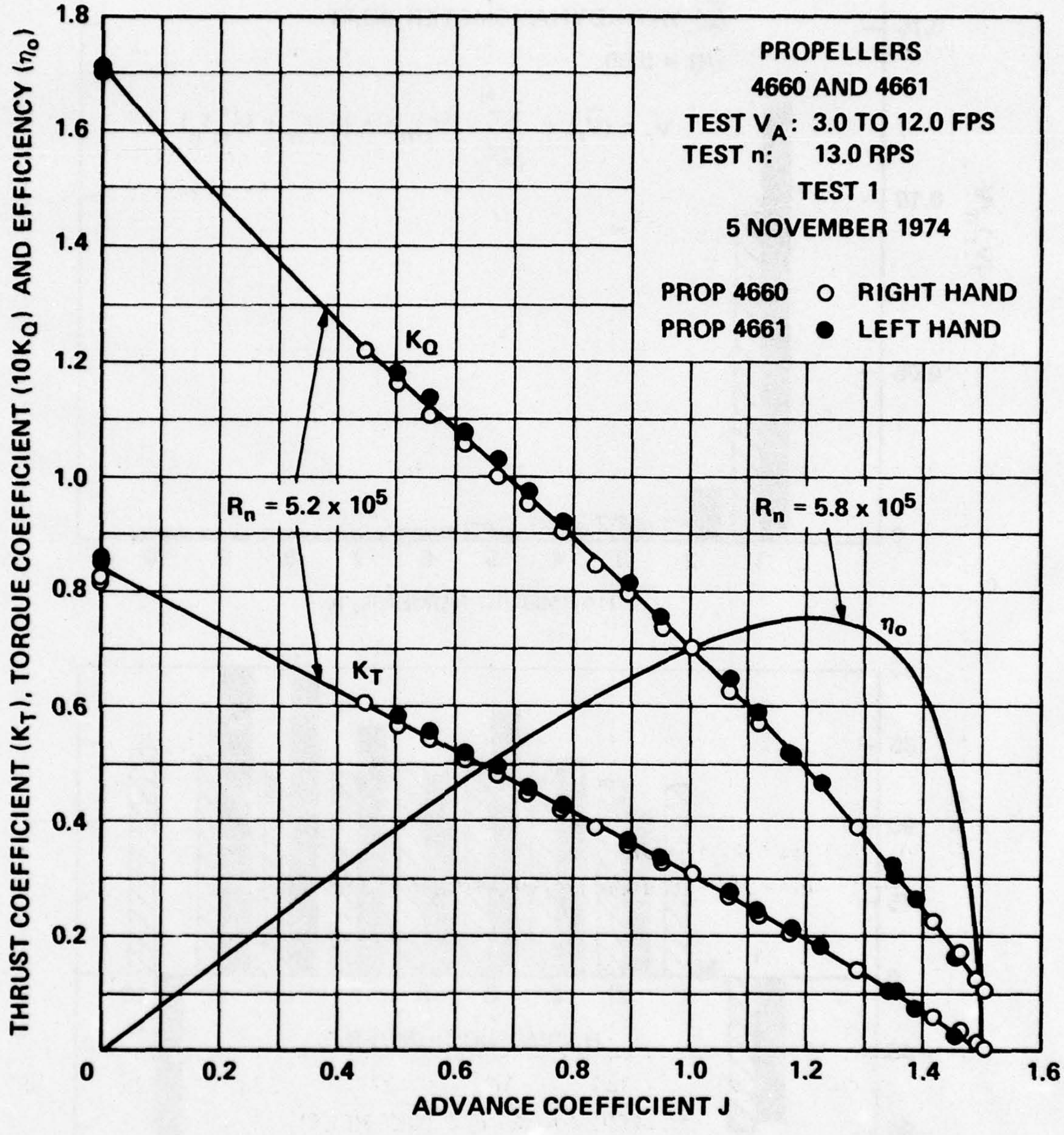

Figure 11 - Open-Water Characteristics of DTNSRDC Model Propellers 4660 and 4661

Figure 12 - Influence of Extraneous Signals on Measured Loads

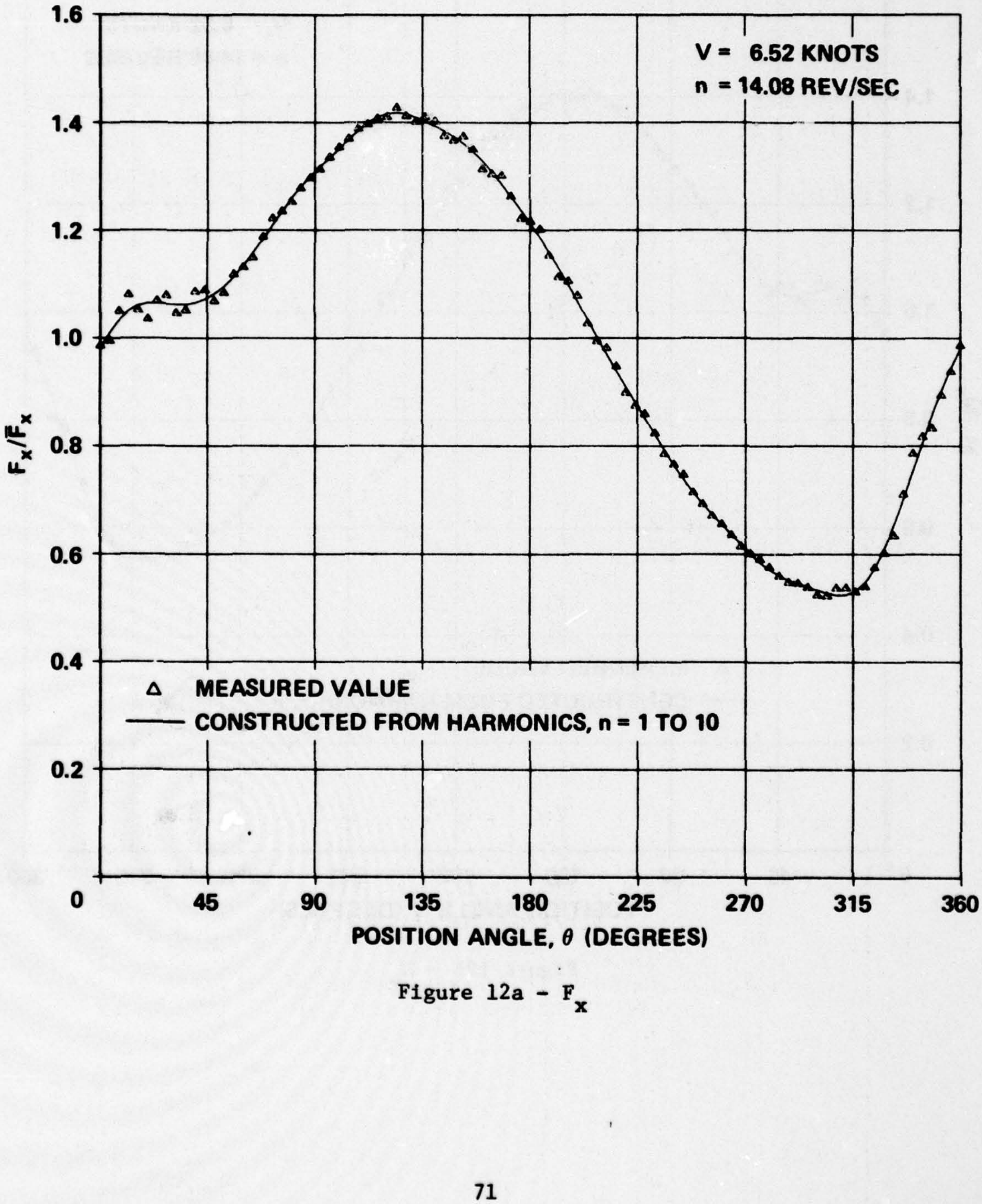

Figure 12a - F_x

Figure 12 (Continued)

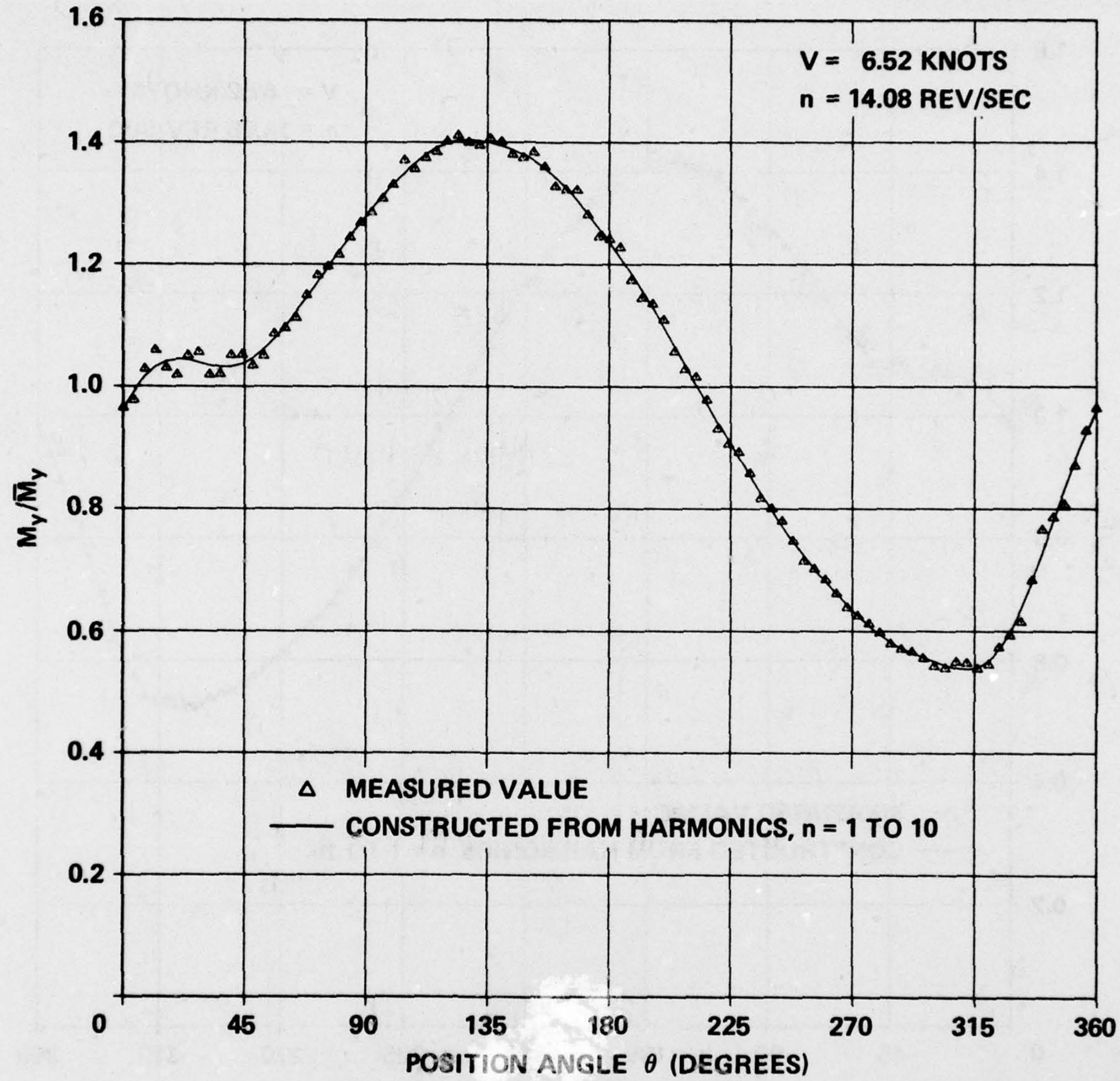

Figure 12b - M_y

Figure 12 (Continued)

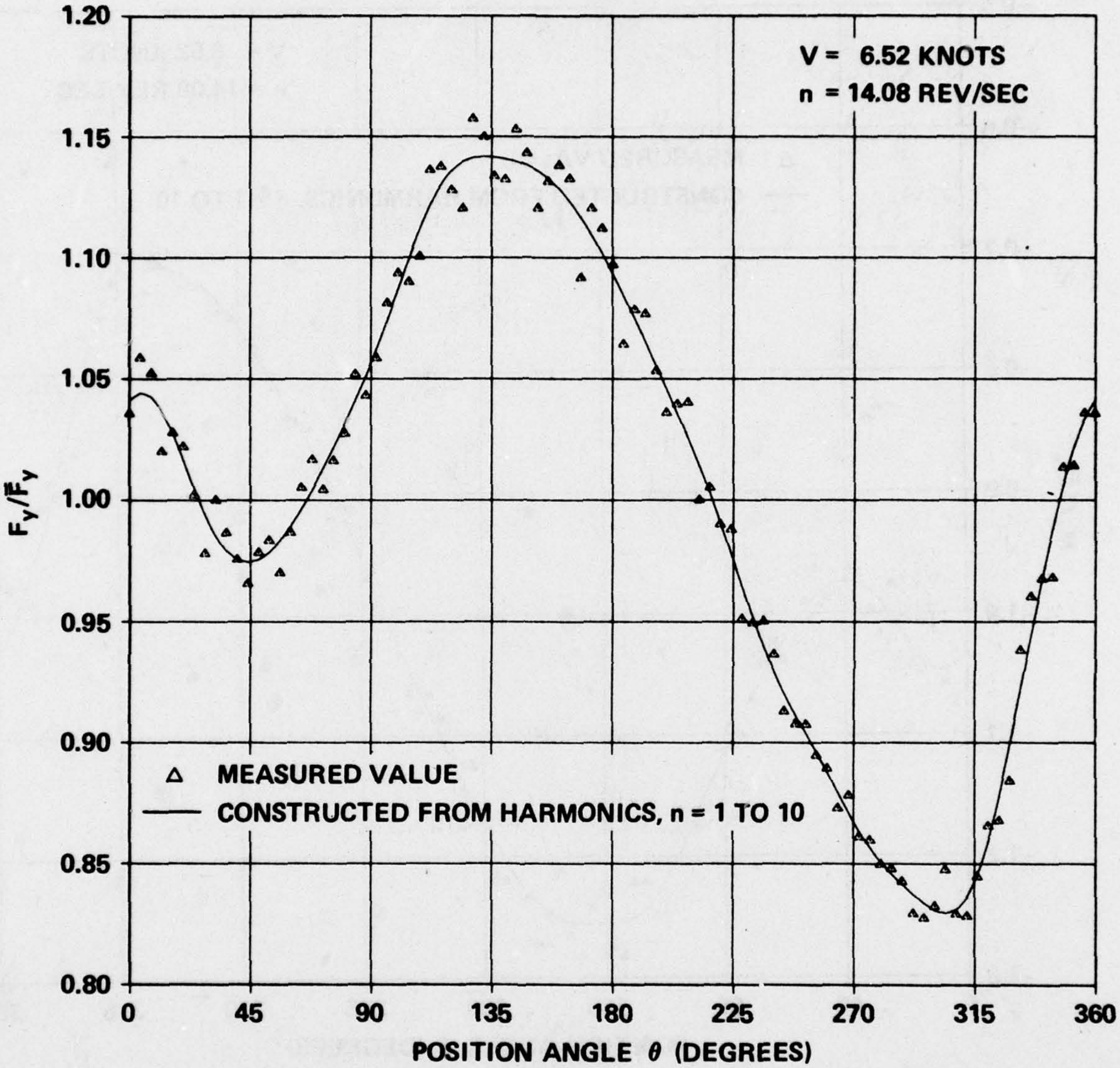

Figure 12c - F_y

Figure 12 (Continued)

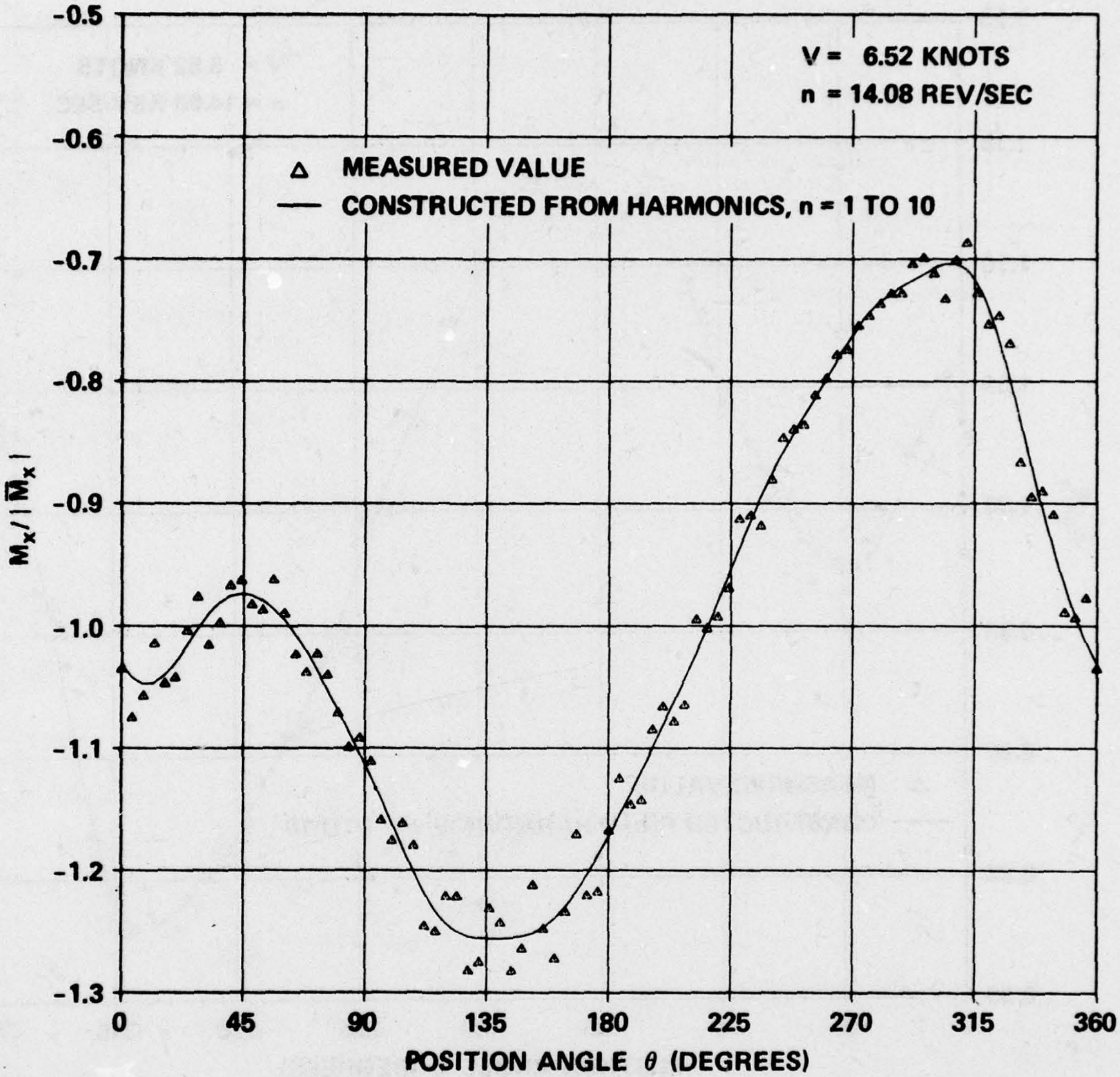

Figure 12d - M_x

Figure 12 (Continued)

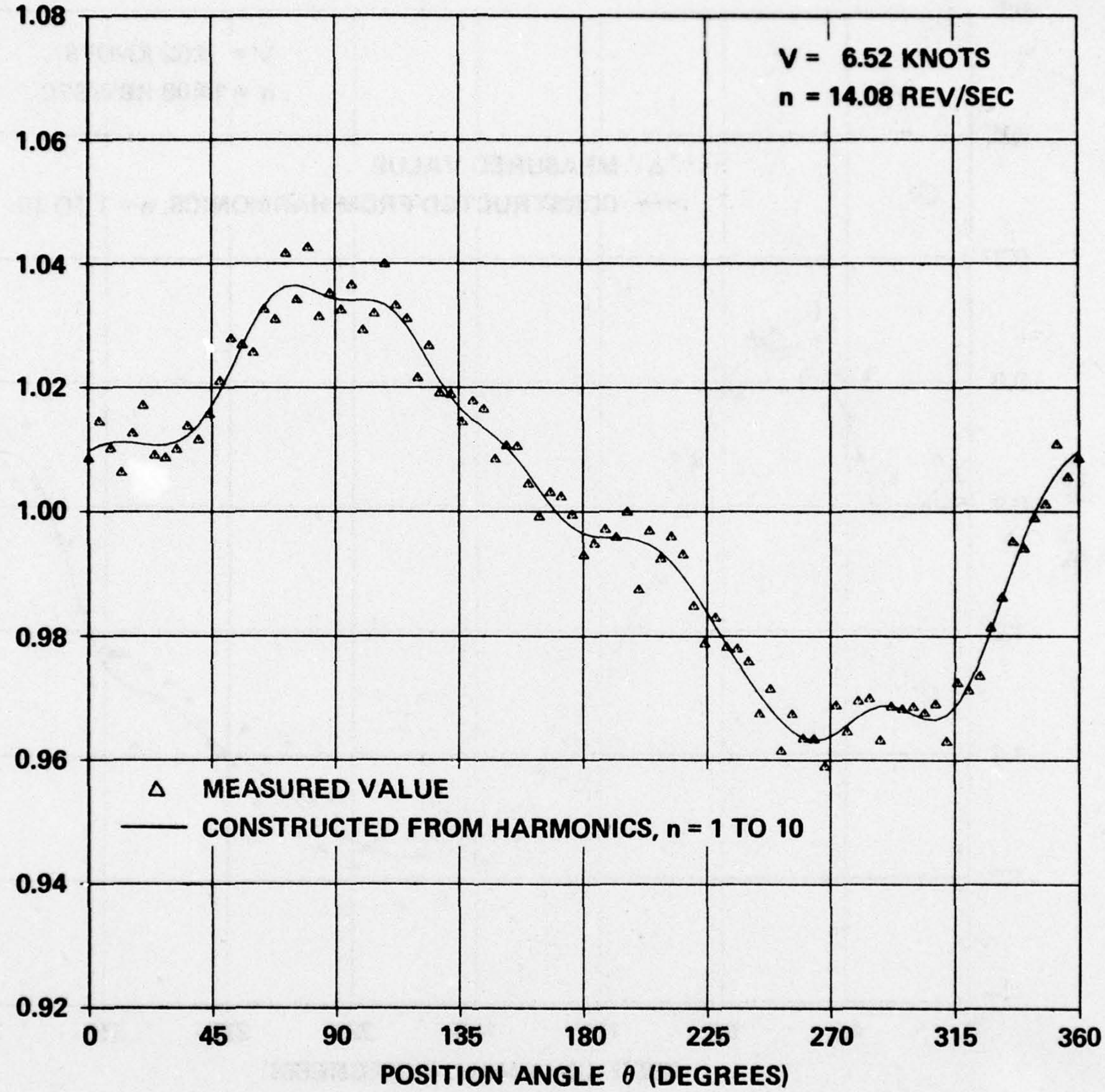

Figure 12e - F_z

Figure 12 (Continued)

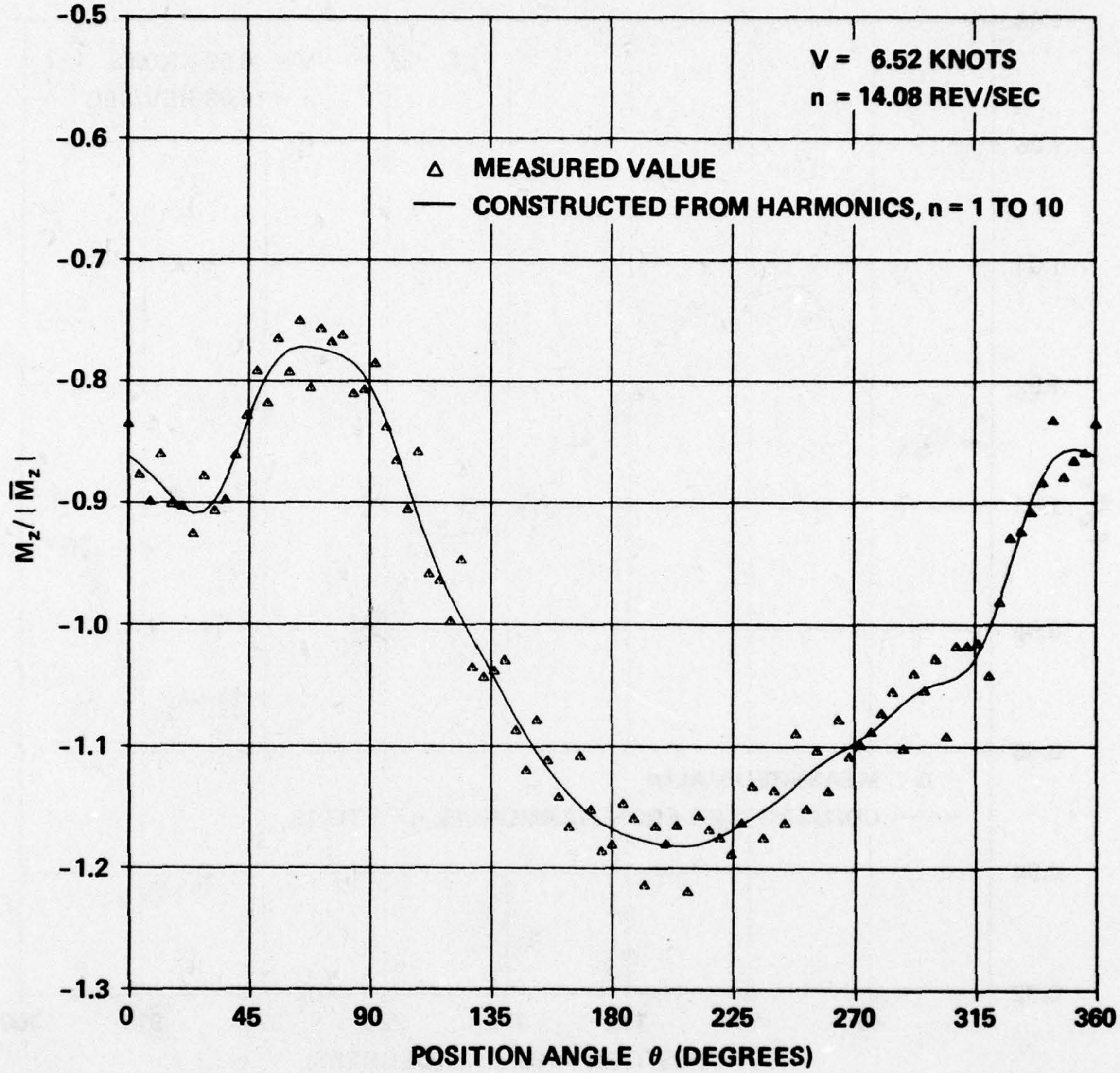

Figure 12f - M_z

Figure 13 - Experimental Data Showing Extraneous Higher Harmonics

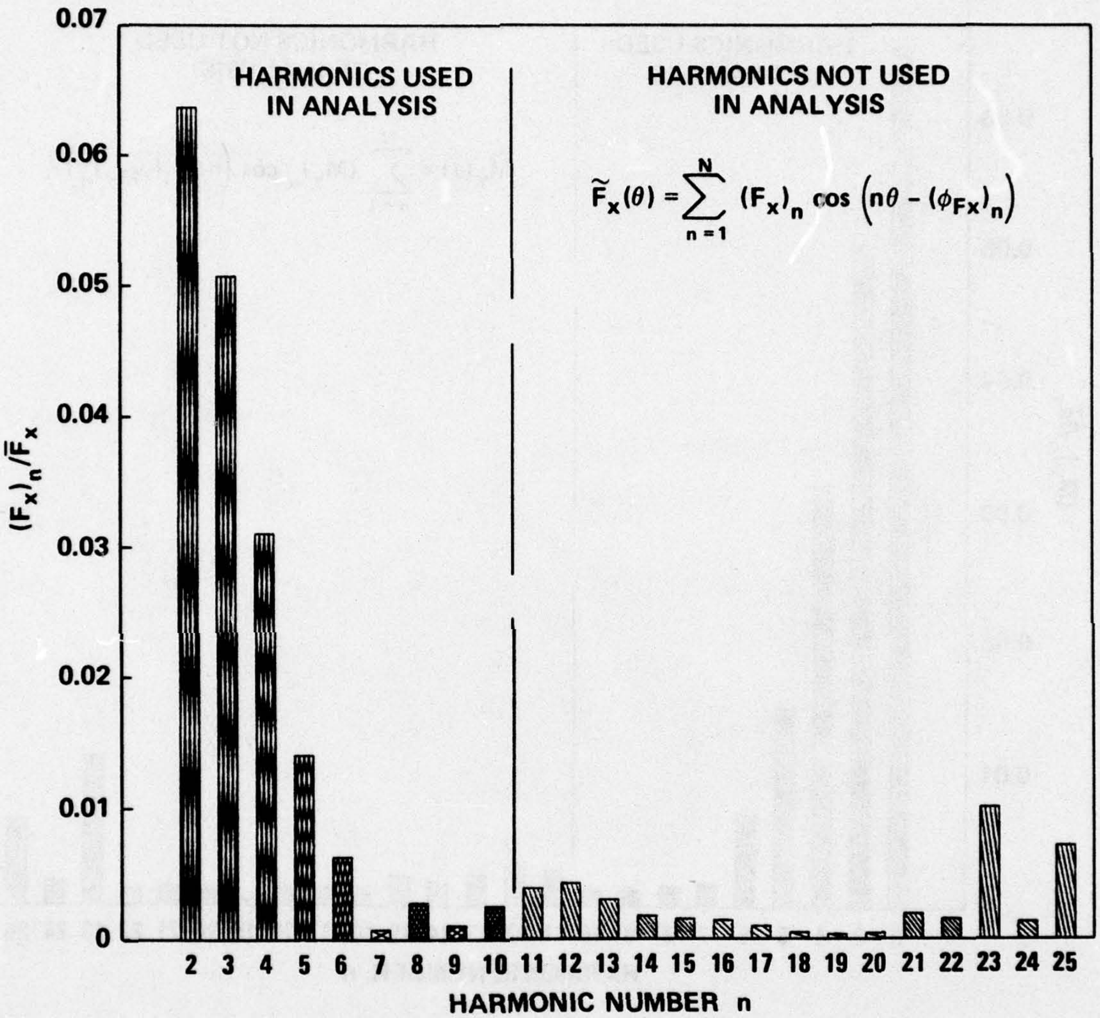

Figure 13a - F_x

Figure 13 (Continued)

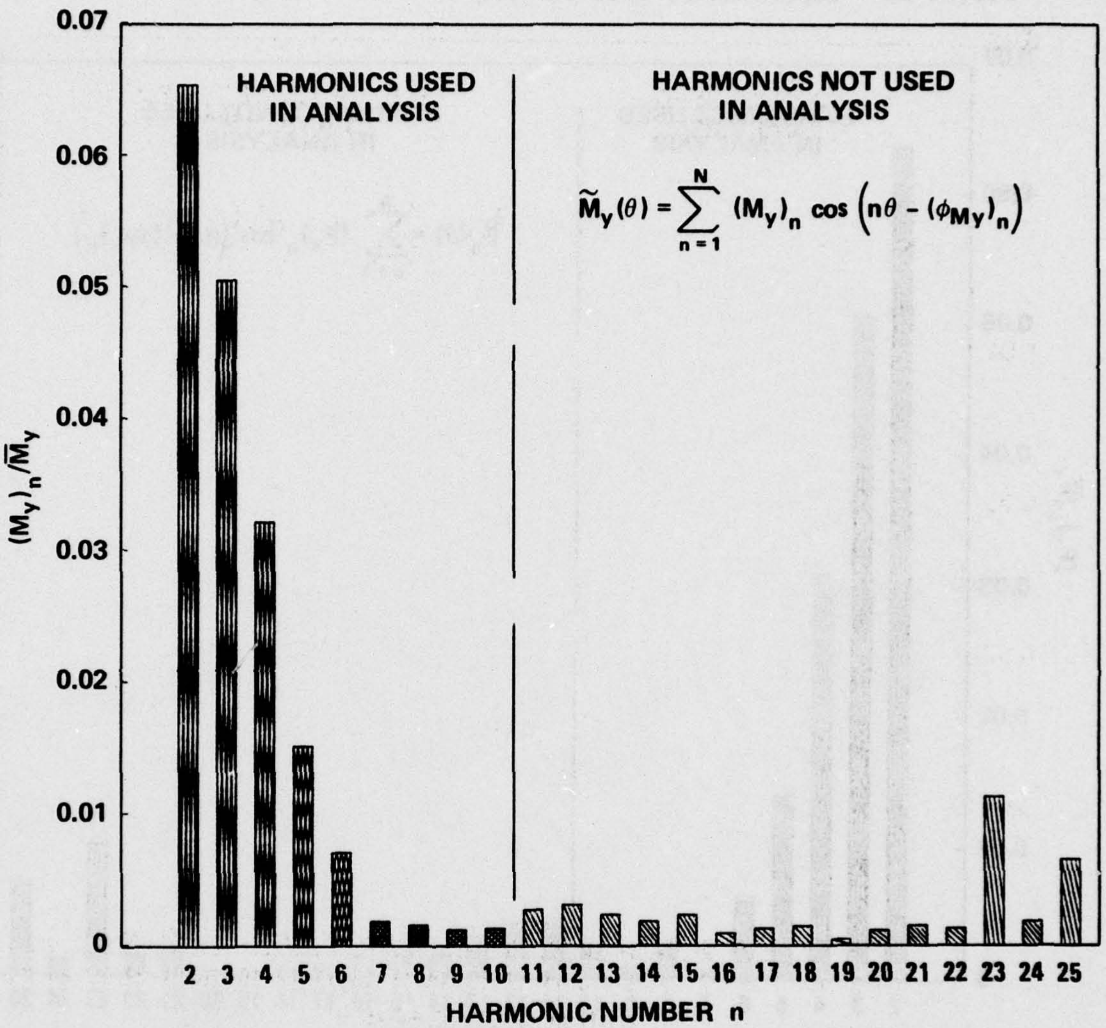

Figure 13b - M_y

Figure 13 (Continued)

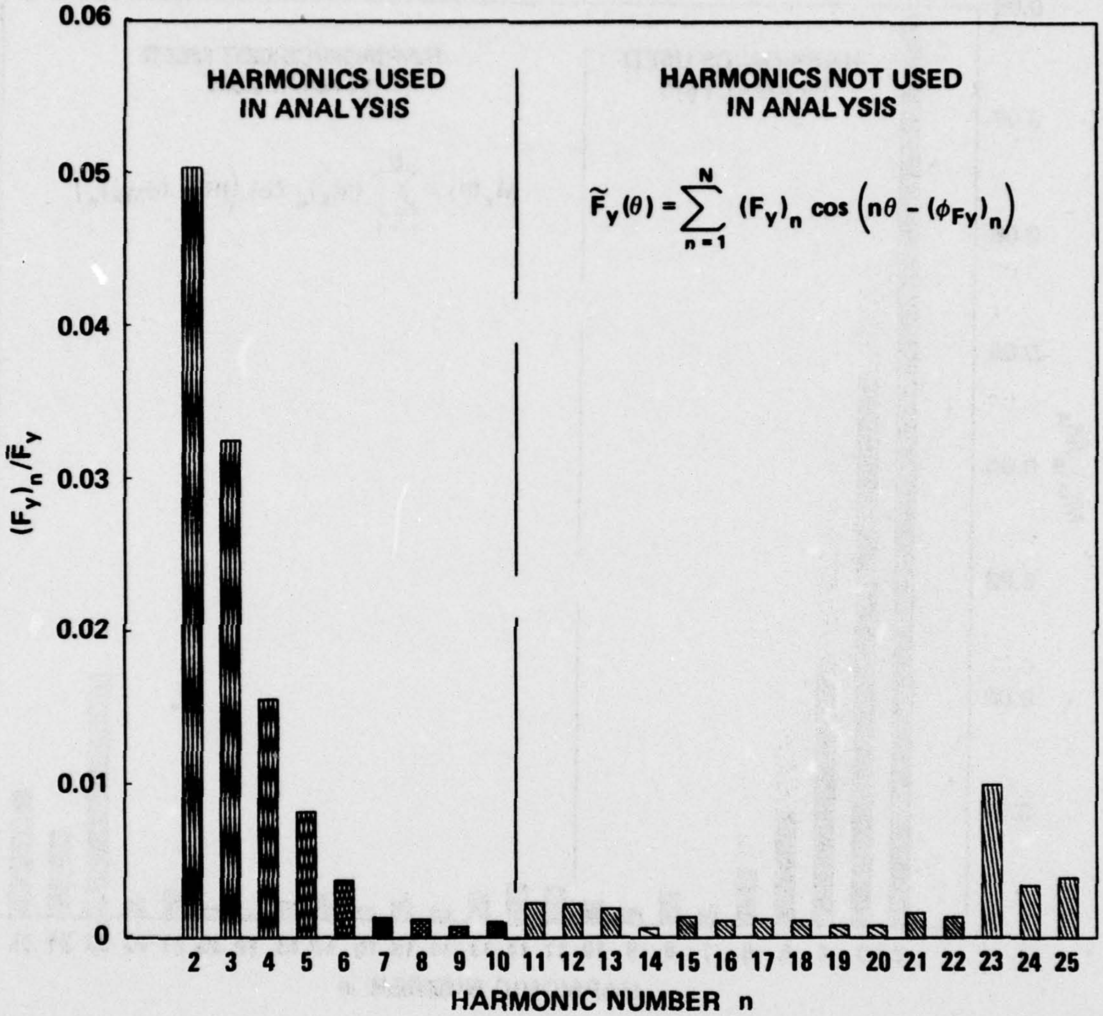

Figure 13c - F_y

Figure 13 (Continued)

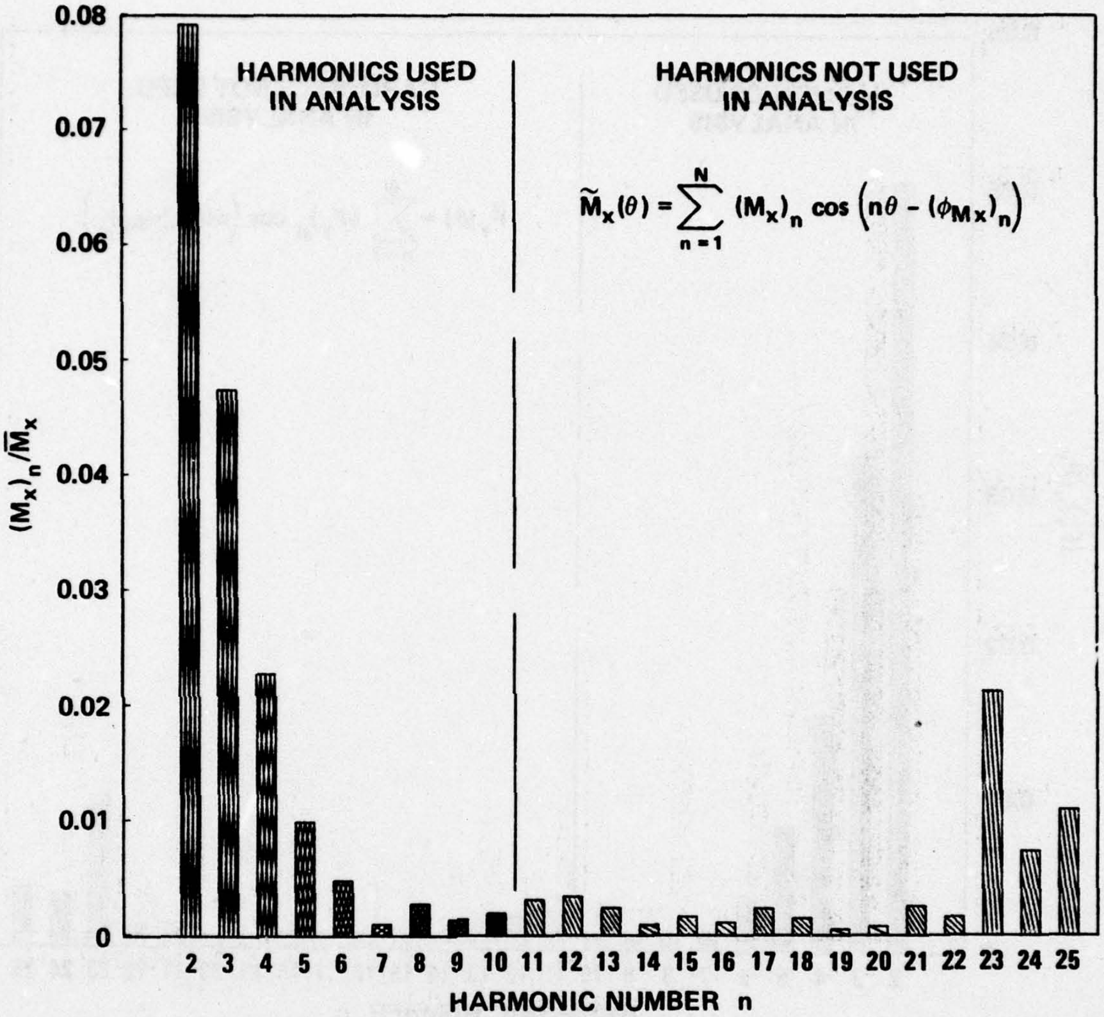

Figure 13d - M_x

Figure 13 (Continued)

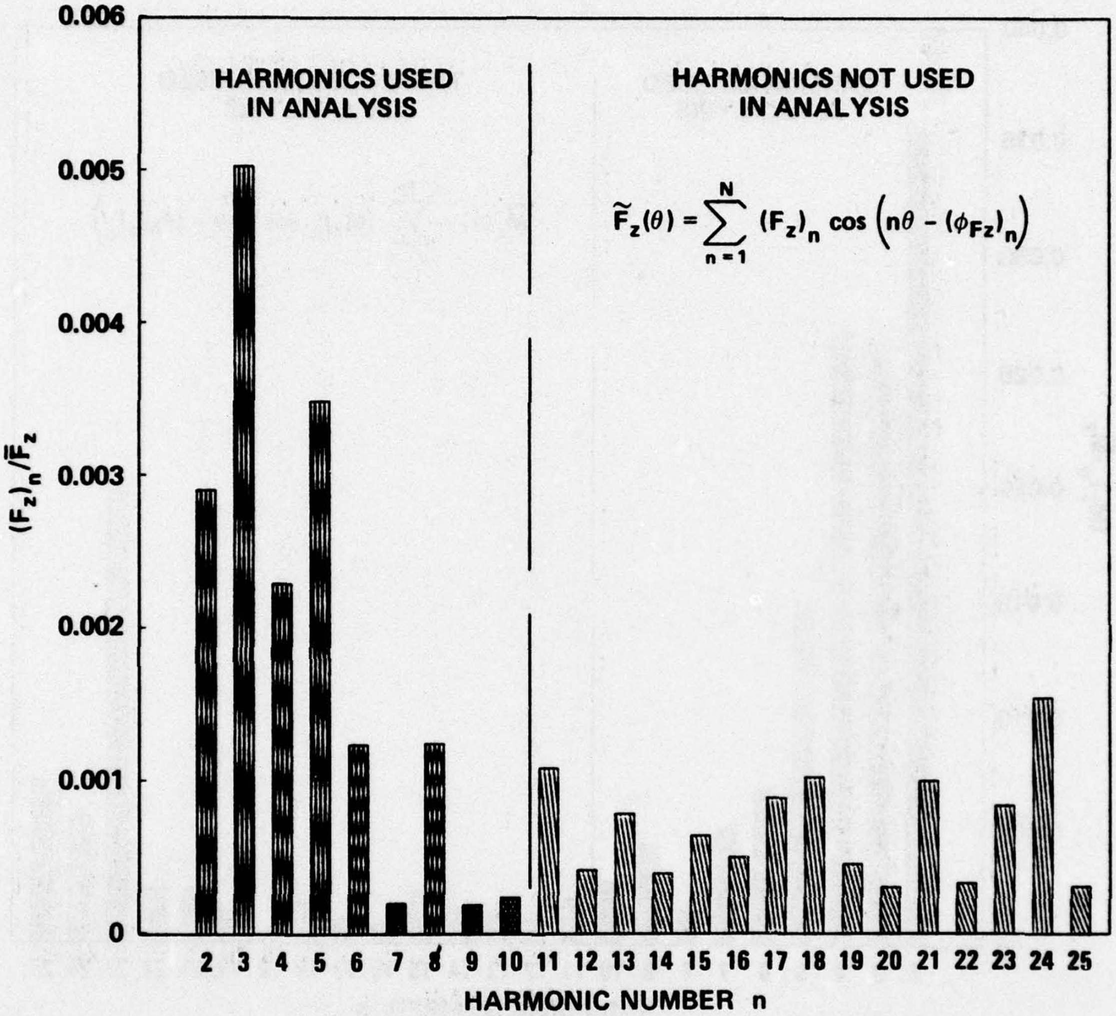

Figure 13e - F_z

Figure 13 (Continued)

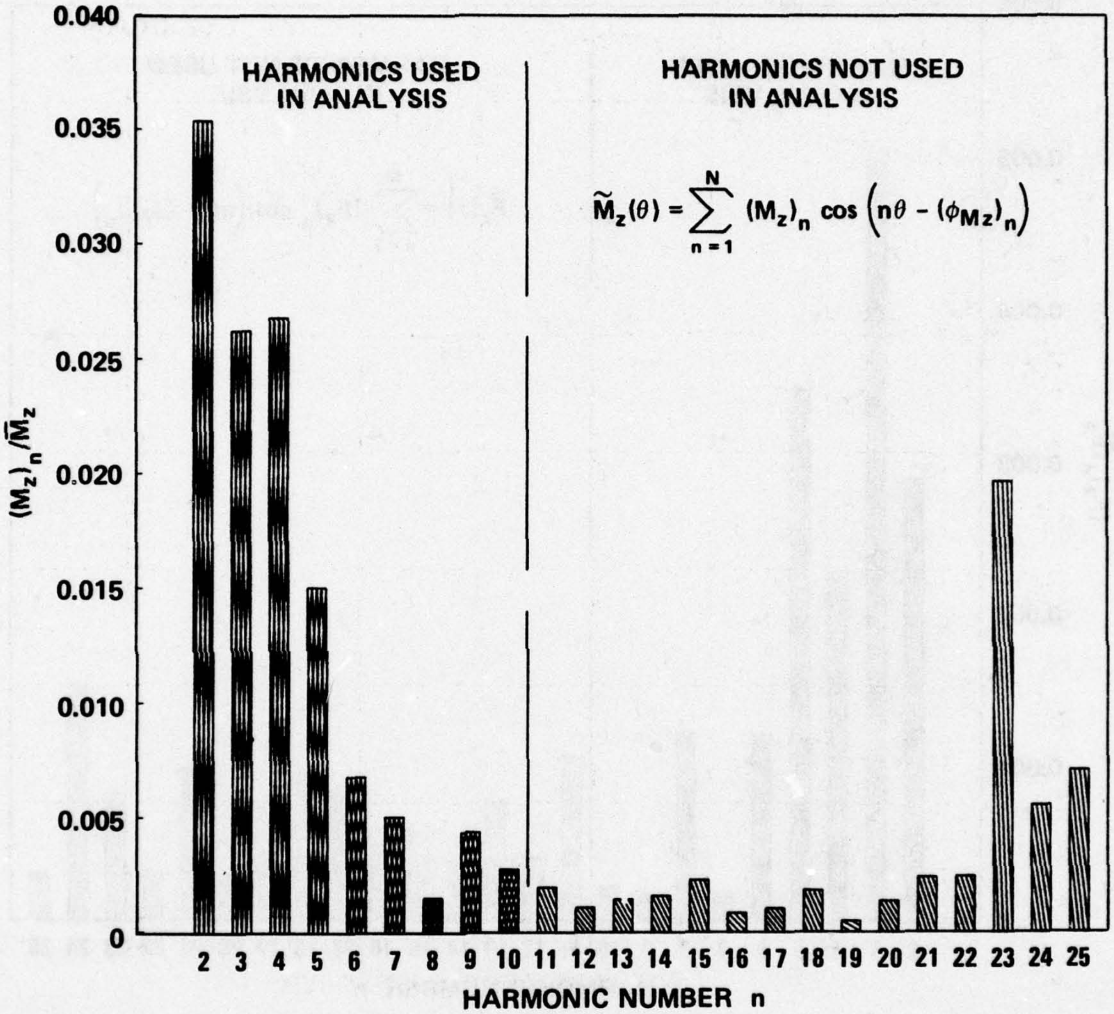

Figure 13f - M_z

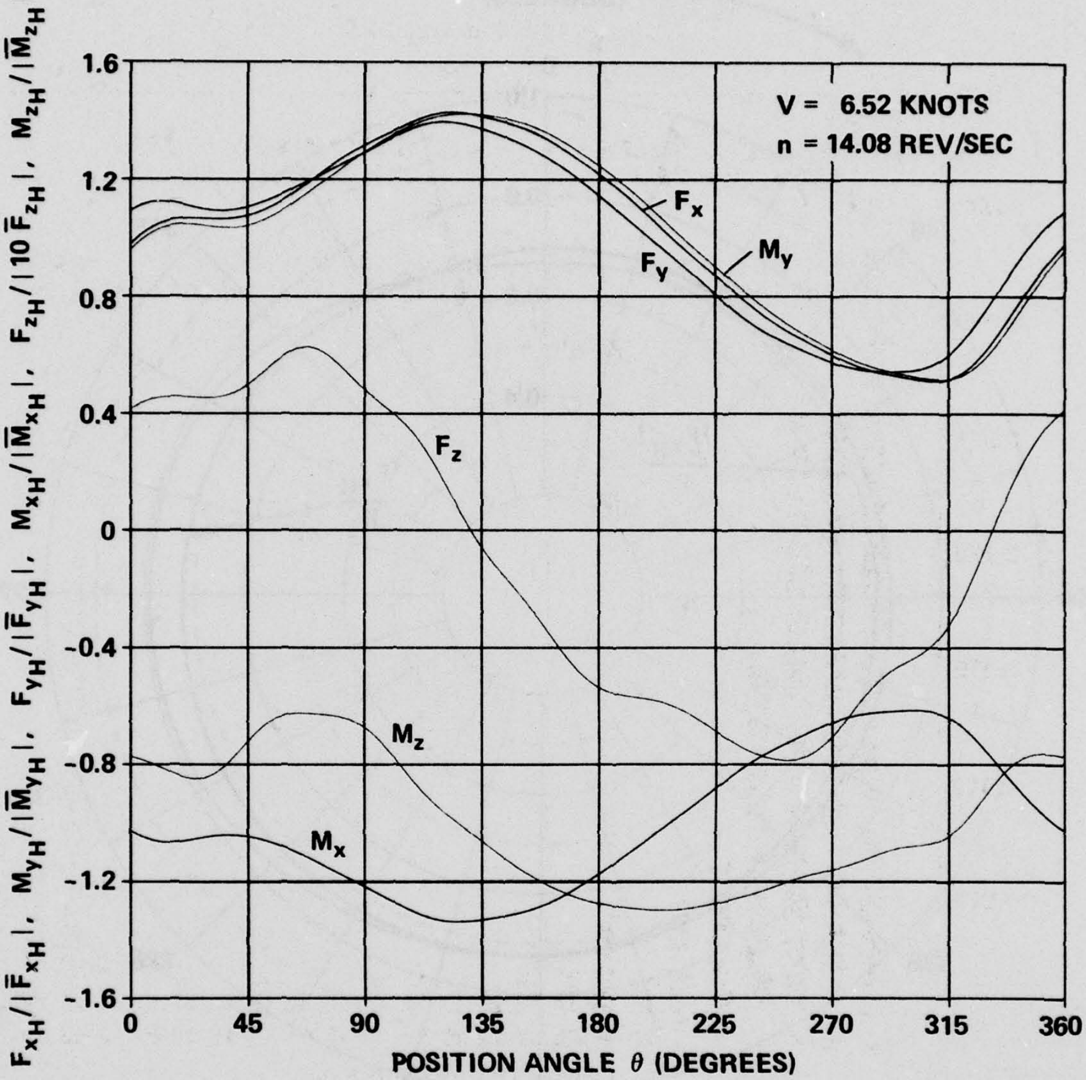

Figure 14 - Variation of Experimental Hydrodynamic Loads
with Angular Position for Steady-Ahead Operation

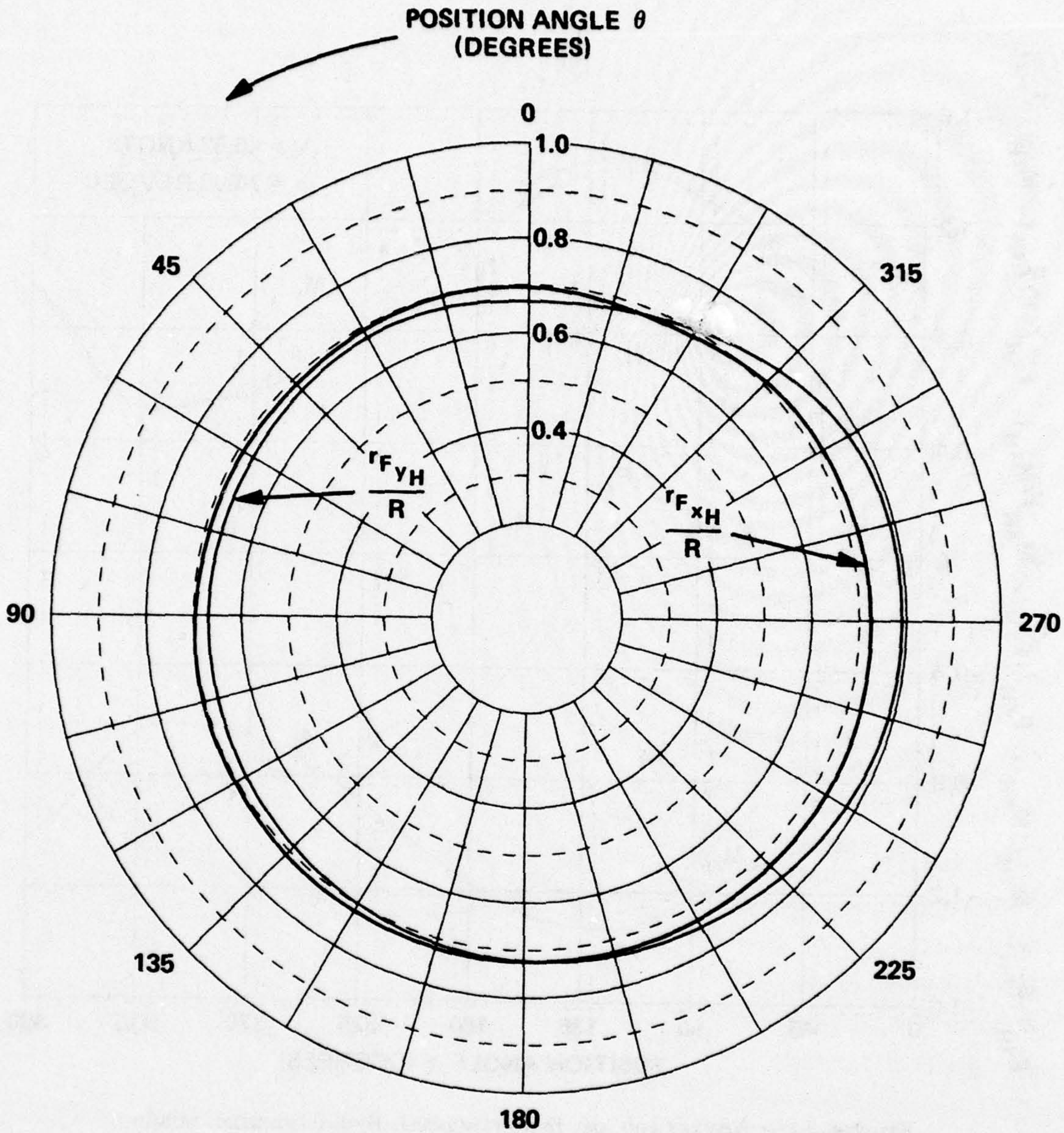

Figure 15 - Variation in Radial Center of Thrust F_{x_H} and Transverse Hydrodynamic Force F_{y_H} with Blade Angular Position for Steady-Ahead Operation

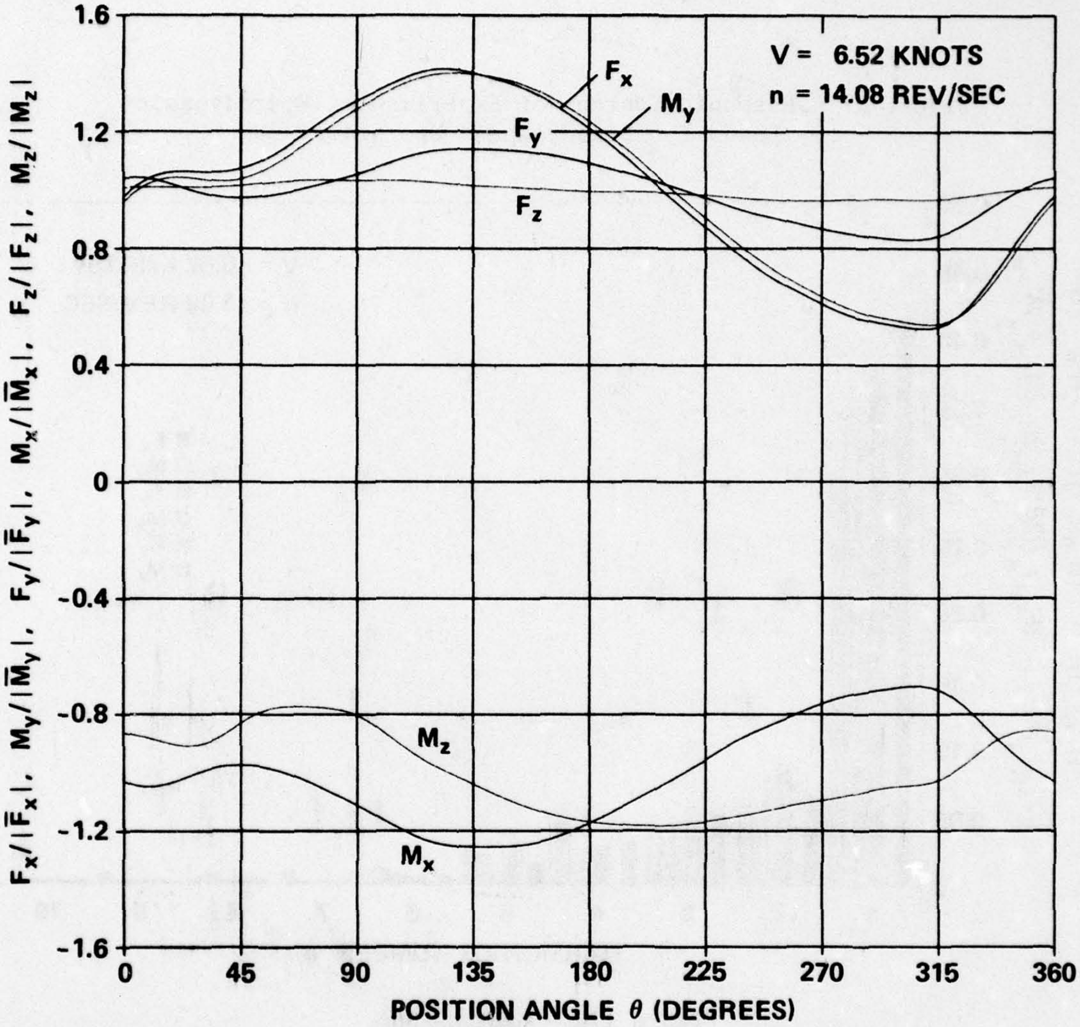

Figure 16 - Variation of Experimental Total Loads with Angular Position for Steady-Ahead Operation

AD-A048 385 DAVID W TAYLOR NAVAL SHIP RESEARCH AND DEVELOPMENT CE--ETC F/G 13/10
EXPERIMENTAL UNSTEADY AND TIME AVERAGE LOADS ON THE BLADES OF T--ETC(U)
DEC 77 S D JESSUP, R J BOSWELL, J J NELKA

UNCLASSIFIED DTNSRDC-77-0110 NL

2 OF 4
AD
A048385

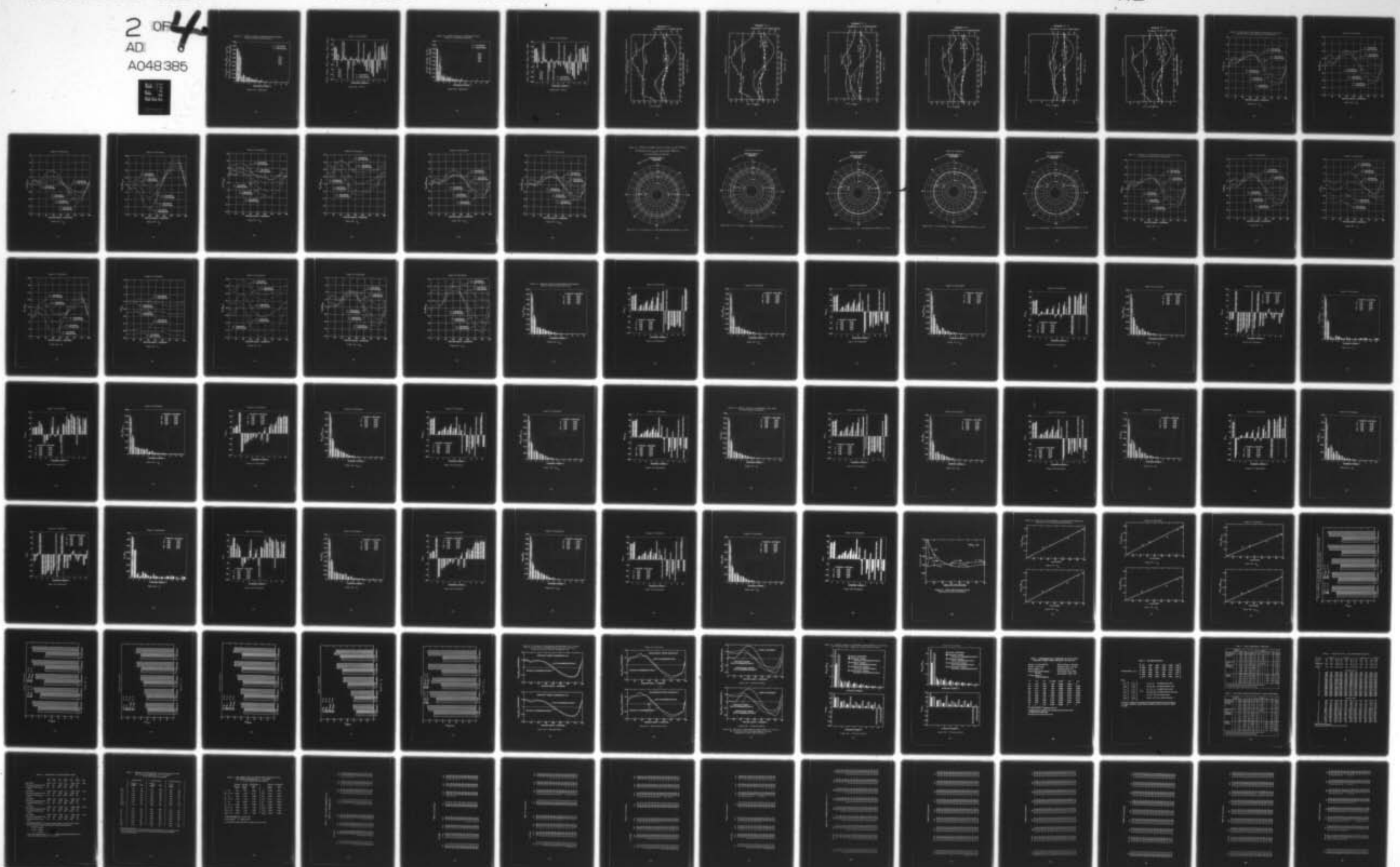

Figure 17 - Harmonic Content of Expe
Loads for Steady-Ahead

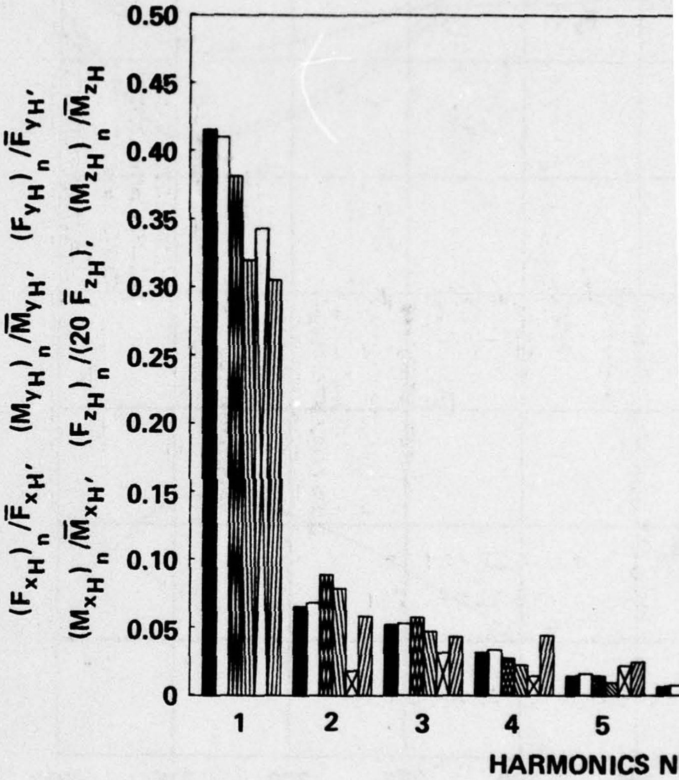

Figure 17a - Amplitu

Figure 17 (Continued)

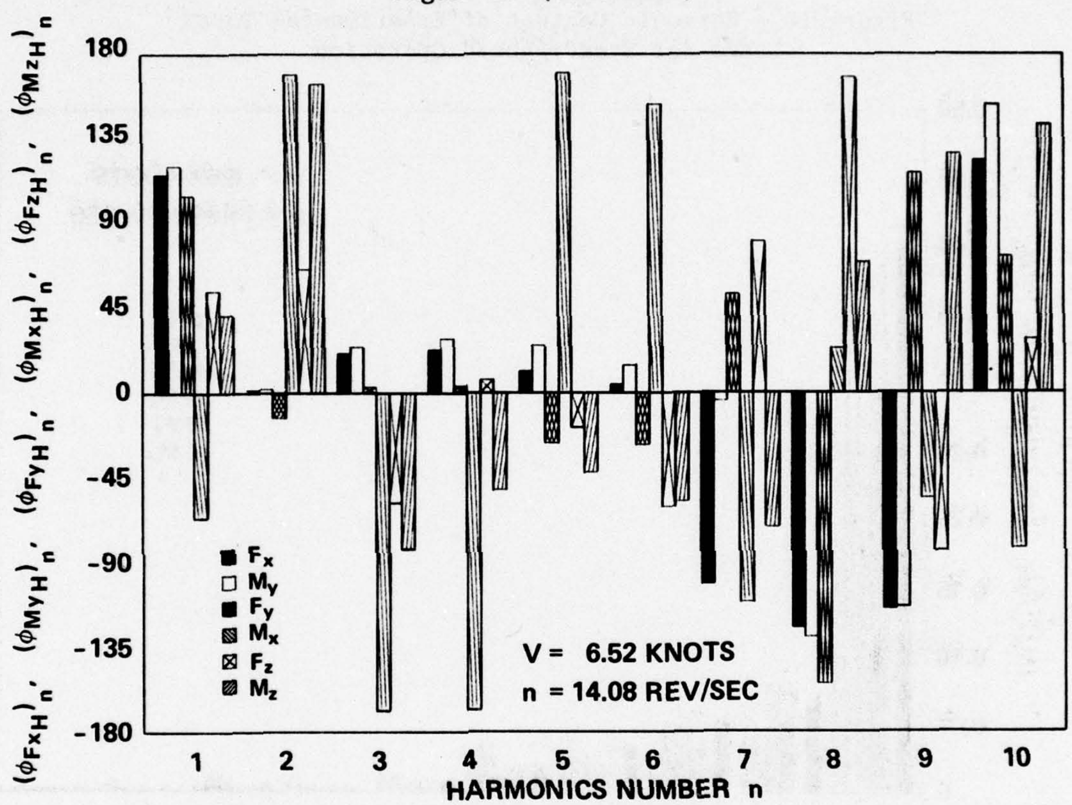

Figure 17b - Phases

Figure 18 - Harmonic Content of Experimental Total Loads for Steady-Ahead Operation

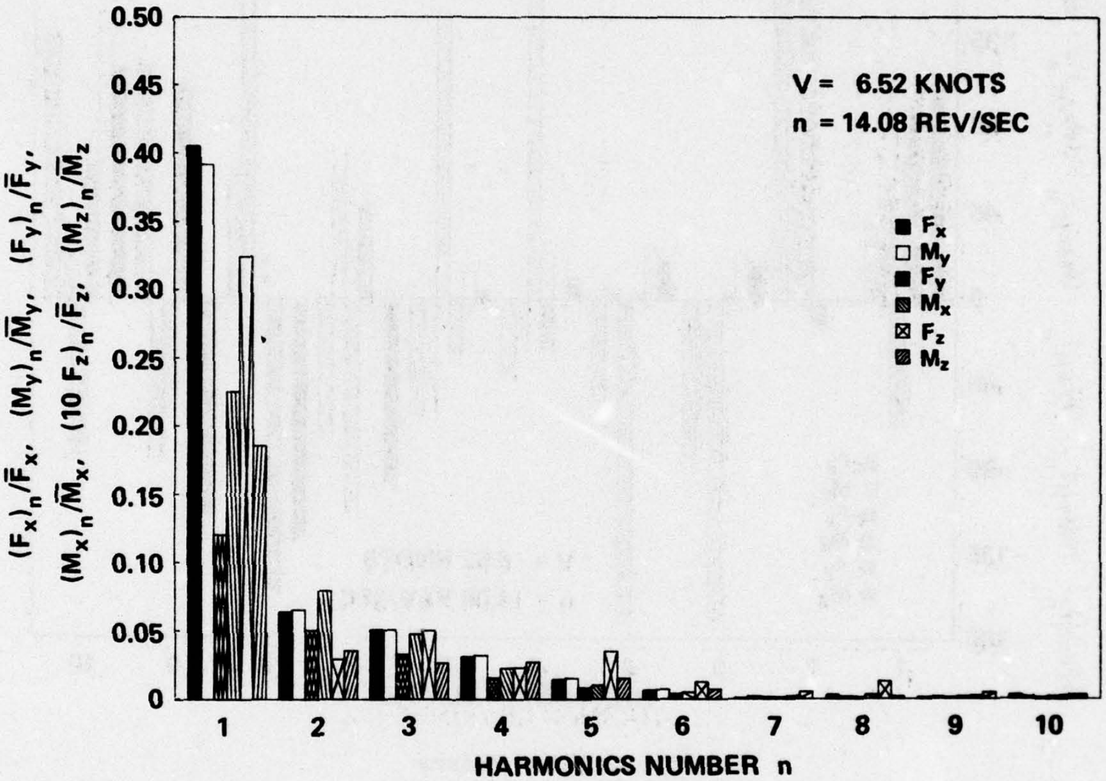

Figure 18a - Amplitudes

Figure 18 (Continued)

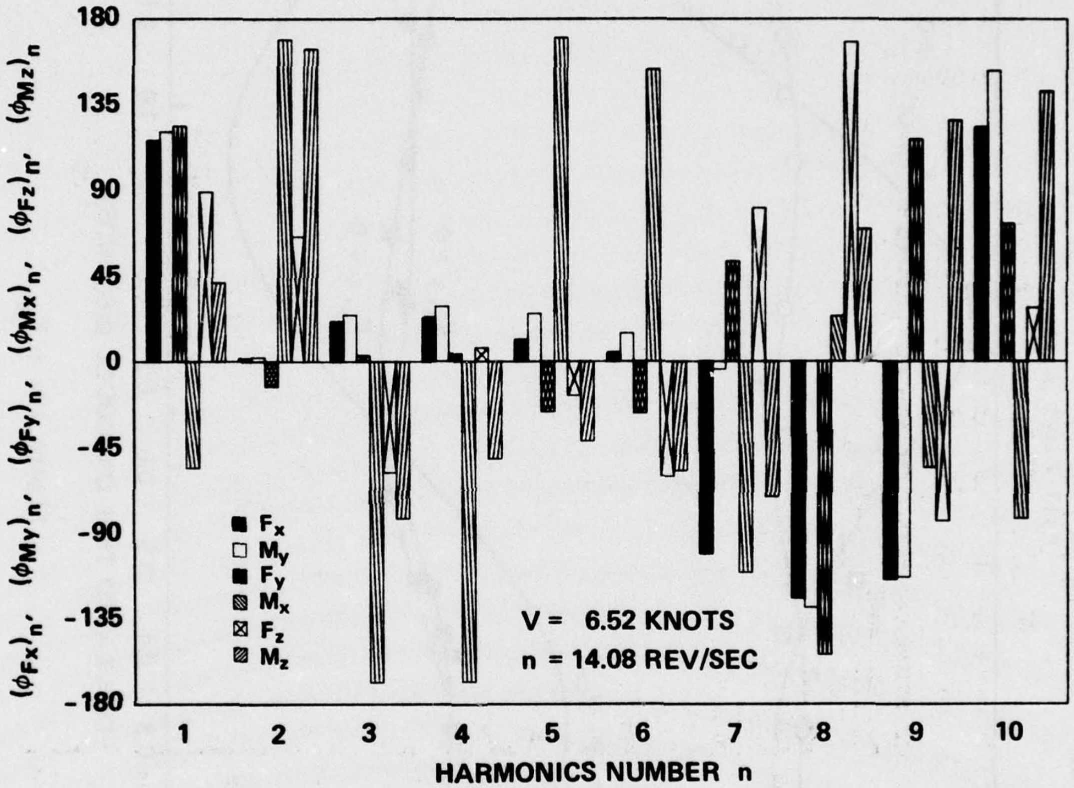

Figure 18b - Phases

Figure 19 - Variation of Components of Total Blade Loading with Hull Pitch Angle

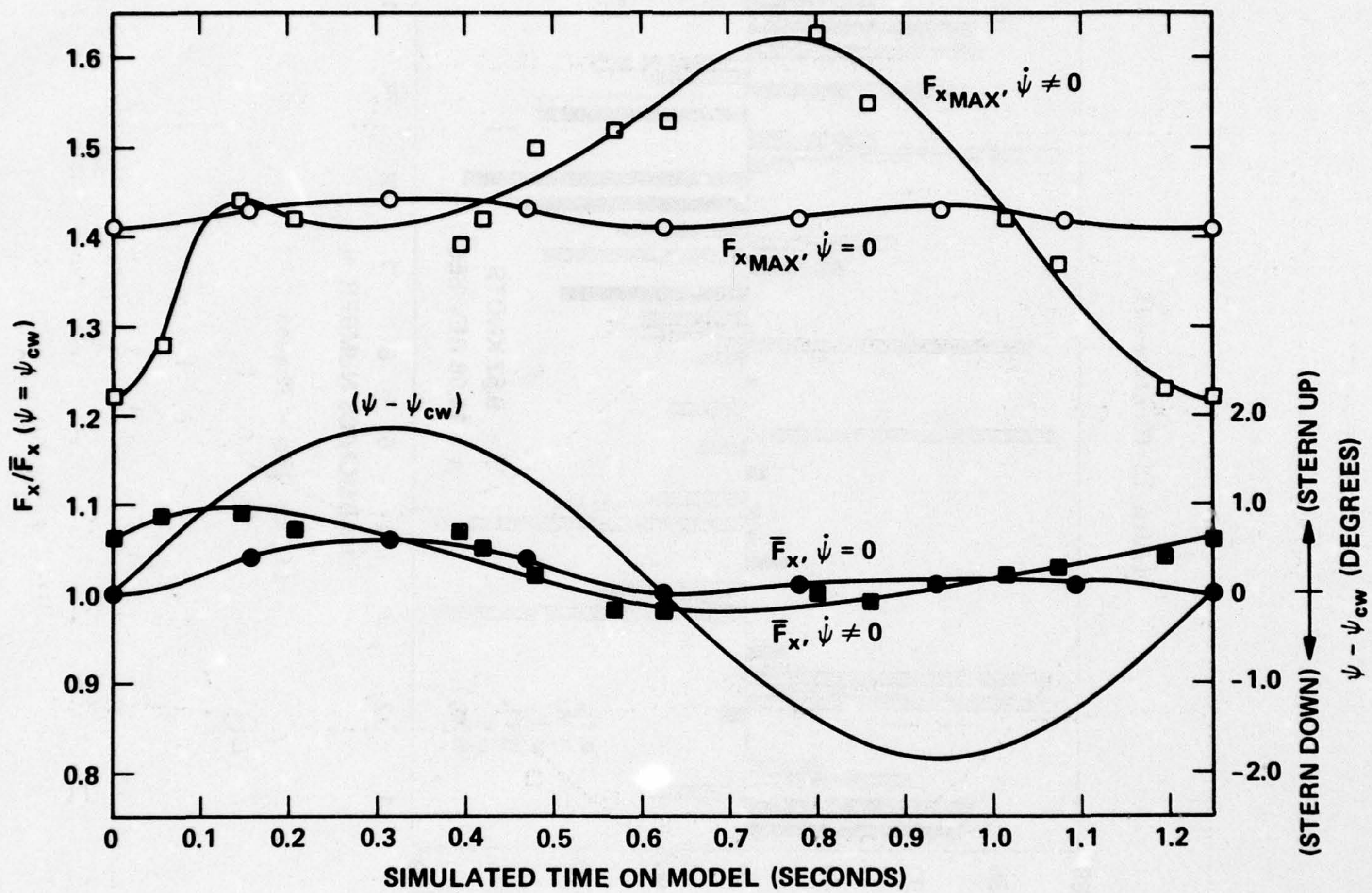

Figure 19a - F_x

Figure 19 (Continued)

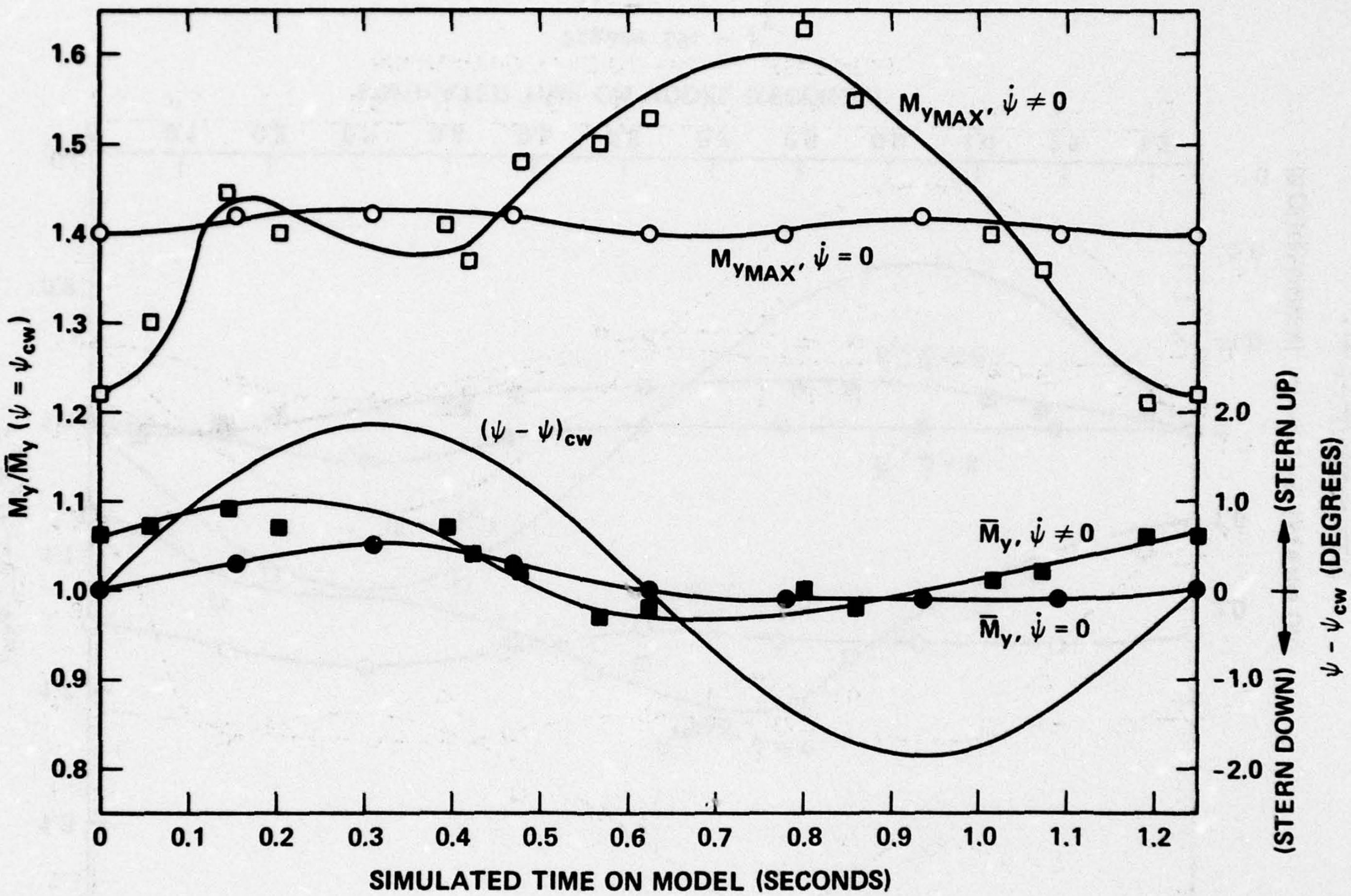

Figure 19b - M_y

Figure 19 (Continued)

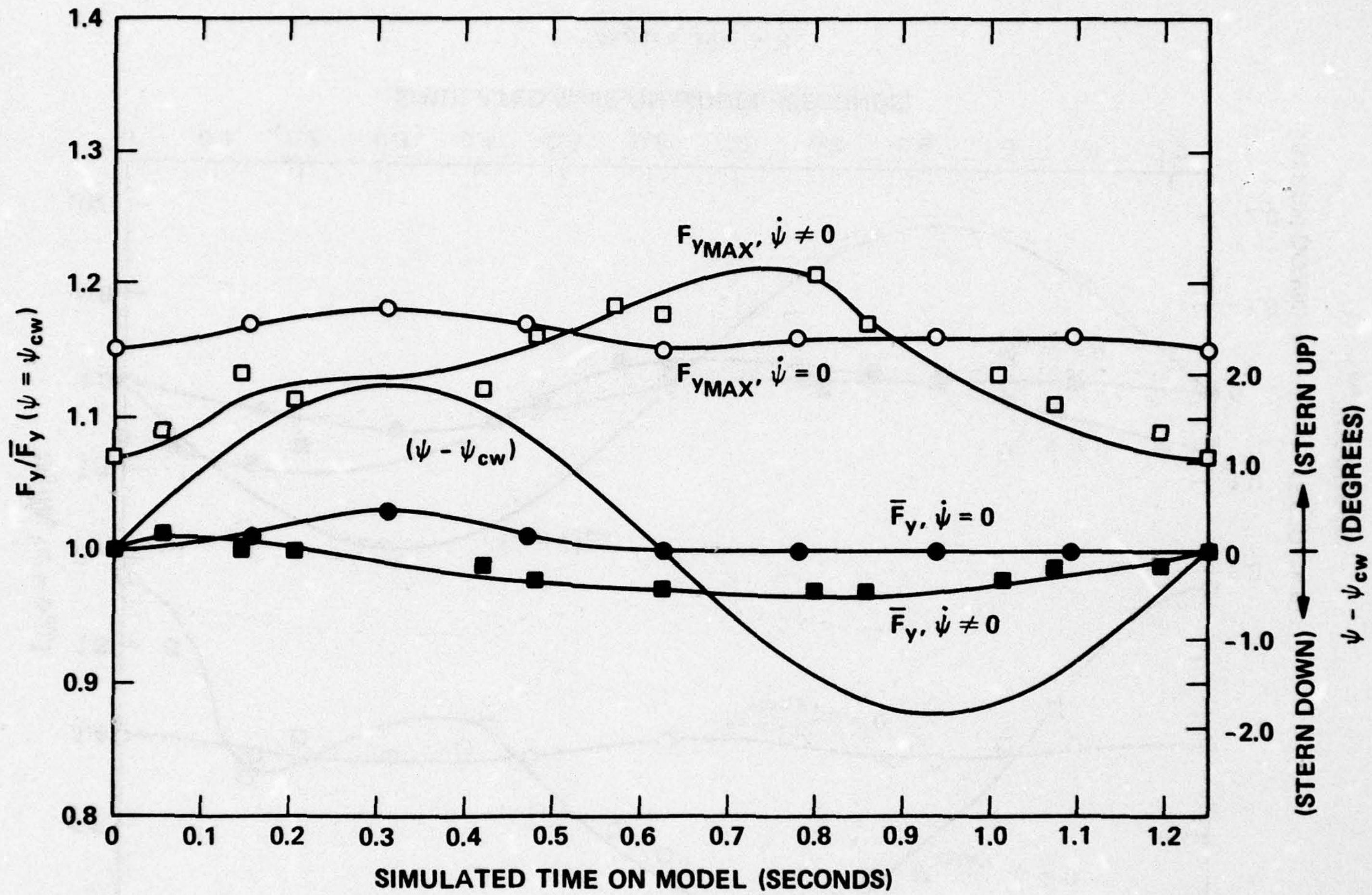

Figure 19c - F_y

Figure 19 (Continued)

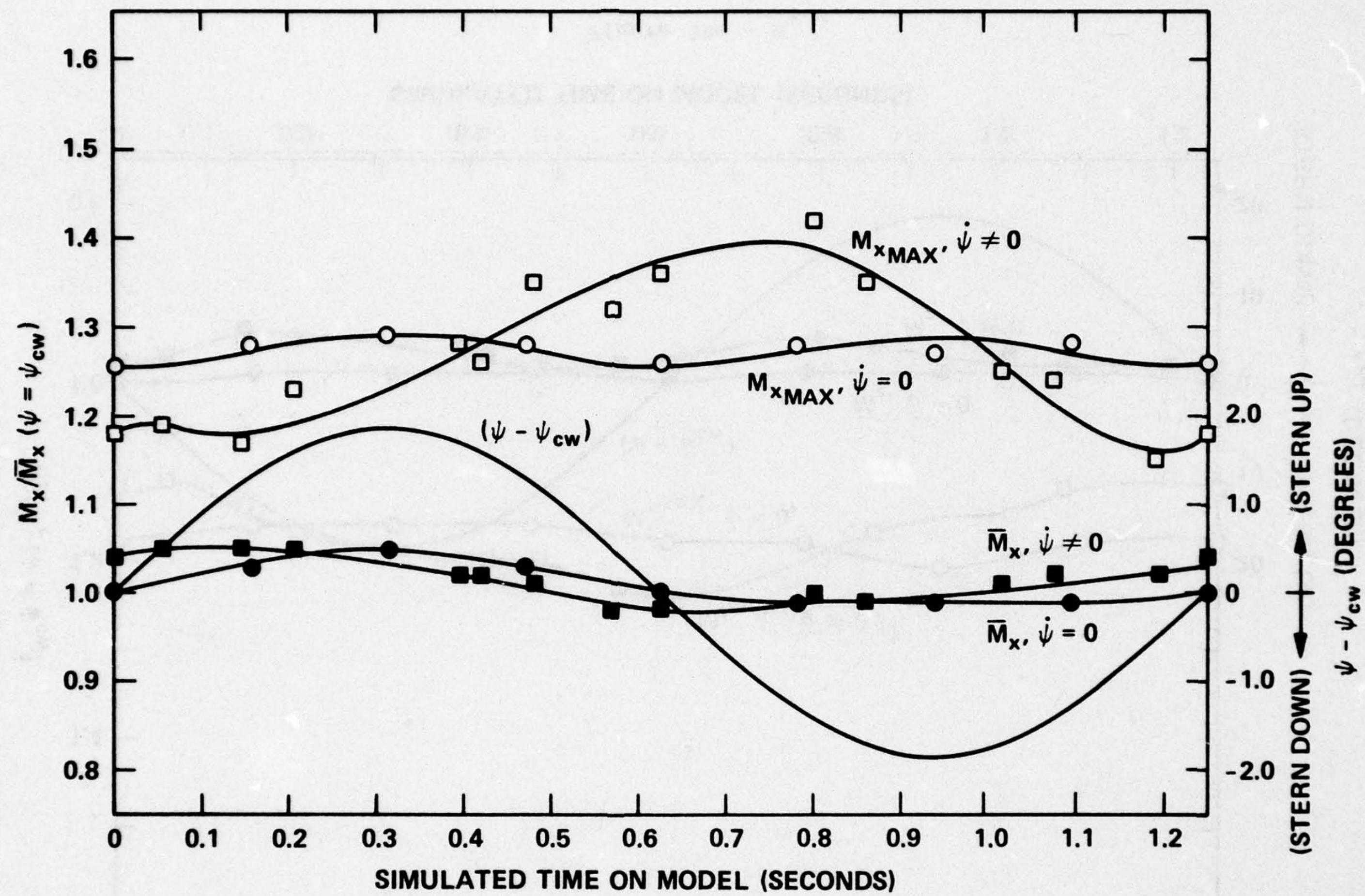

Figure 19d - M_x

Figure 19 (Continued)

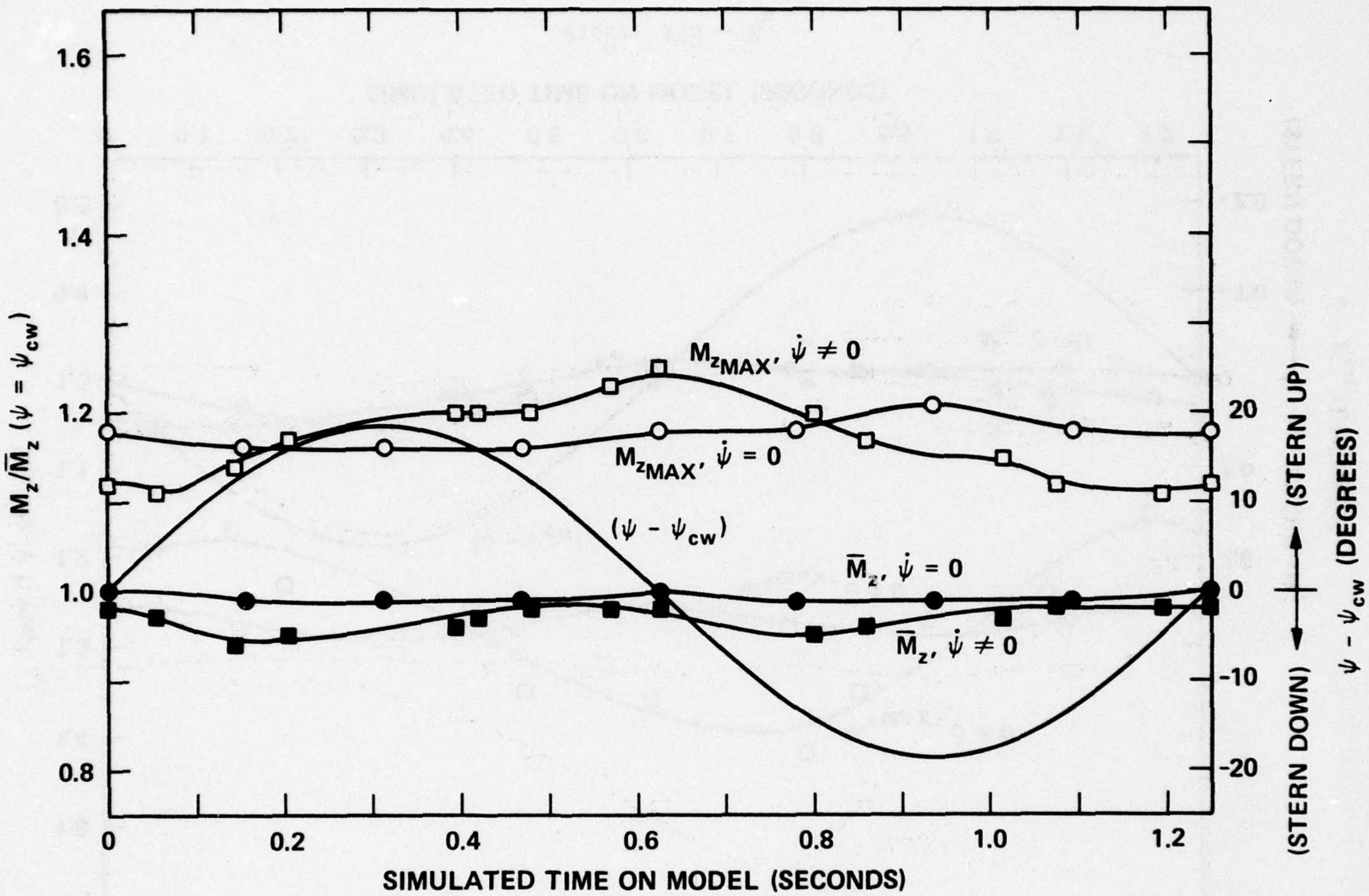

Figure 19e - M_z

Figure 19 (Continued)

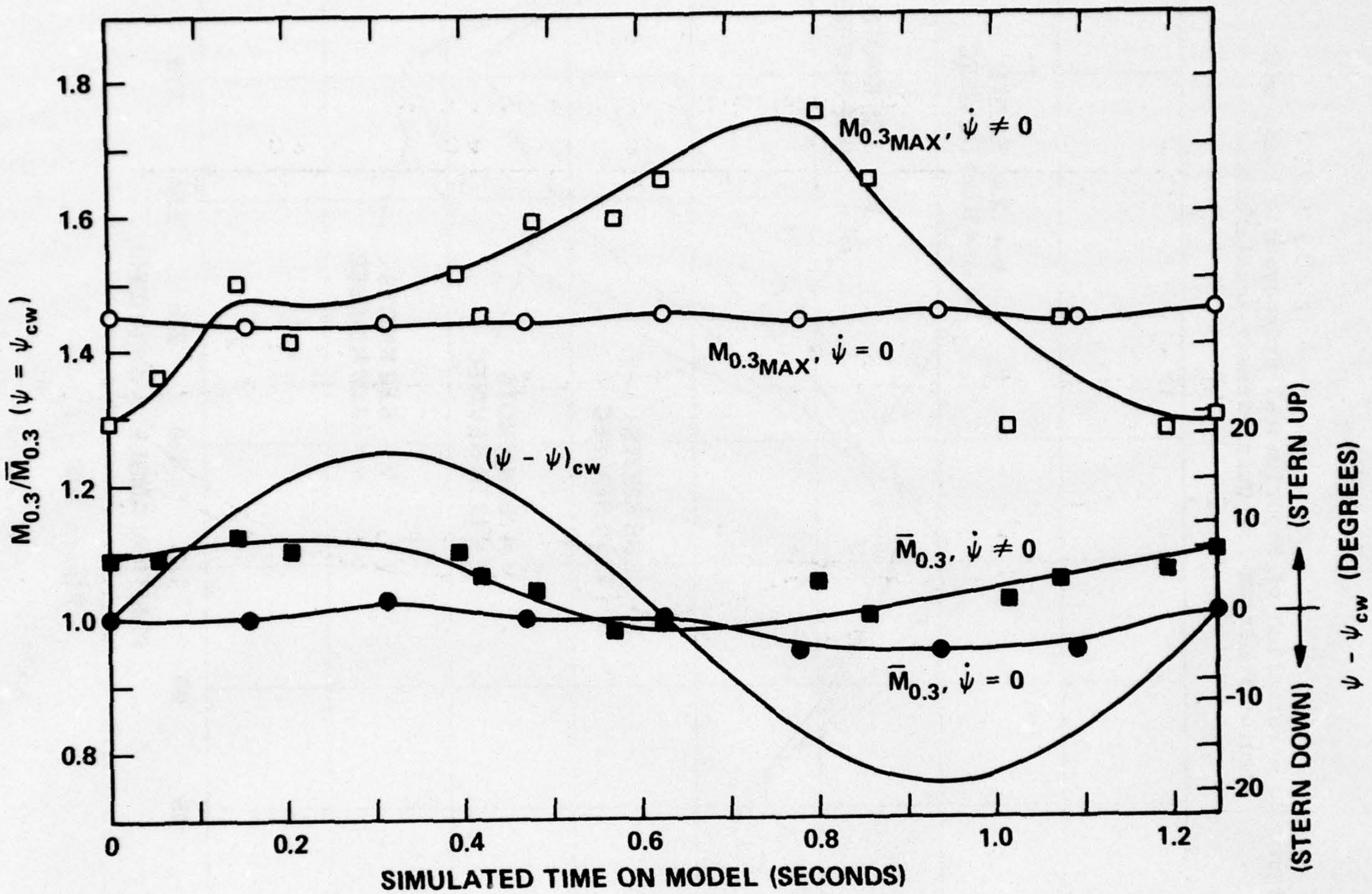

Figure 19f - $M_{0.3}$

Figure 20 - Variation of Experimental Hydrodynamic Loads with Angular Position for Quasi-Steady Acceleration

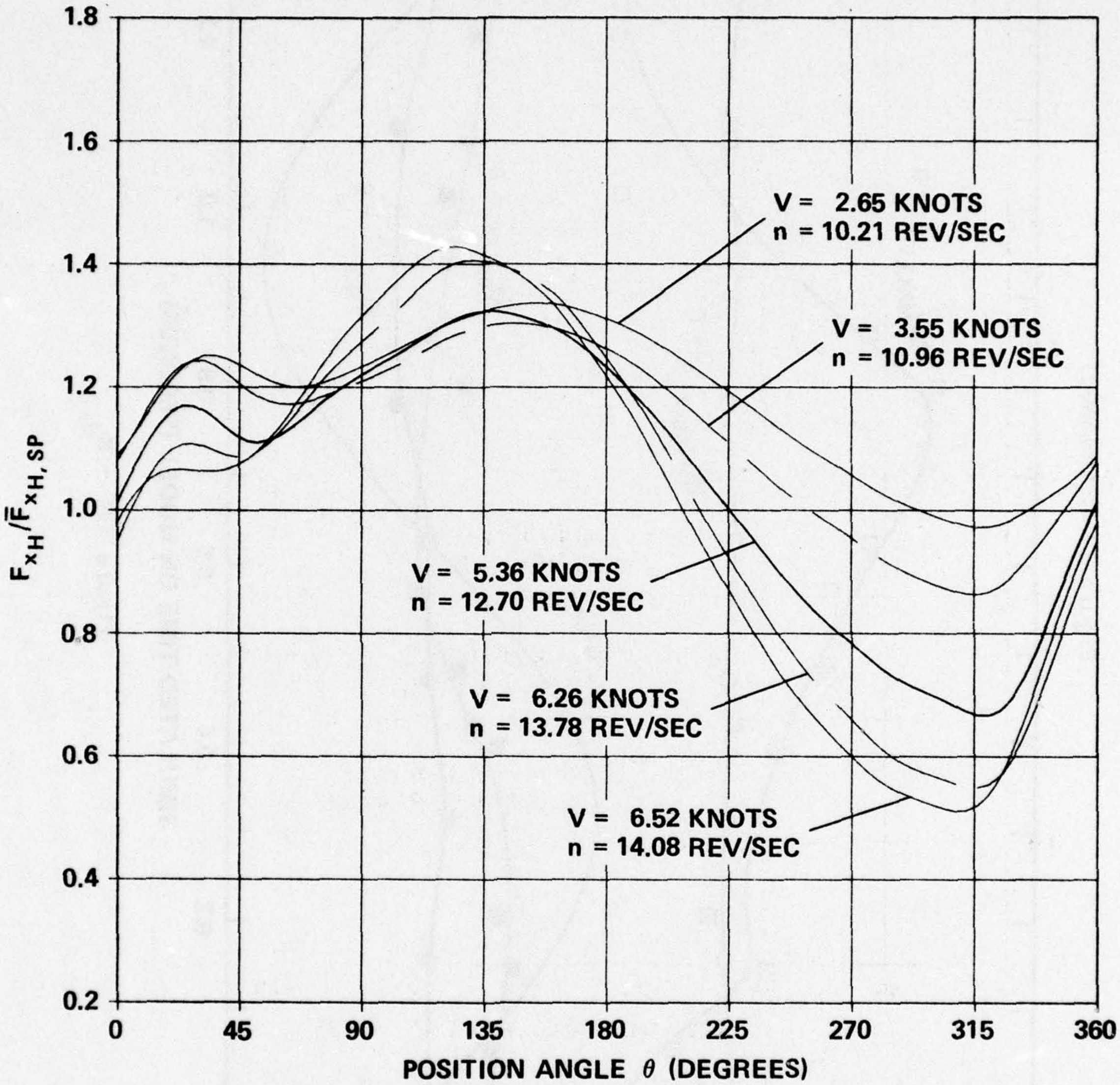

Figure 20a - F_{x_H}

Figure 20 (Continued)

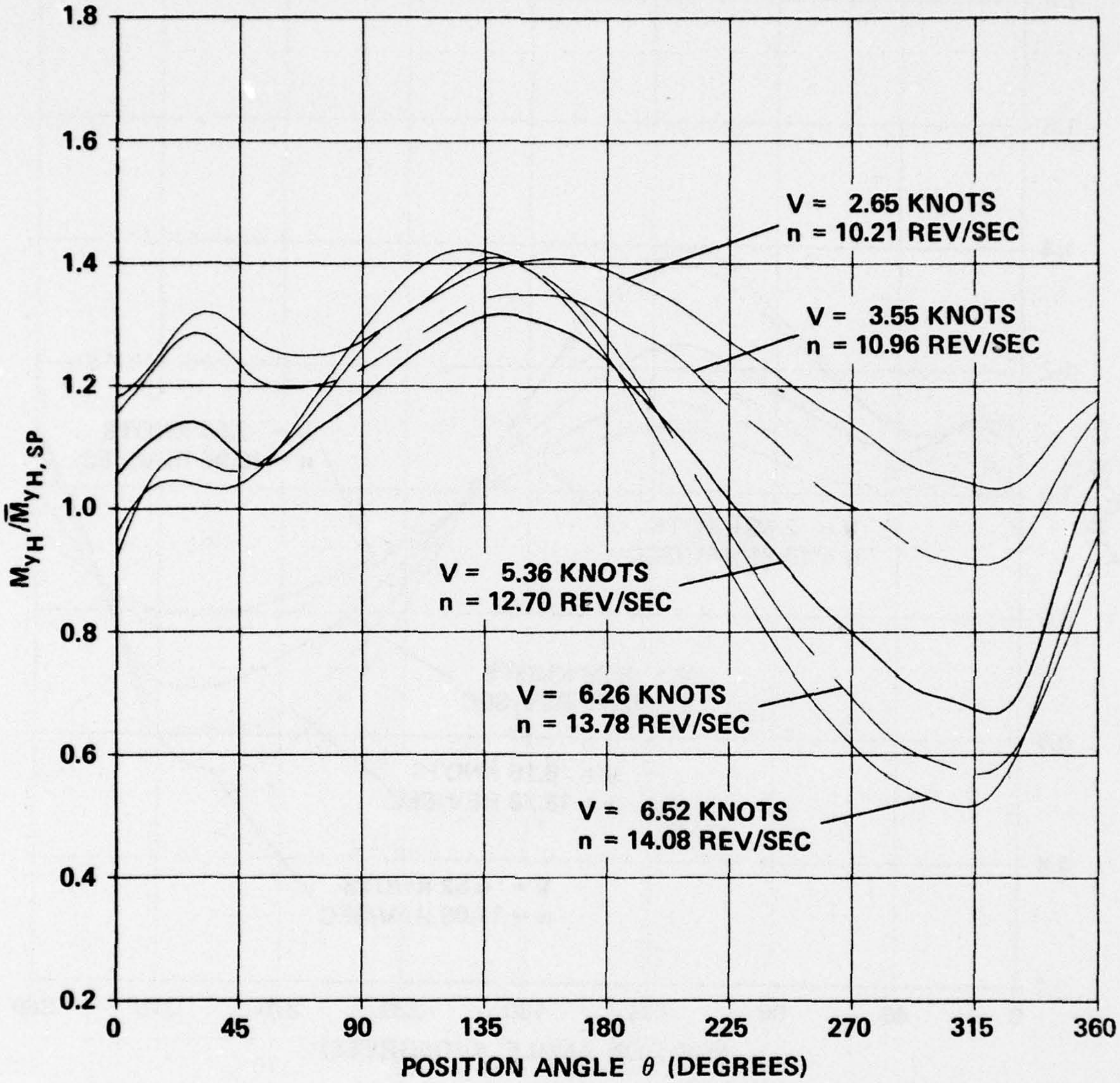

Figure 20b - M_{y_H}

Figure 20 (Continued)

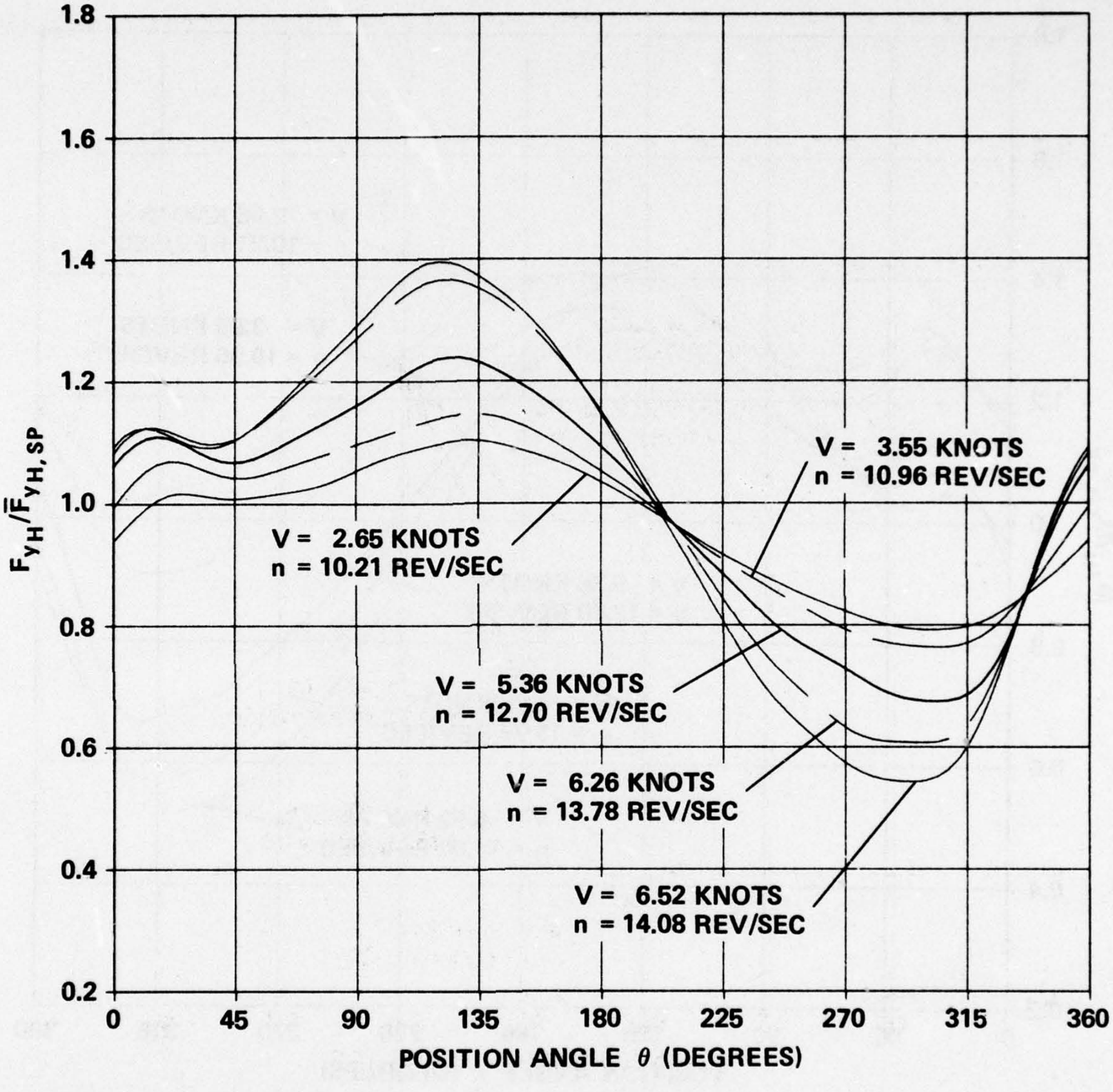

Figure 20c - F_{y_H}

Figure 20 (Continued)

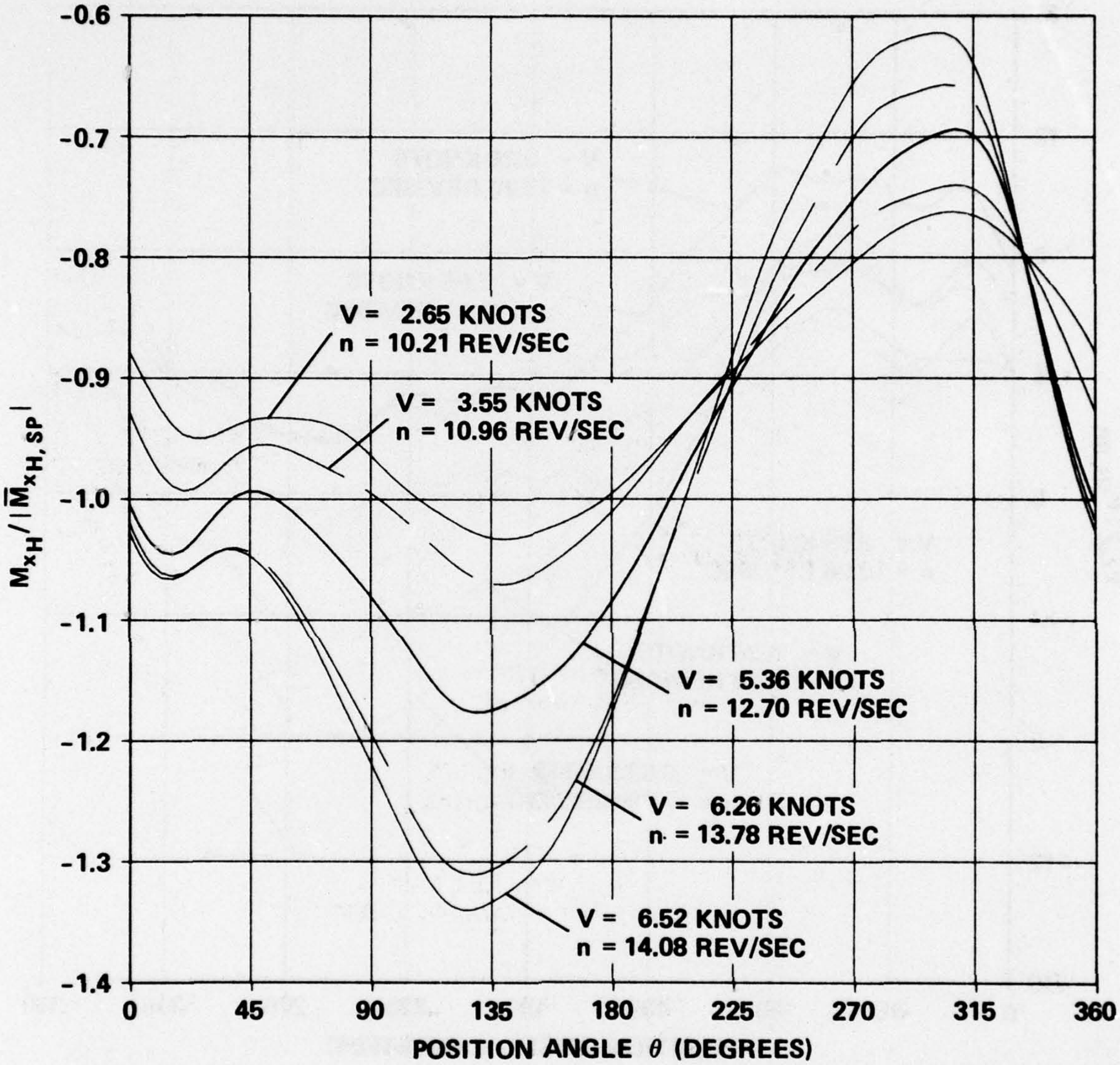

Figure 20d - M_{x_H}

Figure 20 (Continued)

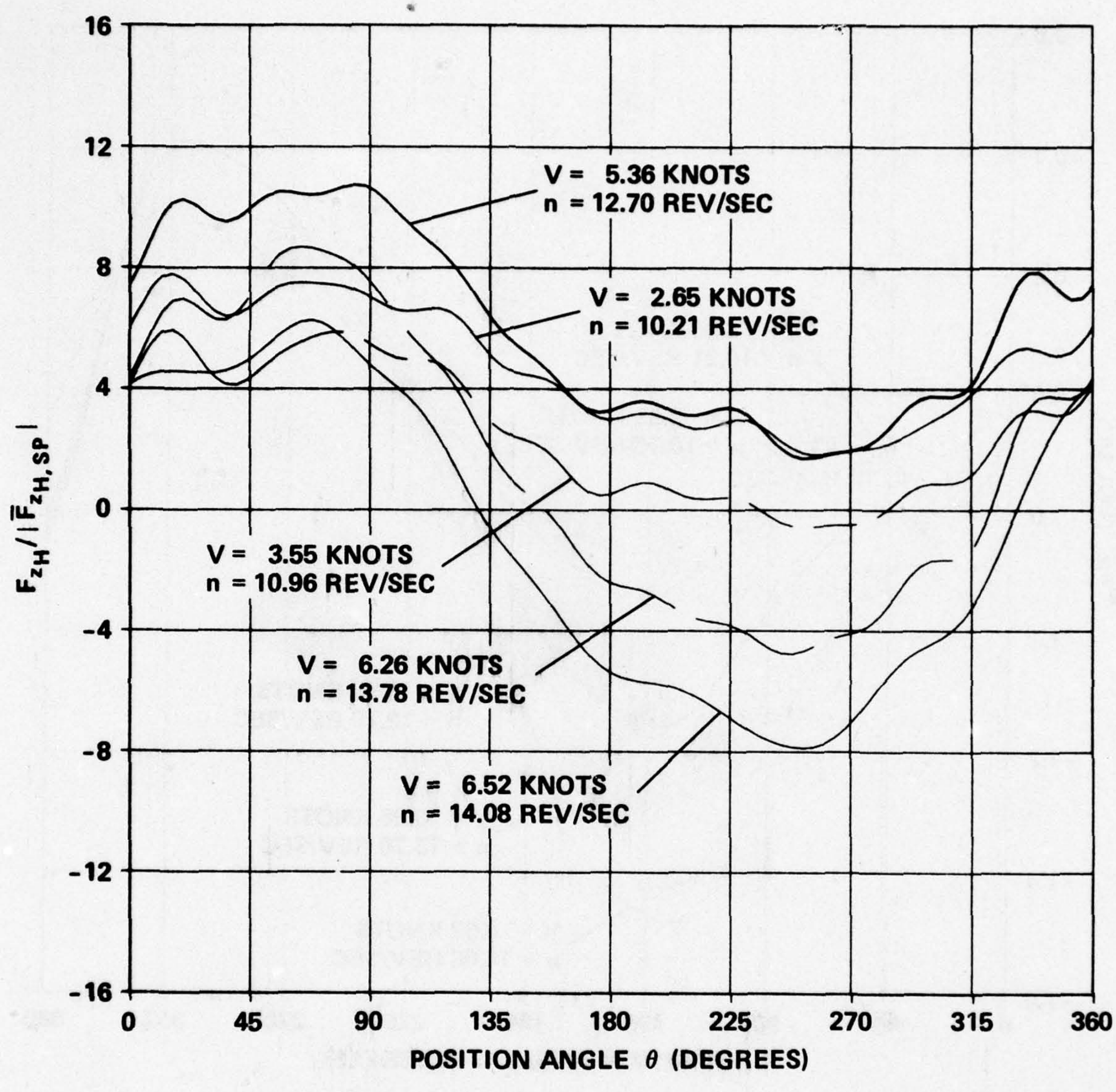

Figure 20e - F_{z_H}

Figure 20 (Continued)

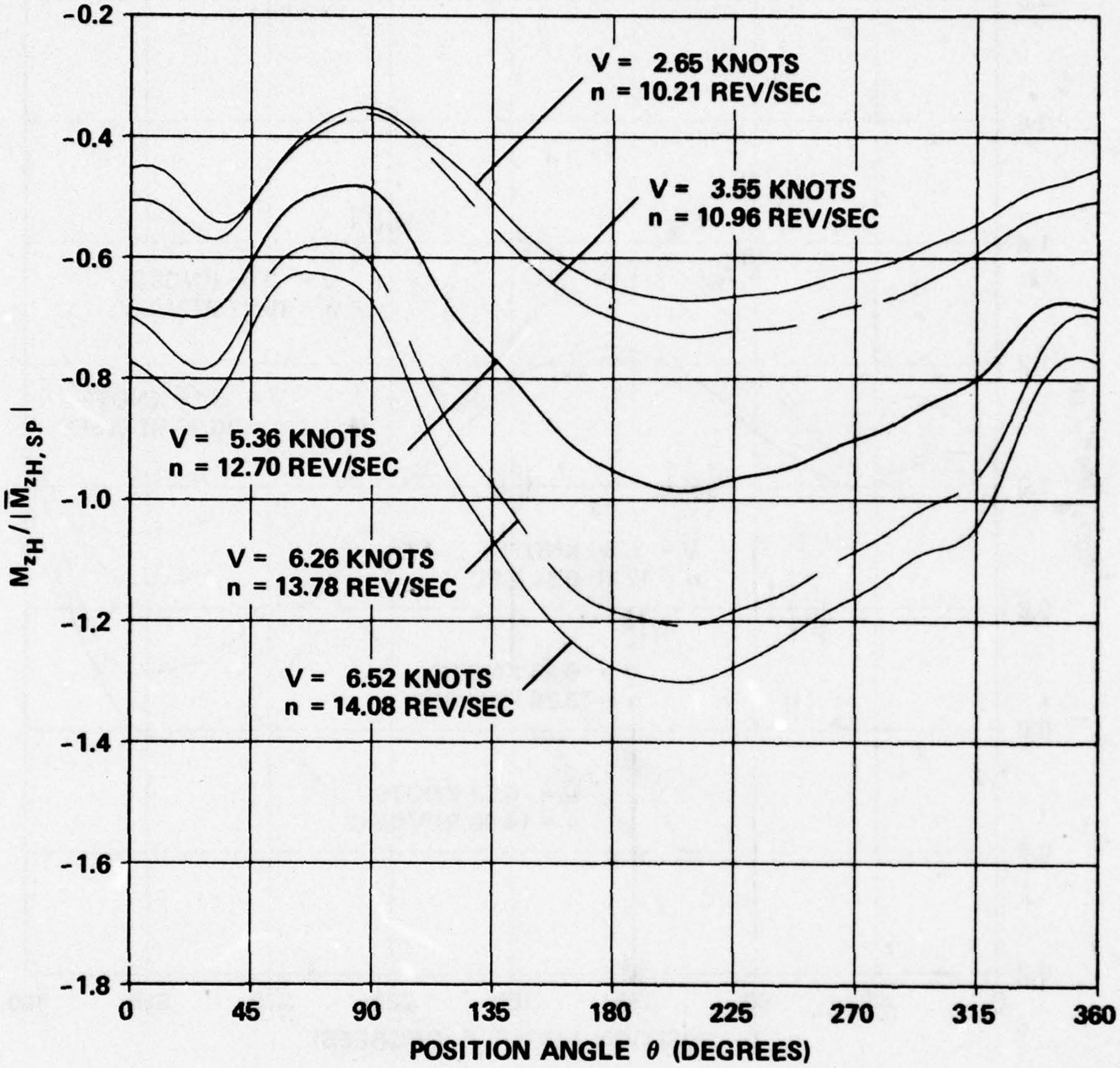

Figure 20f - M_{z_H}

Figure 20 (Continued)

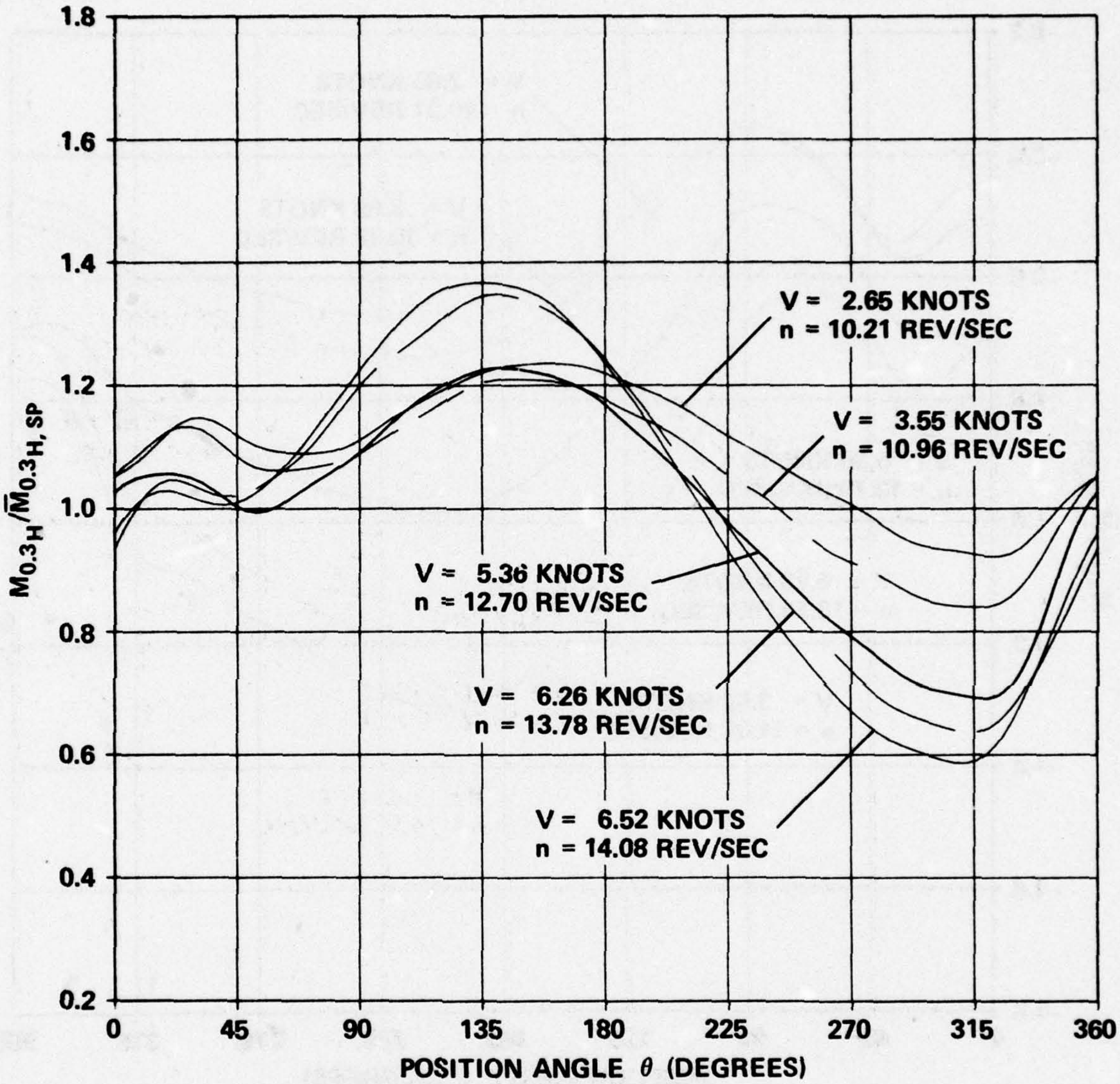

Figure 20g - $M_{0.3_H}$

Figure 20 (Continued)

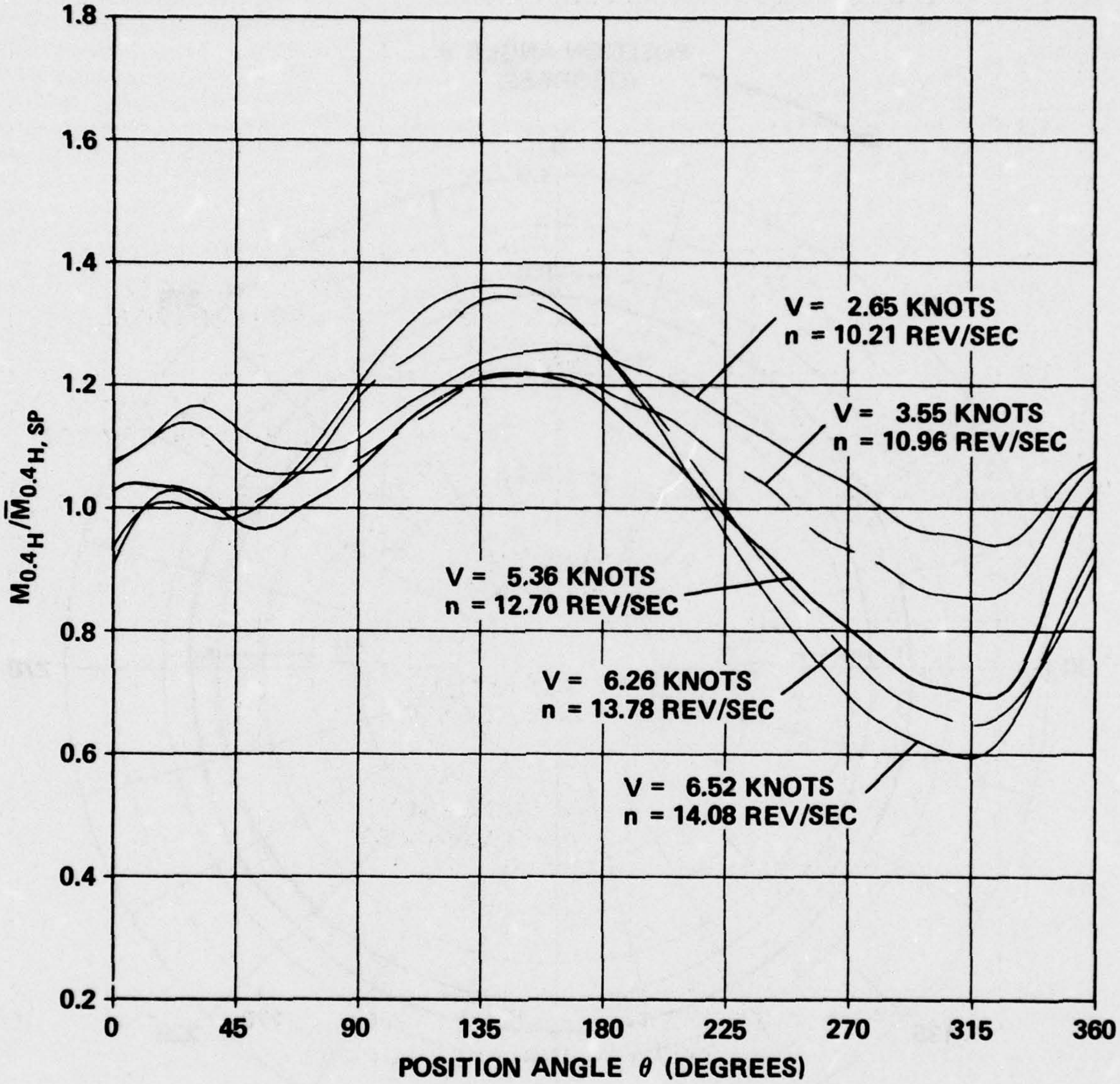

Figure 20h - $M_{0.4_H}$

Figure 21 - Variation in Radial Center of Thrust F_{x_H} and Transverse Hydrodynamic Force F_{y_H} with Blade Angular Position for Quasi-Steady Acceleration

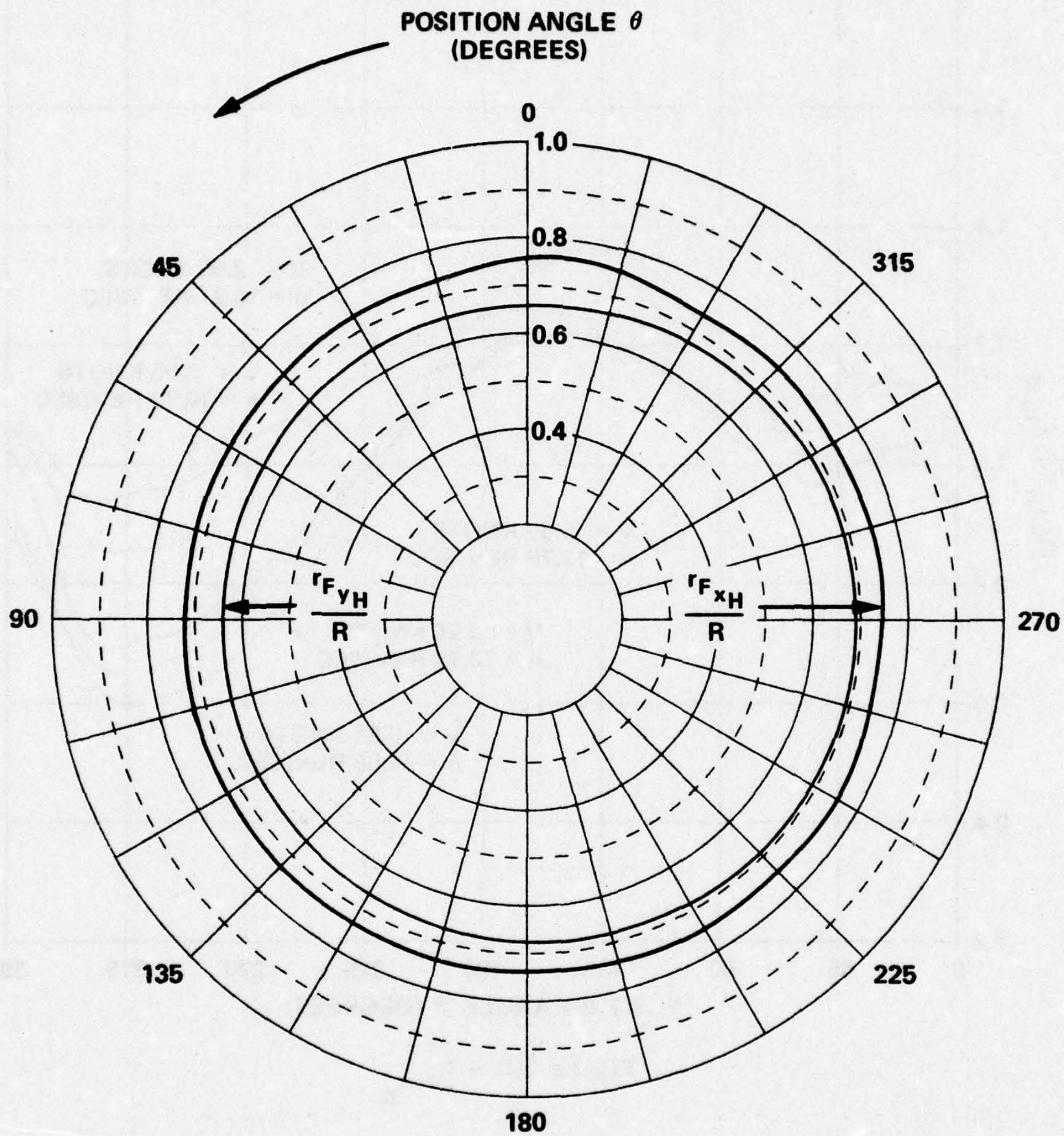

Figure 21a - V = 2.65 Knots, n = 10.21 Revolutions per Second, J_v = 0.64

Figure 21 (Continued)

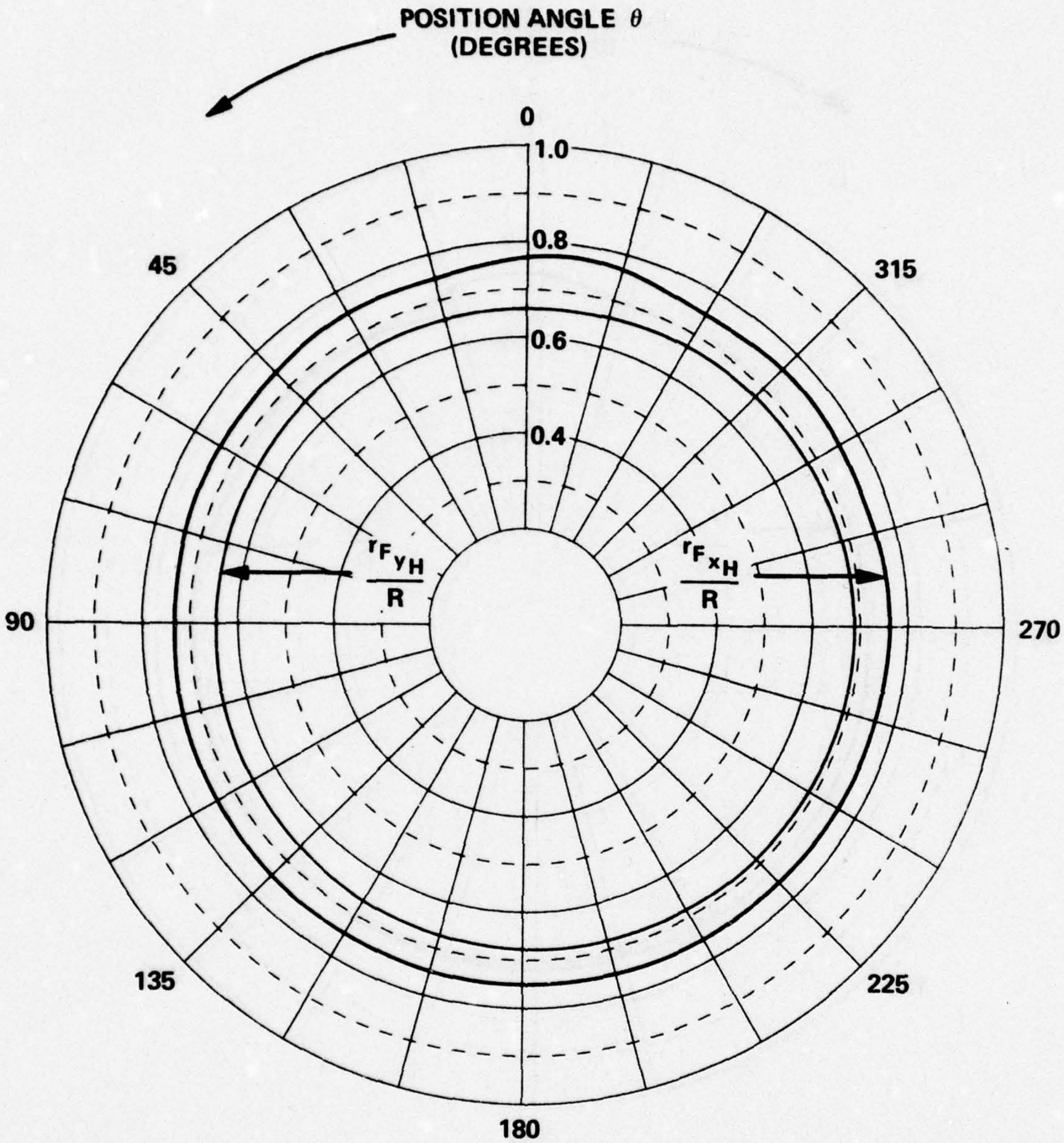

Figure 21b - V = 3.55 Knots, n = 10.96 Revolutions per Second, J_V = 0.80

Figure 21 (Continued)

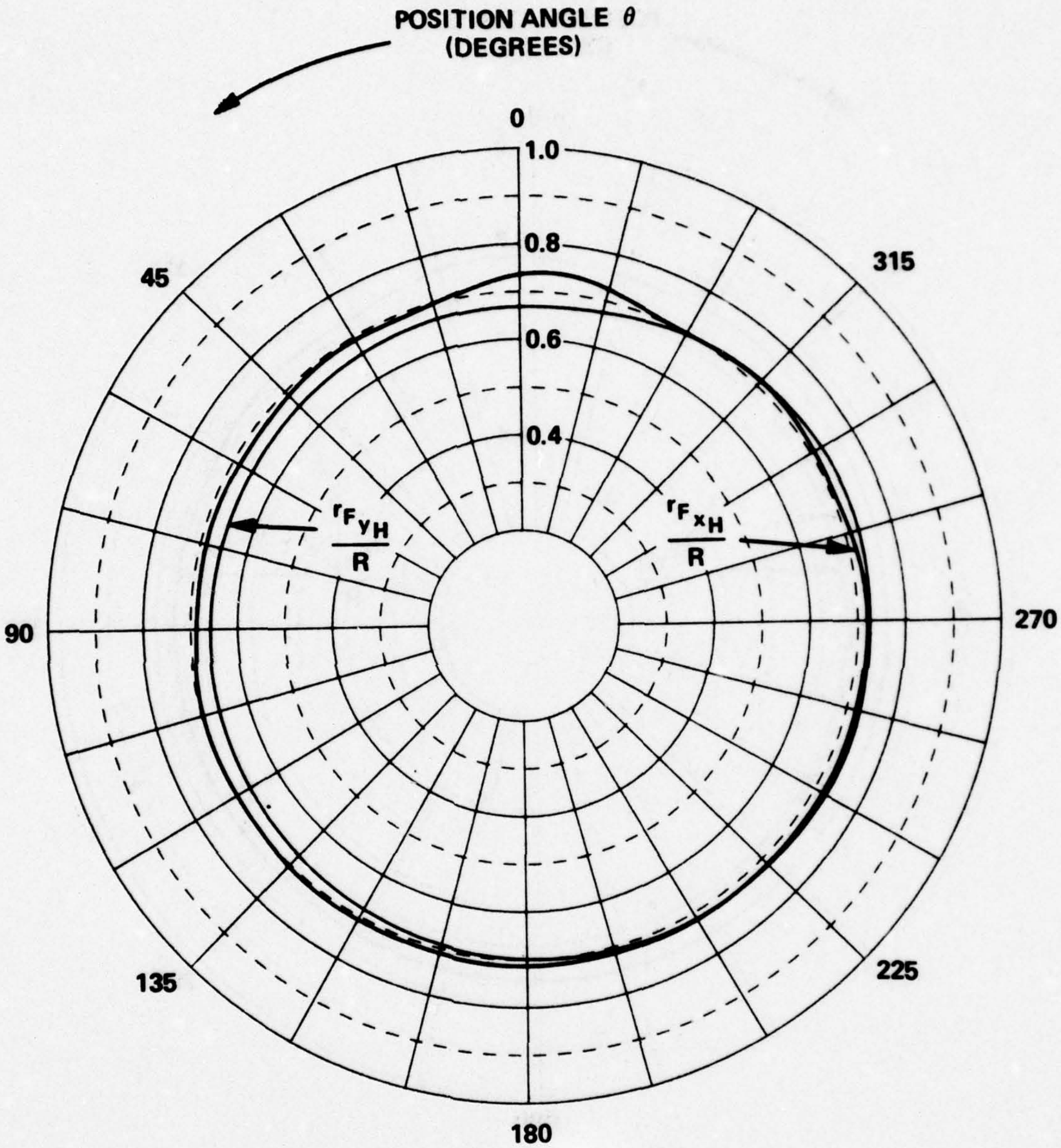

Figure 21c - V = 5.36 Knots, n = 12.70 Revolutions per Second, $J_V = 1.04$

Figure 21 (Continued)

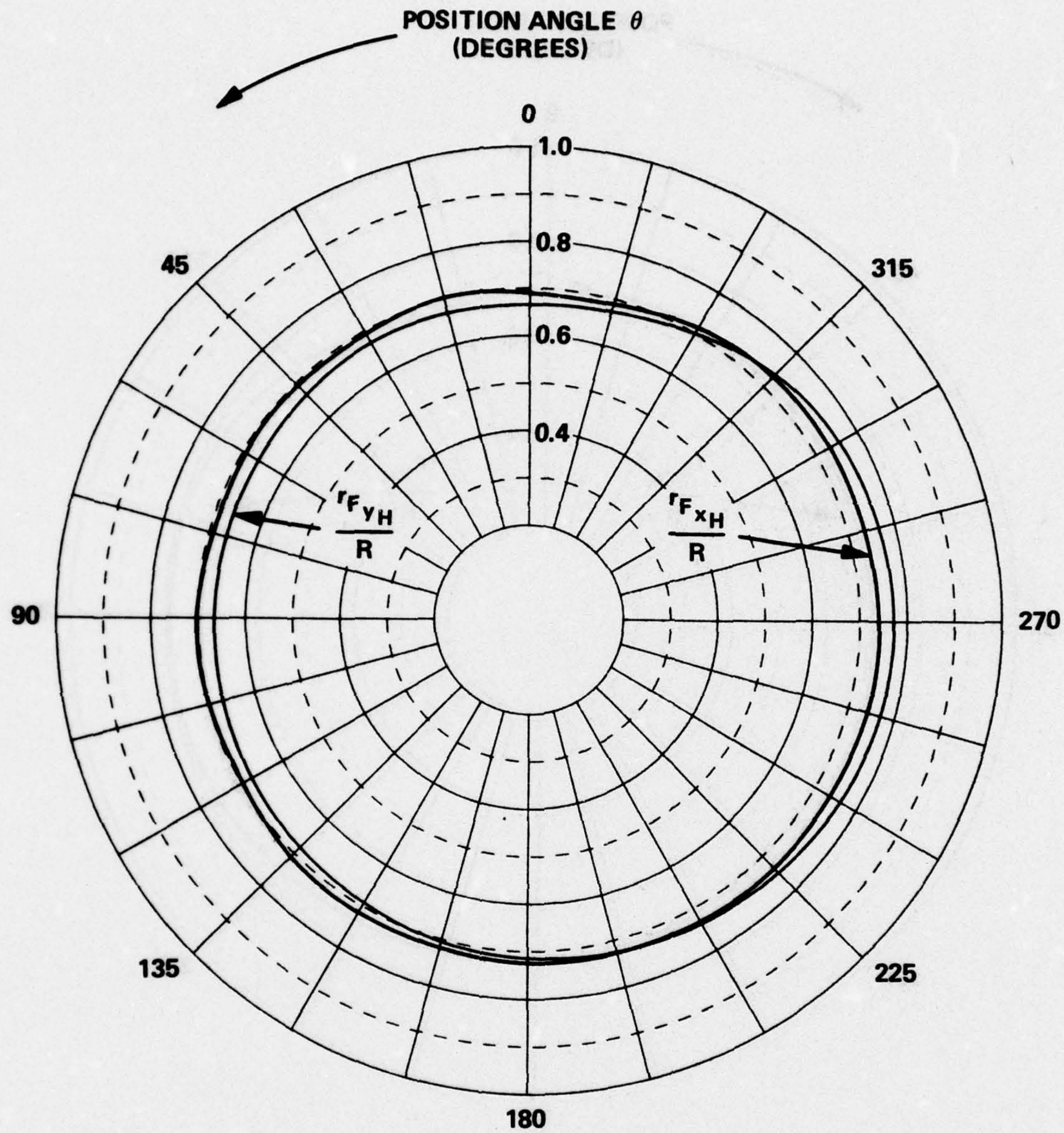

Figure 21d - V = 6.26 Knots, n = 13.78 Revolutions per Second, J_v = 1.12

Figure 21 (Continued)

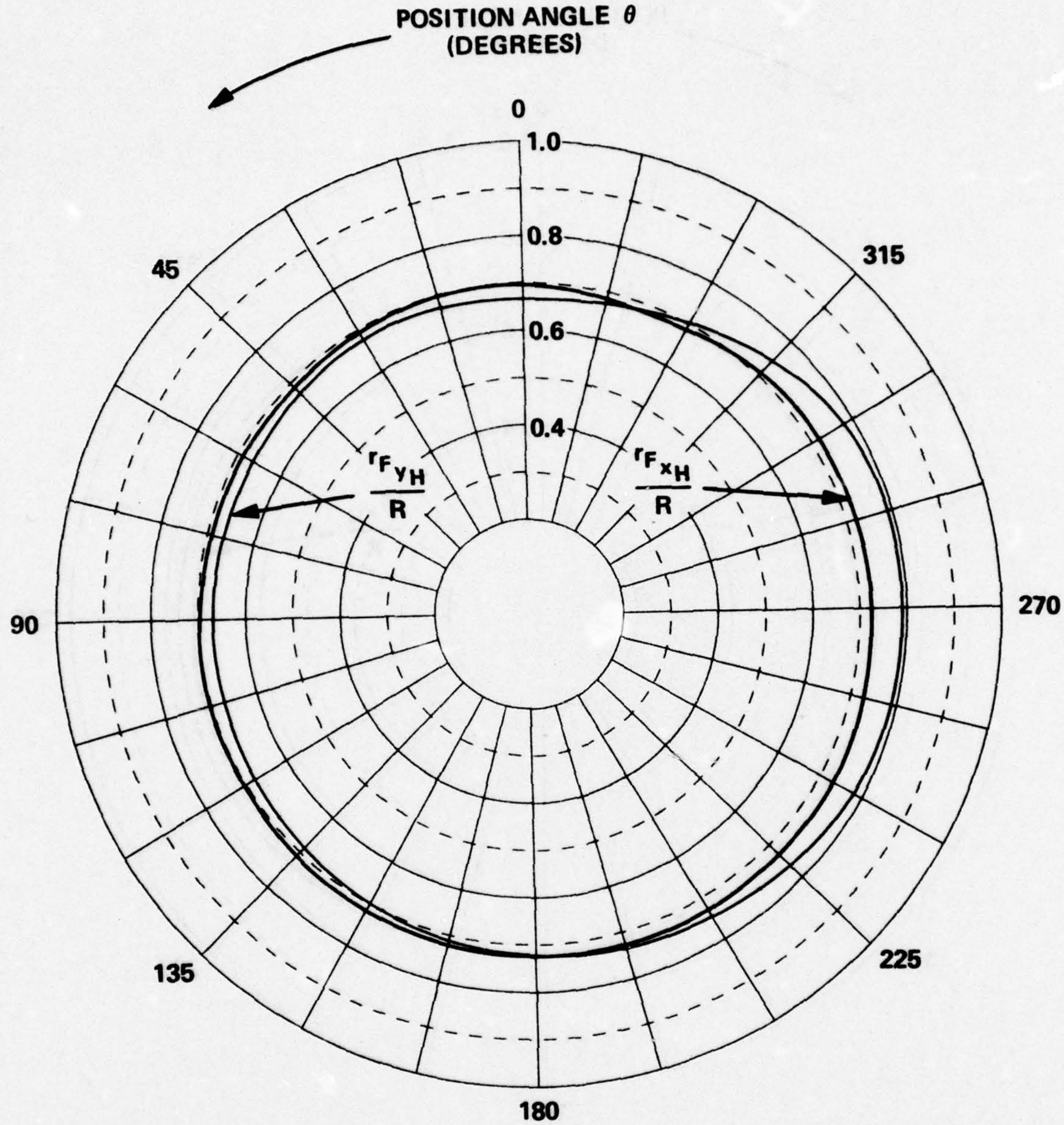

Figure 21e - V = 6.52 Knots, n = 14.08 Revolutions per Second, J_v = 1.14

Figure 22 - Variation of Experimental Total Loads with Angular Position for Quasi-Steady Acceleration

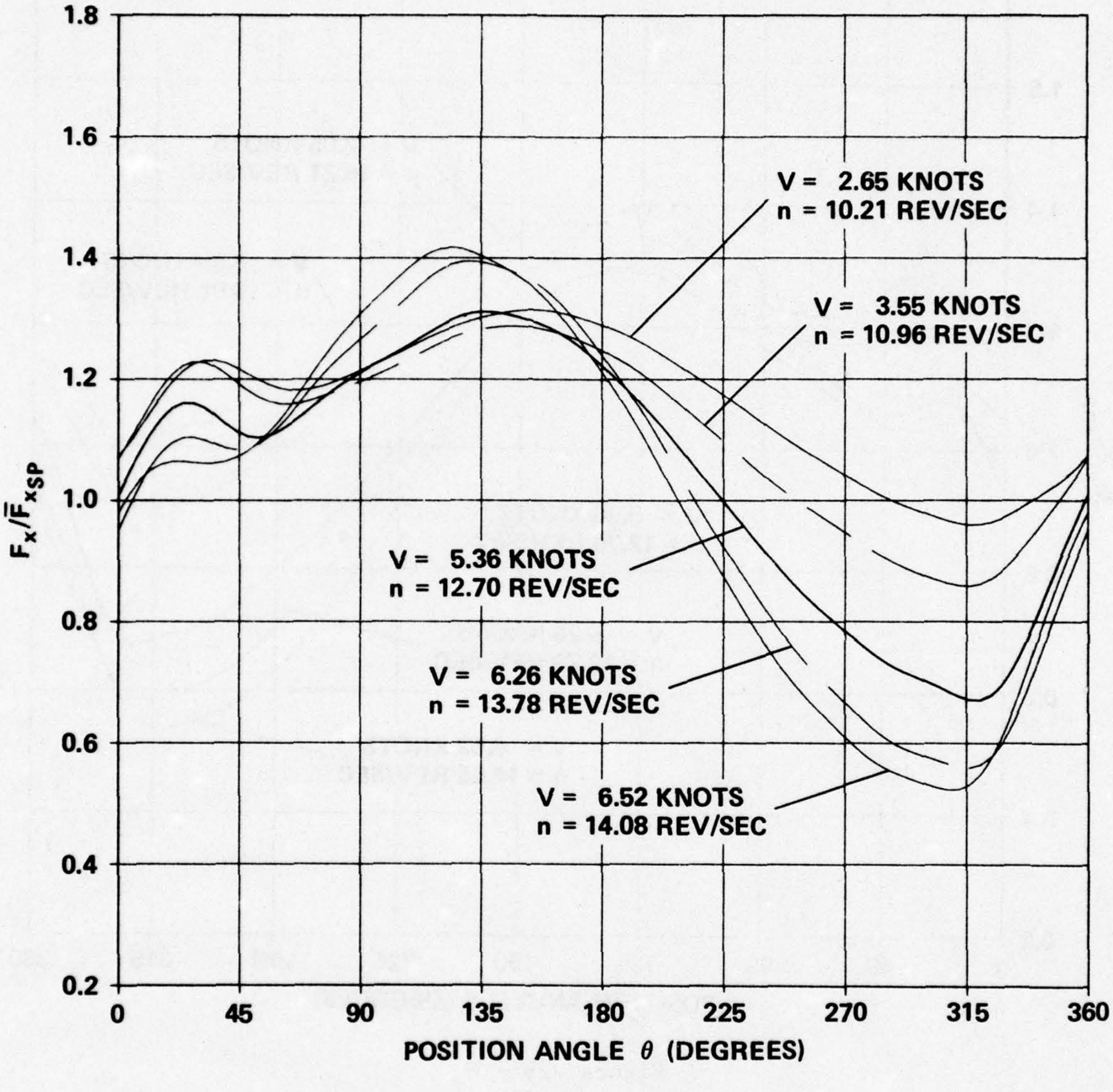

Figure 22a - F_x

Figure 22 (Continued)

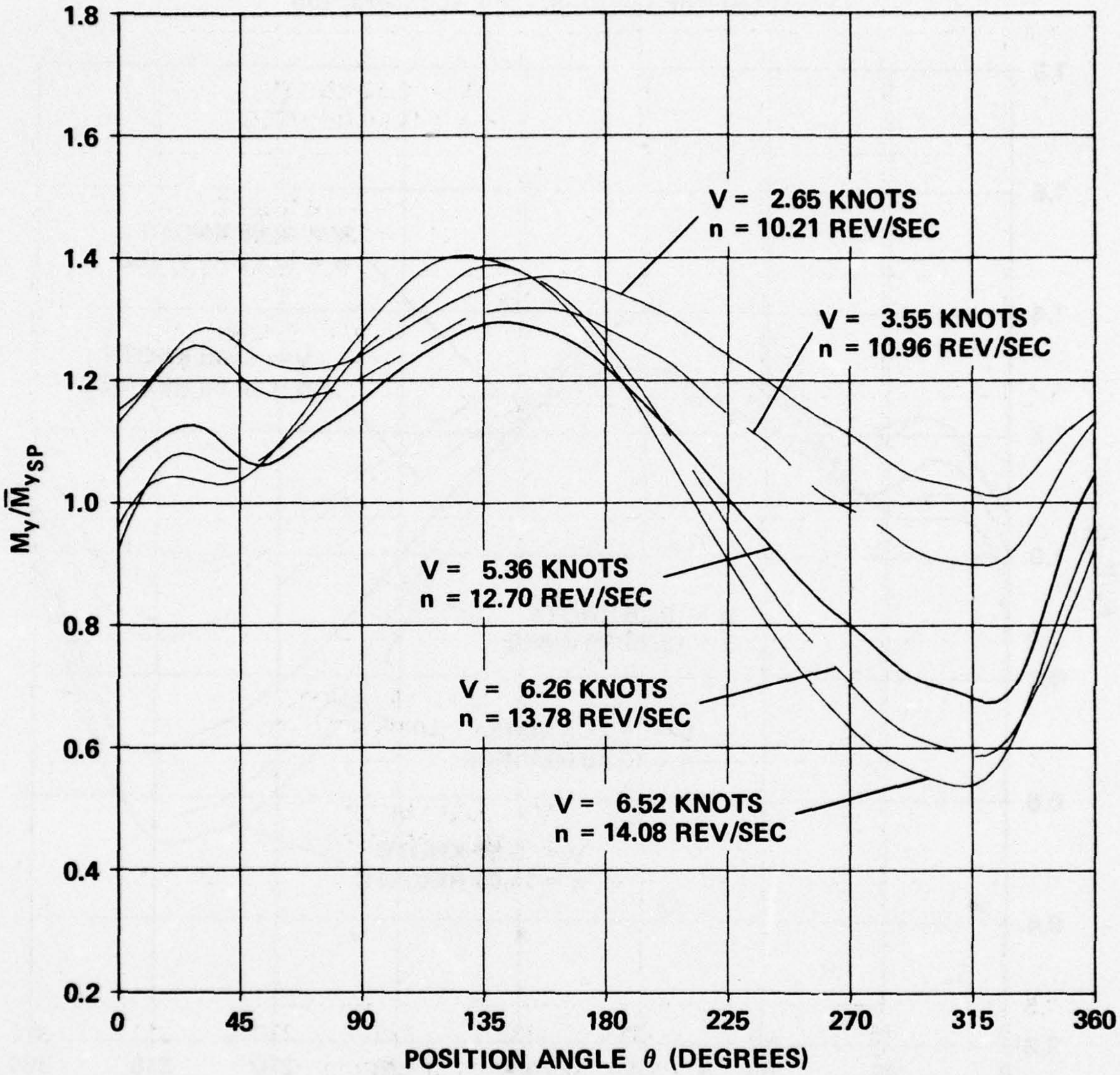

Figure 22b - M_y

Figure 22 (Continued)

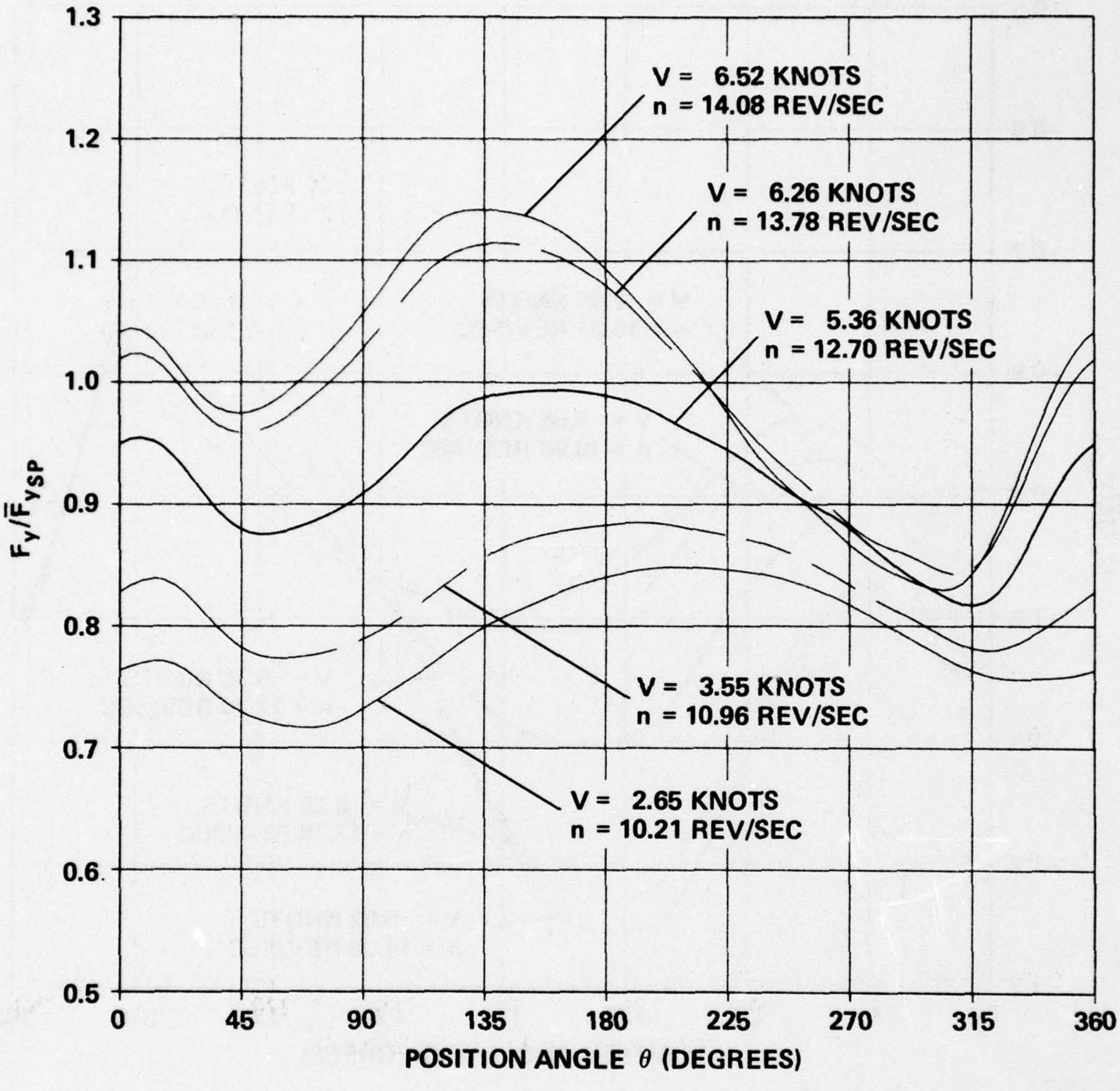

Figure 22c - F_y

Figure 22 (Continued)

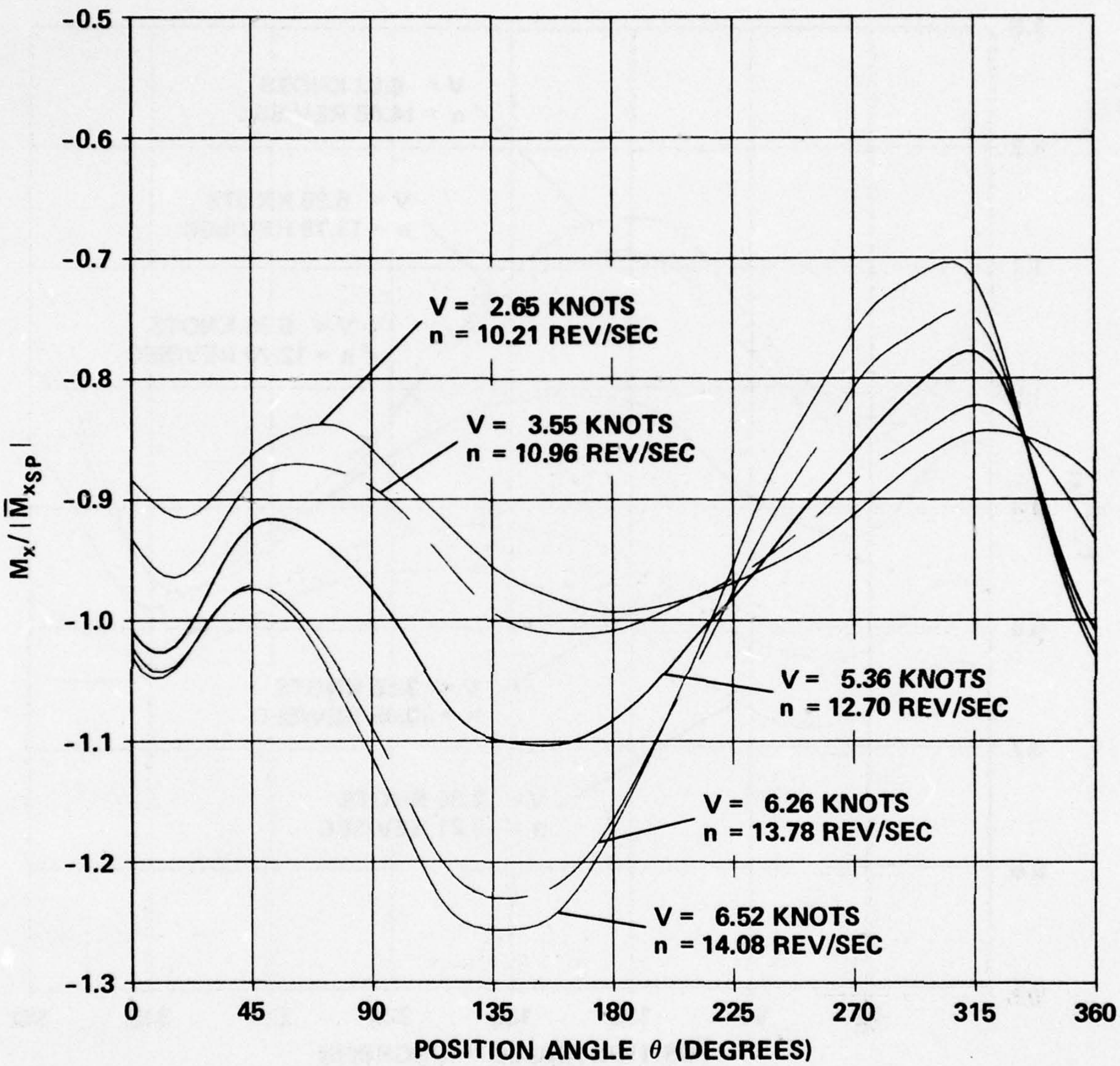

Figure 22d - M_x

Figure 22 (Continued)

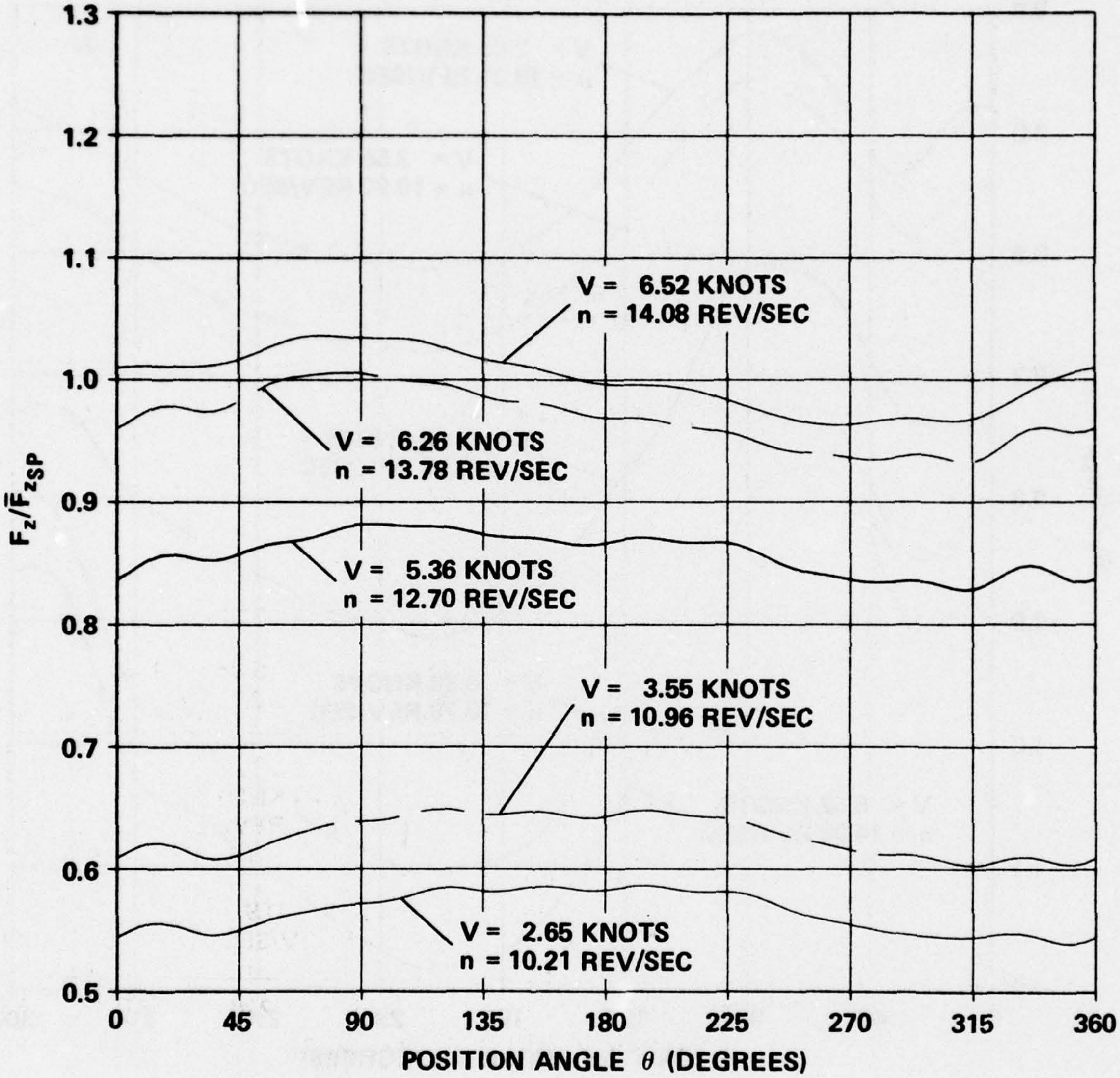

Figure 22e - F_z

Figure 22 (Continued)

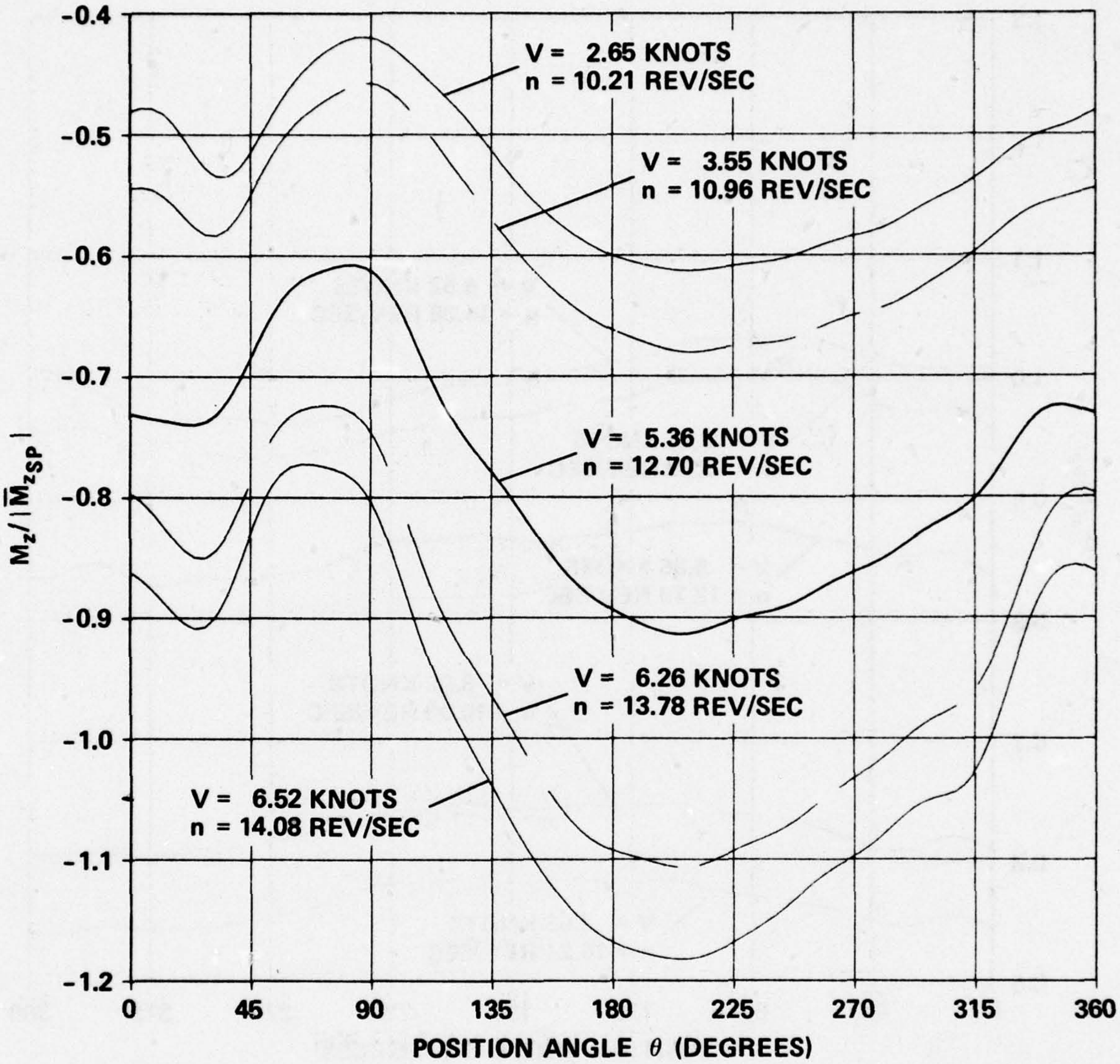

Figure 22f - M_z

Figure 22 (Continued)

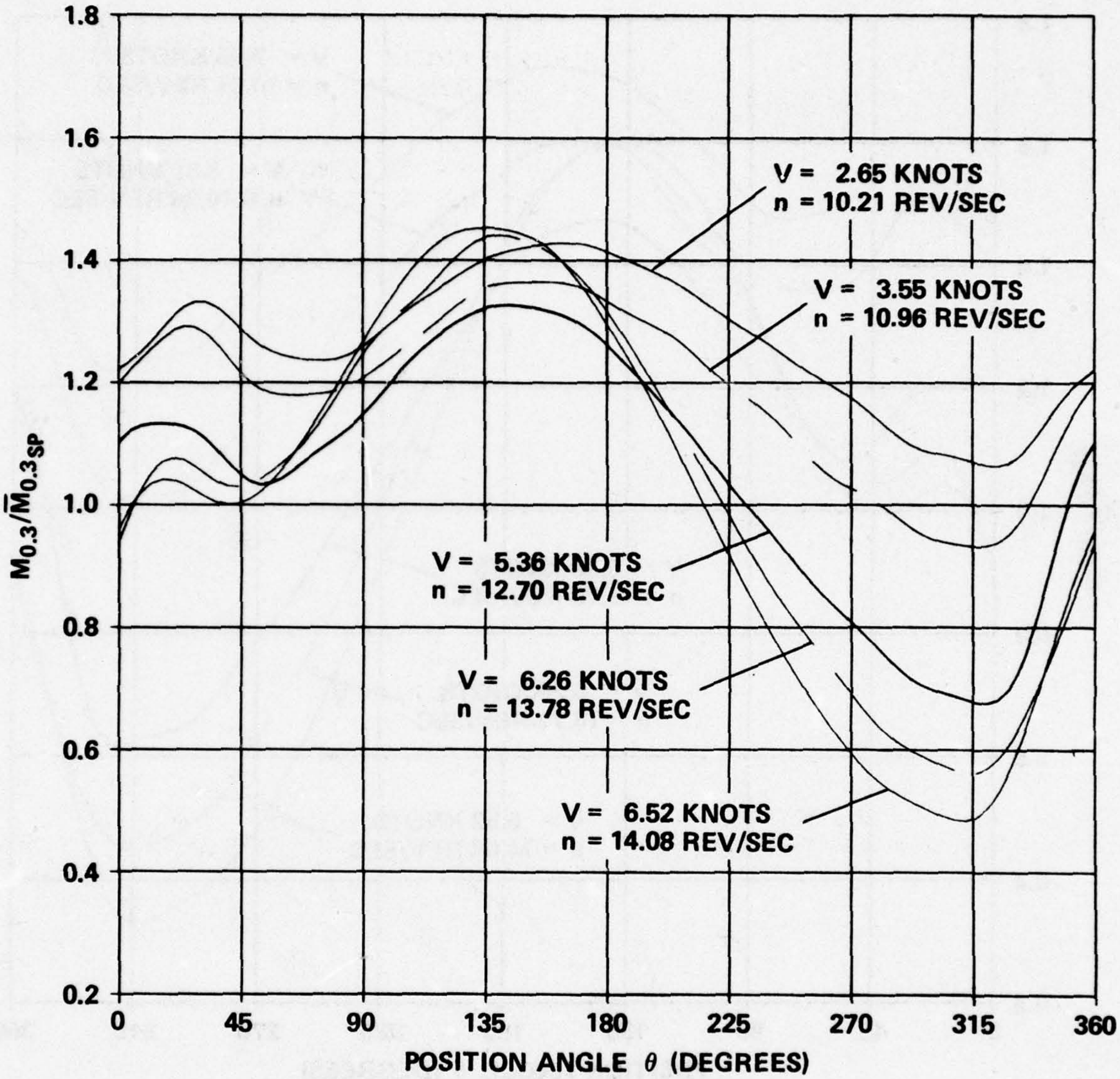

Figure 22g - $M_{0.3}$

Figure 22 (Continued)

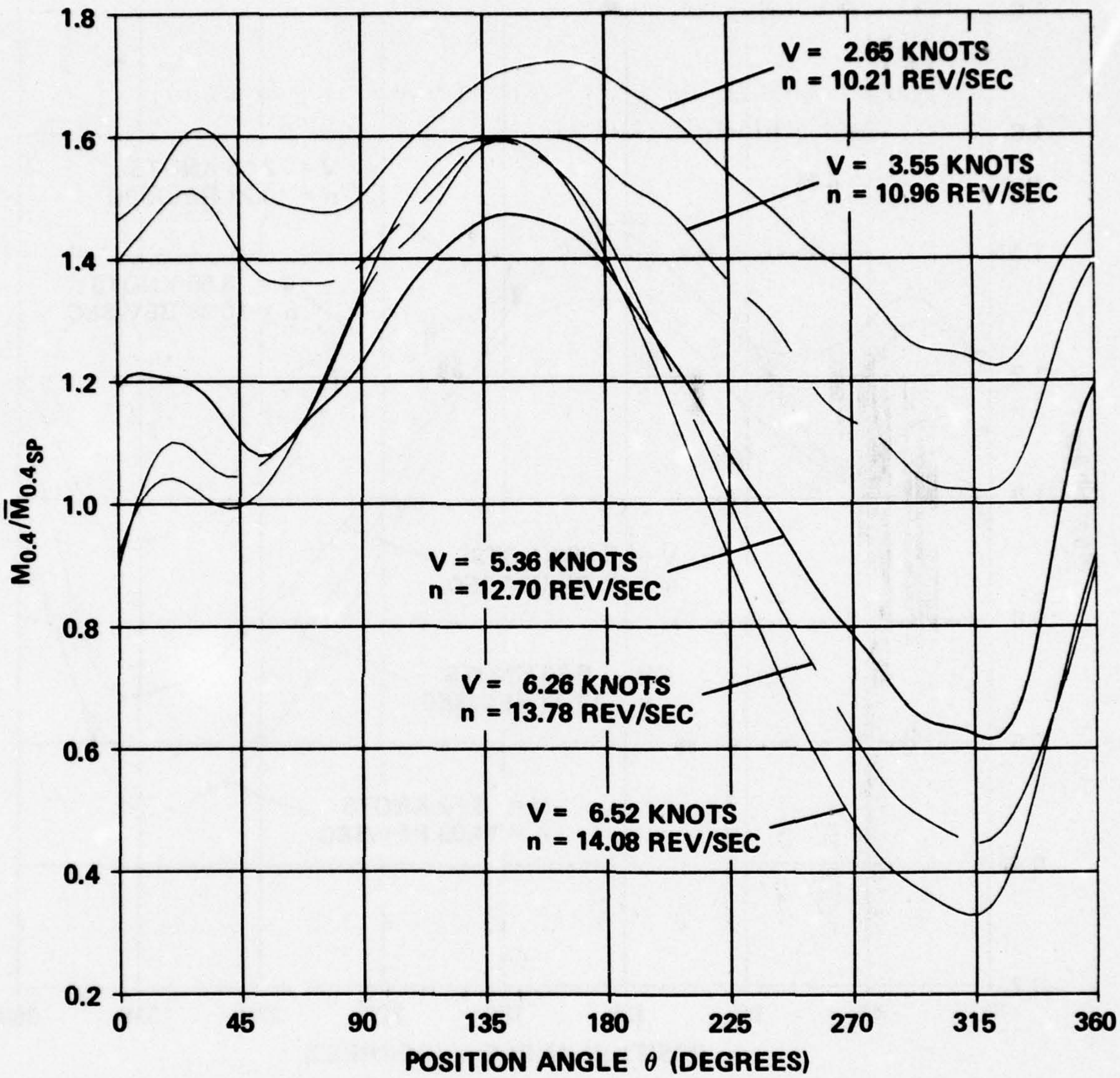

Figure 22h - $M_{0.4}$

Figure 23 - Harmonic Content of Experimental Hydrodynamic Loads for Quasi-Steady Acceleration

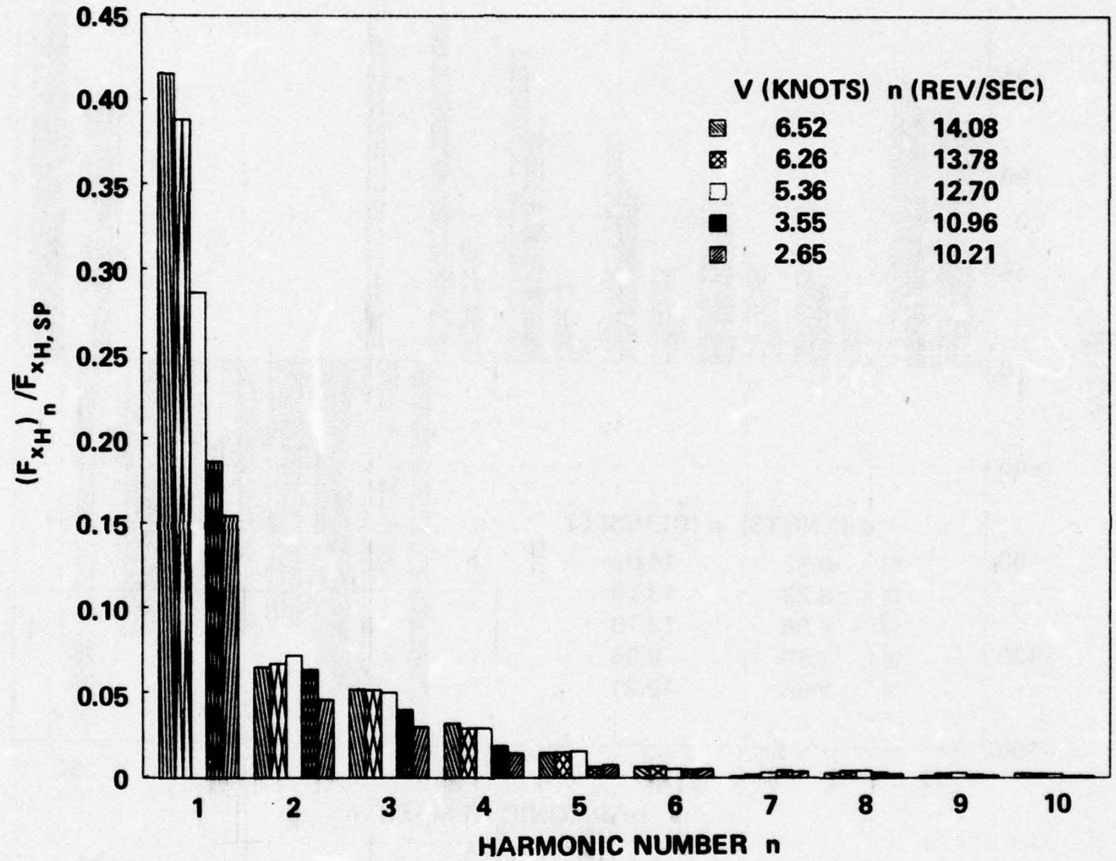

Figure 23a - F_{x_H}

Figure 23 (Continued)

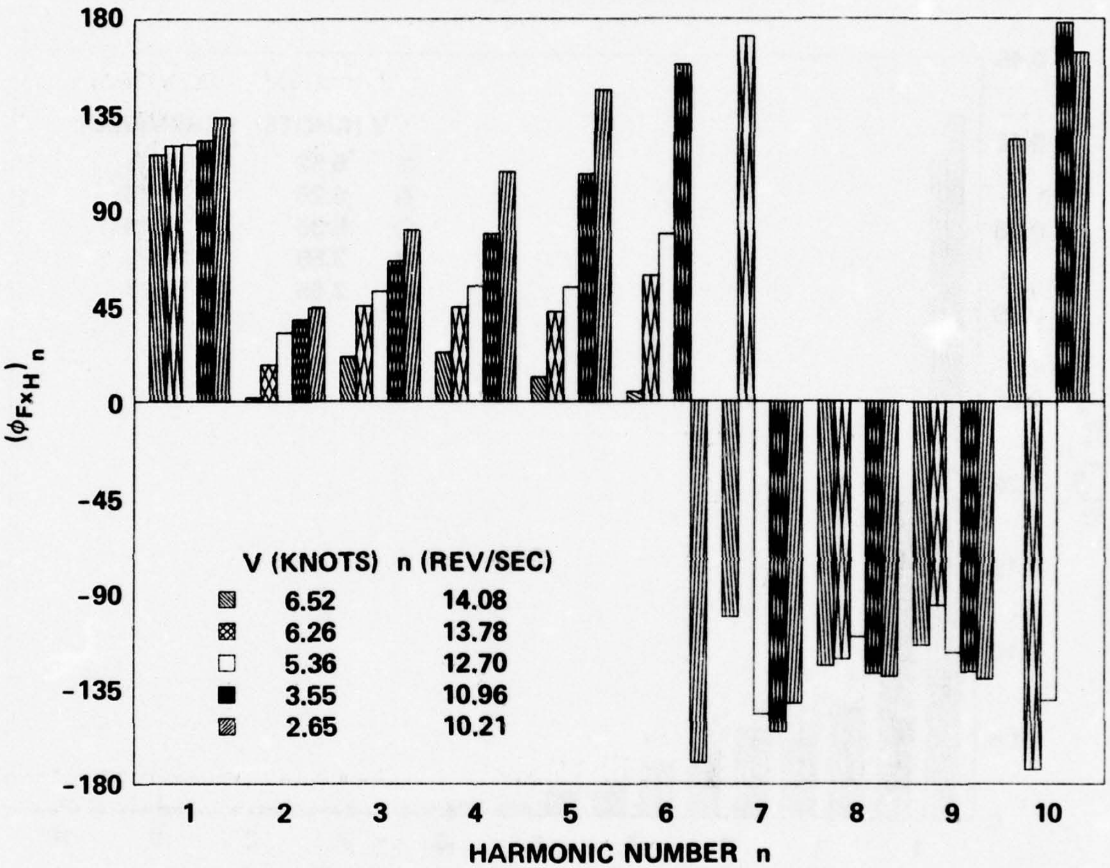

Figure 23a (Continued)

Figure 23 (Continued)

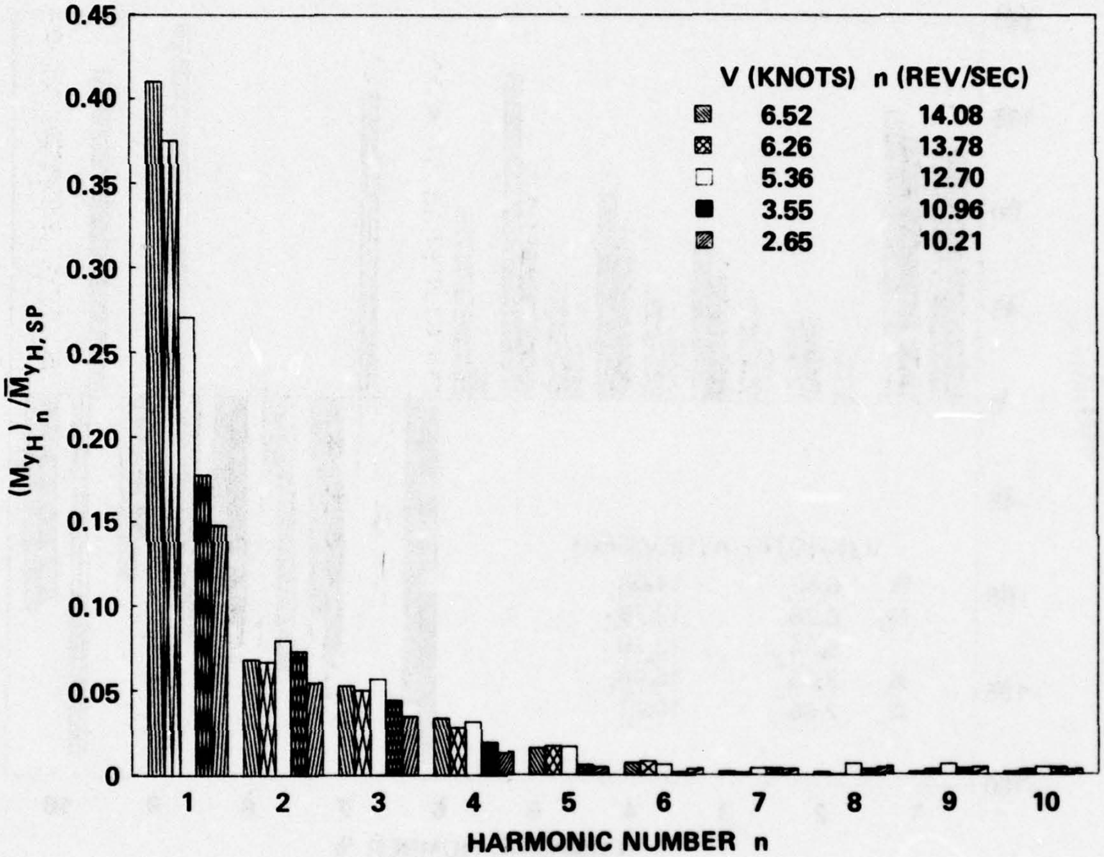

Figure 23b - M_{y_H}

Figure 23 (Continued)

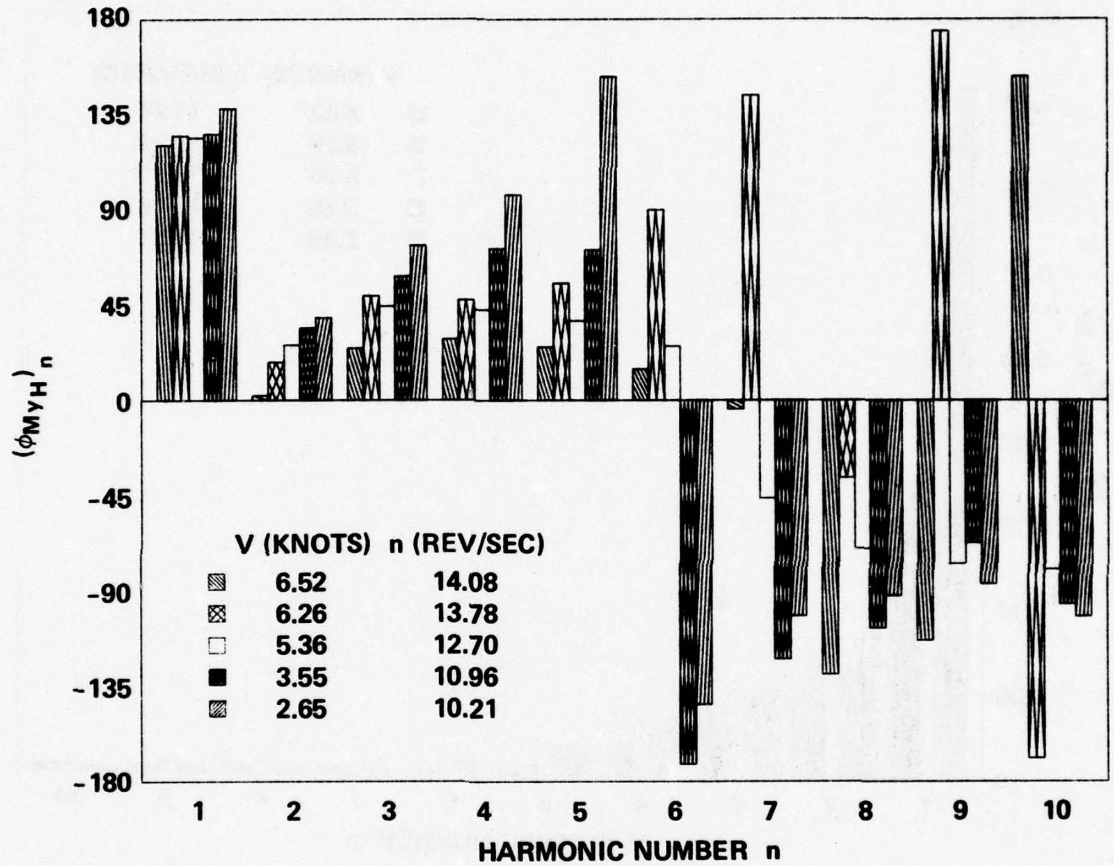

Figure 23b (Continued)

Figure 23 (Continued)

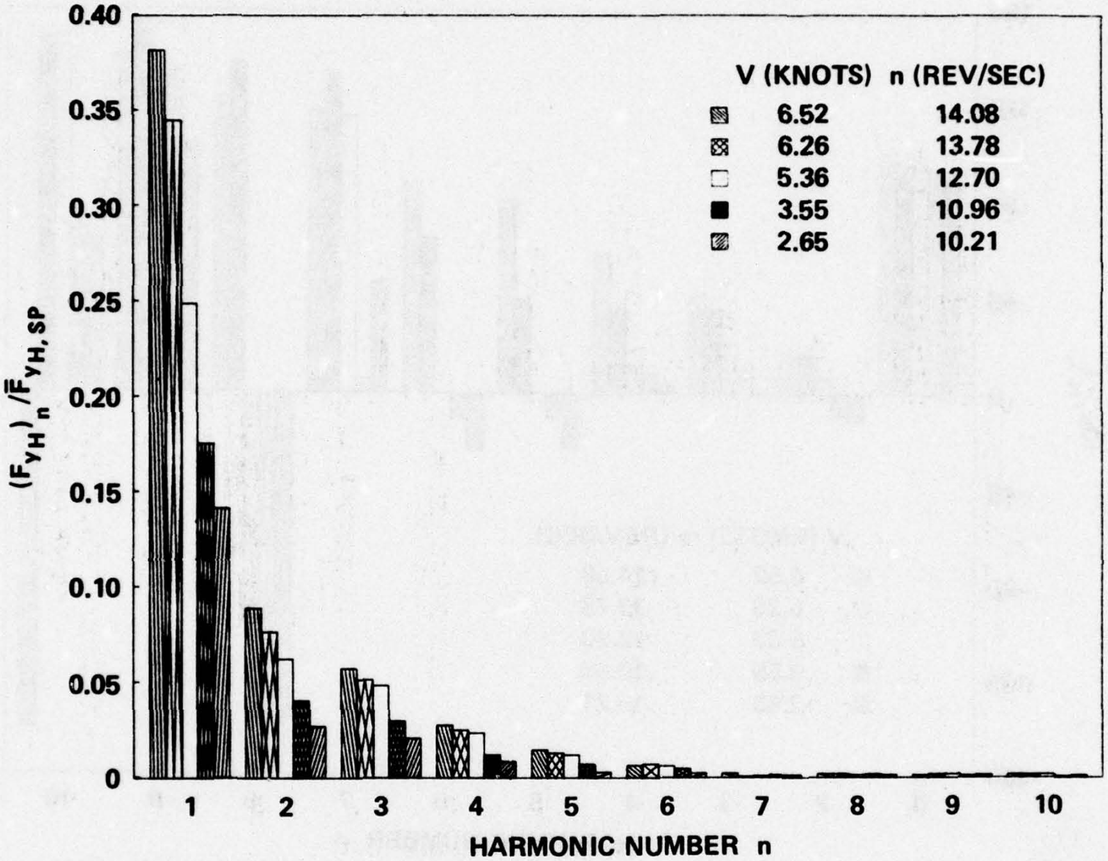

Figure 23c - F_{y_H}

Figure 23 (Continued)

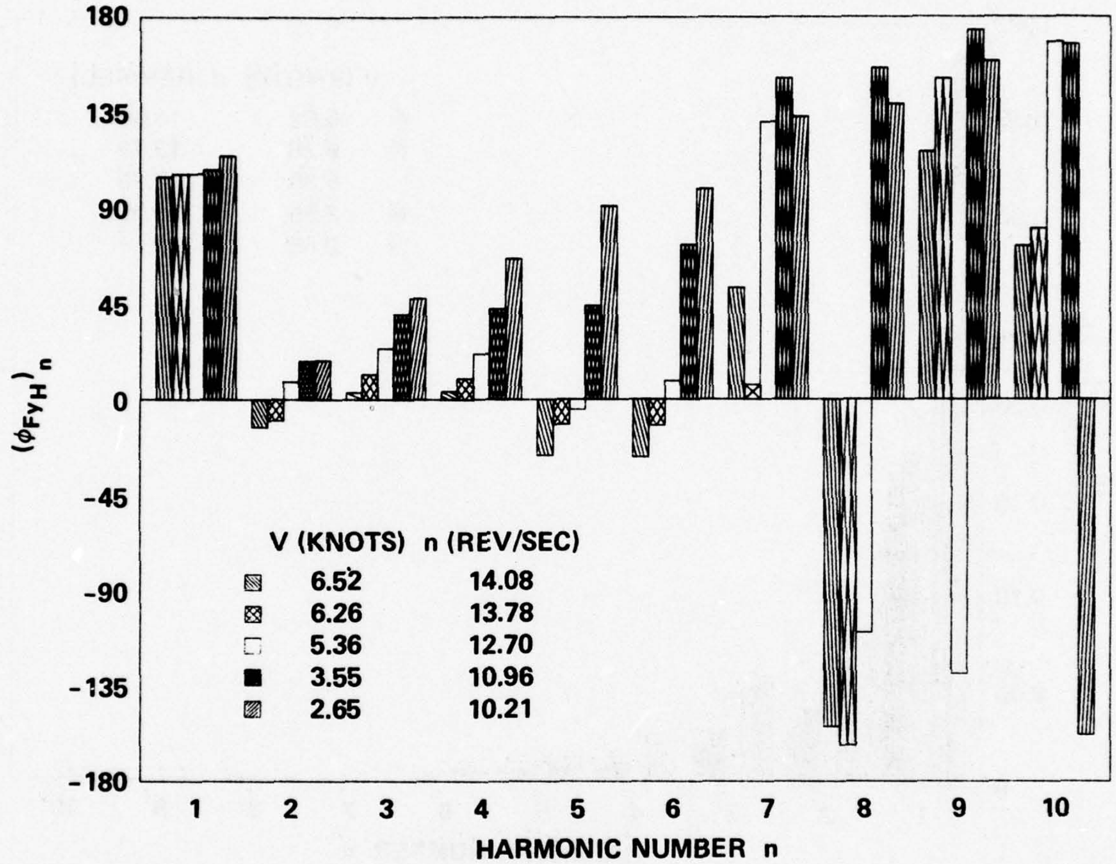

Figure 23c (Continued)

Figure 23 (Continued)

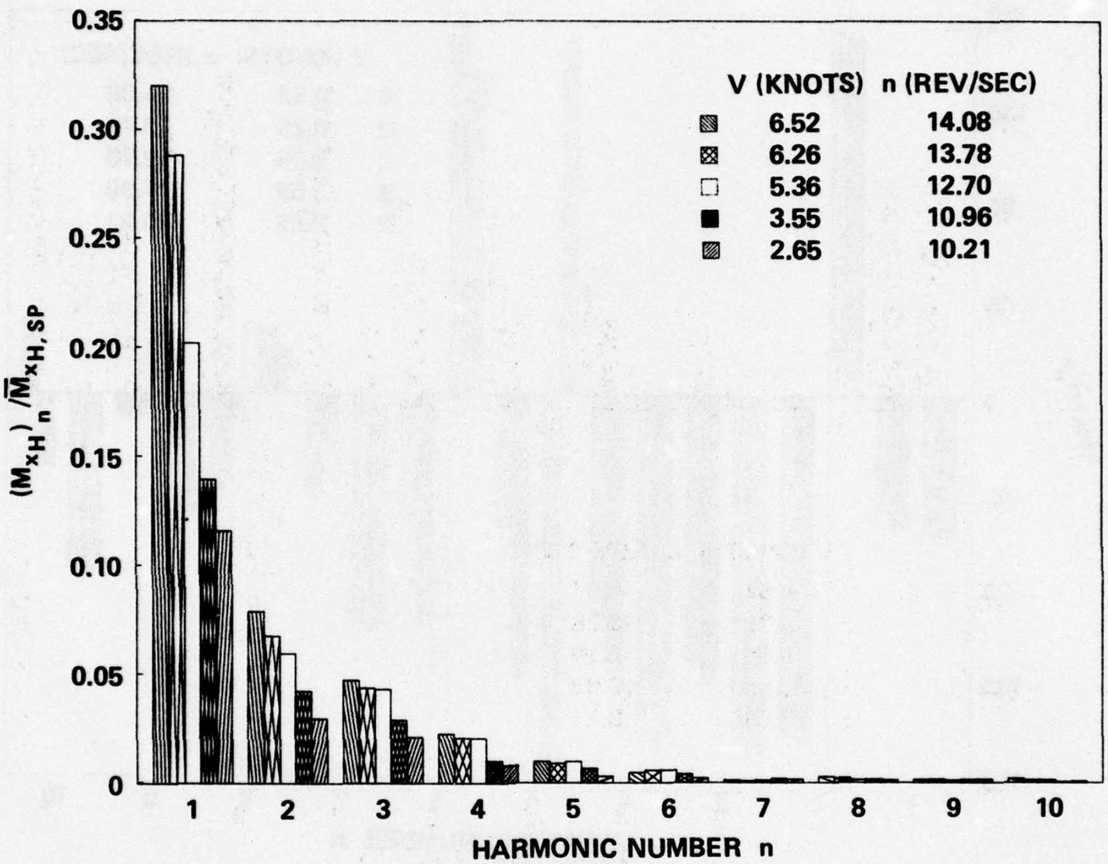

Figure 23d - M_{x_H}

Figure 23 (Continued)

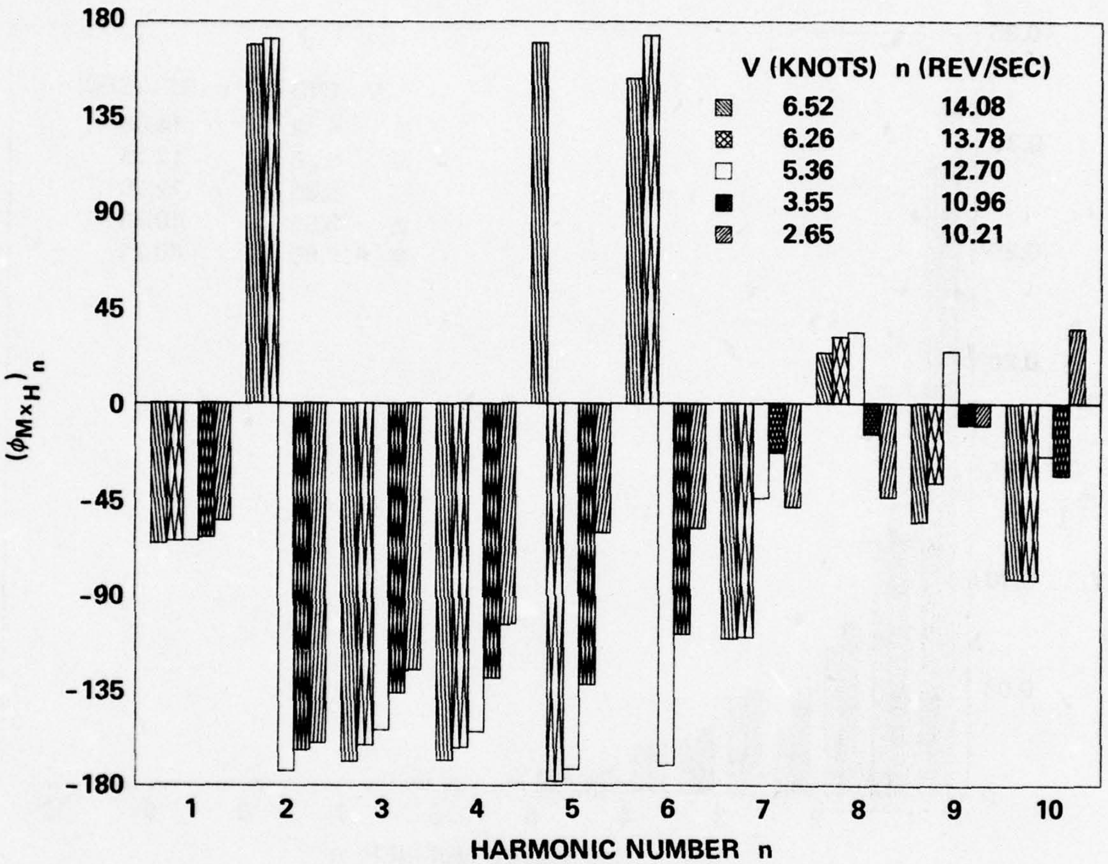

Figure 23d (Continued)

Figure 23 (Continued)

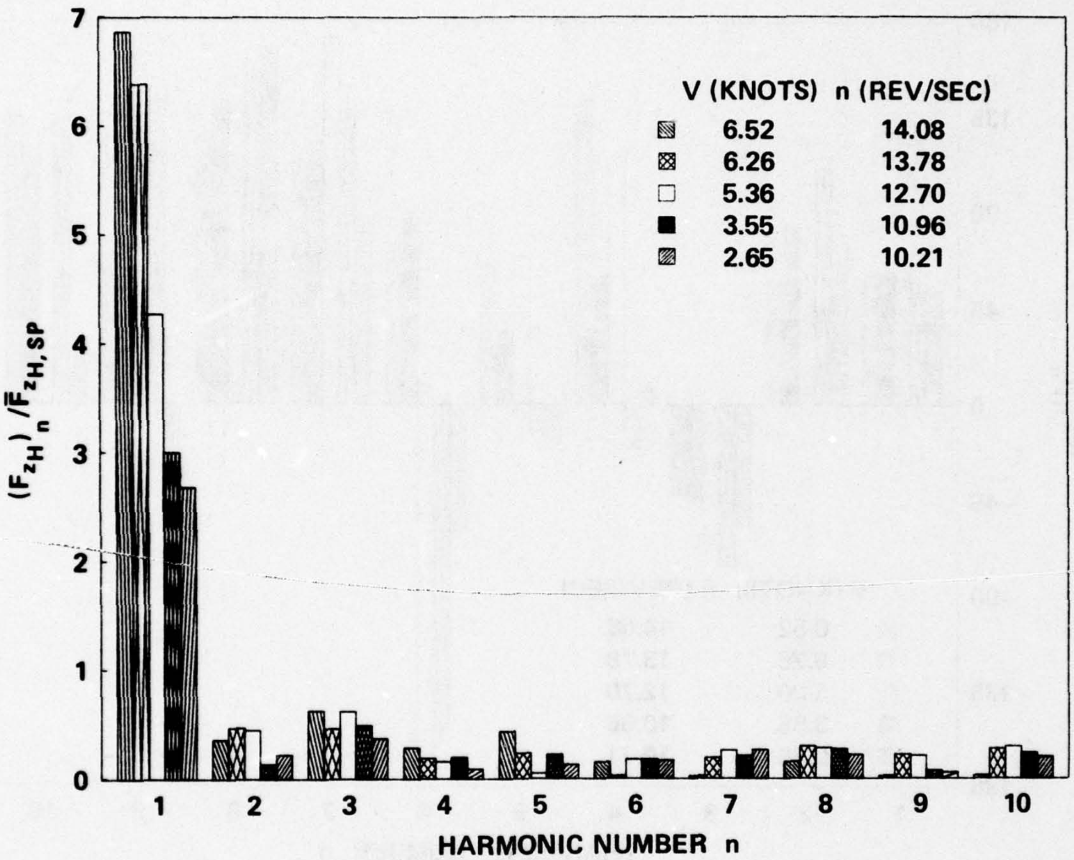

Figure 23e - F_z

Figure 23 (Continued)

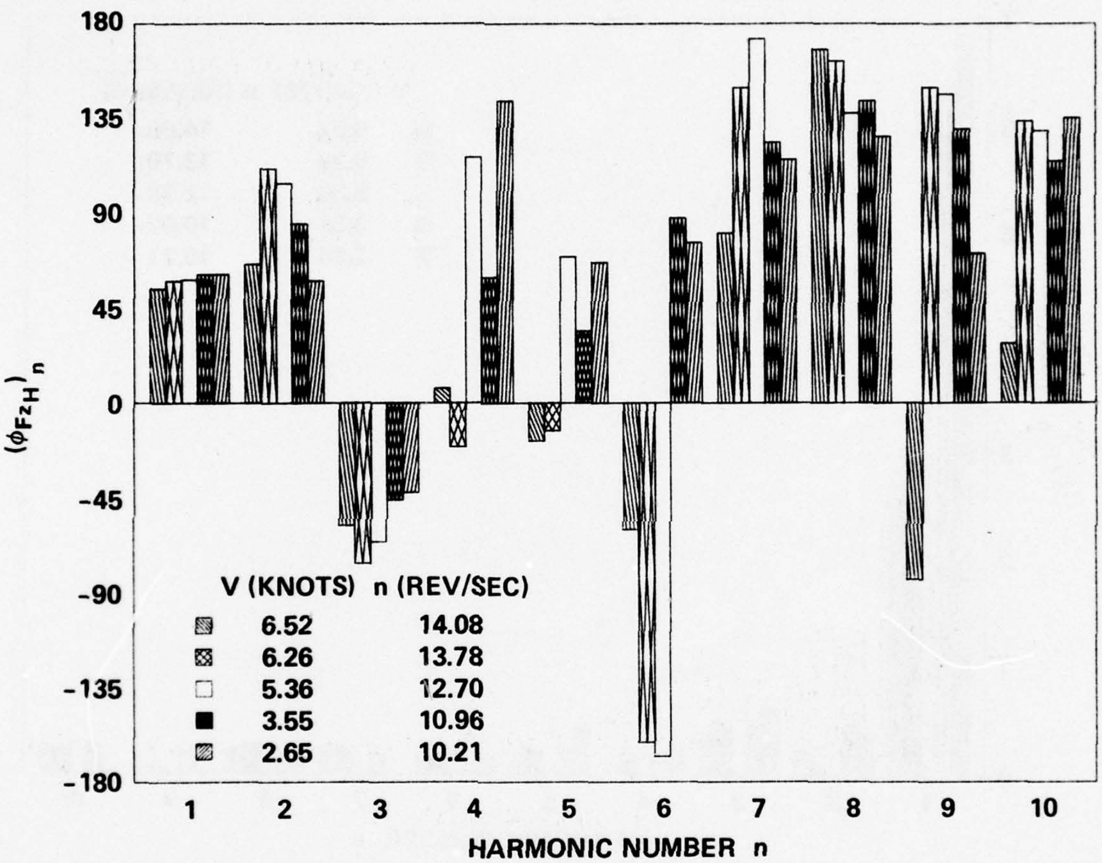

Figure 23e (Continued)

Figure 23 (Continued)

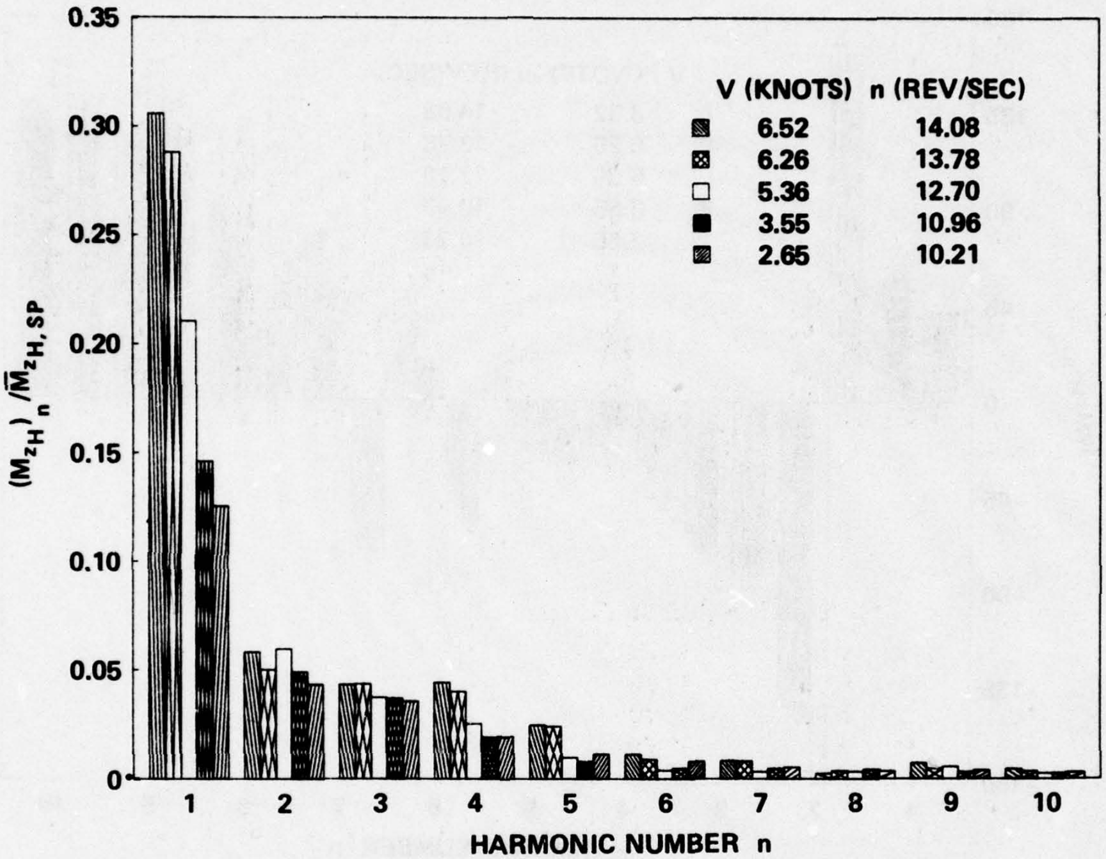

Figure 23f - M_{z_H}

Figure 23 (Continued)

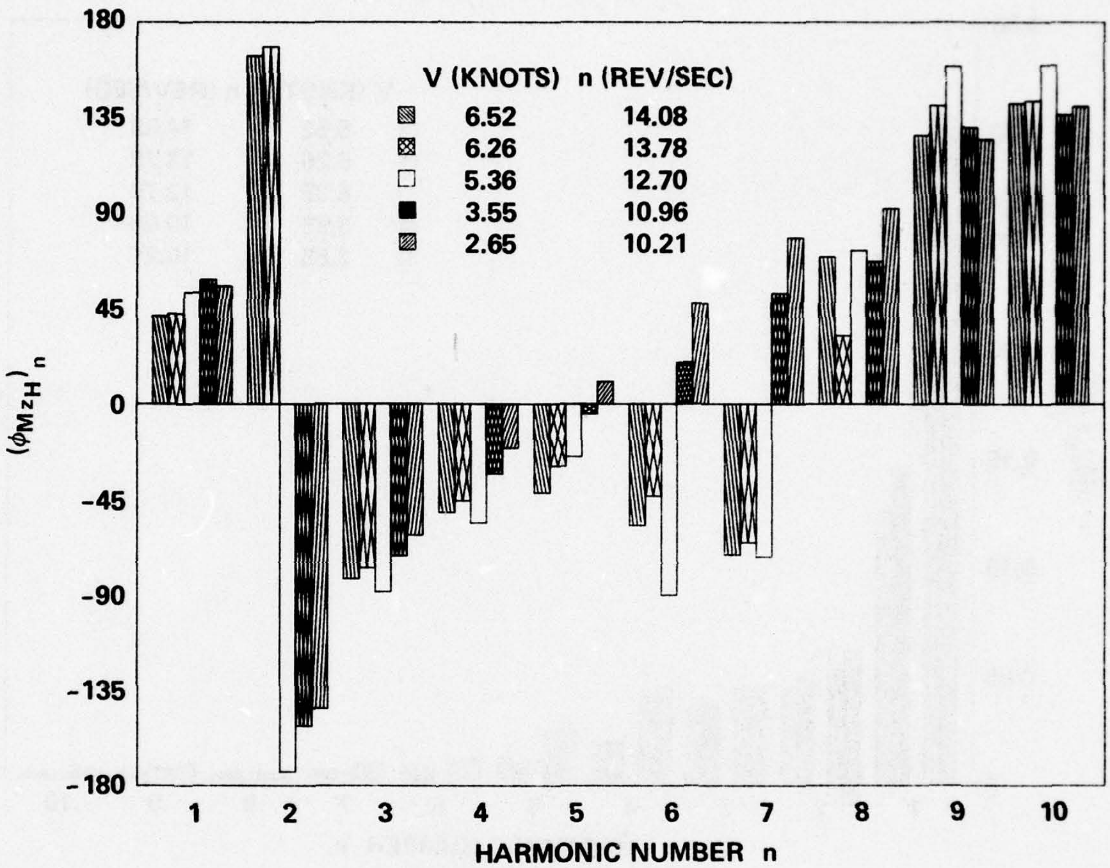

Figure 23f (Continued)

Figure 23 (Continued)

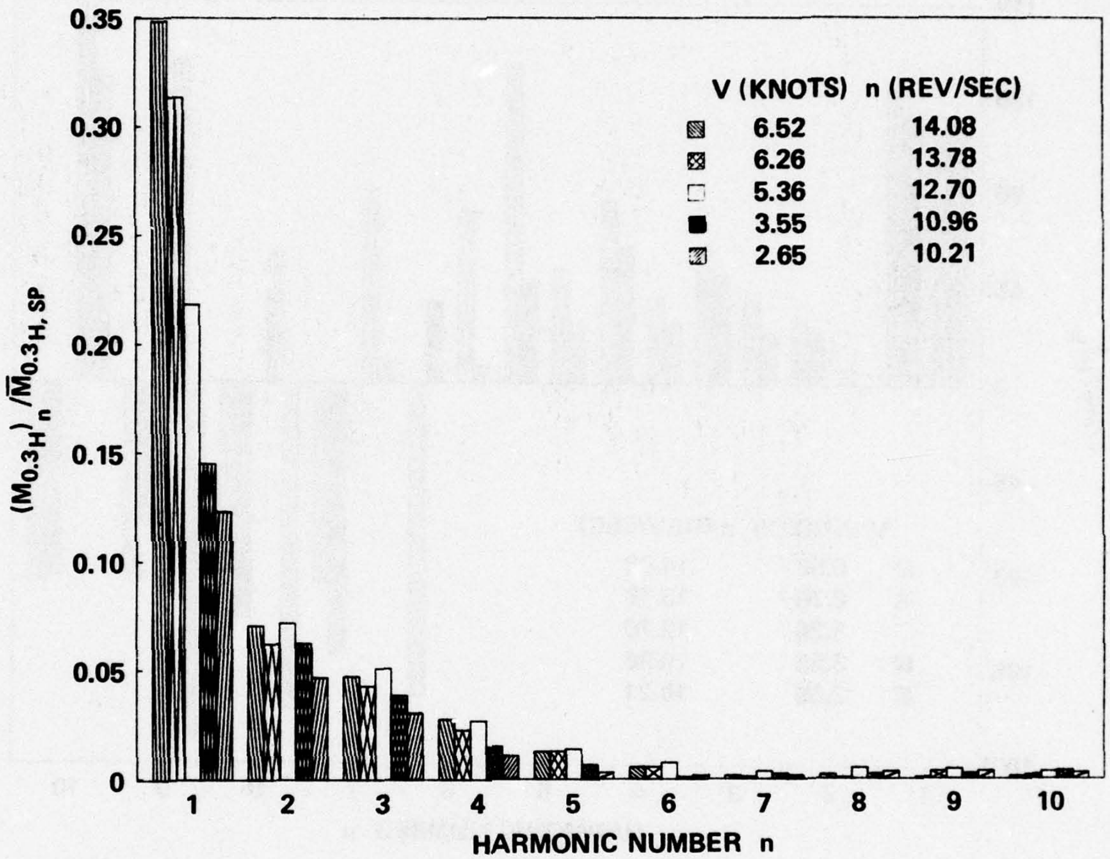

Figure 23g - $M_{0.3_H}$

Figure 23 (Continued)

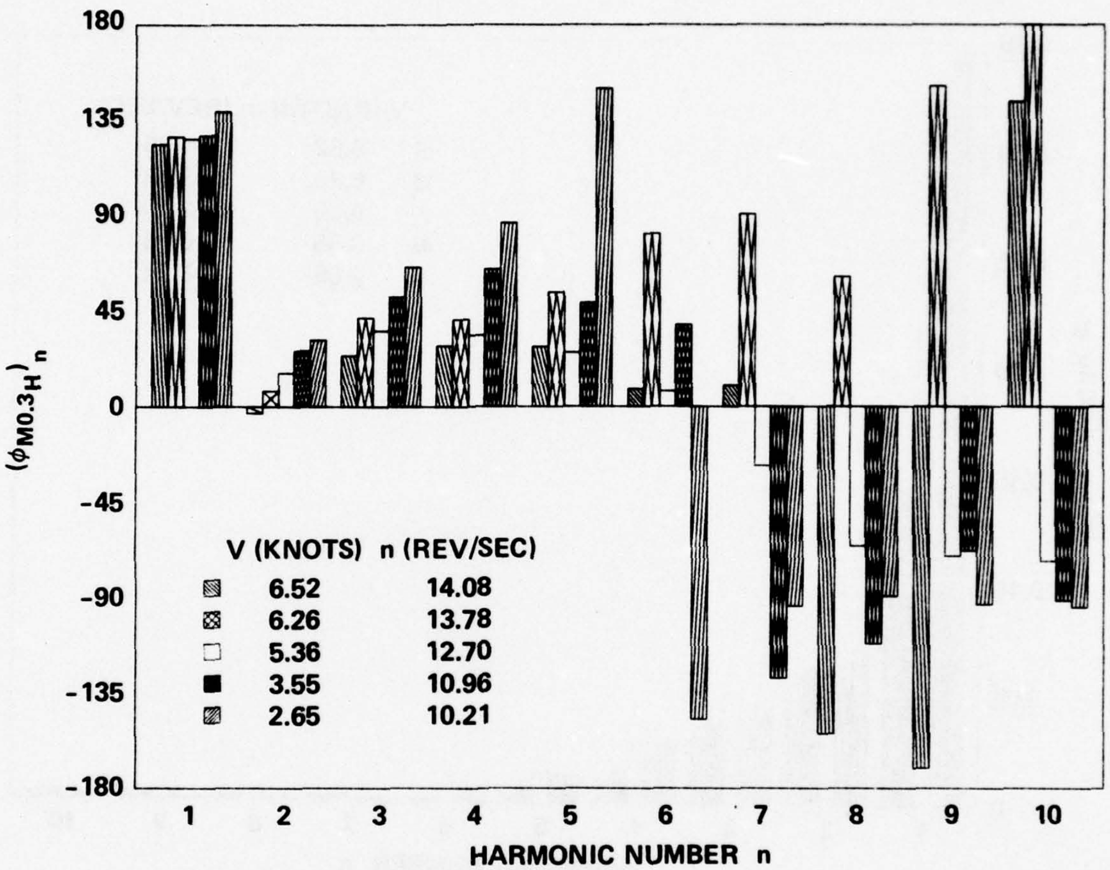

Figure 23g (Continued)

Figure 23 (Continued)

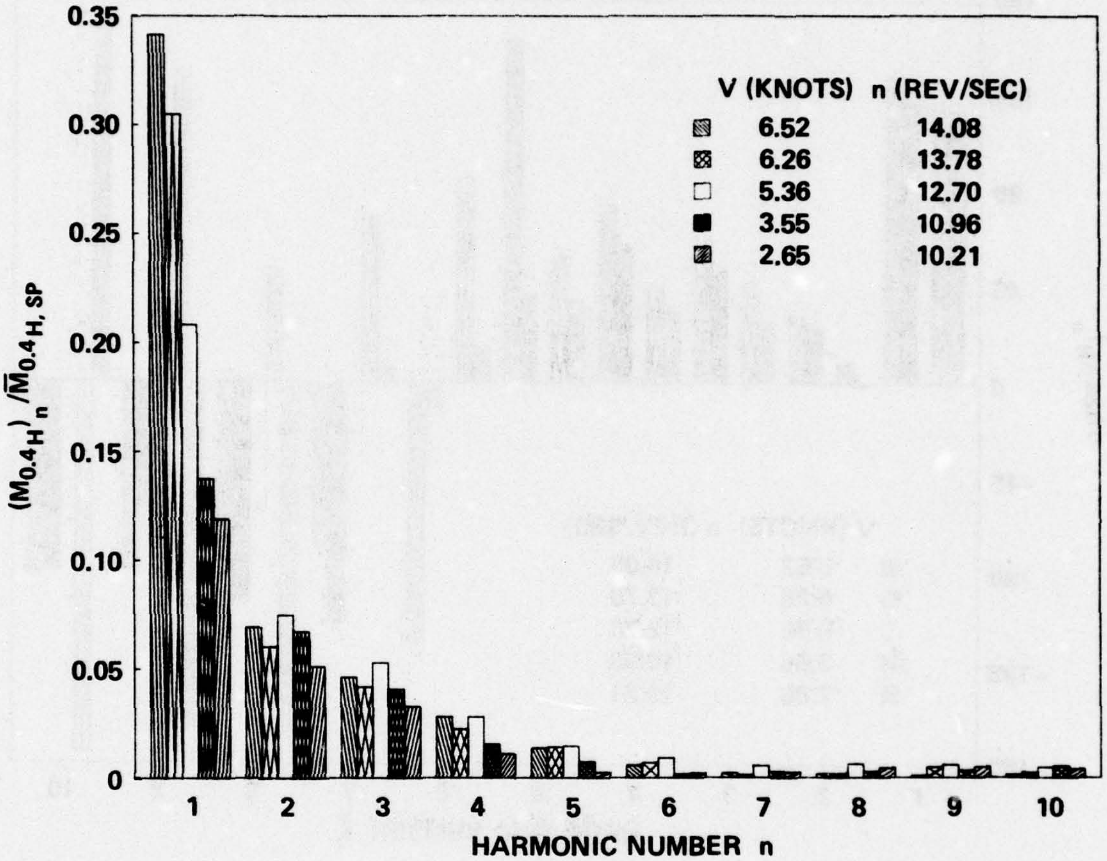

Figure 23h - $M_{0.4_H}$

Figure 23 (Continued)

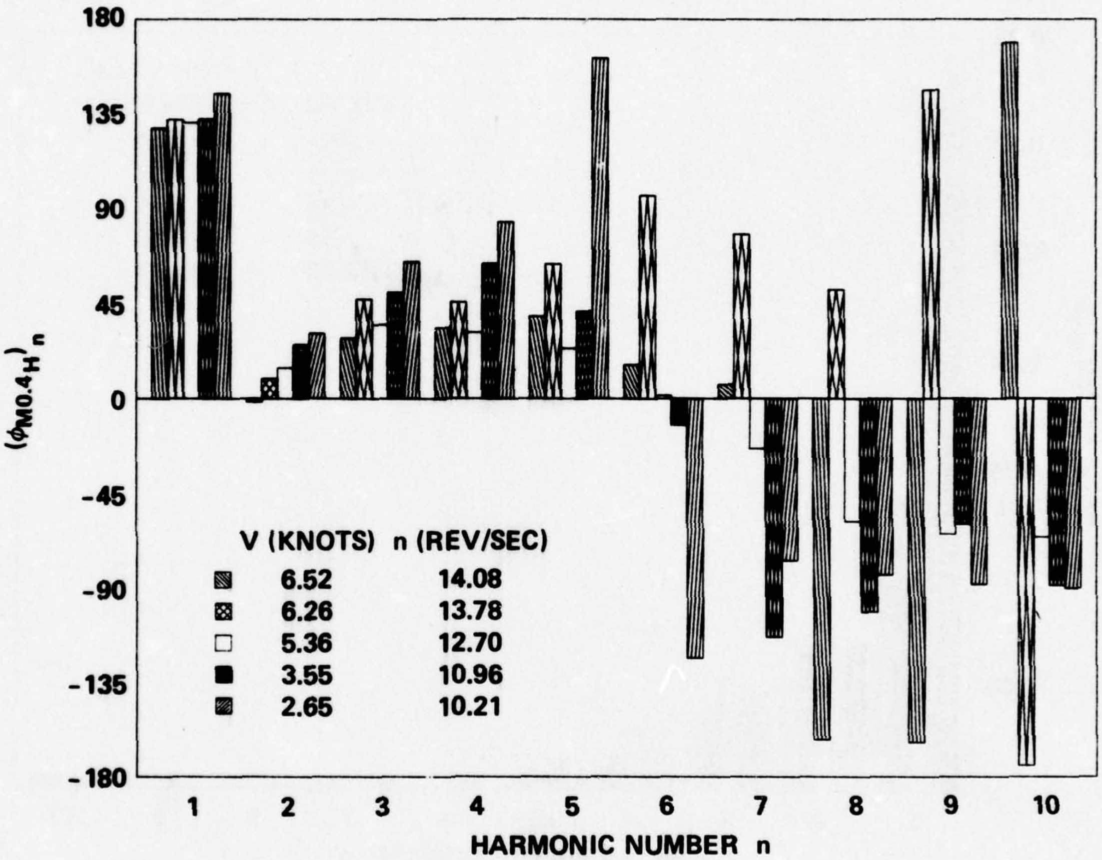

Figure 23h (Continued)

Figure 24 - Harmonic Content of Experimental Total Loads for Quasi-Steady Acceleration

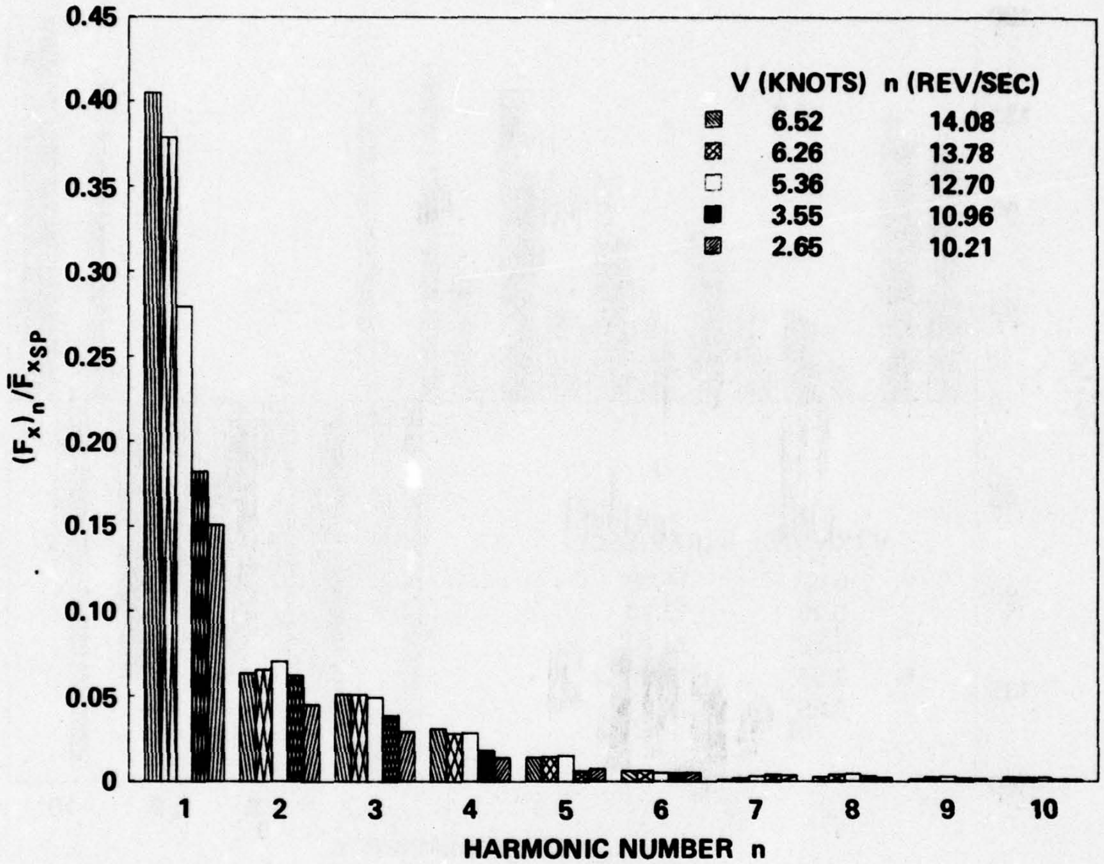

Figure 24a - F_x

Figure 24 (Continued)

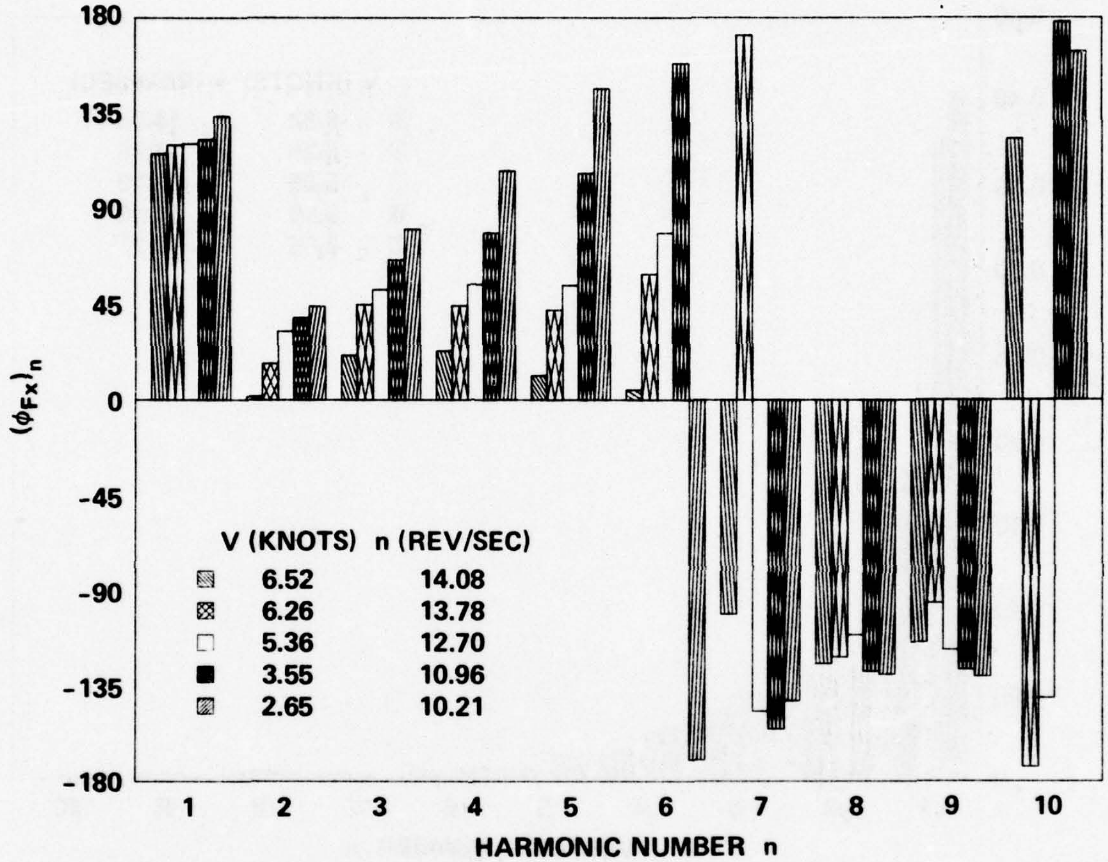

Figure 24a (Continued)

Figure 24 (Continued)

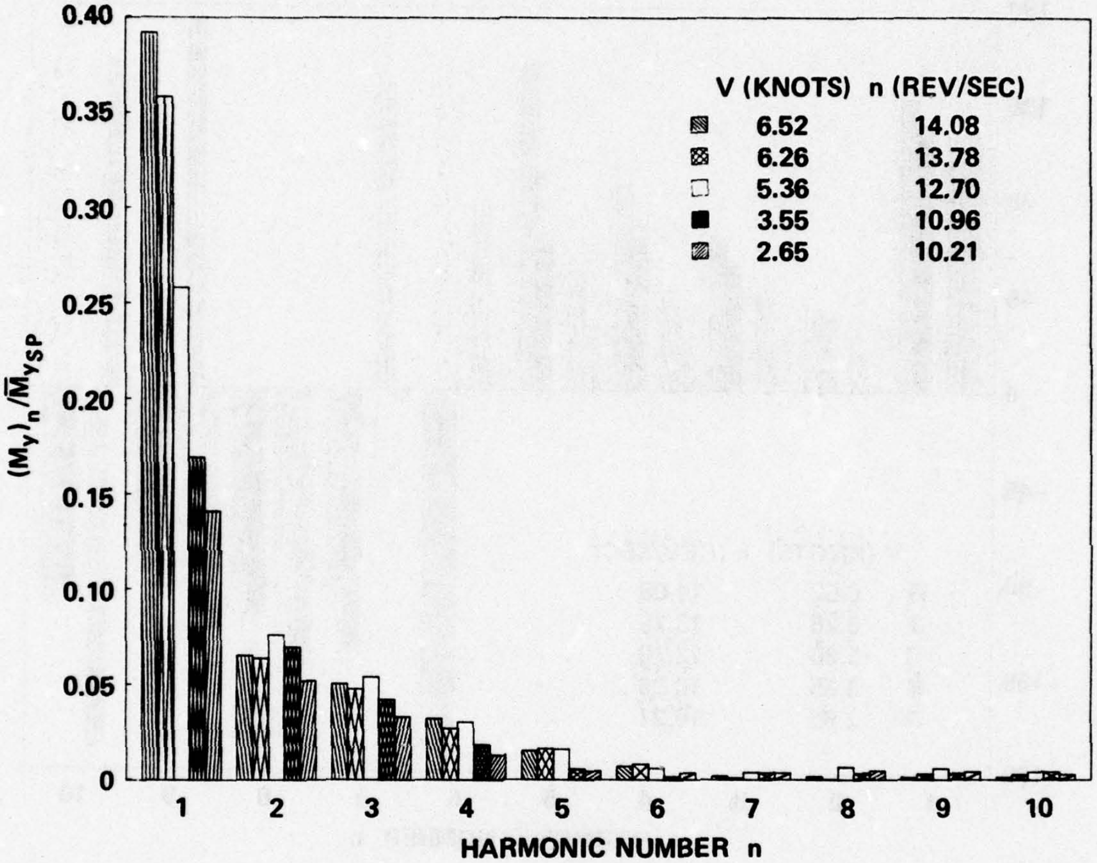

Figure 24b - M_y

Figure 24 (Continued)

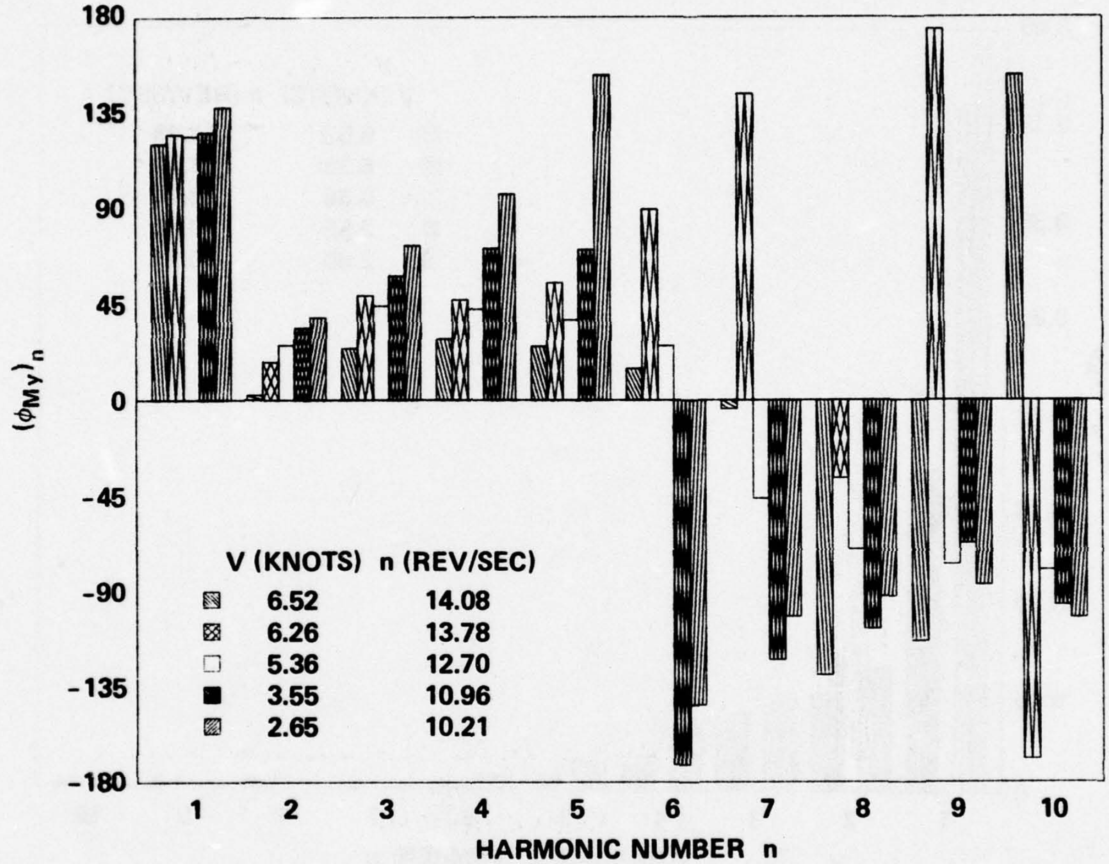

Figure 24b (Continued)

Figure 24 (Continued)

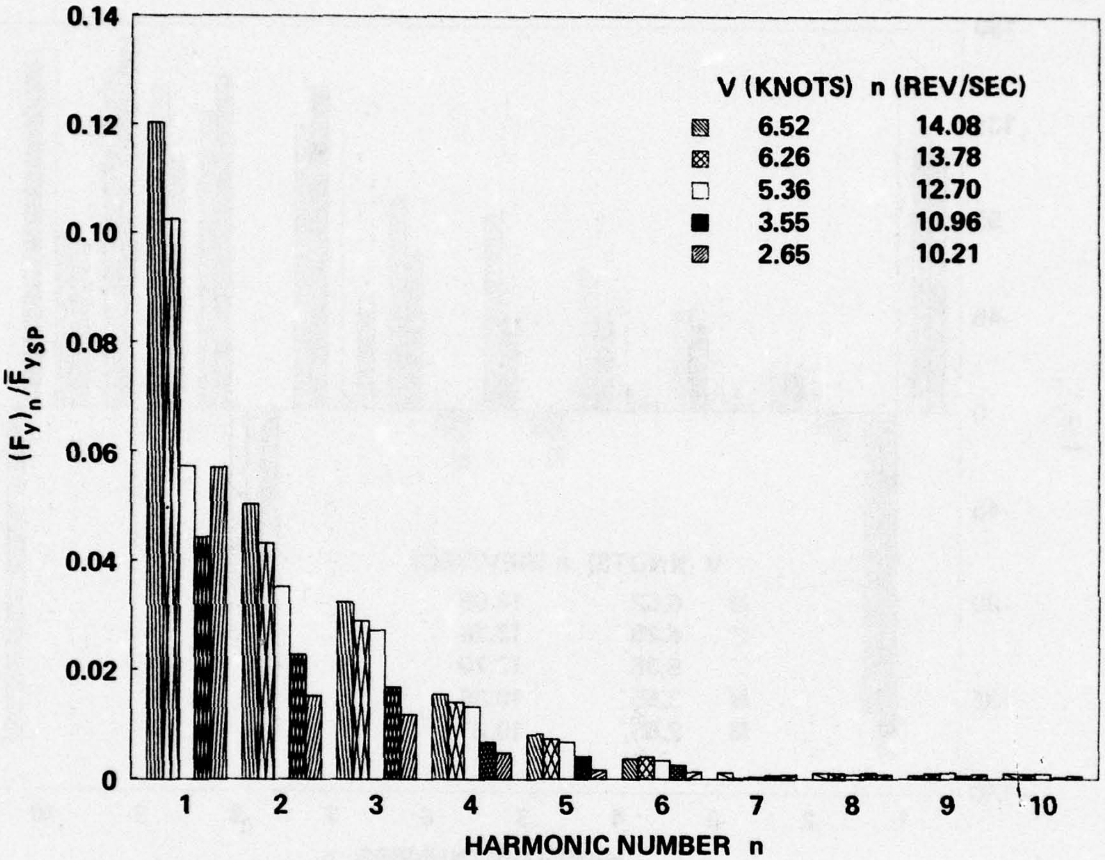

Figure 24c - M_y

Figure 24 (Continued)

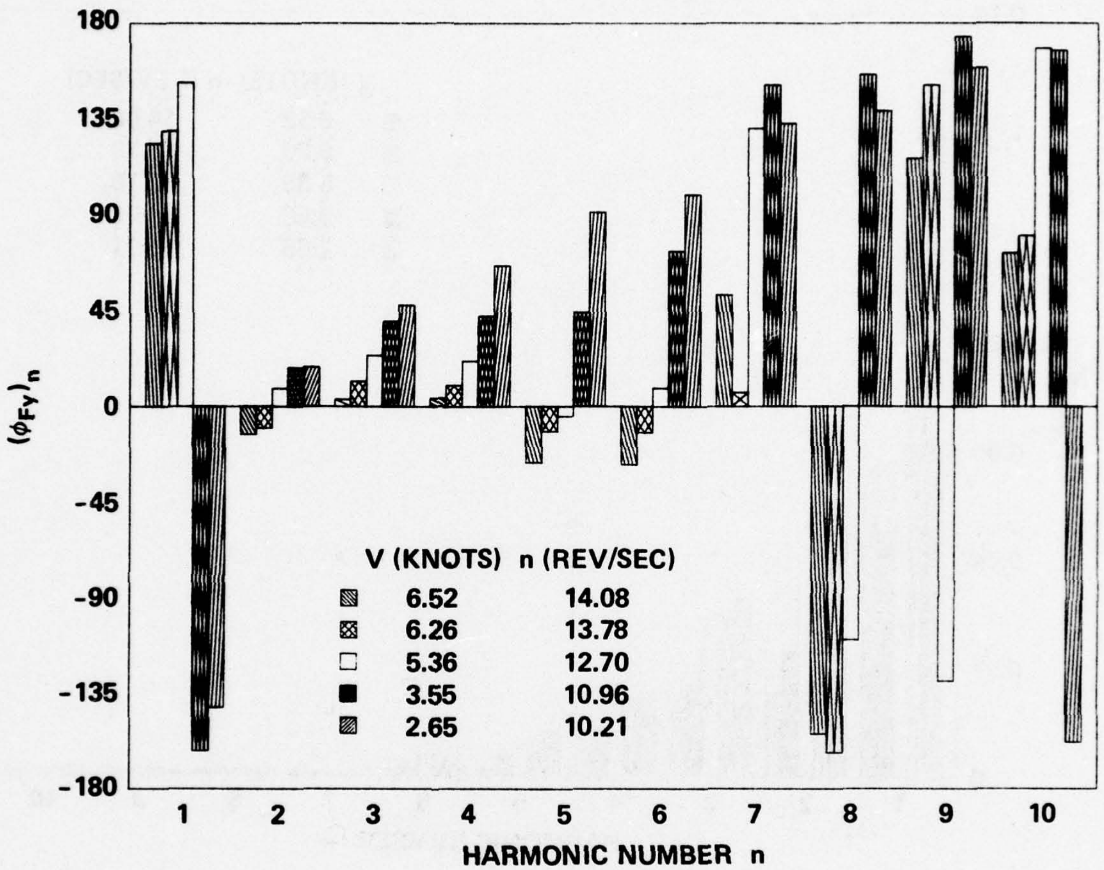

Figure 24c (Continued)

Figure 24 (Continued)

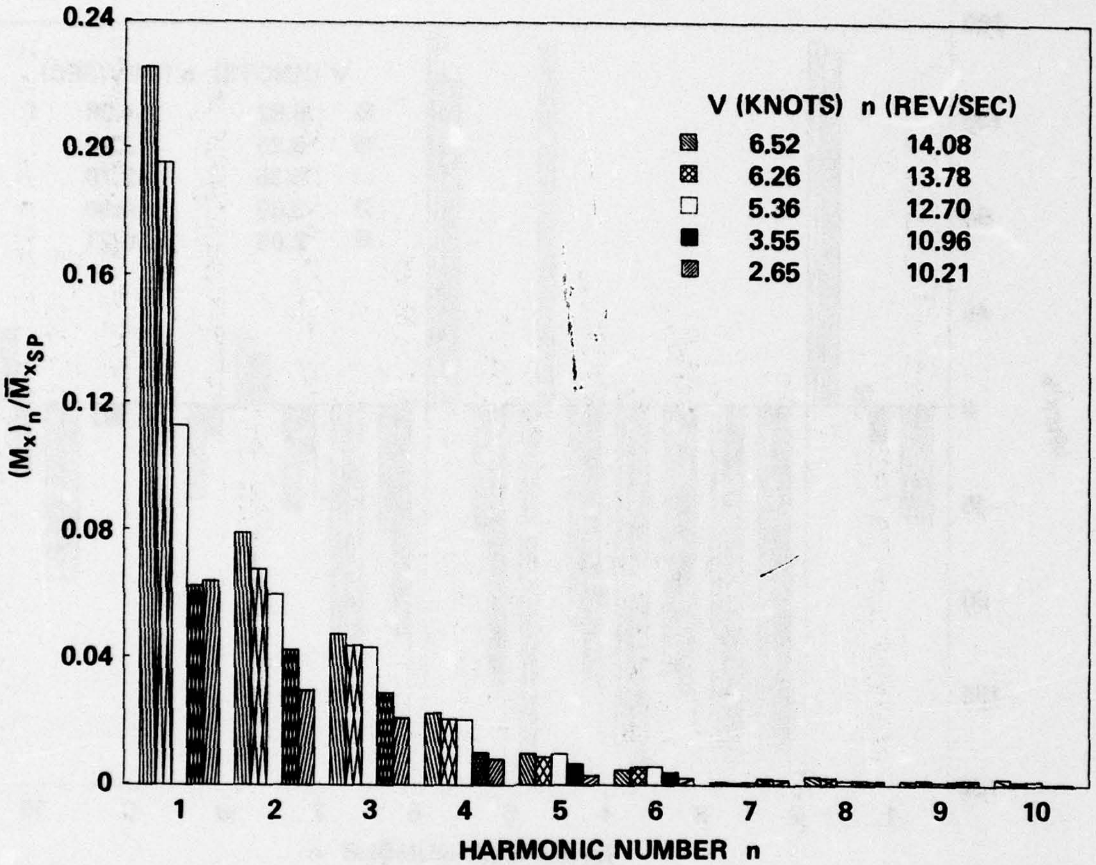

Figure 24d - M_x

Figure 24 (Continued)

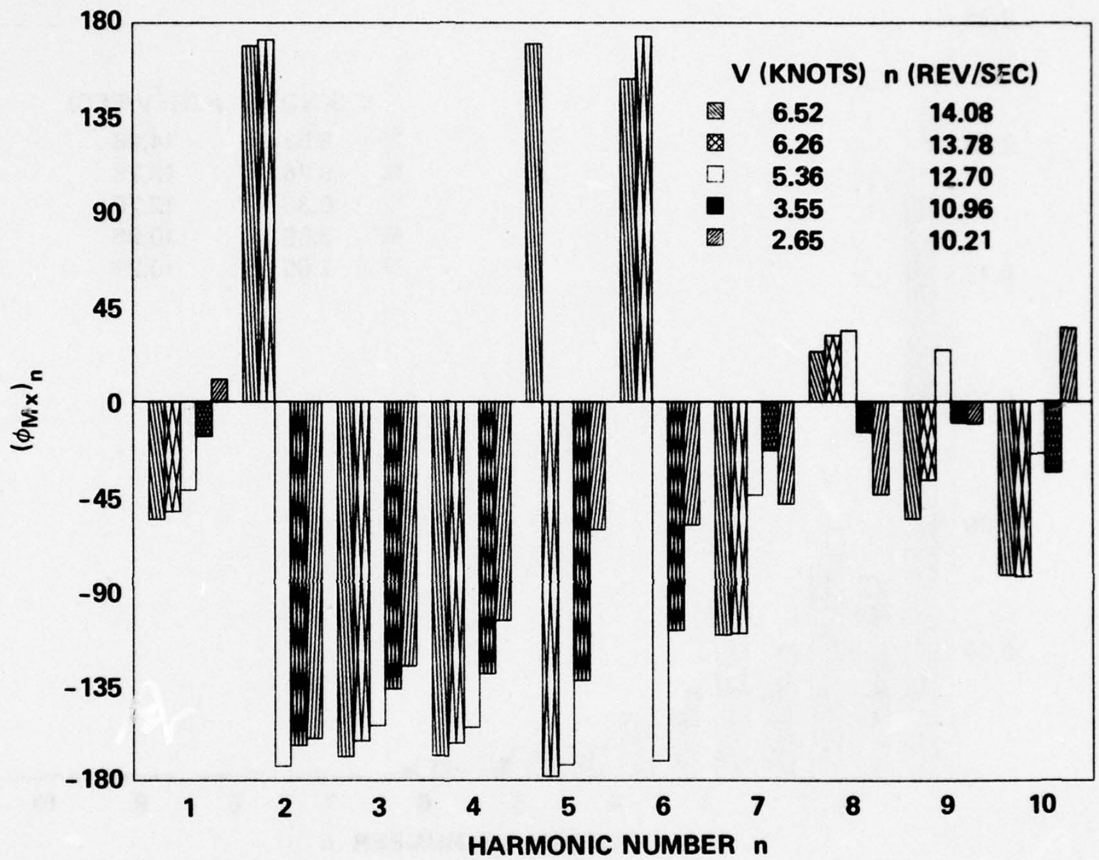

Figure 24d (Continued)

Figure 24 (Continued)

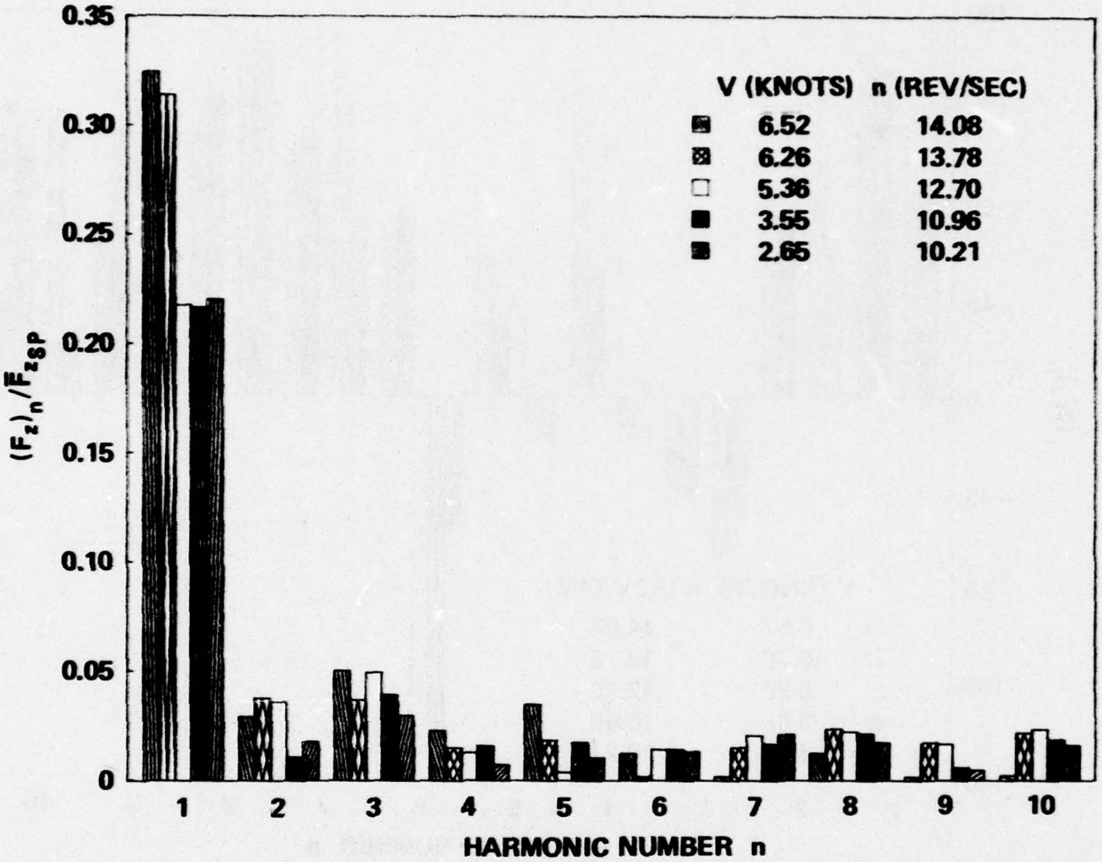

Figure 24e - F_z

Figure 24 (Continued)

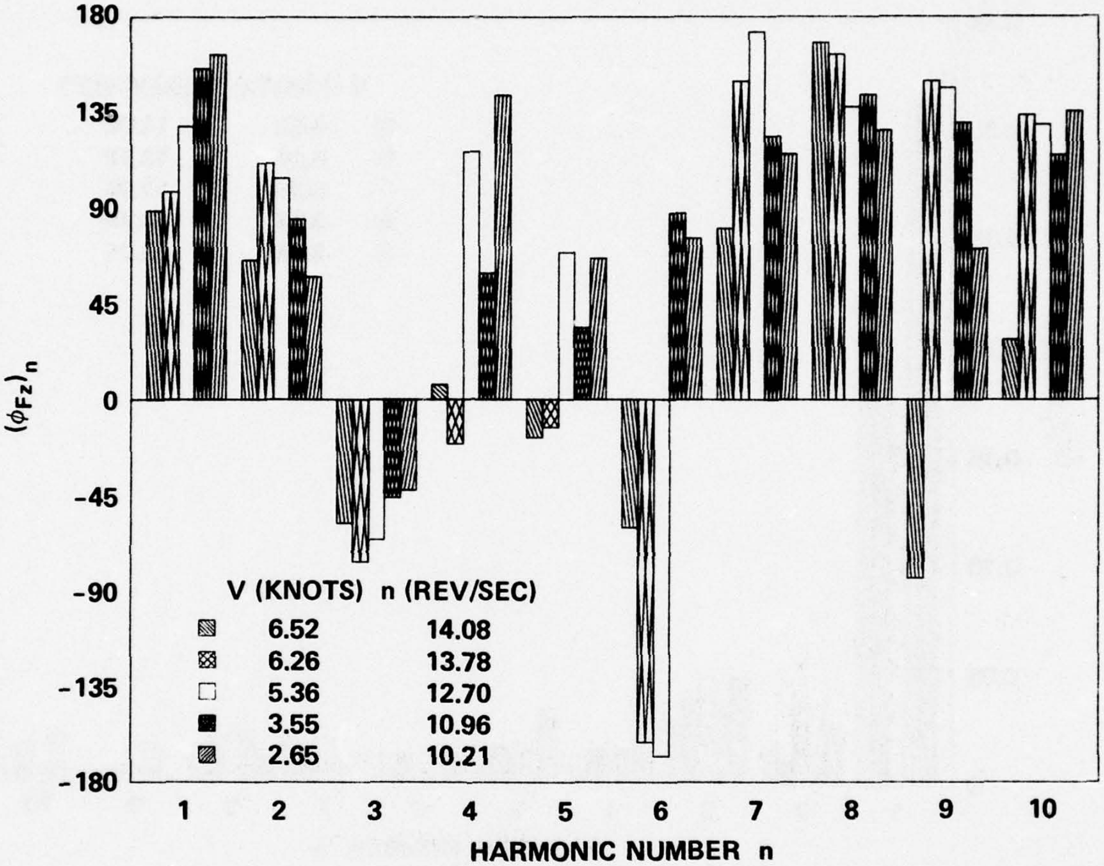

Figure 24e (Continued)

Figure 24 (Continued)

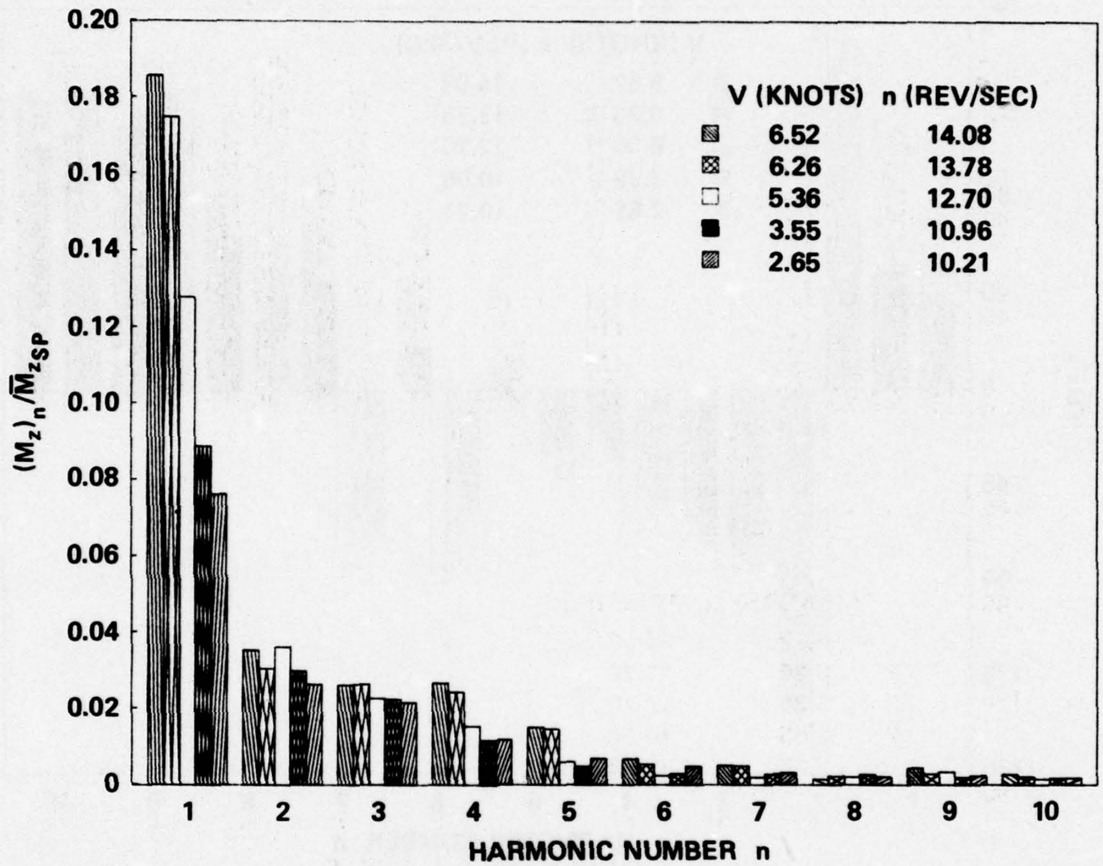

Figure 24f - M_z

Figure 24 (Continued)

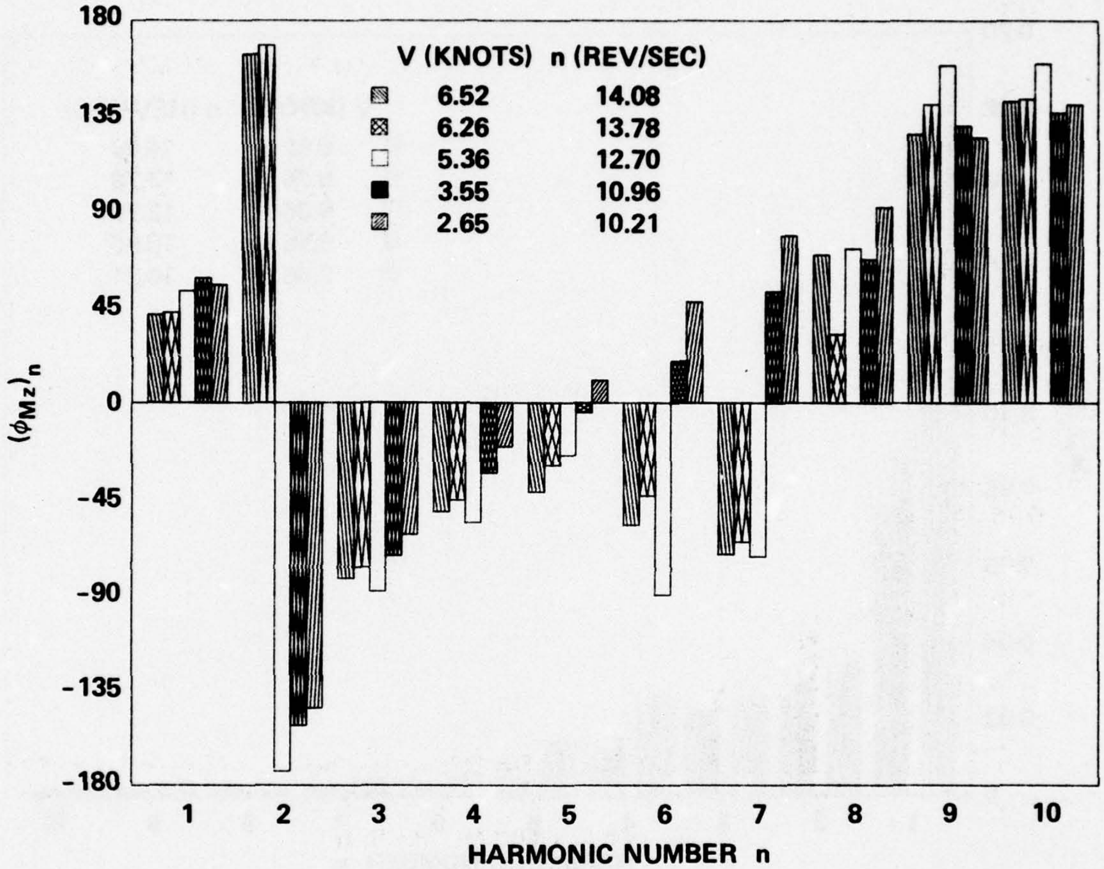

Figure 24f (Continued)

Figure 24 (Continued)

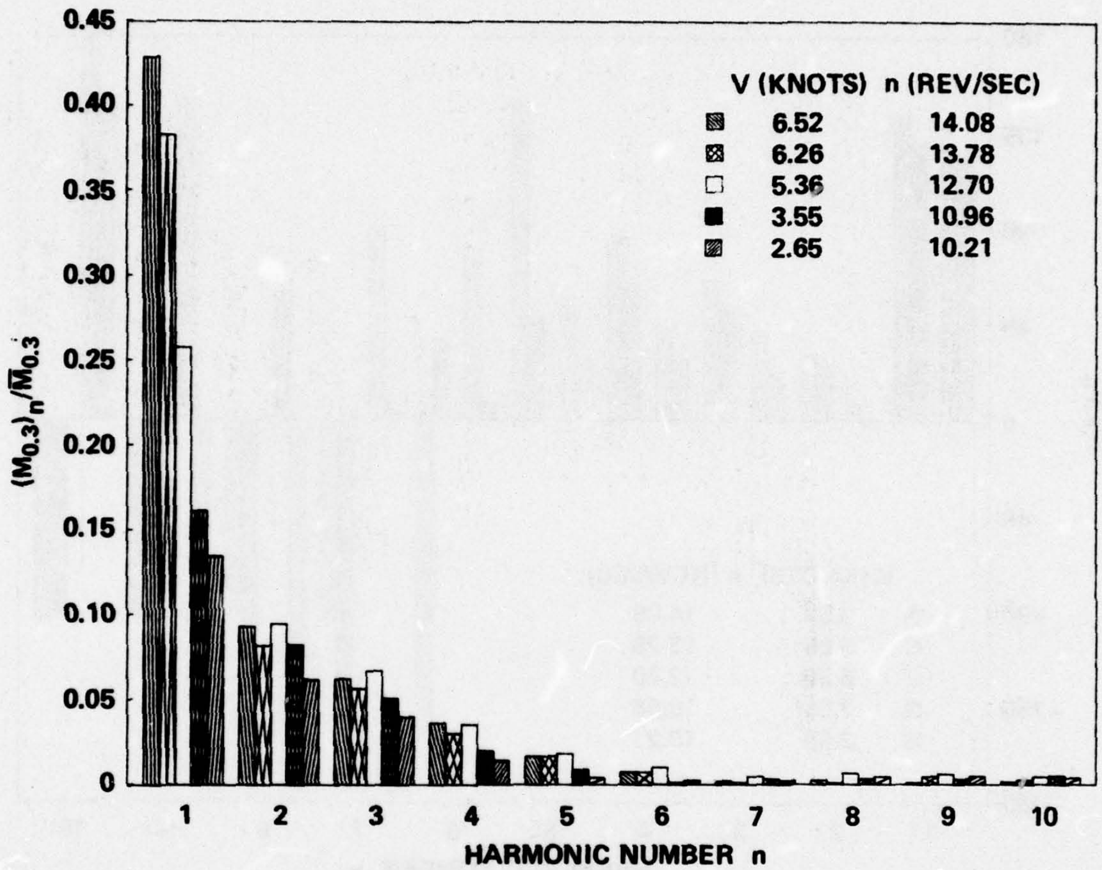

Figure 24g - $M_{0.3}$

Figure 24 (Continued)

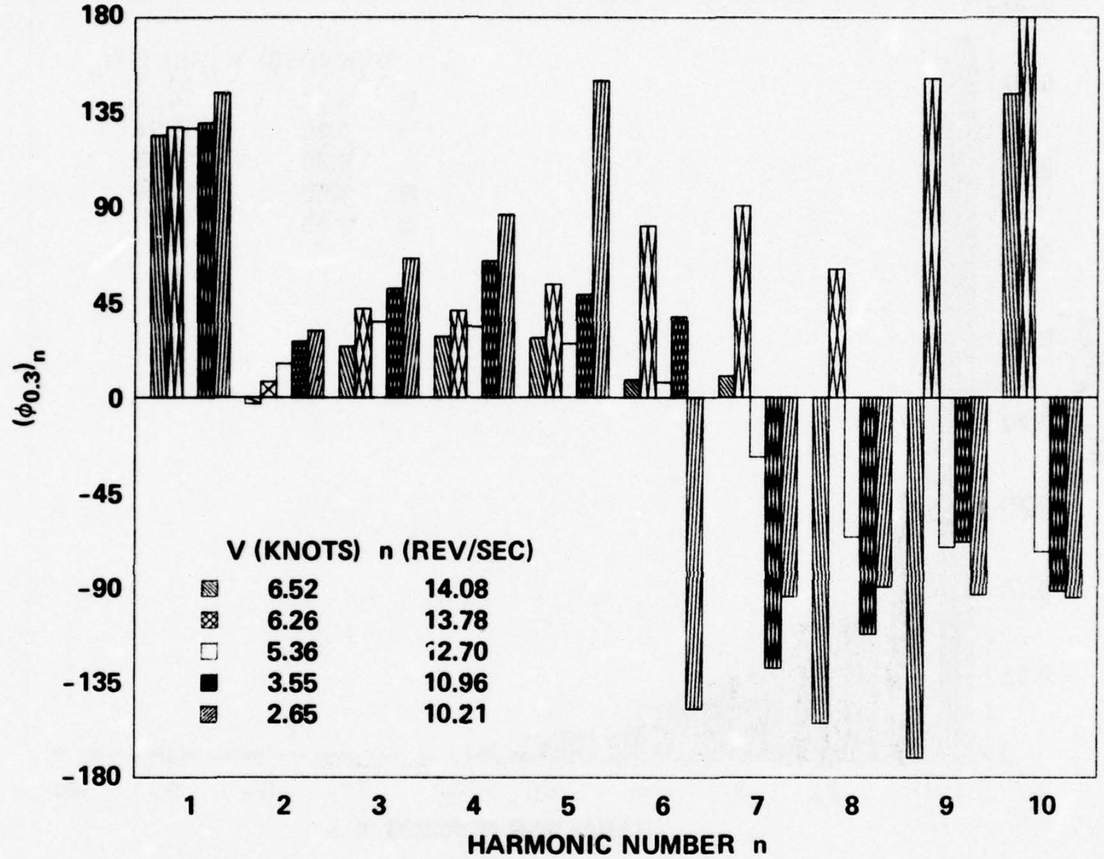

Figure 24g (Continued)

Figure 24 (Continued)

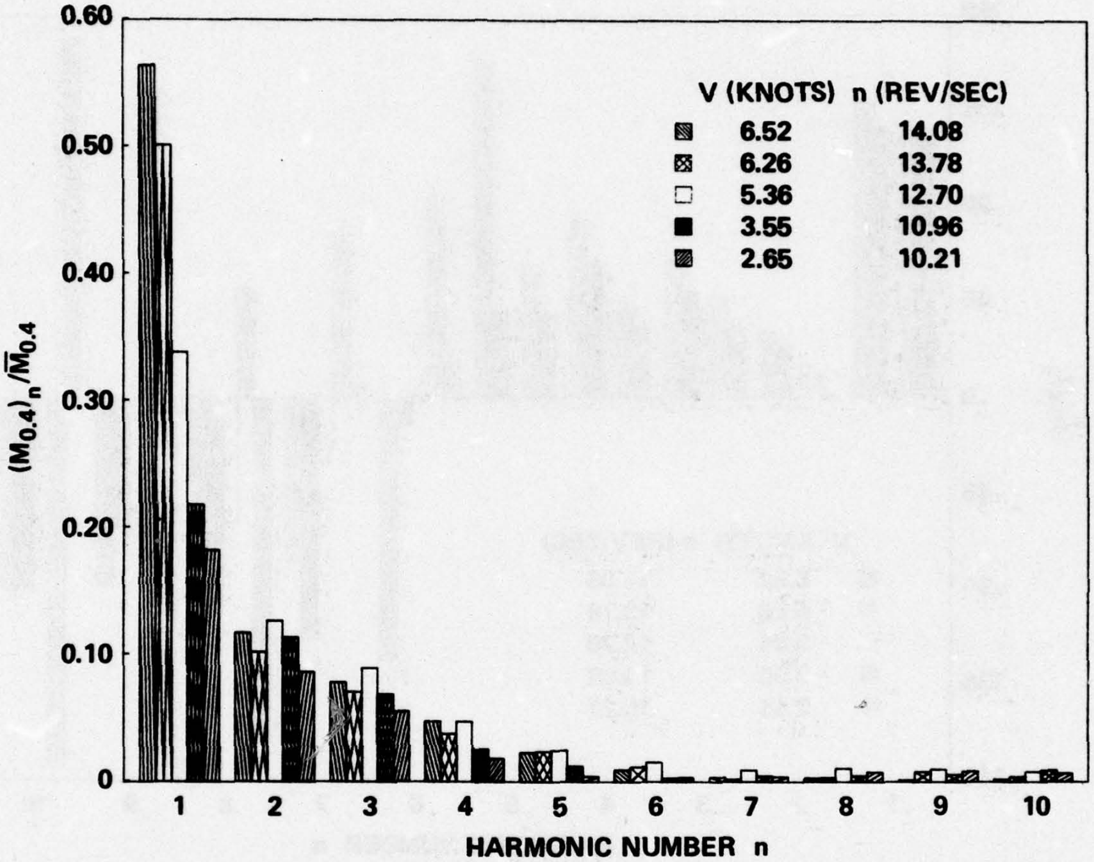

Figure 24h - $M_{0.4}$

Figure 24 (Continued)

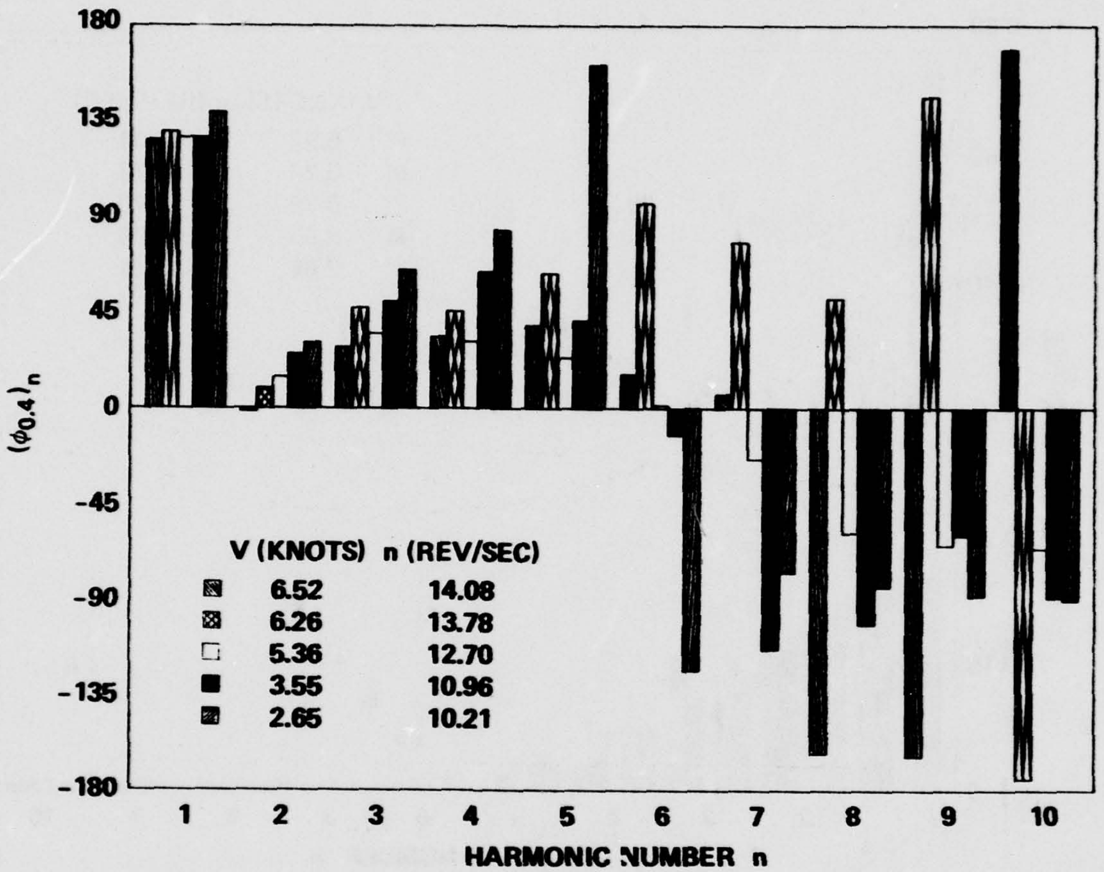

Figure 24h (Continued)

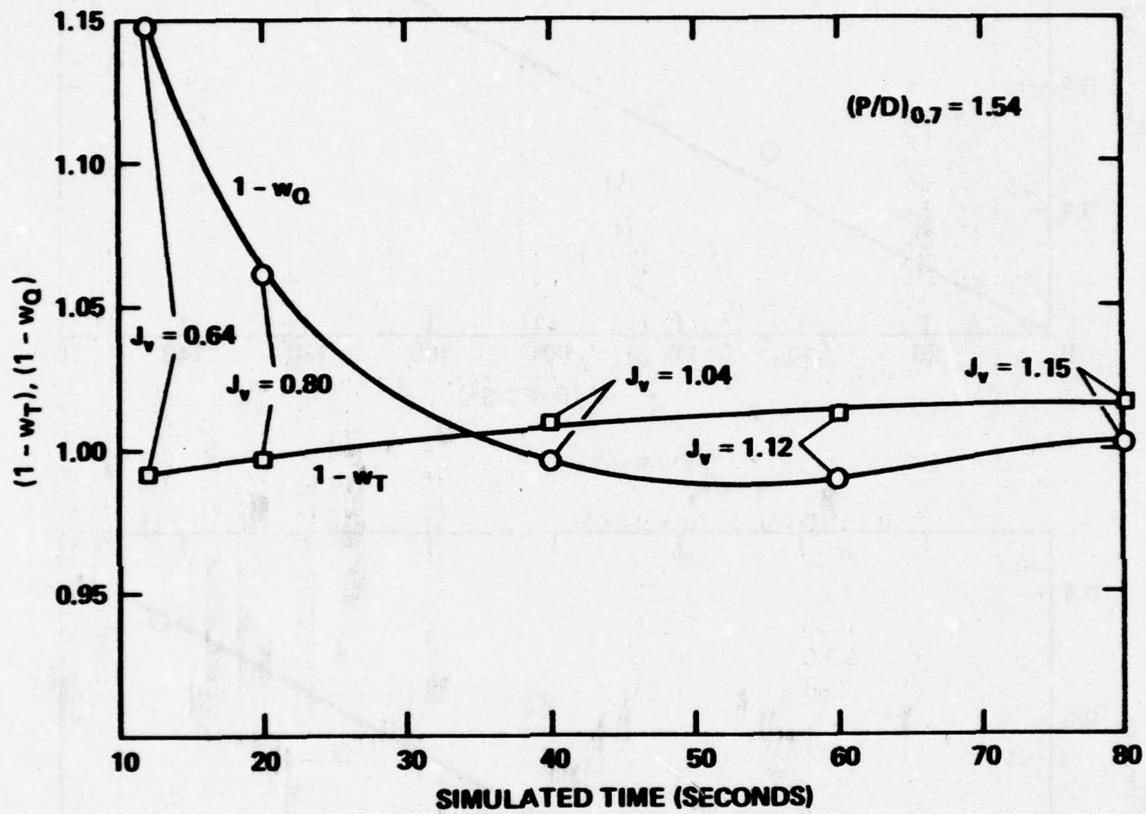

Figure 25 - Taylor Wake Fractions during Simulated Acceleration Maneuvers

Figure 26 - Variation of First Harmonic of Experimental Hydrodynamic Loads with nV for Quasi-Steady Acceleration

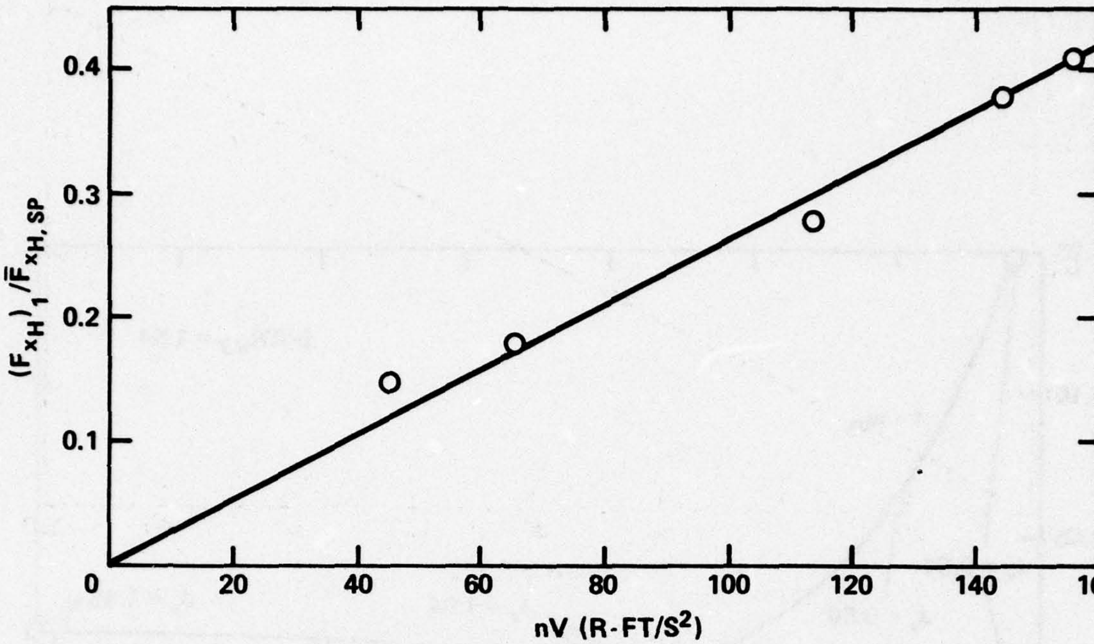

Figure 26a - F_{x_H}

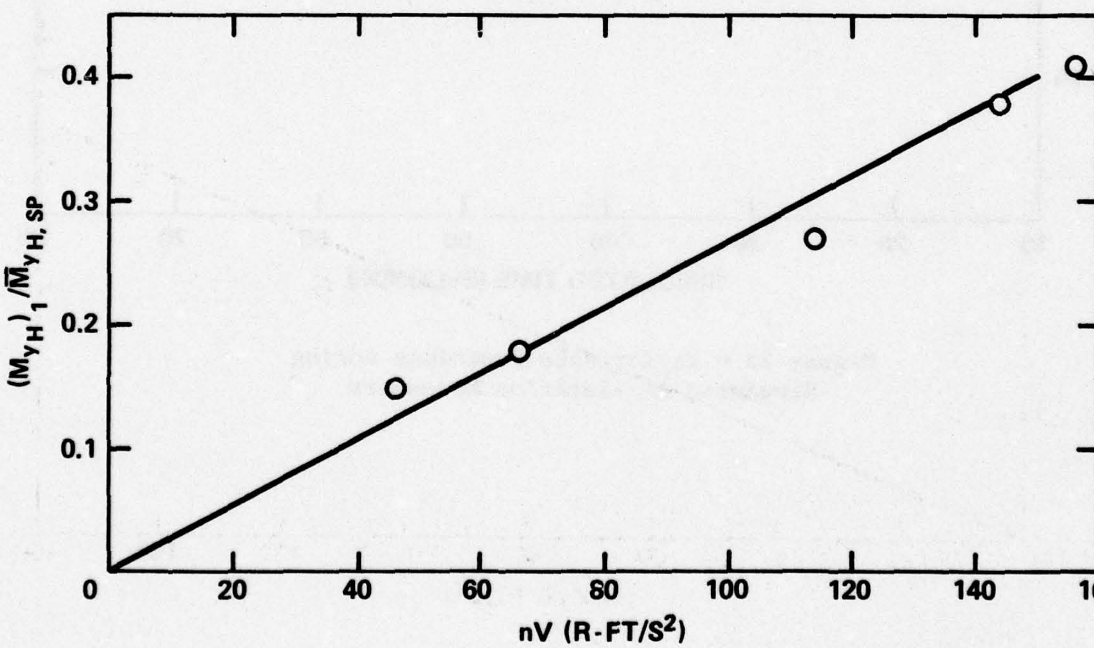

Figure 26b - M_{y_H}

Figure 26 (Continued)

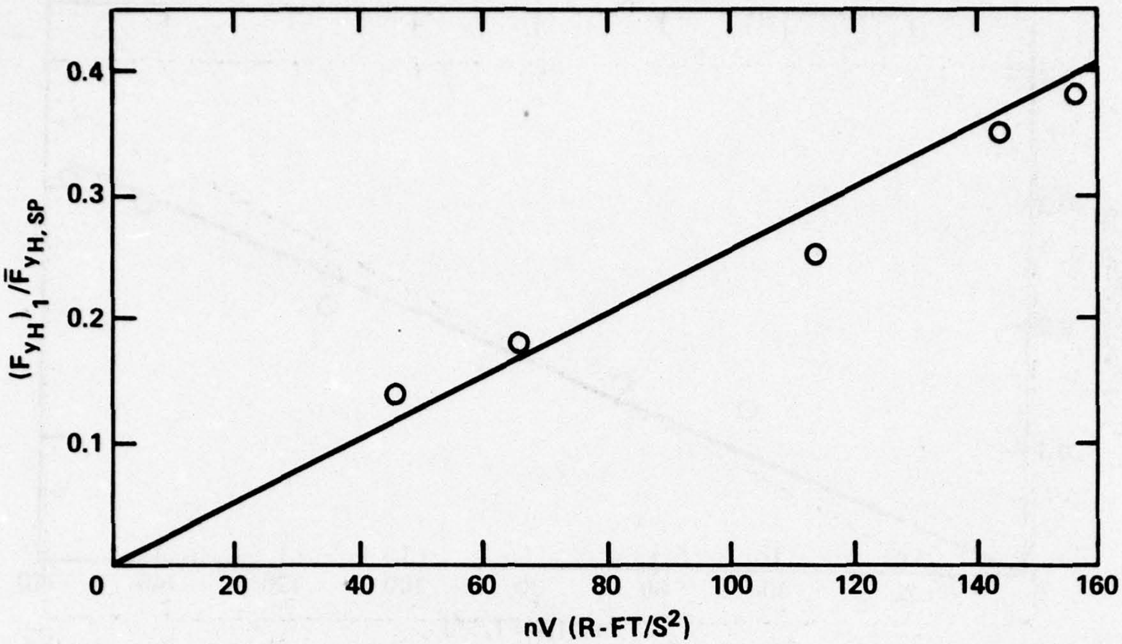

Figure 26c - F_{y_H}

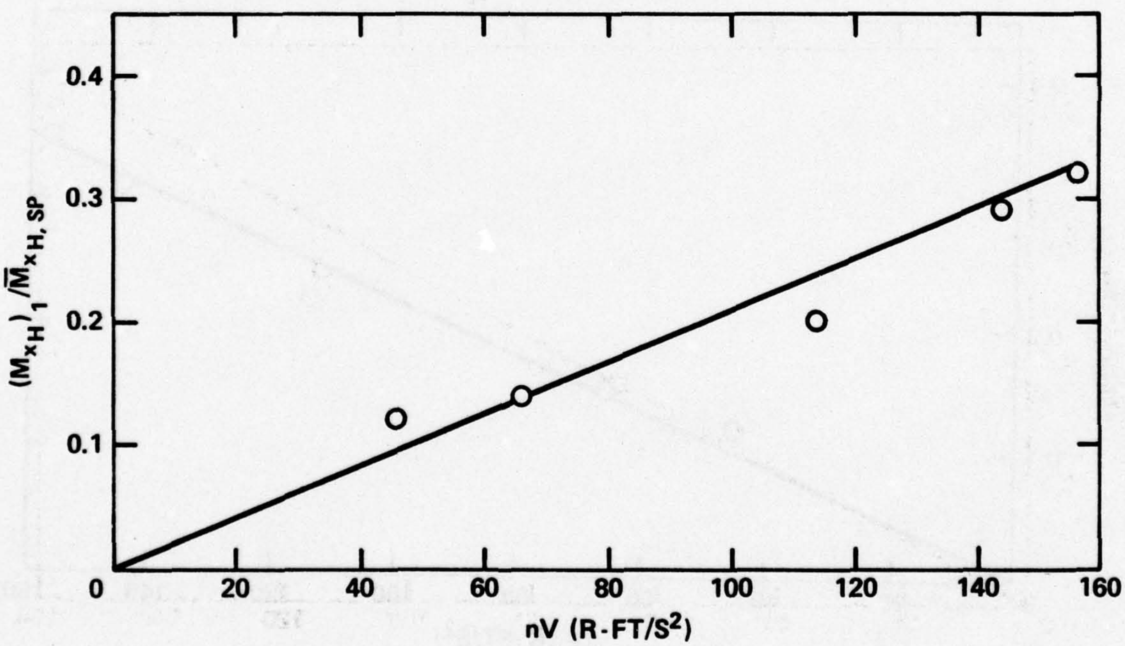

Figure 26d - M_{x_H}

Figure 26 (Continued)

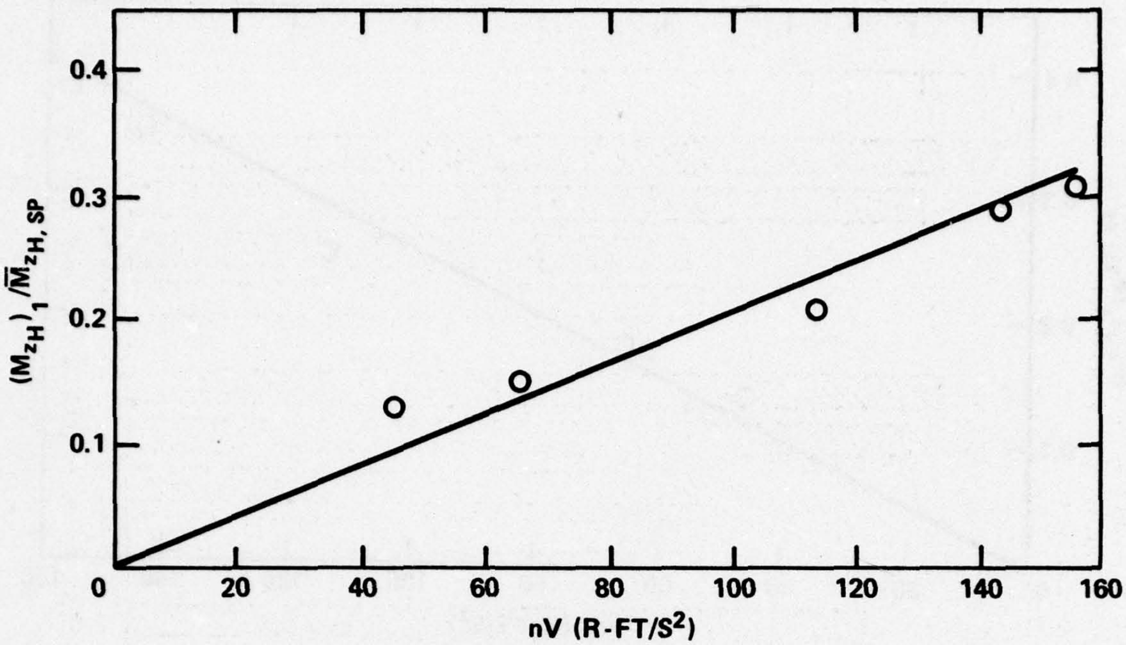

Figure 26e - M_{z_H}

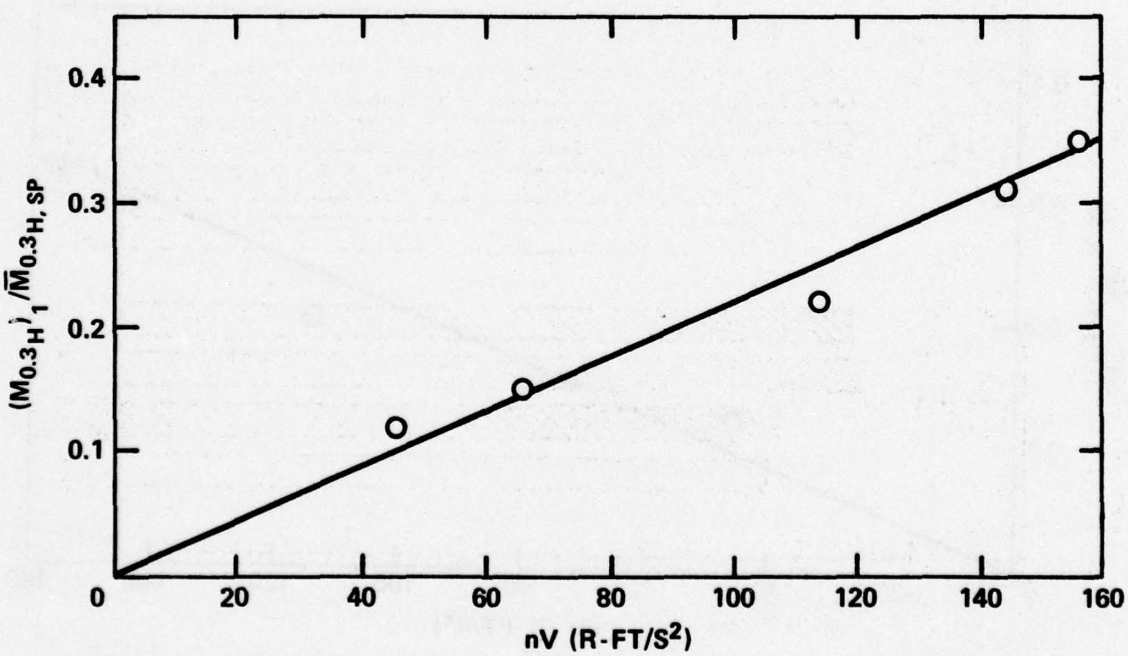

Figure 26f - $M_{0.3_H}$

Figure 27 - Comparison of Time-Average Values per Revolution and Peak Values of Various Components of Experimental Total Blade Loading for Quasi-Steady and Unsteady Simulated Acceleration

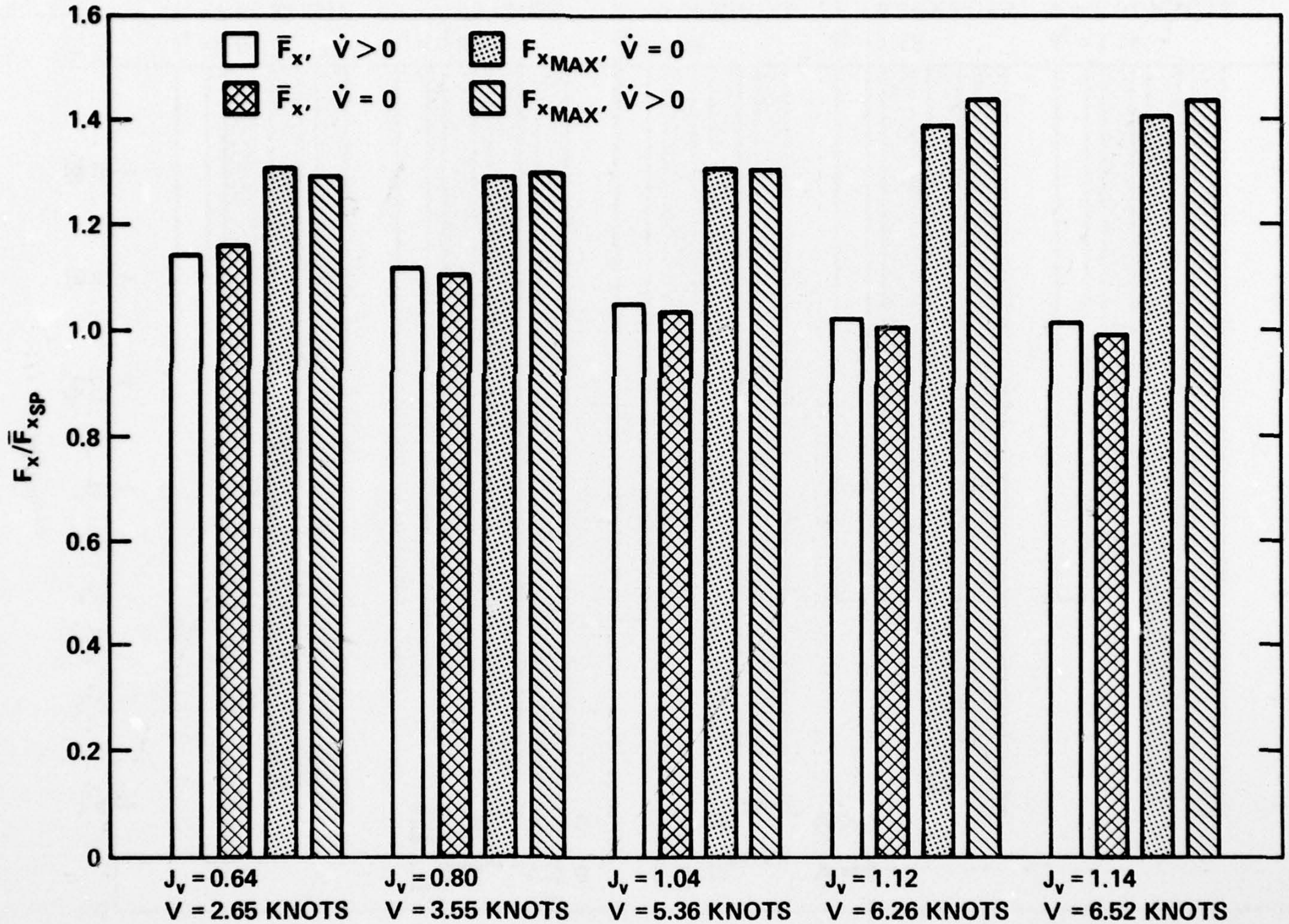

Figure 27a - F_x

Figure 27 (Continued)

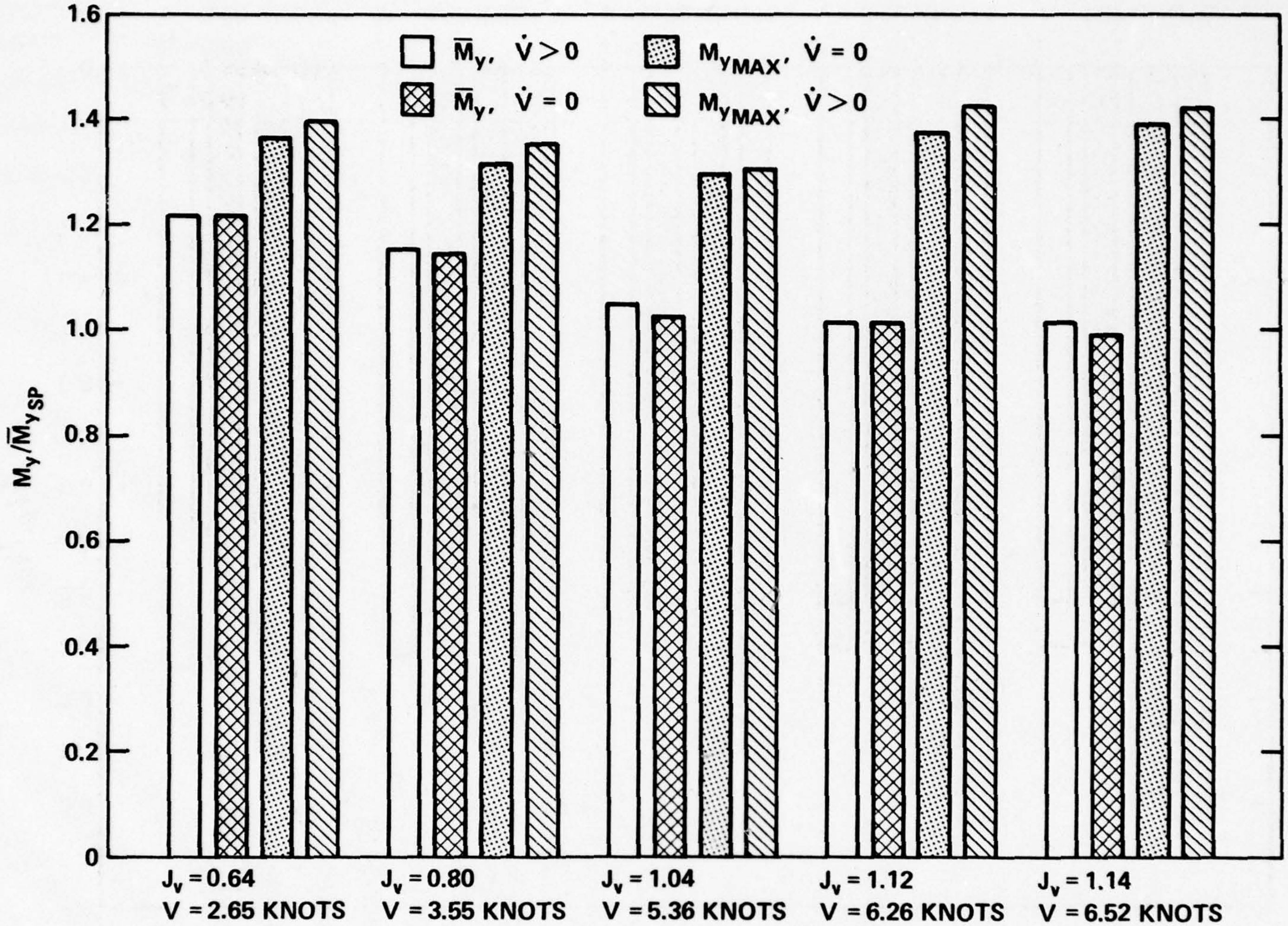

Figure 27b - M_y

Figure 27 (Continued)

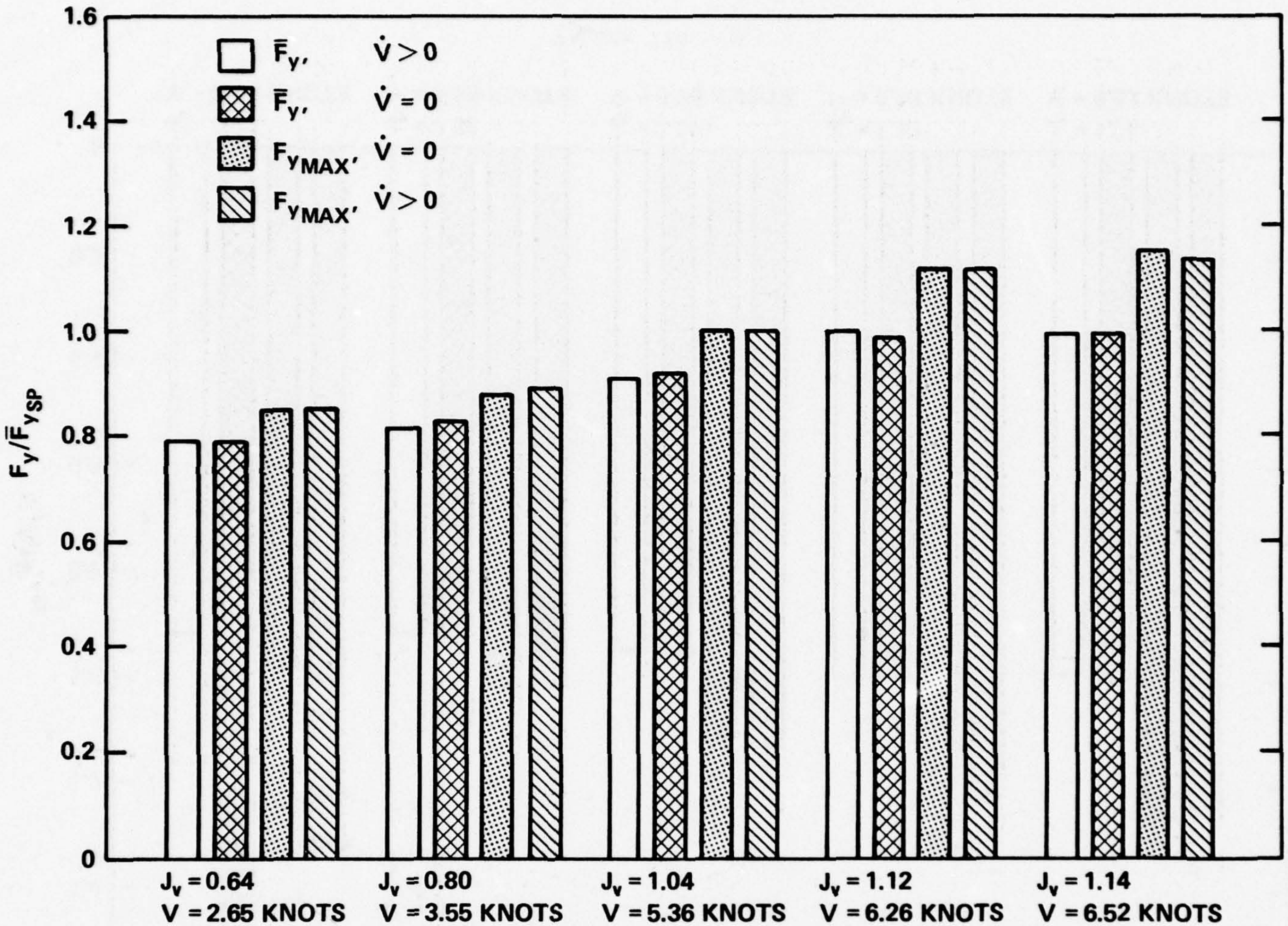

Figure 27c - F_y

Figure 27 (Continued)

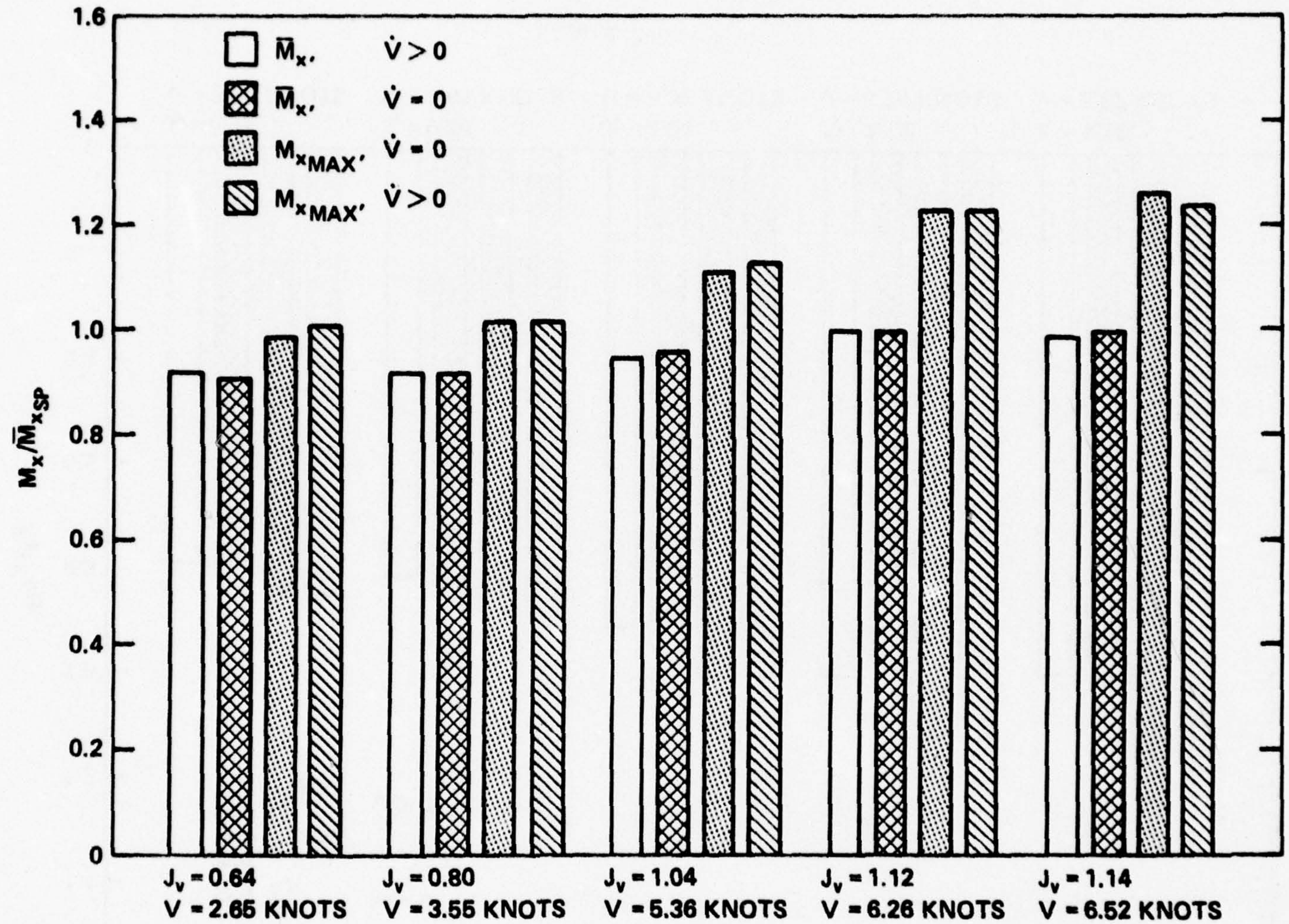

Figure 27d - M_x

Figure 27 (Continued)

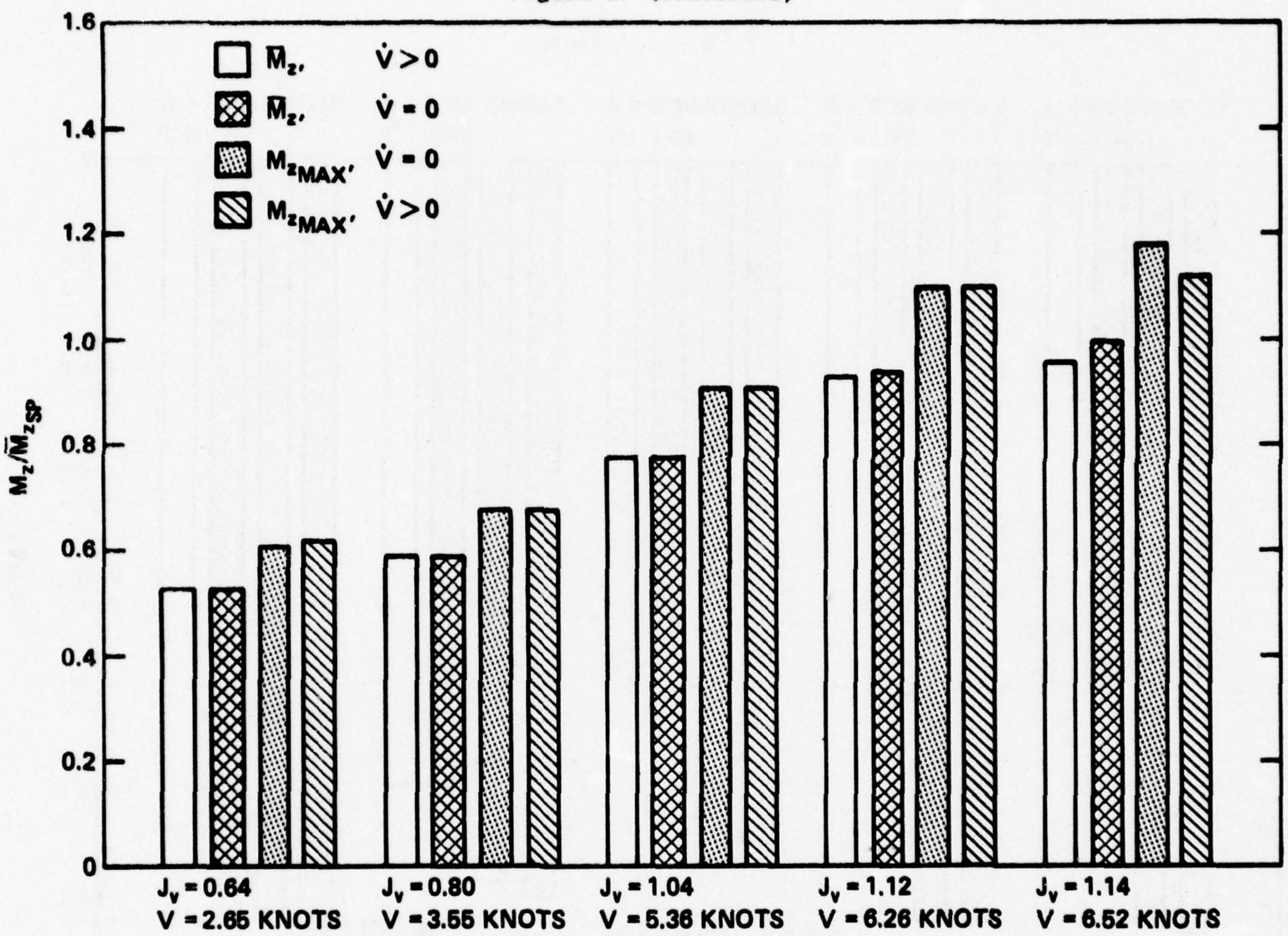

Figure 27e - M_z

Figure 27 (Continued)

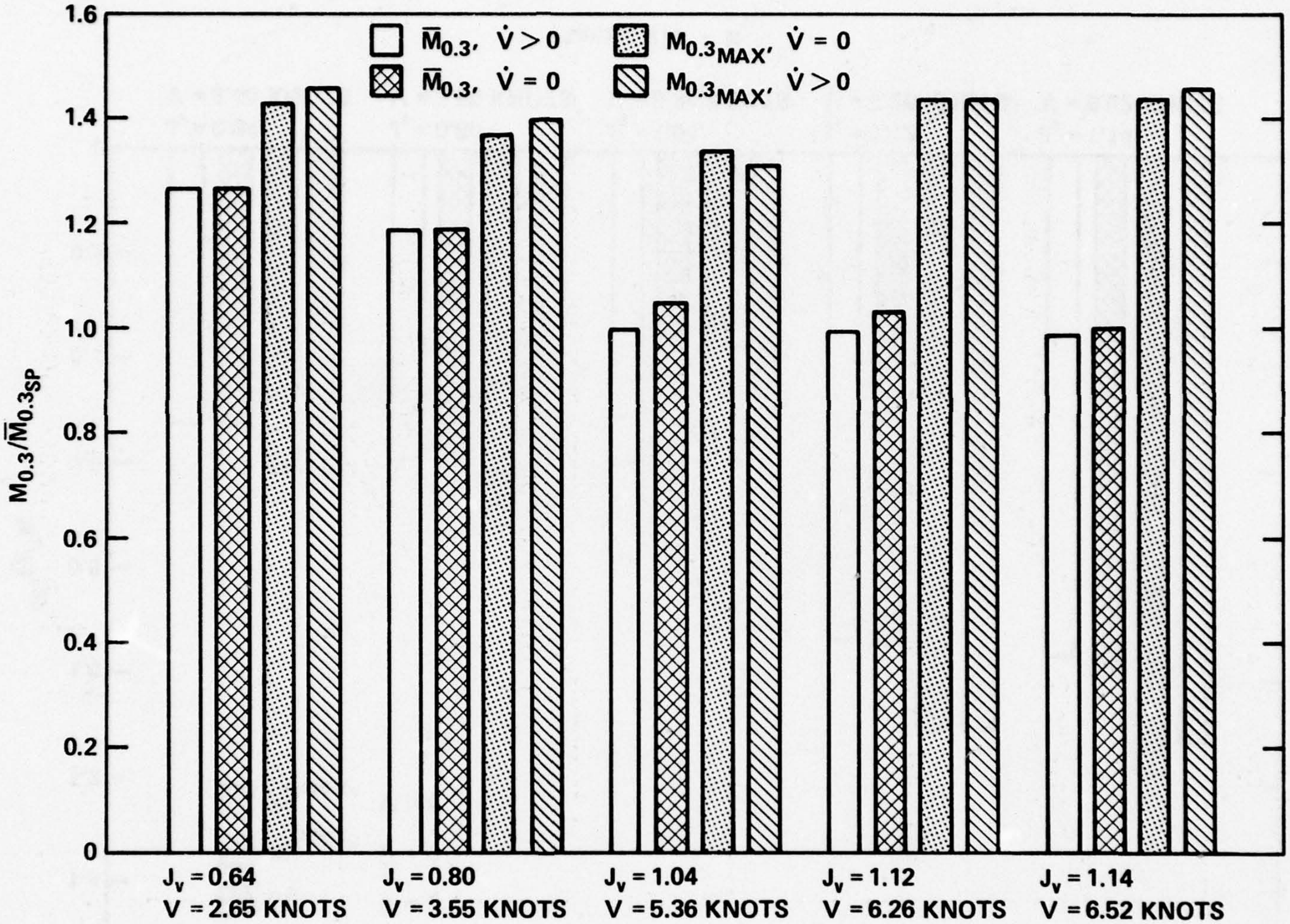

Figure 27f - $M_{0.3}$

Figure 28 - Variation of Hydrodynamic Bending Moment at 30 Percent and 40 Percent Radii with Blade Angular Position, Theoretical Prediction With and Without Dynamometer Boat

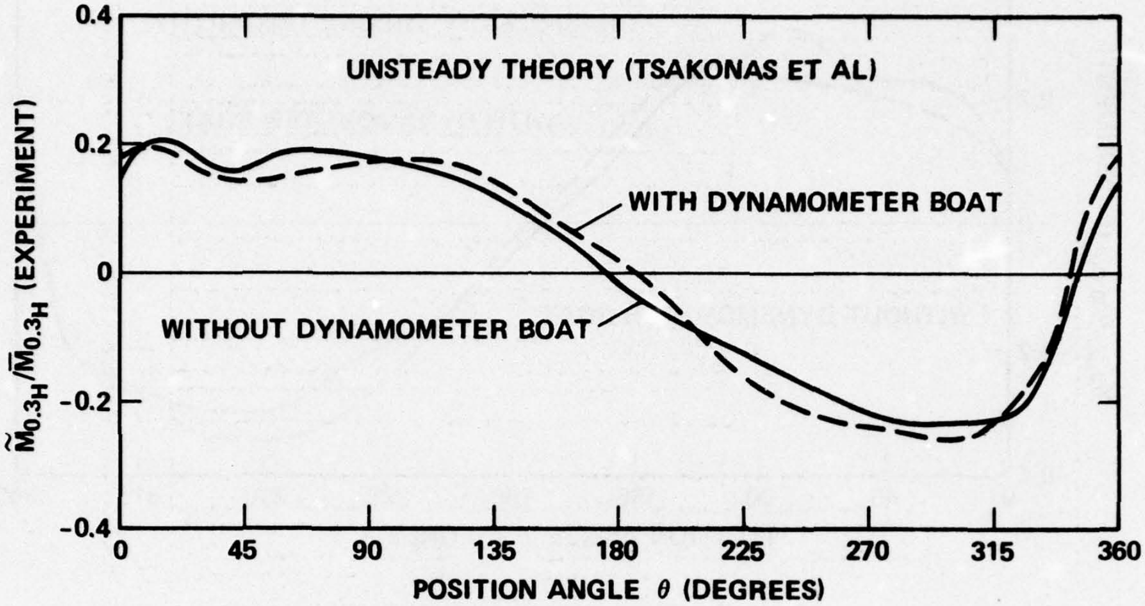

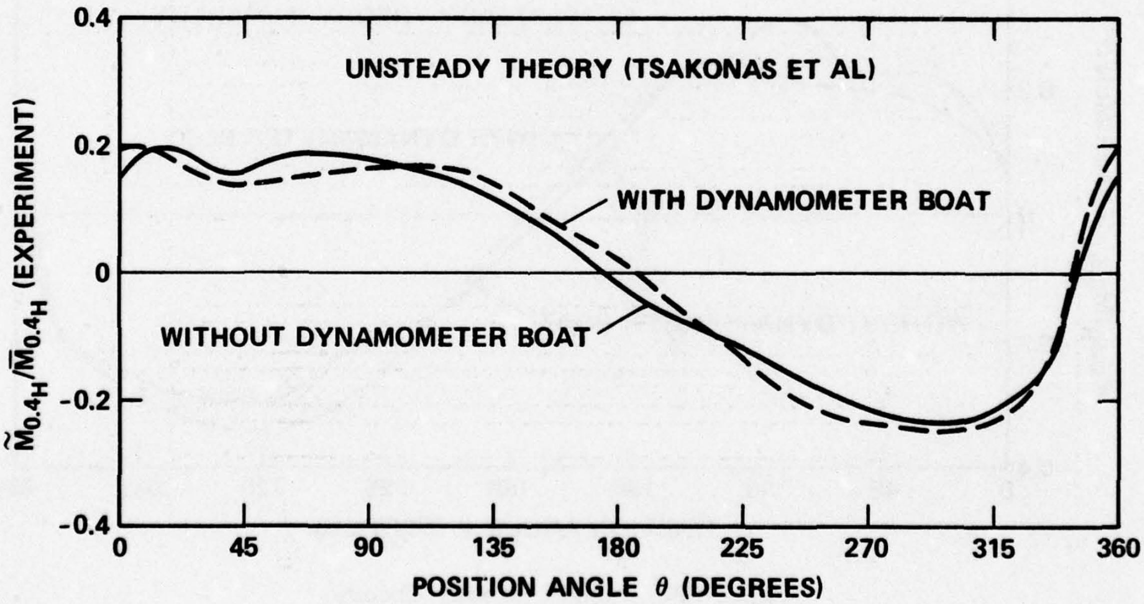

Figure 28a - Unsteady Theory

Figure 28 (Continued)

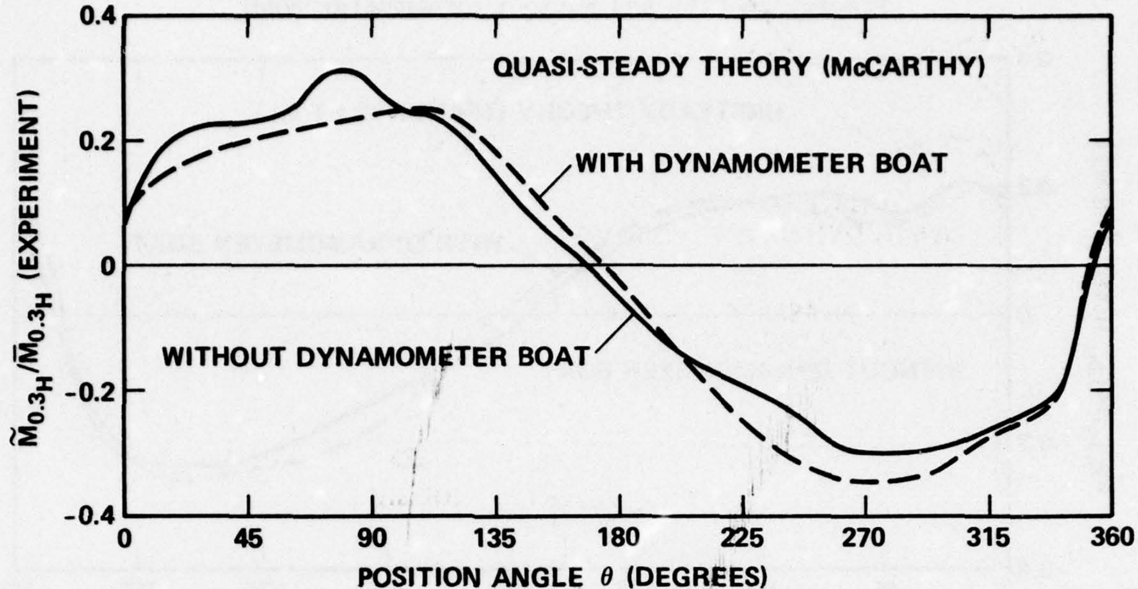

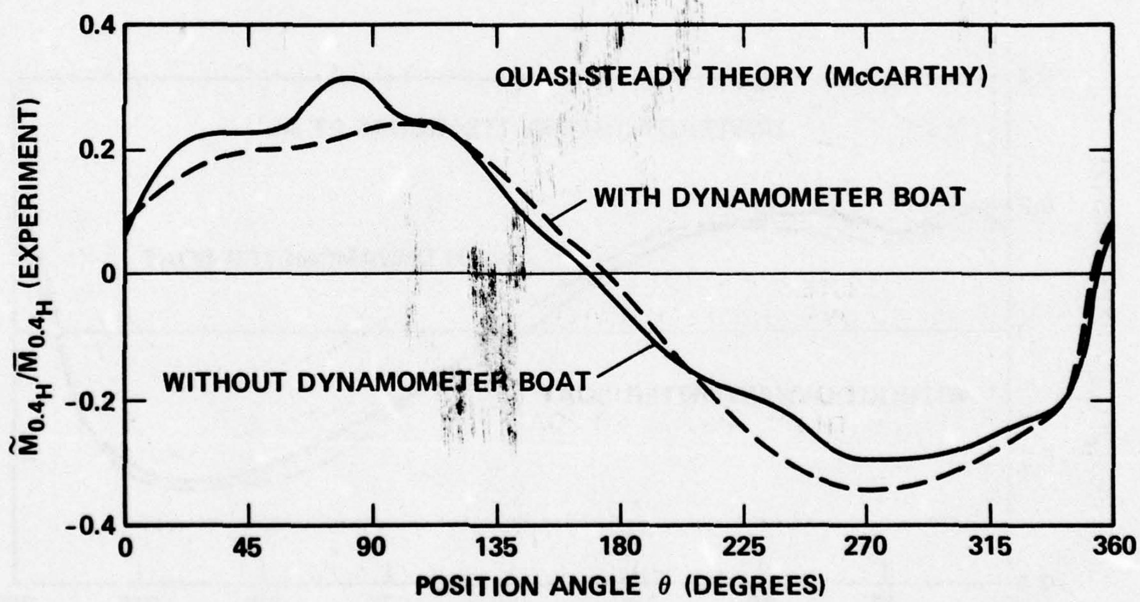

Figure 28b - Quasi-Steady Theory

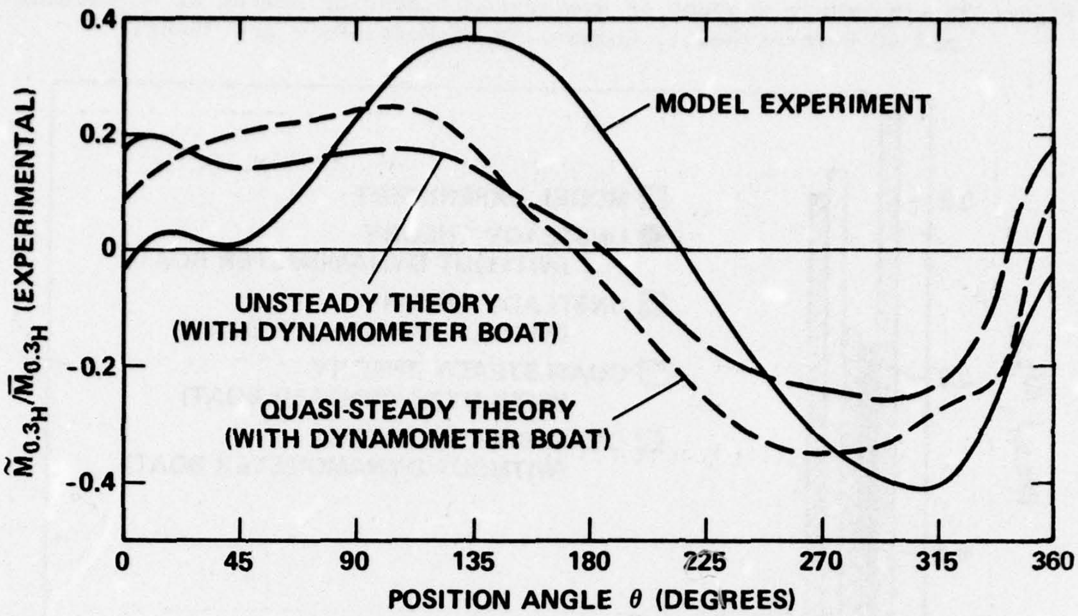

Figure 29a - 30 Percent Radius

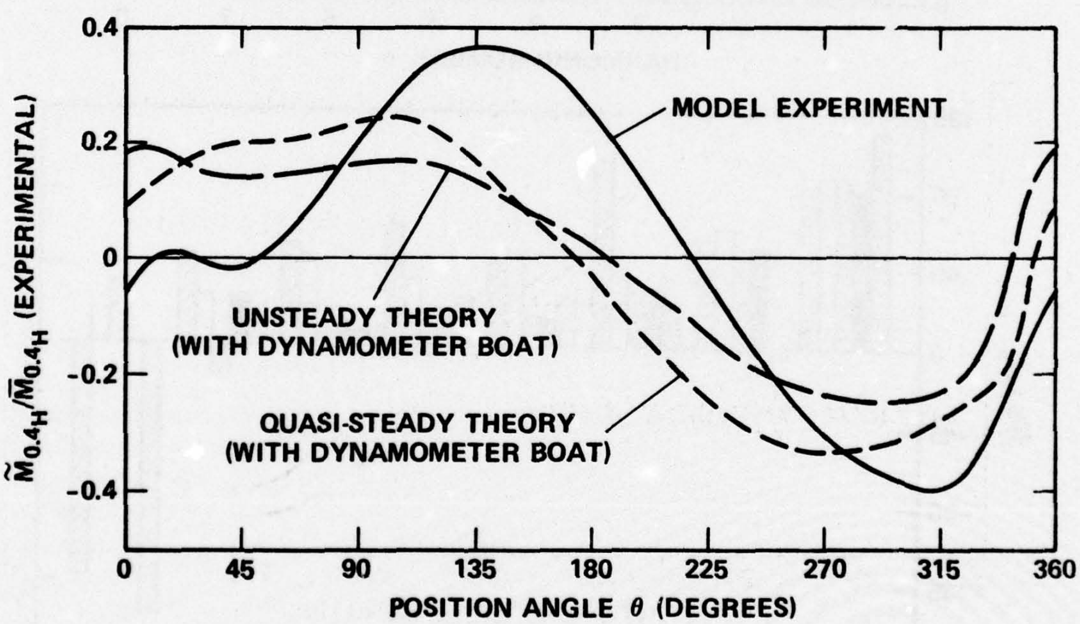

Figure 29b - 40 Percent Radius

Figure 29 - Variation of Hydrodynamic Bending Moment at 30 Percent and 40 Percent Radii with Blade Angular Position, Comparison of Model Data with Theory

Figure 30 - Harmonic Content of Hydrodynamic Bending Moment at 30 Percent and 40 Percent Radii, Comparison of Model Data and Theory

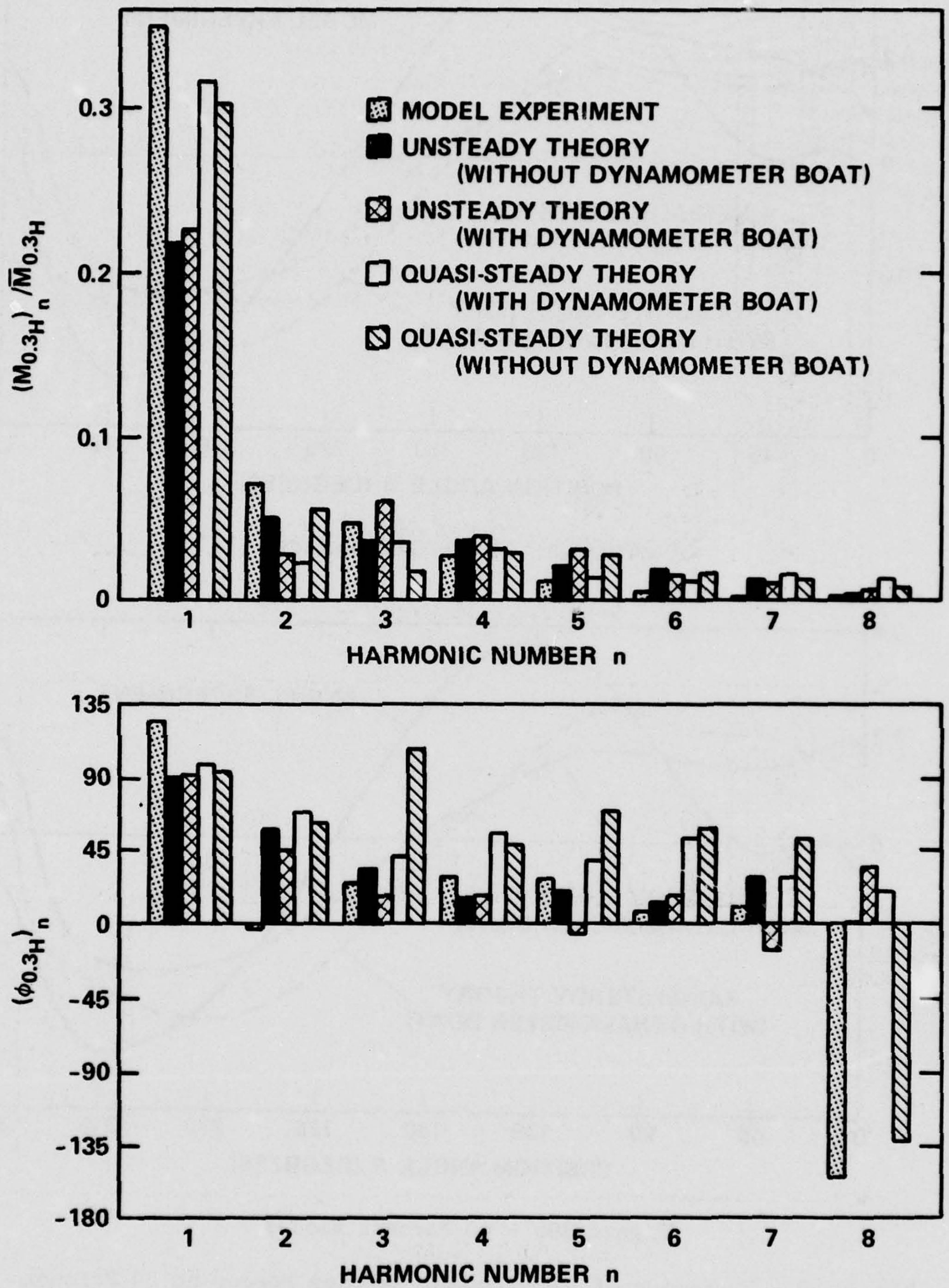

Figure 30a - 30 Percent Radius

Figure 30 (Continued)

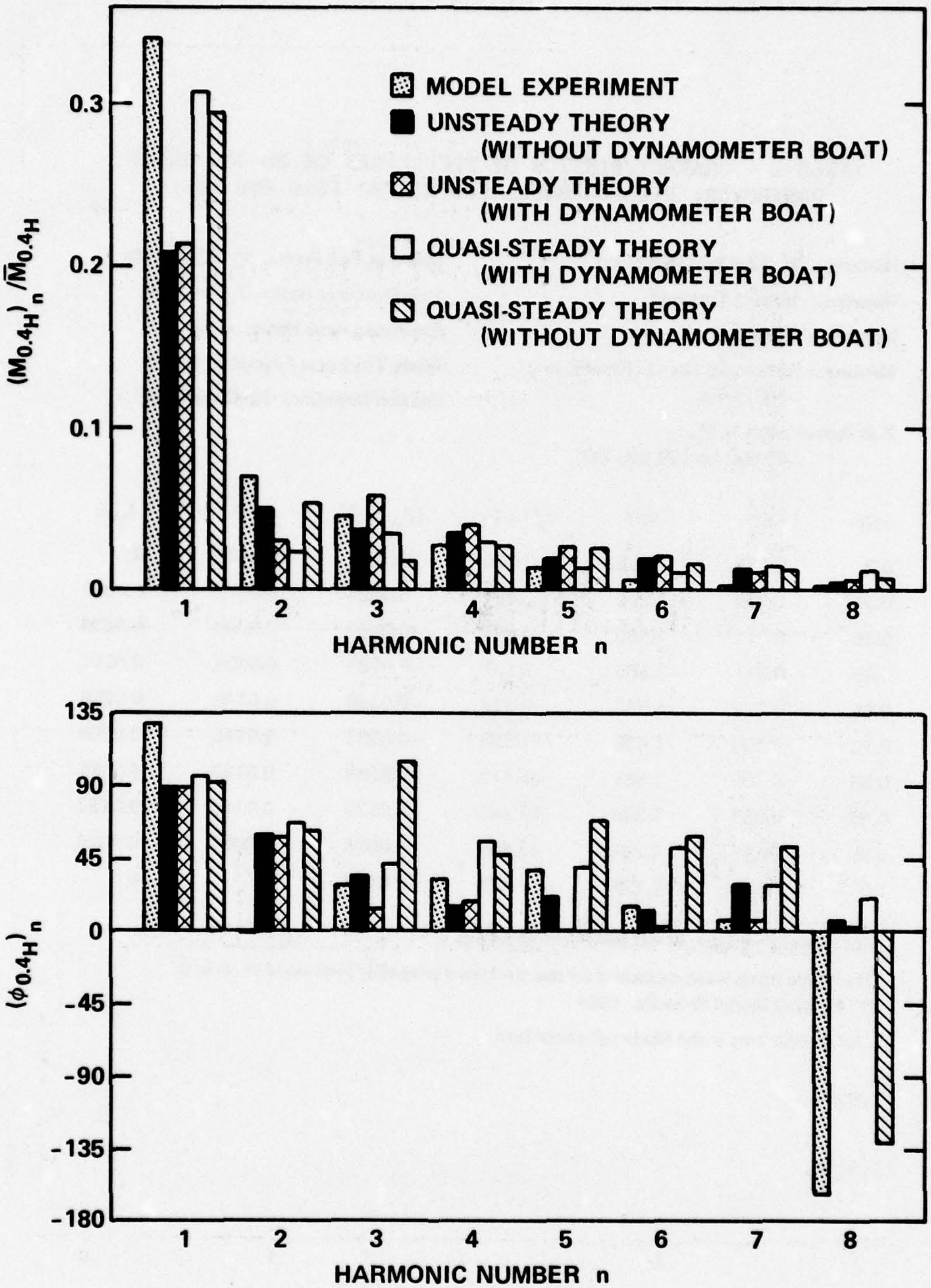

Figure 30b - 40 Percent Radius

TABLE 1 - CHARACTERISTICS OF PROPELLERS ON DD-963 CLASS DESTROYER; DTNSRDC MODEL PROPELLERS 4660 AND 4661

Diameter, D: 17.0 feet (5.577 m)+

Rotation: Inward Turning*

Number of Blades, Z: 5

Maximum Rotational Speed (Rated), n: 168 r/min

Full Power (Rated), P_D: 40,000 hp (29,800 kW)

Speed at Full Power, V: 32.5 knots

Hub-Diameter Ratio, D_h/D: 0.30

Expanded Area Ratio: 0.73

Blade Thickness Fraction: 0.054

Section Meanline: NACA a = 0.8

r/R	c/D	P/D	θ_s** (deg)	(Z_R/D)**	t/D	f_M/c
0.3	0.178	1.165	2.985	-0.0006	0.0420	0
0.35	0.210	1.296	3.481	-0.0022	0.0372	0.0050
0.45	0.271	1.480	4.810	-0.0095	0.0290	0.0209
0.55	0.327	1.566	6.631	-0.0185	0.0226	0.0267
0.65	0.374	1.566	8.978	-0.0288	0.0178	0.0256
0.75	0.406	1.498	11.895	-0.0392	0.0146	0.0209
0.85	0.409	1.381	15.410	-0.0488	0.0122	0.0151
0.90	0.387	1.306	17.403	-0.0529	0.0110	0.0122
0.95	0.326	1.222	19.557	-0.0561	0.0091	0.0094
1.0	0	1.128	21.876	-0.0583	0	0

+For model propeller, D = 0.6848 feet (22.47 cm)

*The blade loads were measured on the starboard propeller (left-hand rotation); DTNSRDC Model Propeller 4661

**The spindle axis is the blade reference line.

TABLE 2 - CALIBRATION MATRIX

$$\text{Calibration Matrix} = (C_{i,j}) = \begin{bmatrix} -3.33 & -0.099 & 0.058 & -0.002 & -0.090 & -0.066 \\ -0.008 & 5.00 & -0.002 & 0.084 & -0.168 & -0.196 \\ -0.071 & 0.048 & -3.34 & 0.070 & -0.014 & 0.058 \\ 0.009 & -0.033 & 0.103 & 4.99 & -0.071 & 0.297 \\ -0.234 & -0.367 & 0.291 & -0.861 & -9.99 & -1.87 \\ 0.079 & -0.103 & 0.223 & 0.020 & -0.034 & -5.02 \end{bmatrix}$$

where,

$$\begin{bmatrix} F_{x_I} \\ M_{y_I} \\ F_{y_I} \\ M_{x_I} \\ F_{z_I} \\ M_{z_I} \end{bmatrix} = \begin{bmatrix} F_{x_A} \\ M_{y_A} \\ F_{y_A} \\ M_{x_A} \\ F_{z_A} \\ M_{z_A} \end{bmatrix} \cdot (C_{i,j})$$

$F_{x_I}, F_{y_I}, F_{z_I}$ are indicated forces in volts

$M_{x_I}, M_{y_I}, M_{z_I}$ are indicated moments in volts

$F_{x_A}, F_{y_A}, F_{z_A}$ are applied forces in pounds

$M_{x_A}, M_{y_A}, M_{z_A}$ are applied moments in inch-pound

C_{ij} for j = 1, 3, 5 are in volts per pound

C_{ij} for j = 2, 4, 6 are in volts per inch-pound

The arrays are arranged by the coupling of the force and moment pairs of the three flexures; i.e., Flexure 1 measures F_x and M_y, Flexure 2 measures F_y and M_x, and Flexure 3 measures F_z and M_z.

TABLE 3 - MODEL EXPERIMENTAL CONDITIONS

	Condition Number	V knot	(M/s)	n r/s	J_V	$(P/D)_{0.7}$	$\psi-\psi_{CW}$ degree	$\dot{V}$ knot/s	(M/s^2)	$t-t_o$ s
Self Propulsion	1	6.52	(3.61)	14.08	1.14	1.54	0	0	(0)	N/A
Quasi-Steady Hull Pitch	2	6.52	(3.61)	14.08	1.14	1.54	-1.85	0	(0)	N/A
	3	6.52	(3.61)	14.08	1.14	1.54	-0.92	0	(0)	N/A
	4	6.52	(3.61)	14.08	1.14	1.54	0.92	0	(0)	N/A
	5	6.52	(3.61)	14.08	1.14	1.54	1.85	0	(0)	N/A
Unsteady Hull Pitch	6	6.52	(3.61)	14.08	1.14	1.54	variable*	0	(0)	N/A
Quasi-Steady Acceleration	7	2.65	(1.47)	10.21	0.64	1.54	0	0	(0)	N/A
	8	3.55	(1.96)	10.96	0.80	1.54	0	0	(0)	N/A
	9	5.36	(2.97)	12.70	1.04	1.54	0	0	(0)	N/A
	10	6.26	(3.47)	13.78	1.12	1.54	0	0	(0)	N/A
	11	6.52	(3.61)	14.08	1.14	1.54	0	0	(0)	N/A
Unsteady Acceleration	12	2.65**	(1.47)**	10.21	0.64	1.54	0	0.56**	(0.31)**	2.41
	13	3.55**	(1.96)**	10.96	0.80	1.54	0	0.56**	(0.31)**	4.01
	14	5.36**	(2.97)**	12.70	1.04	1.54	0	0.32**	(0.18)**	8.03
	15	6.26**	(3.47)**	13.78	1.12	1.54	0	0.08**	(0.04)**	12.04
	16	6.52**	(3.61)**	14.08	1.14	1.54	0	0**	(0)**	16.05

*Sinusoidal with amplitude equal to 1.85 degrees, frequency equal to 0.8 Hz.

**Varies with time (Figure 7); value shown is at time of interest.

TABLE 4 - FULL-SCALE CONDITIONS SIMULATED BY MODEL EXPERIMENTS

	Condition Number	V knot	(M/s)	n r/min	J_V	$(P/D)_{0.7}$	$\psi-\psi_{CW}$ degree	$\dot{V}$ knot/s	(M/s^2)	$t-t_o$ s
Self Propulsion	1	32.5	(18.0)	169	1.14	1.54	0	0	(0)	N/A
Quasi-Steady Hull Pitch	2	32.5	(18.0)	169	1.14	1.54	-1.85	0	(0)	N/A
	3	32.5	(18.0)	169	1.14	1.54	-0.92	0	(0)	N/A
	4	32.5	(18.0)	169	1.14	1.54	0.92	0	(0)	N/A
	5	32.5	(18.0)	169	1.14	1.54	1.85	0	(0)	N/A
Unsteady Hull Pitch	6	32.5	(18.0)	169	1.14	1.54	variable*	0	(0)	N/A
Quasi-Steady Acceleration	7	13.2	(7.3)	123	0.64	1.54	0	0	(0)	N/A
	8	17.7	(9.8)	132	0.80	1.54	0	0	(0)	N/A
	9	26.7	(14.8)	153	1.04	1.54	0	0	(0)	N/A
	10	31.2	(17.3)	166	1.12	1.54	0	0	(0)	N/A
	11	32.5	(18.0)	169	1.14	1.54	0	0	(0)	N/A
Unsteady Acceleration	12	13.2	(7.3)	123	0.64	1.54	0	0.56**	(0.31)**	12.0
	13	17.7	(9.8)	132	0.80	1.54	0	0.56**	(0.31)**	20.0
	14	26.7	(14.8)	153	1.04	1.54	0	0.32**	(0.18)**	40.0
	15	31.2	(17.3)	166	1.12	1.54	0	0.08**	(0.04)**	60.0
	16	32.5	(18.0)	169	1.14	1.54	0	0**	(0)**	80.0

*Sinusoidal with amplitude equal to 1.85 degrees, frequency equal to 0.16 Hz.

**Varies with time (Figure 7); value shown is at time of interest.

TABLE 5 - REPEAT RUNS FOR F_x FOR STEADY-AHEAD OPERATION

Date of Run:	18 Dec 76			21 Dec 76			28 Dec 76				30 Dec 76
Time of Run:	1100	1300	1410	1740	1052	1613	1120	1310	1315	1335	1000
Run No.:	45	50	55	57	65	92	114	115*	116	117	128
Propeller Speed, n (r/s)	14.08	14.08	14.08	14.08	14.08	14.01	14.08	14.08	14.02	14.08	14.00
Velocity, V (ft/s)	11.04	11.04	11.03	11.07	11.05	11.04	10.97	10.97	10.97	10.97	10.97
n	Amplitudes $(F_x)_n^{**}$ (lb)										
0	4.380	4.392	4.408	4.520	4.635	4.528	4.321	4.495	4.434	4.457	4.528
1	1.628	1.631	1.632	1.532	1.631	1.622	1.563	1.608	1.594	1.588	1.610
2	0.306	0.303	0.305	0.340	0.335	0.330	0.255	0.257	0.261	0.255	0.292
3	0.215	0.210	0.211	0.221	0.228	0.234	0.201	0.203	0.204	0.201	0.229
4	0.115	0.117	0.117	0.110	0.118	0.123	0.119	0.123	0.123	0.121	0.127
5	0.060	0.061	0.059	0.054	0.063	0.069	0.054	0.055	0.051	0.052	0.056
6	0.028	0.027	0.024	0.028	0.031	0.033	0.021	0.025	0.022	0.021	0.027
7	0.008	0.010	0.008	0.007	0.003	0.002	0.003	0.002	0.002	0.003	0.005
8	0.015	0.016	0.017	0.008	0.010	0.008	0.010	0.010	0.011	0.011	0.013
9	0.009	0.009	0.011	0.010	0.002	0.004	0.003	0.003	0.004	0.005	0.008
10	0.008	0.007	0.009	0.009	0.010	0.011	0.010	0.009	0.009	0.010	0.010
11	0.008	0.009	0.009	0.012	0.011	0.011	0.012	0.014	0.014	0.016	0.012
12	0.013	0.013	0.014	0.015	0.014	0.015	0.017	0.016	0.017	0.019	0.018
13	0.009	0.009	0.010	0.012	0.010	0.011	0.012	0.011	0.011	0.014	0.014
14	0.006	0.006	0.007	0.008	0.007	0.007	0.008	0.006	0.005	0.008	0.008
15	0.005	0.004	0.006	0.003	0.002	0.004	0.005	0.006	0.005	0.005	0.006
16	0.007	0.006	0.008	0.005	0.003	0.003	0.005	0.005	0.006	0.006	0.006
	Phases $(\phi_x)_n^{**}$ (deg)										
1	118.8	118.6	119.0	115.3	116.8	116.5	116.7	116.5	116.3	116.2	118.7
2	12.0	11.2	11.6	3.5	-0.0	-0.2	1.2	1.3	3.4	3.2	-2.7
3	38.2	37.3	37.9	19.1	24.1	23.8	21.6	21.4	21.7	20.7	26.0
4	37.7	36.8	36.6	17.6	20.9	19.2	24.8	23.6	26.5	23.7	30.3
5	31.9	30.4	30.4	-0.6	10.5	9.5	13.5	12.6	15.5	12.2	18.7
6	49.7	46.5	39.8	4.6	13.5	16.4	11.2	5.8	6.2	3.0	35.5
7	167.9	-169.0	-166.5	107.7	113.7	116.5	-159.1	-92.1	161.0	-168.8	101.7
8	-126.4	-125.5	-121.0	-171.6	-155.3	179.3	-137.8	-123.6	-127.9	-140.6	-147.2
9	-135.2	-126.3	-133.4	140.1	171.2	136.1	-157.9	-113.9	-120.8	127.9	172.0
10	172.9	-178.3	-176.1	107.8	128.3	125.0	130.7	123.6	119.1	120.3	143.5
11	[illegible]5.3	161.8	176.2	106.7	130.6	111.9	127.5	118.4	122.3	121.3	146.1
12	141.7	140.9	143.8	91.5	112.1	100.1	114.5	115.0	114.3	122.1	143.7
13	133.7	135.6	143.2	95.4	114.5	108.3	123.8	121.2	119.7	123.2	132.1
14	116.9	112.7	117.6	75.5	113.2	97.0	84.3	78.3	85.8	85.0	90.6
15	90.6	98.8	113.7	110.8	96.1	74.4	60.3	58.2	36.6	56.8	26.1
16	77.9	78.4	88.6	55.1	74.6	61.0	83.8	47.7	68.3	85.6	92.8

*Run 115 used for detailed analysis

**Raw data without corrections for interactions or downstream body

TABLE 6 - CENTRIFUGAL AND GRAVITATIONAL LOADS*

	F_X (lb)	M_Y (in.-lb)	F_Y (lb)	M_X (in.-lb)	F_Z (lb)	M_Z (in.-lb)	n (r/s)
Mean, $(\overline{F, M})$	0.036	0.191	0.774	0.0	7.300	-0.510	14.08
First Harmonic Amplitude, $(F, M)_1$	0.0	0.0	0.194	0.314	0.244	0.0	
First Harmonic Phase, $(\phi_{F, M})_1$, (deg)	0.0	0.0	-96.0	96.0	-159.0	0.0	
Mean, $(\overline{F, M})$	0.035	0.184	0.744	0.0	6.930	-0.485	13.76
First Harmonic Amplitude, $(F, M)_1$	0.0	0.0	0.194	0.314	0.244	0.0	
First Harmonic Phase, $(\phi_{F, M})_1$, (deg)	0.0	0.0	-96.0	96.0	-159.0	0.0	
Mean, $(\overline{F, M})$	0.030	0.161	0.642	0.0	5.860	-0.410	12.65
First Harmonic Amplitude, $(F, M)_1$	0.0	0.0	0.194	0.314	0.244	0.0	
First Harmonic Phase, $(\phi_{F, M})_1$, (deg)	0.0	0.0	-96.0	96.0	-159.0	0.0	
Mean, $(\overline{F, M})$	0.024	0.127	0.493	0.0	4.400	-0.308	10.96
First Harmonic Amplitude, $(F, M)_1$	0.0	0.0	0.194	0.314	0.244	0.0	
First Harmonic Phase, $(\phi_{F, M})_1$, (deg)	0.0	0.0	-96.0	96.0	-159.0	0.0	
Mean, $(\overline{F, M})$	0.016	0.108	0.434	0.0	3.820	-0.207	10.21
First Harmonic Amplitude, $(F, M)_1$	0.0	0.0	0.194	0.314	0.244	0.0	
First Harmonic Phase, $(\phi_{F, M})_1$, (deg)	0.0	0.0	-96.0	96.0	-159.0	0.0	

*The results shown here are for an Aluminum model propeller, $\rho_P = 5.44\ lbf\text{-}s^2/ft^4$ and were obtained by fairing the experimental air-spin data using the following restraints:

$(\overline{F, M})/n^2$ = constant

(F_1, M_1) = constant

ϕ_1 = constant

Except where indicated in Table 8, all other centrifugal and gravitational loads presented in this report are for a Bronze propeller, $\rho_P = 14.48\ lbf\text{-}s^2/ft^4$

TABLE 7 - SUMMARY OF CIRCUMFERENTIAL VARIATION OF LOADS AT THE SELF PROPULSION CONDITION; V = 6.52 KNOTS, n = 14.08 REVOLUTIONS PER SECOND

	Maximum Values		Minimum Values		First Harmonic Values	
	$\frac{(F,M)_{MAX}}{\lvert \overline{F,M} \rvert}$	ϕ_{MAX}	$\frac{(F,M)_{MIN}}{\lvert \overline{F,M} \rvert}$	ϕ_{MIN}	$\frac{(F,M)_1}{(\overline{F,M})}$	ϕ_1
F_{x_H}	1.43	124	0.51	308	0.42	116
M_{y_H}	1.42	128	0.52	312	0.41	120
F_{y_H}	1.40	120	0.54	292	0.38	105
M_{x_H}	-1.34*	124	-0.61	300	0.32	294
F_{z_H}	-7.88*	252	6.30	68	6.87	54
M_{z_H}	-1.30*	204	-0.63	64	0.31	41
$M_{0.3_H}$	1.37	132	0.59	312	0.35	124
$M_{0.4_H}$	1.36	132	0.60	312	0.34	128
F_x	1.42	124	0.53	308	0.41	116
M_y	1.40	128	0.54	312	0.39	120
F_y	1.14	132	0.83	304	0.12	123
M_x	-1.26*	136	-0.70	308	0.23	304
F_z	1.04	76	0.96	264	0.03	89
M_z	-1.18*	204	-0.77	64	0.19	41
$M_{0.3}$	1.45	136	0.48	312	0.43	124
$M_{0.4}$	1.60	140	0.33	312	0.56	126

*The maximum values shown are the values which have the largest absolute value. For maximum values shown with negative sign, the corresponding time average values are negative using the adopted convention shown in Figure 1.

TABLE 8 - TIME AVERAGE LOADS FOR STEADY-AHEAD OPERATION AT THE SELF PROPULSION CONDITION; V = 6.52 KNOTS, n = 14.08 REVOLUTIONS PER SECOND

		Total with Aluminum Blades	Total with Bronze Blades	Hydrodynamic Loads Only		Total with Bronze Blades	Hydrodynamic Loads Only
$\bar{F}_x$	(lb)	3.722	3.781	3.686	$\bar{K}_{F_x}$	0.0448	0.0437
$\bar{M}_y$	(in. - lb)	10.903	11.220	10.712	$\bar{K}_{M_y}$	0.0161	0.0154
$\bar{F}_y$	(lb)	3.456	4.742	2.682	$\bar{K}_{F_y}$	0.0562	0.0318
$\bar{M}_x$	(in. - lb)	-7.765	-7.765	-7.765	$\bar{K}_{M_x}$	-0.0112	-0.0112
$\bar{F}_z$	(lb)	7.145	19.279	-0.154	$\bar{K}_{F_z}$	0.2253	-0.0018
$\bar{M}_z$	(in. - lb)	-2.608	-3.456	-2.098	$\bar{K}_{M_z}$	-0.0049	-0.0030
$\bar{M}_{0.3}$	(in. - lb)	6.659	5.563	7.322	$\bar{K}_{M_{0.3}}$	0.0080	0.0106
$\bar{M}_{0.4}$	(in. - lb)	4.653	3.314	5.609	$\bar{K}_{M_{0.4}}$	0.0048	0.0081
$\bar{M}_{0.5}$	(in. - lb)	2.790	1.079	3.820	$\bar{K}_{M_{0.5}}$	0.0016	0.0055

For Aluminum blades ρ_P = 5.44 lbf - s^2/ft^4

For Bronze blades ρ_P = 14.48 lbf - s^2/ft^4

$\bar{K}_F = \bar{F}/(\rho n^2 D^4)$ and $\bar{K}_M = \bar{M}/(\rho n^2 D^5)$ are based on the density of water

TABLE 9 - WAKE WITHOUT DYNAMOMETER BOAT

TABLE 9A - MEASURED DATA

r/R = 0.370

θ_w	V_x/V	V_t/V	V_r/V	θ_w	V_x/V	V_t/V	V_r/V
0.0	.906	.031	-.011	45.0	1.098	-.151	-.059
1.6	.917	.027	-.014	54.1	1.111	-.163	-.046
3.0	.917	.019	-.017	54.1	1.101	-.165	-.046
3.0	.906	.025	-.018	63.1	1.120	-.172	-.036
5.2	.918	.016	-.018	72.1	1.109	-.180	-.026
5.2	.894	.015	-.018	80.0	1.116	-.180	-.018
6.0	.902	-.009	-.014	90.2	1.124	-.176	-.008
8.8	.894	-.032	-.011	99.2	1.117	-.172	-.000
10.6	.933	-.064	.001	107.0	1.131	-.161	.007
14.3	.979	-.117	.009	117.2	1.130	-.148	.016
17.9	1.028	-.166	.011	117.2	1.119	-.151	.015
17.9	1.023	-.165	.015	126.3	1.123	-.133	.022
21.5	1.120	-.167	-.009	135.3	1.128	-.113	.027
25.1	1.132	-.147	-.048	144.2	1.111	-.095	.032
26.9	1.105	-.143	-.058	153.0	1.121	-.073	.034
28.9	1.112	-.135	-.065	162.3	1.127	-.049	.038
32.4	1.117	-.131	-.068	171.3	1.117	-.024	.040
35.0	1.116	-.133	-.068	180.0	1.133	.004	.039
35.9	1.093	-.136	-.069	184.1	1.119	.016	.039
39.0	1.100	-.142	-.064				

TABLE 9A (Continued)

r/R = 0.370

θ_w	V_x/V	V_t/V	V_r/V	θ_w	V_x/V	V_t/V	V_r/V
184.1	1.119	.016	.039	315.0	1.110	.114	-.041
187.7	1.122	.028	.037	324.0	1.088	.130	-.018
189.0	1.119	.032	.038	324.2	1.086	.134	-.018
191.3	1.107	.039	.038	327.8	1.063	.138	-.015
198.3	1.106	.061	.036	331.4	1.010	.138	-.013
207.2	1.111	.085	.031	333.0	1.000	.126	-.011
216.2	1.124	.108	.027	333.1	.974	.124	-.013
225.2	1.118	.130	.020	335.0	.930	.109	-.007
234.3	1.125	.144	.012	338.6	.909	.055	.000
243.0	1.137	.154	.005	342.0	.922	.022	.006
243.4	1.123	.157	.004	345.8	.936	.019	.012
252.2	1.119	.163	-.002	349.0	.940	.021	.009
261.0	1.114	.165	-.010	351.1	.939	.026	.012
270.0	1.108	.166	-.020	353.0	.927	.027	.006
279.1	1.109	.158	-.029	354.8	.931	.031	.002
288.2	1.113	.146	-.037	356.0	.911	.032	-.003
291.8	1.102	.141	-.041	358.0	.909	.030	-.007
297.0	1.097	.132	-.047	358.0	.916	.031	-.009
297.1	1.098	.132	-.046	359.0	.920	.029	-.008
305.0	1.089	.118	-.051				

TABLE 9A (Continued)

r/R = 0.574

θ_w	V_x/V	V_t/V	V_r/V	θ_w	V_x/V	V_t/V	V_r/V
-1.5	1.027	-.059	-.023	189.1	1.129	.034	.110
4.0	.987	-.099	-.055	199.9	1.128	.038	.104
7.0	1.026	-.115	-.080	208.8	1.125	.046	.096
7.0	1.023	-.127	-.078	217.0	1.125	.057	.087
11.1	1.051	-.130	-.093	219.6	1.126	.064	.084
14.8	1.087	-.122	-.096	239.5	1.124	.088	.055
18.3	1.078	-.118	-.096	255.7	1.128	.096	.028
18.3	1.085	-.098	-.098	279.0	1.105	.102	-.015
21.0	1.078	-.119	-.091	298.0	1.096	.083	-.047
25.4	1.081	-.120	-.086	309.0	1.100	.064	-.058
29.1	1.090	-.119	-.081	317.0	1.101	.060	-.061
32.0	1.085	-.123	-.077	318.9	1.102	.060	-.062
36.2	1.086	-.128	-.069	320.0	1.083	.063	-.056
39.8	1.086	-.132	-.063	322.5	1.064	.067	-.069
39.9	1.099	-.128	-.062	324.3	1.053	.065	-.069
59.7	1.096	-.143	-.029	328.0	.998	.050	-.075
79.4	1.110	-.146	.007	331.5	.997	.017	-.072
99.1	1.115	-.136	.039	338.7	1.007	-.028	-.046
120.0	1.114	-.109	.072	338.8	1.009	-.027	-.046
140.2	1.126	-.074	.094	342.0	1.017	-.040	-.032
160.1	1.141	-.046	.106	347.7	1.020	-.046	-.018
169.4	1.128	-.026	.111	353.1	1.034	-.060	-.013
179.0	1.142	-.003	.111	358.0	1.023	-.071	-.018
189.1	1.129	.004	.110	358.5	1.027	-.059	-.023

TABLE 9A (Continued)

r/R = 0.798

θ_w	V_x/V	V_t/V	V_r/V	θ_w	V_x/V	V_t/V	V_r/V
0.0	.962	-.063	-.117	200.4	1.036	.042	.103
3.9	.973	-.061	-.115	220.0	1.061	.078	.084
7.0	.987	-.051	-.106	239.9	1.048	.110	.052
9.4	.943	-.068	-.104	254.1	1.063	.117	.021
12.0	.962	-.100	-.105	254.1	1.059	.119	.021
14.7	.992	-.115	-.116	259.0	1.062	.123	.011
16.0	1.017	-.108	-.115	259.0	1.061	.124	.011
19.9	1.023	-.096	-.112	279.4	1.034	.125	-.039
25.3	1.031	-.096	-.102	290.0	1.031	.117	-.062
39.0	1.019	-.111	-.083	299.2	1.045	.102	-.081
50.6	1.030	-.117	-.064	310.0	1.043	.080	-.102
59.6	1.032	-.121	-.046	318.0	1.041	.077	-.108
70.0	1.028	-.126	-.029	318.9	1.036	.077	-.105
79.4	1.024	-.126	-.012	320.9	1.009	.084	-.112
99.2	1.030	-.120	.024	322.0	.998	.074	-.111
106.5	1.018	-.116	.041	326.1	.989	.021	-.116
119.2	1.010	-.104	.063	328.0	1.001	.010	-.124
124.0	1.022	-.096	.070	329.0	1.017	.018	-.128
138.9	1.024	-.076	.088	331.5	1.029	.024	-.128
142.0	1.023	-.072	.091	333.5	1.002	.030	-.124
160.0	1.030	-.042	.106	336.0	1.008	.027	-.117
180.0	1.044	-.002	.111	340.7	.968	.022	-.112
182.2	1.041	-.000	.113	349.6	.940	-.017	-.104
200.1	1.058	.040	.104	358.6	.957	-.062	-.119
200.4	1.036	.042	.103	360.0	.962	-.063	-.117

TABLE 9A (Continued)

r/R = 1.022

θ_w	V_x/V	V_t/V	V_r/V	θ_w	V_x/V	V_t/V	V_r/V
0.0	.925	-.074	-.105	199.9	1.075	.028	.111
1.0	.944	-.079	-.109	219.6	1.072	.054	.088
3.0	.965	-.083	-.116	239.0	1.067	.078	.057
7.4	1.000	-.070	-.119	259.0	1.083	.103	.015
9.2	.983	-.075	-.113	279.2	1.079	.101	-.028
12.8	1.009	-.105	-.105	299.0	1.064	.081	-.075
14.6	1.024	-.112	-.111	304.0	1.043	.076	-.092
20.0	1.066	-.079	-.108	309.9	1.034	.063	-.102
21.9	1.060	-.103	-.097	315.2	1.027	.051	-.110
27.1	1.060	-.107	-.091	320.9	.996	.063	-.116
32.6	1.064	-.115	-.082	322.0	.970	.056	-.116
37.0	1.057	-.122	-.074	324.3	.955	.008	-.125
39.8	1.067	-.119	-.069	326.0	1.006	.010	-.136
59.0	1.072	-.128	-.032	327.8	1.011	.016	-.136
79.4	1.079	-.133	.002	329.6	1.015	.015	-.132
99.1	1.059	-.131	.037	333.2	1.004	.010	-.131
120.0	1.065	-.103	.073	336.0	.998	.005	-.125
140.4	1.064	-.086	.099	340.4	.982	.007	-.113
162.1	1.076	-.045	.118	346.1	.917	-.001	-.104
169.2	1.080	-.037	.117	351.0	.900	-.029	-.093
181.9	1.085	-.016	.119	356.6	.903	-.049	-.102
189.0	1.083	-.003	.117	360.0	.925	-.074	-.105

TABLE 9B - INTERPOLATED VALUES OF V_x/V

θ_w	r/R = 0.3	0.4	0.5	0.6	0.7	0.8	0.9	1.0
0.0	.852	.925	.973	.988	.975	.962	.948	.933
2.5	.875	.928	.963	.974	.967	.961	.958	.958
5.0	.850	.925	.976	.995	.987	.983	.983	.987
7.5	.806	.923	.999	1.019	.991	.978	.978	.993
10.0	.827	.950	1.022	1.025	.969	.942	.944	.974
12.5	.880	.987	1.049	1.048	.994	.968	.968	.996
15.0	.912	1.012	1.071	1.071	1.024	1.000	.999	1.020
17.5	.969	1.036	1.074	1.071	1.034	1.017	1.021	1.045
20.0	1.074	1.086	1.086	1.068	1.036	1.023	1.031	1.058
22.5	1.152	1.124	1.097	1.068	1.040	1.028	1.032	1.052
25.0	1.152	1.125	1.099	1.071	1.043	1.031	1.034	1.052
27.5	1.103	1.104	1.097	1.076	1.045	1.031	1.033	1.054
30.0	1.119	1.113	1.102	1.077	1.044	1.029	1.033	1.055
32.5	1.124	1.113	1.098	1.073	1.040	1.026	1.032	1.056
35.0	1.107	1.105	1.096	1.072	1.038	1.023	1.027	1.051
37.5	1.095	1.102	1.098	1.075	1.037	1.020	1.024	1.050
40.0	1.087	1.102	1.102	1.078	1.037	1.019	1.026	1.058
42.5	1.084	1.101	1.104	1.081	1.038	1.022	1.030	1.063
45.0	1.083	1.102	1.105	1.083	1.041	1.024	1.033	1.067
47.5	1.085	1.103	1.106	1.084	1.043	1.027	1.035	1.069
50.0	1.089	1.104	1.106	1.085	1.045	1.029	1.037	1.069
52.5	1.094	1.107	1.107	1.085	1.046	1.031	1.038	1.068
55.0	1.100	1.109	1.107	1.084	1.047	1.031	1.038	1.067
57.5	1.108	1.113	1.107	1.084	1.047	1.032	1.037	1.064
60.0	1.115	1.116	1.108	1.083	1.047	1.032	1.037	1.063

TABLE 9B (Continued)

θ_w	r/R = 0.3	0.4	0.5	0.6	0.7	0.8	0.9	1.0
60.0	1.115	1.116	1.108	1.083	1.047	1.032	1.037	1.063
62.5	1.118	1.119	1.110	1.085	1.047	1.031	1.037	1.064
65.0	1.115	1.118	1.111	1.086	1.047	1.030	1.036	1.065
67.5	1.108	1.116	1.112	1.087	1.046	1.029	1.036	1.066
70.0	1.101	1.114	1.113	1.088	1.046	1.028	1.035	1.067
72.5	1.096	1.113	1.114	1.089	1.045	1.027	1.034	1.067
75.0	1.097	1.114	1.116	1.090	1.045	1.025	1.033	1.067
77.5	1.099	1.117	1.118	1.092	1.044	1.024	1.032	1.067
80.0	1.102	1.119	1.120	1.093	1.044	1.024	1.031	1.066
82.5	1.105	1.122	1.122	1.094	1.046	1.025	1.031	1.065
85.0	1.109	1.124	1.123	1.095	1.048	1.026	1.031	1.063
87.5	1.111	1.125	1.124	1.097	1.049	1.028	1.032	1.061
90.0	1.113	1.126	1.125	1.098	1.051	1.029	1.032	1.059
92.5	1.109	1.125	1.125	1.098	1.053	1.030	1.032	1.056
95.0	1.105	1.123	1.124	1.099	1.053	1.031	1.031	1.054
97.5	1.102	1.122	1.124	1.099	1.053	1.030	1.030	1.052
100.0	1.102	1.122	1.125	1.099	1.052	1.028	1.028	1.050
102.5	1.108	1.126	1.126	1.098	1.048	1.024	1.024	1.050
105.0	1.115	1.130	1.128	1.097	1.045	1.020	1.021	1.049
107.5	1.121	1.133	1.129	1.096	1.042	1.016	1.018	1.049
110.0	1.119	1.133	1.129	1.095	1.038	1.012	1.015	1.049
112.5	1.116	1.132	1.128	1.094	1.036	1.009	1.013	1.049
115.0	1.112	1.130	1.128	1.093	1.034	1.007	1.013	1.050
117.5	1.109	1.128	1.127	1.093	1.035	1.008	1.013	1.051
120.0	1.108	1.127	1.127	1.094	1.037	1.012	1.017	1.052

TABLE 9B (Continued)

θ_w	r/R = 0.3	0.4	0.5	0.6	0.7	0.8	0.9	1.0
120.0	1.108	1.127	1.127	1.094	1.037	1.012	1.017	1.052
122.5	1.107	1.126	1.127	1.097	1.043	1.018	1.022	1.054
125.0	1.107	1.126	1.127	1.099	1.048	1.023	1.026	1.054
127.5	1.108	1.127	1.128	1.100	1.050	1.026	1.027	1.055
130.0	1.111	1.129	1.130	1.102	1.051	1.027	1.028	1.055
132.5	1.112	1.131	1.132	1.103	1.052	1.026	1.027	1.054
135.0	1.112	1.132	1.134	1.104	1.051	1.026	1.026	1.054
137.5	1.104	1.130	1.134	1.105	1.051	1.024	1.025	1.054
140.0	1.094	1.126	1.135	1.107	1.051	1.023	1.024	1.054
142.5	1.084	1.123	1.136	1.109	1.051	1.022	1.023	1.054
145.0	1.078	1.122	1.138	1.112	1.051	1.022	1.023	1.055
147.5	1.079	1.124	1.141	1.114	1.052	1.022	1.023	1.056
150.0	1.082	1.127	1.144	1.116	1.054	1.023	1.024	1.057
152.5	1.086	1.130	1.146	1.118	1.055	1.024	1.025	1.058
155.0	1.090	1.133	1.148	1.119	1.057	1.026	1.027	1.060
157.5	1.093	1.135	1.149	1.120	1.058	1.028	1.029	1.062
160.0	1.096	1.135	1.148	1.120	1.059	1.030	1.031	1.063
162.5	1.101	1.134	1.144	1.117	1.061	1.034	1.035	1.066
165.0	1.099	1.131	1.140	1.115	1.063	1.037	1.039	1.068
167.5	1.097	1.127	1.136	1.113	1.064	1.041	1.043	1.070
170.0	1.094	1.125	1.134	1.113	1.066	1.044	1.046	1.072
172.5	1.096	1.127	1.138	1.116	1.068	1.046	1.047	1.073
175.0	1.104	1.134	1.143	1.119	1.070	1.046	1.048	1.074
177.5	1.109	1.139	1.147	1.122	1.071	1.046	1.047	1.075
180.0	1.110	1.140	1.149	1.123	1.069	1.044	1.046	1.075

TABLE 9B (Continued)

θ_w	r/R = 0.3	0.4	0.5	0.6	0.7	0.8	0.9	1.0
180.0	1.110	1.140	1.149	1.123	1.069	1.044	1.046	1.075
182.5	1.096	1.132	1.145	1.120	1.066	1.040	1.043	1.075
185.0	1.092	1.128	1.141	1.116	1.063	1.038	1.041	1.074
187.5	1.097	1.128	1.138	1.113	1.061	1.037	1.041	1.073
190.0	1.087	1.121	1.134	1.111	1.061	1.037	1.041	1.072
192.5	1.073	1.114	1.131	1.111	1.062	1.039	1.041	1.070
195.0	1.071	1.113	1.130	1.111	1.064	1.041	1.042	1.069
197.5	1.074	1.114	1.131	1.112	1.066	1.043	1.044	1.068
200.0	1.077	1.115	1.131	1.113	1.069	1.046	1.046	1.067
202.5	1.080	1.116	1.130	1.113	1.070	1.048	1.047	1.067
205.0	1.084	1.117	1.130	1.113	1.072	1.051	1.049	1.067
207.5	1.089	1.118	1.129	1.112	1.073	1.053	1.051	1.067
210.0	1.096	1.121	1.130	1.112	1.075	1.055	1.052	1.067
212.5	1.103	1.124	1.130	1.112	1.076	1.057	1.054	1.067
215.0	1.109	1.127	1.130	1.112	1.078	1.058	1.055	1.068
217.5	1.110	1.127	1.131	1.113	1.079	1.060	1.056	1.068
220.0	1.106	1.127	1.132	1.115	1.080	1.061	1.057	1.068
222.5	1.102	1.125	1.132	1.116	1.079	1.059	1.055	1.066
225.0	1.099	1.124	1.132	1.115	1.078	1.057	1.053	1.065
227.5	1.100	1.125	1.133	1.115	1.077	1.055	1.051	1.064
230.0	1.103	1.126	1.133	1.114	1.075	1.053	1.049	1.063
232.5	1.106	1.128	1.133	1.113	1.073	1.051	1.048	1.062
235.0	1.110	1.130	1.133	1.112	1.072	1.050	1.046	1.061
237.5	1.114	1.131	1.133	1.111	1.071	1.049	1.045	1.061
240.0	1.117	1.132	1.133	1.111	1.070	1.048	1.045	1.061

TABLE 9B (Continued)

θ_w	r/R = 0.3	0.4	0.5	0.6	0.7	0.8	0.9	1.0
240.0	1.117	1.132	1.133	1.111	1.070	1.048	1.045	1.061
242.5	1.118	1.133	1.134	1.112	1.072	1.050	1.047	1.063
245.0	1.116	1.132	1.134	1.113	1.074	1.053	1.050	1.065
247.5	1.111	1.130	1.133	1.114	1.076	1.056	1.053	1.068
250.0	1.106	1.127	1.133	1.115	1.078	1.058	1.055	1.070
252.5	1.101	1.125	1.132	1.115	1.079	1.060	1.058	1.072
255.0	1.096	1.123	1.132	1.116	1.080	1.061	1.059	1.074
257.5	1.097	1.122	1.130	1.115	1.079	1.061	1.060	1.076
260.0	1.096	1.120	1.128	1.113	1.078	1.061	1.060	1.077
262.5	1.095	1.118	1.126	1.111	1.076	1.059	1.059	1.077
265.0	1.093	1.116	1.124	1.108	1.073	1.056	1.057	1.077
267.5	1.091	1.114	1.122	1.105	1.069	1.052	1.055	1.076
270.0	1.090	1.113	1.119	1.102	1.065	1.049	1.052	1.075
272.5	1.091	1.112	1.117	1.099	1.061	1.044	1.049	1.074
275.0	1.093	1.112	1.115	1.095	1.057	1.040	1.046	1.072
277.5	1.096	1.112	1.114	1.092	1.053	1.037	1.043	1.071
280.0	1.099	1.113	1.112	1.090	1.050	1.034	1.040	1.070
282.5	1.105	1.115	1.112	1.088	1.048	1.032	1.039	1.071
285.0	1.109	1.115	1.111	1.086	1.046	1.030	1.039	1.071
287.5	1.108	1.114	1.109	1.085	1.045	1.030	1.039	1.071
290.0	1.099	1.109	1.107	1.084	1.045	1.031	1.039	1.070
292.5	1.091	1.103	1.104	1.084	1.049	1.034	1.041	1.069
295.0	1.088	1.101	1.102	1.085	1.052	1.039	1.043	1.066
297.5	1.086	1.099	1.101	1.086	1.056	1.043	1.045	1.062
300.0	1.081	1.097	1.101	1.087	1.060	1.046	1.044	1.055

TABLE 9B (Continued)

θ_w	r/R = 0.3	0.4	0.5	0.6	0.7	0.8	0.9	1.0
300.0	1.081	1.097	1.101	1.087	1.060	1.046	1.044	1.055
302.5	1.077	1.095	1.101	1.089	1.062	1.046	1.041	1.046
305.0	1.074	1.094	1.101	1.090	1.063	1.046	1.038	1.039
307.5	1.081	1.096	1.103	1.090	1.063	1.044	1.035	1.036
310.0	1.088	1.104	1.107	1.092	1.063	1.043	1.033	1.033
312.5	1.097	1.109	1.110	1.096	1.070	1.050	1.038	1.033
315.0	1.103	1.112	1.111	1.097	1.072	1.052	1.038	1.029
317.5	1.102	1.110	1.108	1.092	1.066	1.044	1.028	1.016
320.0	1.099	1.104	1.099	1.078	1.044	1.019	1.003	.996
322.5	1.099	1.092	1.078	1.054	1.021	.995	.976	.963
325.0	1.094	1.078	1.060	1.035	1.006	.987	.976	.975
327.5	1.099	1.054	1.021	1.003	1.000	1.000	1.003	1.010
330.0	1.059	1.022	1.000	.999	1.016	1.024	1.025	1.017
332.5	.999	.996	.996	1.001	1.011	1.015	1.015	1.009
335.0	.891	.944	.983	1.001	1.003	1.003	1.002	1.001
337.5	.652	.928	.981	1.005	1.002	1.000	.997	.995
340.0	.849	.935	.990	1.005	.986	.976	.974	.981
342.5	.859	.946	1.000	1.008	.976	.957	.950	.956
345.0	.870	.955	1.004	1.008	.972	.947	.932	.928
347.5	.878	.960	1.007	1.008	.970	.941	.921	.910
350.0	.874	.963	1.013	1.014	.971	.939	.916	.903
352.5	.854	.956	1.016	1.020	.975	.940	.915	.899
355.0	.348	.947	1.006	1.013	.976	.945	.920	.902
357.5	.836	.938	1.000	1.012	.980	.952	.929	.311
360.0	.852	.925	.973	.988	.975	.962	.948	.933

AD-A048 385 DAVID W TAYLOR NAVAL SHIP RESEARCH AND DEVELOPMENT CE--ETC F/G 13/10
EXPERIMENTAL UNSTEADY AND TIME AVERAGE LOADS ON THE BLADES OF T--ETC(U)
DEC 77 S D JESSUP, R J BOSWELL, J J NELKA

UNCLASSIFIED DTNSRDC-77-0110 NL

3 OF 4
AD
A048385

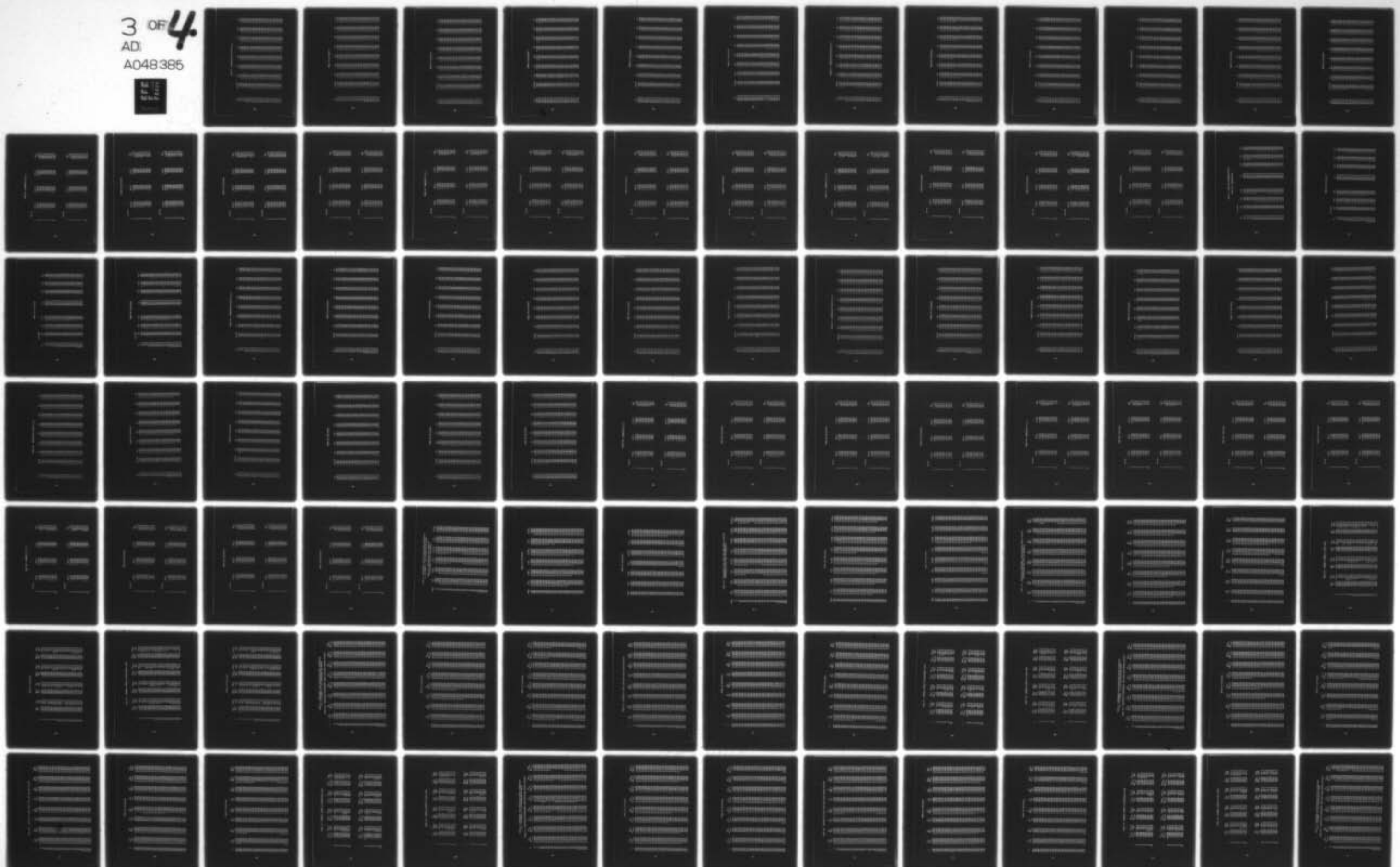

TABLE 9C - INTERPOLATED VALUES OF V_t/V

θ_w	r/R = 0.3	0.4	0.5	0.6	0.7	0.8	0.9	1.0
0.0	.088	.010	-.044	-.067	-.063	-.063	-.065	-.071
2.5	.090	-.001	-.061	-.083	-.071	-.066	-.069	-.080
5.0	.100	-.010	-.081	-.097	-.069	-.055	-.056	-.071
7.5	.042	-.050	-.106	-.110	-.073	-.053	-.050	-.065
10.0	.001	-.072	-.116	-.120	-.092	-.075	-.070	-.077
12.5	-.068	-.101	-.122	-.124	-.111	-.103	-.100	-.102
15.0	-.129	-.127	-.124	-.119	-.114	-.111	-.110	-.110
17.5	-.190	-.151	-.123	-.110	-.109	-.106	-.100	-.092
20.0	-.198	-.160	-.130	-.112	-.104	-.096	-.088	-.081
22.5	-.179	-.154	-.133	-.115	-.101	-.094	-.095	-.104
25.0	-.158	-.143	-.129	-.115	-.101	-.096	-.098	-.109
27.5	-.149	-.138	-.127	-.115	-.103	-.097	-.098	-.105
30.0	-.135	-.131	-.125	-.116	-.105	-.100	-.101	-.109
32.5	-.130	-.130	-.127	-.119	-.108	-.102	-.104	-.112
35.0	-.134	-.134	-.131	-.123	-.111	-.106	-.108	-.117
37.5	-.140	-.138	-.133	-.125	-.114	-.109	-.111	-.119
40.0	-.147	-.141	-.135	-.126	-.116	-.111	-.112	-.117
42.5	-.152	-.145	-.137	-.128	-.118	-.113	-.112	-.116
45.0	-.157	-.148	-.139	-.130	-.120	-.114	-.113	-.116
47.5	-.162	-.151	-.141	-.131	-.121	-.116	-.114	-.117
50.0	-.167	-.155	-.144	-.133	-.123	-.117	-.115	-.118
52.5	-.171	-.158	-.146	-.135	-.124	-.118	-.117	-.120
55.0	-.175	-.161	-.148	-.136	-.125	-.119	-.118	-.122
57.5	-.178	-.163	-.150	-.138	-.126	-.120	-.120	-.125
60.0	-.180	-.165	-.152	-.139	-.128	-.122	-.121	-.126

TABLE 9C (Continued)

θ_w	r/R = 0.3	0.4	0.5	0.6	0.7	0.8	0.9	1.0
60.0	-.180	-.165	-.152	-.139	-.128	-.122	-.121	-.126
62.5	-.183	-.167	-.153	-.140	-.129	-.123	-.122	-.127
65.0	-.186	-.169	-.154	-.141	-.130	-.124	-.123	-.128
67.5	-.190	-.171	-.156	-.142	-.131	-.125	-.124	-.129
70.0	-.193	-.173	-.156	-.142	-.131	-.126	-.125	-.130
72.5	-.195	-.174	-.157	-.143	-.132	-.126	-.126	-.130
75.0	-.196	-.175	-.157	-.143	-.132	-.126	-.126	-.131
77.5	-.196	-.175	-.157	-.143	-.132	-.126	-.126	-.131
80.0	-.196	-.174	-.157	-.142	-.132	-.126	-.126	-.132
82.5	-.195	-.174	-.156	-.142	-.131	-.126	-.126	-.132
85.0	-.194	-.173	-.155	-.141	-.130	-.125	-.126	-.132
87.5	-.192	-.171	-.154	-.140	-.130	-.125	-.125	-.132
90.0	-.191	-.170	-.153	-.139	-.129	-.124	-.125	-.131
92.5	-.191	-.169	-.152	-.138	-.127	-.123	-.124	-.131
95.0	-.190	-.168	-.150	-.136	-.126	-.122	-.123	-.130
97.5	-.189	-.167	-.148	-.134	-.125	-.121	-.122	-.129
100.0	-.188	-.164	-.146	-.132	-.123	-.119	-.121	-.128
102.5	-.184	-.161	-.143	-.130	-.122	-.118	-.119	-.125
105.0	-.181	-.158	-.140	-.128	-.120	-.117	-.118	-.122
107.5	-.177	-.155	-.137	-.125	-.118	-.115	-.116	-.119
110.0	-.175	-.152	-.134	-.122	-.116	-.113	-.113	-.116
112.5	-.173	-.149	-.130	-.119	-.114	-.111	-.111	-.113
115.0	-.171	-.146	-.127	-.116	-.111	-.109	-.108	-.110
117.5	-.168	-.142	-.123	-.112	-.108	-.106	-.105	-.106
120.0	-.164	-.138	-.119	-.108	-.105	-.103	-.102	-.103

TABLE 9C (Continued)

θ_w	r/R = 0.3	0.4	0.5	0.6	0.7	0.8	0.9	1.0
120.0	-.164	-.138	-.119	-.108	-.105	-.103	-.102	-.103
122.5	-.159	-.134	-.115	-.104	-.100	-.099	-.099	-.101
125.0	-.154	-.129	-.110	-.100	-.096	-.095	-.096	-.098
127.5	-.149	-.124	-.106	-.095	-.092	-.091	-.093	-.096
130.0	-.143	-.119	-.101	-.091	-.088	-.088	-.090	-.094
132.5	-.136	-.113	-.096	-.087	-.085	-.085	-.087	-.092
135.0	-.130	-.108	-.091	-.083	-.081	-.081	-.084	-.089
137.5	-.125	-.103	-.087	-.078	-.077	-.078	-.081	-.087
140.0	-.120	-.098	-.082	-.074	-.073	-.075	-.078	-.084
142.5	-.113	-.093	-.078	-.071	-.070	-.071	-.075	-.080
145.0	-.107	-.088	-.074	-.067	-.067	-.068	-.071	-.075
147.5	-.099	-.082	-.070	-.064	-.063	-.064	-.066	-.071
150.0	-.091	-.077	-.066	-.061	-.059	-.060	-.062	-.066
152.5	-.083	-.071	-.062	-.057	-.055	-.055	-.057	-.061
155.0	-.075	-.065	-.058	-.053	-.051	-.051	-.053	-.056
157.5	-.067	-.059	-.053	-.049	-.047	-.047	-.048	-.052
160.0	-.059	-.053	-.048	-.045	-.042	-.042	-.044	-.047
162.5	-.051	-.047	-.043	-.040	-.036	-.036	-.038	-.043
165.0	-.044	-.041	-.038	-.034	-.030	-.030	-.033	-.040
167.5	-.036	-.034	-.032	-.028	-.024	-.024	-.028	-.037
170.0	-.029	-.028	-.026	-.022	-.018	-.019	-.024	-.033
172.5	-.021	-.020	-.019	-.016	-.012	-.013	-.019	-.029
175.0	-.012	-.012	-.012	-.010	-.007	-.009	-.015	-.025
177.5	-.003	-.005	-.005	-.005	-.003	-.005	-.011	-.021
180.0	.007	.003	0.000	-.001	0.000	-.002	-.008	-.017

TABLE 9C (Continued)

θ_w	r/R = 0.3	0.4	0.5	0.6	0.7	0.8	0.9	1.0
180.0	.007	.003	0.000	-.001	0.000	-.002	-.008	-.017
182.5	.017	.009	.002	0.000	.002	0.000	-.005	-.013
185.0	.029	.015	.005	.002	.004	.004	-.001	-.009
187.5	.042	.022	.008	.004	.008	.008	.004	-.004
190.0	.053	.029	.013	.008	.013	.013	.010	.002
192.5	.060	.037	.021	.016	.019	.019	.016	.008
195.0	.068	.045	.030	.024	.027	.026	.022	.016
197.5	.075	.053	.038	.032	.034	.033	.029	.023
200.0	.082	.060	.045	.039	.041	.040	.036	.030
202.5	.092	.066	.049	.042	.045	.045	.042	.035
205.0	.101	.072	.052	.045	.050	.050	.047	.040
207.5	.111	.077	.054	.047	.054	.055	.052	.044
210.0	.120	.082	.057	.050	.058	.060	.056	.047
212.5	.129	.088	.061	.053	.062	.064	.061	.050
215.0	.136	.093	.065	.057	.066	.069	.065	.053
217.5	.143	.099	.070	.062	.071	.073	.068	.056
220.0	.150	.106	.077	.068	.077	.078	.072	.059
222.5	.156	.112	.082	.073	.082	.083	.076	.062
225.0	.163	.117	.087	.078	.086	.087	.080	.065
227.5	.168	.122	.091	.082	.091	.092	.084	.069
230.0	.173	.125	.094	.085	.095	.096	.088	.072
232.5	.176	.129	.096	.088	.099	.100	.092	.075
235.0	.183	.132	.099	.090	.102	.104	.096	.078
237.5	.187	.135	.100	.092	.105	.107	.100	.082
240.0	.192	.137	.102	.094	.107	.110	.103	.085

TABLE 9C (Continued)

θ_w	r/R = 0.3	0.4	0.5	0.6	0.7	0.8	0.9	1.0
240.0	.192	.137	.102	.094	.107	.110	.103	.085
242.5	.195	.140	.104	.095	.108	.112	.105	.088
245.0	.198	.142	.106	.096	.109	.113	.107	.091
247.5	.201	.145	.108	.098	.110	.114	.108	.094
250.0	.204	.146	.109	.099	.111	.115	.110	.097
252.5	.206	.148	.110	.100	.112	.117	.113	.100
255.0	.207	.149	.111	.101	.114	.119	.115	.103
257.5	.208	.149	.112	.102	.117	.122	.118	.105
260.0	.208	.150	.113	.104	.119	.124	.121	.107
262.5	.208	.151	.114	.105	.120	.126	.122	.108
265.0	.209	.151	.114	.106	.122	.127	.123	.109
267.5	.209	.152	.115	.107	.123	.128	.124	.109
270.0	.208	.151	.116	.108	.123	.128	.124	.109
272.5	.205	.150	.116	.108	.123	.128	.123	.108
275.0	.202	.149	.115	.108	.123	.127	.122	.107
277.5	.198	.147	.115	.108	.122	.126	.121	.106
280.0	.193	.144	.113	.107	.121	.125	.120	.105
282.5	.189	.141	.111	.105	.119	.124	.118	.102
285.0	.184	.138	.109	.104	.118	.122	.116	.100
287.5	.180	.135	.107	.101	.115	.119	.113	.098
290.0	.176	.132	.104	.099	.113	.117	.111	.095
292.5	.172	.129	.101	.096	.109	.113	.108	.092
295.0	.167	.125	.098	.093	.106	.109	.104	.089
297.5	.162	.120	.094	.089	.101	.105	.100	.086
300.0	.157	.116	.089	.084	.096	.100	.096	.084

TABLE 9C (Continued)

θ_w	r/R = 0.3	0.4	0.5	0.6	0.7	0.8	0.9	1.0
300.0	.157	.116	.089	.084	.096	.100	.096	.084
302.5	.153	.111	.084	.079	.091	.095	.092	.081
305.0	.149	.107	.080	.074	.085	.090	.087	.077
307.5	.147	.104	.076	.070	.081	.085	.081	.072
310.0	.146	.102	.074	.066	.077	.080	.077	.066
312.5	.146	.101	.072	.065	.075	.078	.073	.060
315.0	.147	.102	.072	.064	.074	.076	.070	.056
317.5	.153	.105	.073	.064	.073	.076	.074	.066
320.0	.160	.109	.076	.067	.076	.080	.078	.070
322.5	.162	.116	.083	.069	.072	.068	.058	.041
325.0	.167	.121	.084	.060	.046	.034	.022	.010
327.5	.178	.123	.078	.047	.027	.015	.011	.013
330.0	.200	.120	.061	.030	.023	.018	.015	.015
332.5	.201	.104	.038	.013	.024	.027	.024	.014
335.0	.183	.083	.018	0.000	.020	.029	.026	.012
337.5	.134	.050	-.003	-.013	.014	.026	.025	.010
340.0	.090	.021	-.021	-.023	.007	.023	.024	.011
342.5	.066	.004	-.031	-.031	-.001	.016	.020	.010
345.0	.063	.002	-.033	-.035	-.009	.006	.011	.005
347.5	.063	.003	-.033	-.039	-.018	-.006	-.002	-.006
350.0	.072	.006	-.036	-.046	-.029	-.019	-.016	-.021
352.5	.079	.008	-.040	-.055	-.042	-.035	-.031	-.033
355.0	.101	.006	-.057	-.077	-.060	-.048	-.042	-.041
357.5	.096	.007	-.053	-.076	-.065	-.058	-.054	-.054
360.0	.088	.010	-.044	-.067	-.063	-.063	-.065	-.071

TABLE 9D - INTERPOLATED VALUES OF V_r/V

θ_w	r/R = 0.3	0.4	0.5	0.6	0.7	0.8	0.9	1.0
0.0	-.020	-.010	-.014	-.043	-.090	-.117	-.124	-.111
2.5	-.016	-.018	-.029	-.056	-.095	-.118	-.126	-.118
5.0	-.002	-.025	-.047	-.071	-.096	-.112	-.120	-.121
7.5	.023	-.025	-.062	-.085	-.096	-.106	-.113	-.118
10.0	.044	-.021	-.068	-.093	-.099	-.104	-.107	-.109
12.5	.062	-.014	-.068	-.097	-.103	-.106	-.107	-.105
15.0	.068	-.010	-.067	-.099	-.109	-.114	-.116	-.113
17.5	.072	-.008	-.067	-.100	-.110	-.115	-.117	-.115
20.0	.054	-.016	-.067	-.096	-.106	-.112	-.113	-.109
22.5	.015	-.033	-.070	-.093	-.103	-.108	-.105	-.097
25.0	-.029	-.055	-.075	-.090	-.099	-.102	-.101	-.093
27.5	-.051	-.065	-.076	-.086	-.095	-.098	-.098	-.092
30.0	-.063	-.069	-.075	-.082	-.091	-.095	-.094	-.088
32.5	-.067	-.069	-.072	-.079	-.088	-.092	-.090	-.084
35.0	-.070	-.068	-.069	-.075	-.084	-.088	-.087	-.079
37.5	-.069	-.065	-.065	-.071	-.081	-.085	-.083	-.075
40.0	-.067	-.062	-.060	-.066	-.077	-.082	-.080	-.071
42.5	-.067	-.059	-.056	-.062	-.073	-.078	-.076	-.067
45.0	-.067	-.057	-.053	-.057	-.069	-.074	-.072	-.062
47.5	-.064	-.053	-.049	-.053	-.065	-.069	-.067	-.058
50.0	-.061	-.050	-.044	-.049	-.060	-.065	-.063	-.053
52.5	-.057	-.046	-.040	-.044	-.056	-.060	-.057	-.048
55.0	-.054	-.042	-.037	-.040	-.051	-.055	-.052	-.043
57.5	-.051	-.039	-.033	-.036	-.046	-.050	-.047	-.038
60.0	-.049	-.036	-.029	-.032	-.041	-.045	-.042	-.033

TABLE 9D (Continued)

θ_w	r/R = 0.3	0.4	0.5	0.6	0.7	0.8	0.9	1.0
60.0	-.049	-.036	-.029	-.032	-.041	-.045	-.042	-.033
62.5	-.047	-.033	-.025	-.027	-.037	-.041	-.038	-.029
65.0	-.045	-.030	-.021	-.023	-.033	-.037	-.034	-.025
67.5	-.044	-.026	-.017	-.018	-.029	-.033	-.030	-.021
70.0	-.042	-.023	-.013	-.014	-.025	-.029	-.026	-.016
72.5	-.041	-.020	-.009	-.009	-.020	-.024	-.022	-.012
75.0	-.039	-.017	-.005	-.005	-.016	-.020	-.017	-.008
77.5	-.038	-.014	-.001	0.000	-.011	-.015	-.013	-.004
80.0	-.036	-.012	.003	.004	-.007	-.011	-.009	0.000
82.5	-.035	-.009	.007	.008	-.002	-.007	-.004	.004
85.0	-.033	-.006	.011	.012	.002	-.002	0.000	.009
87.5	-.032	-.003	.014	.016	.006	.002	.004	.013
90.0	-.031	-.001	.018	.021	.010	.006	.009	.018
92.5	-.029	.002	.021	.025	.015	.011	.013	.022
95.0	-.028	.004	.025	.029	.019	.016	.018	.027
97.5	-.027	.007	.028	.033	.024	.021	.023	.031
100.0	-.025	.009	.032	.037	.029	.026	.028	.036
102.5	-.023	.012	.035	.042	.035	.032	.034	.041
105.0	-.022	.015	.039	.046	.040	.038	.040	.046
107.5	-.020	.017	.042	.051	.045	.043	.045	.050
110.0	-.019	.020	.046	.055	.050	.048	.050	.055
112.5	-.018	.022	.049	.059	.054	.052	.054	.059
115.0	-.017	.025	.053	.063	.058	.056	.058	.063
117.5	-.016	.027	.056	.067	.062	.060	.062	.068
120.0	-.015	.029	.059	.070	.065	.064	.066	.071

TABLE 9D (Continued)

θ_w	r/R = 0.3	0.4	0.5	0.6	0.7	0.8	0.9	1.0
120.0	-.015	.029	.059	.070	.065	.064	.066	.071
122.5	-.014	.031	.062	.073	.069	.067	.070	.075
125.0	-.013	.033	.065	.077	.072	.071	.073	.079
127.5	-.012	.035	.067	.080	.075	.074	.076	.082
130.0	-.011	.037	.070	.082	.078	.077	.080	.085
132.5	-.010	.039	.072	.085	.081	.080	.083	.088
135.0	-.009	.040	.074	.088	.084	.083	.086	.091
137.5	-.008	.042	.076	.090	.086	.086	.088	.094
140.0	-.007	.043	.078	.092	.089	.089	.091	.097
142.5	-.006	.045	.080	.094	.092	.092	.094	.100
145.0	-.005	.046	.081	.096	.094	.094	.097	.103
147.5	-.005	.046	.082	.098	.096	.097	.100	.106
150.0	-.005	.047	.084	.100	.098	.099	.102	.108
152.5	-.004	.048	.085	.101	.100	.101	.105	.111
155.0	-.003	.049	.086	.103	.102	.103	.107	.112
157.5	-.002	.050	.087	.104	.103	.105	.108	.114
160.0	-.002	.051	.088	.105	.105	.106	.110	.115
162.5	-.001	.053	.090	.107	.105	.106	.110	.116
165.0	-.001	.053	.092	.108	.106	.107	.110	.116
167.5	-.001	.054	.093	.109	.107	.107	.110	.115
170.0	-.001	.055	.094	.110	.107	.107	.110	.115
172.5	-.001	.055	.094	.110	.108	.108	.110	.116
175.0	-.001	.055	.094	.110	.108	.108	.111	.117
177.5	-.001	.054	.093	.110	.109	.110	.112	.117
180.0	-.001	.054	.093	.110	.110	.111	.114	.118

TABLE 9D (Continued)

θ_w	r/R = 0.3	0.4	0.5	0.6	0.7	0.8	0.9	1.0
180.0	-.001	.054	.093	.110	.110	.111	.114	.118
182.5	0.000	.054	.092	.111	.112	.114	.116	.119
185.0	-.001	.053	.092	.111	.113	.115	.116	.118
187.5	-.002	.052	.091	.110	.113	.115	.116	.118
190.0	-.001	.052	.091	.110	.112	.114	.115	.117
192.5	0.000	.053	.090	.109	.110	.112	.114	.115
195.0	-.001	.052	.089	.107	.108	.110	.111	.114
197.5	-.002	.050	.088	.105	.106	.107	.109	.112
200.0	-.004	.049	.086	.103	.103	.104	.106	.110
202.5	-.004	.048	.084	.101	.101	.102	.104	.108
205.0	-.005	.046	.082	.099	.099	.100	.102	.105
207.5	-.006	.045	.080	.097	.097	.097	.100	.103
210.0	-.006	.043	.078	.094	.094	.095	.097	.100
212.5	-.006	.042	.076	.092	.092	.093	.094	.097
215.0	-.007	.041	.074	.089	.089	.090	.091	.094
217.5	-.007	.039	.071	.086	.086	.087	.088	.091
220.0	-.009	.037	.069	.083	.083	.084	.085	.087
222.5	-.011	.034	.066	.080	.080	.081	.082	.084
225.0	-.012	.032	.063	.077	.077	.077	.078	.080
227.5	-.013	.029	.059	.073	.073	.073	.074	.076
230.0	-.015	.027	.056	.070	.069	.069	.070	.072
232.5	-.016	.025	.053	.066	.065	.065	.066	.068
235.0	-.017	.022	.050	.062	.061	.061	.062	.064
237.5	-.018	.020	.046	.058	.056	.056	.057	.059
240.0	-.020	.017	.043	.054	.052	.052	.053	.055

TABLE 9D (Continued)

θ_w	r/R = 0.3	0.4	0.5	0.6	0.7	0.8	0.9	1.0
240.0	-.020	.017	.043	.054	.052	.052	.053	.055
242.5	-.021	.015	.039	.049	.047	.046	.047	.050
245.0	-.022	.012	.036	.045	.042	.041	.042	.045
247.5	-.023	.010	.032	.041	.037	.036	.036	.039
250.0	-.024	.008	.029	.036	.032	.030	.031	.034
252.5	-.025	.005	.026	.032	.027	.025	.025	.029
255.0	-.026	.003	.022	.028	.022	.019	.020	.023
257.5	-.027	0.000	.018	.023	.017	.014	.014	.018
260.0	-.028	-.002	.014	.018	.012	.009	.009	.012
262.5	-.030	-.005	.010	.014	.006	.003	.003	.007
265.0	-.032	-.008	.006	.009	.001	-.003	-.003	.001
267.5	-.034	-.011	.002	.004	-.005	-.009	-.009	-.004
270.0	-.036	-.014	-.002	-.001	-.011	-.015	-.015	-.010
272.5	-.037	-.017	-.006	-.006	-.017	-.022	-.021	-.016
275.0	-.038	-.020	-.010	-.011	-.022	-.028	-.027	-.021
277.5	-.040	-.023	-.014	-.016	-.028	-.034	-.033	-.027
280.0	-.041	-.025	-.018	-.021	-.034	-.040	-.039	-.032
282.5	-.042	-.028	-.022	-.026	-.039	-.046	-.045	-.038
285.0	-.043	-.031	-.026	-.031	-.045	-.051	-.051	-.043
287.5	-.044	-.034	-.030	-.036	-.050	-.057	-.056	-.048
290.0	-.047	-.037	-.033	-.040	-.055	-.062	-.062	-.054
292.5	-.049	-.040	-.037	-.044	-.060	-.068	-.068	-.060
295.0	-.051	-.042	-.040	-.048	-.064	-.073	-.073	-.066
297.5	-.053	-.045	-.044	-.052	-.069	-.078	-.079	-.073
300.0	-.055	-.047	-.046	-.055	-.073	-.083	-.085	-.081

TABLE 9D (Continued)

θ_w	r/R = 0.3	0.4	0.5	0.6	0.7	0.8	0.9	1.0
300.0	-.055	-.047	-.046	-.055	-.073	-.083	-.085	-.081
302.5	-.056	-.049	-.049	-.059	-.077	-.088	-.092	-.089
305.0	-.057	-.050	-.050	-.061	-.081	-.093	-.098	-.095
307.5	-.055	-.050	-.051	-.064	-.085	-.098	-.103	-.100
310.0	-.052	-.048	-.052	-.066	-.088	-.102	-.107	-.104
312.5	-.047	-.046	-.051	-.066	-.088	-.103	-.109	-.108
315.0	-.040	-.043	-.051	-.067	-.089	-.104	-.111	-.111
317.5	-.027	-.037	-.050	-.069	-.091	-.106	-.113	-.113
320.0	-.015	-.032	-.051	-.072	-.095	-.109	-.116	-.115
322.5	-.002	-.029	-.053	-.076	-.098	-.112	-.119	-.119
325.0	.004	-.025	-.052	-.076	-.098	-.114	-.124	-.129
327.5	.008	-.025	-.054	-.081	-.105	-.122	-.133	-.137
330.0	.009	-.023	-.053	-.083	-.111	-.129	-.136	-.133
332.5	.008	-.021	-.050	-.079	-.108	-.126	-.135	-.133
335.0	.012	-.015	-.042	-.071	-.100	-.120	-.129	-.129
337.5	.014	-.009	-.033	-.062	-.094	-.115	-.124	-.123
340.0	.013	-.002	-.022	-.052	-.090	-.113	-.122	-.117
342.5	.011	.004	-.012	-.043	-.085	-.110	-.120	-.113
345.0	.013	.009	-.006	-.037	-.081	-.108	-.117	-.110
347.5	.009	.009	-.002	-.033	-.078	-.105	-.114	-.105
350.0	.007	.011	.001	-.030	-.077	-.105	-.112	-.100
352.5	0.000	.009	.002	-.030	-.081	-.110	-.117	-.101
355.0	-.016	.004	.004	-.028	-.084	-.115	-.123	-.106
357.5	-.024	-.003	-.002	-.033	-.087	-.118	-.126	-.110
360.0	-.020	-.010	-.014	-.043	-.090	-.117	-.124	-.111

TABLE 9E - HARMONICS OF V_x/V

$r/R = 0.3$

n	$(A_x)_n/V$	$(B_x)_n/V$	$(V_x)_n/V$	$(\phi_x^*)_n$
0	1.0697	0.0000	0.0000	0.0
1	-.0569	.0093	.0577	279.3
2	-.0571	.0118	.0583	281.7
3	-.0395	.0116	.0412	286.4
4	-.0361	.0127	.0383	289.3
5	-.0291	.0142	.0324	296.0
6	-.0147	.0067	.0161	294.4
7	-.0140	.0075	.0159	298.1
8	-.0032	-.0014	.0035	246.3
9	.0017	-.0041	.0045	157.2
10	.0076	-.0147	.0165	152.7

$r/R = 0.4$

n	$(A_x)_n/V$	$(B_x)_n/V$	$(V_x)_n/V$	$(\phi_x^*)_n$
0	1.0963	0.0000	0.0000	0.0
1	-.0532	.0085	.0539	279.1
2	-.0378	.0096	.0390	284.2
3	-.0259	.0121	.0286	295.1
4	-.0208	.0094	.0228	294.4
5	-.0164	.0120	.0203	306.3
6	-.0074	.0057	.0093	307.7
7	-.0052	.0035	.0063	303.7
8	-.0006	-.0018	.0019	199.8
9	.0007	-.0056	.0056	172.7
10	.0022	-.0095	.0098	166.8

TABLE 9E (Continued)

r/R = 0.5

n	$(A_x)_n/V$	$(B_x)_n/V$	$(V_x)_n/V$	$(\phi_x^*)_n$
0	1.1051	0.0000	0.0000	0.0
1	-.0479	.0061	.0483	277.2
2	-.0241	.0083	.0255	289.1
3	-.0164	.0116	.0201	305.1
4	-.0104	.0068	.0124	303.2
5	-.0077	.0101	.0127	322.5
6	-.0027	.0050	.0057	331.9
7	.0006	.0011	.0012	27.9
8	.0009	-.0021	.0023	155.9
9	-.0005	-.0056	.0056	185.3
10	-.0014	-.0056	.0058	193.9

r/R = 0.6

n	$(A_x)_n/V$	$(B_x)_n/V$	$(V_x)_n/V$	$(\phi_x^*)_n$
0	1.0866	0.0000	0.0000	0.0
1	-.0387	-.0001	.0387	269.9
2	-.0166	.0082	.0185	296.4
3	-.0118	.0085	.0146	305.8
4	-.0067	.0046	.0081	304.4
5	-.0046	.0085	.0097	331.4
6	-.0015	.0049	.0051	342.7
7	.0025	.0006	.0026	75.8
8	.0016	-.0025	.0030	147.0
9	-.0021	-.0039	.0044	208.9
10	-.0028	-.0036	.0045	217.7

TABLE 9E (Continued)

$r/R = 0.7$

n	$(A_x)_n/V$	$(B_x)_n/V$	$(V_x)_n/V$	$(\phi_x^*)_n$
0	1.0466	0.0000	0.0000	0.0
1	-.0270	-.0086	.0283	252.3
2	-.0148	.0091	.0174	301.5
3	-.0117	.0039	.0123	288.4
4	-.0086	.0029	.0091	288.3
5	-.0063	.0073	.0096	319.3
6	-.0034	.0051	.0061	326.6
7	.0012	.0021	.0024	30.9
8	.0013	-.0028	.0031	154.2
9	-.0040	-.0007	.0041	260.4
10	-.0022	-.0030	.0037	216.4

$r/R = 0.8$

n	$(A_x)_n/V$	$(B_x)_n/V$	$(V_x)_n/V$	$(\phi_x^*)_n$
0	1.0265	0.0000	0.0000	0.0
1	-.0221	-.0111	.0247	243.4
2	-.0156	.0107	.0189	304.3
3	-.0132	.0033	.0136	283.9
4	-.0095	.0029	.0099	287.2
5	-.0072	.0062	.0095	310.8
6	-.0047	.0050	.0069	316.9
7	-.0008	.0031	.0032	345.0
8	.0001	-.0022	.0022	176.3
9	-.0052	.0019	.0055	289.7
10	-.0020	-.0013	.0024	236.3

TABLE 9E (Continued)

$r/R = 0.9$

n	$(A_x)_n/V$	$(B_x)_n/V$	$(V_x)_n/V$	$(\phi_x^*)_n$
0	1.0264	0.0000	0.0000	0.0
1	-.0241	-.0074	.0252	252.9
2	-.0189	.0129	.0229	304.2
3	-.0165	.0067	.0178	292.1
4	-.0089	.0047	.0101	297.8
5	-.0074	.0053	.0091	305.7
6	-.0056	.0048	.0074	310.3
7	-.0036	.0036	.0051	315.1
8	-.0020	-.0006	.0021	252.2
9	-.0057	.0038	.0068	303.6
10	-.0022	.0013	.0026	300.4

$r/R = 1.0$

n	$(A_x)_n/V$	$(B_x)_n/V$	$(V_x)_n/V$	$(\phi_x^*)_n$
0	1.0463	0.0000	0.0000	0.0
1	-.0329	.0023	.0330	274.0
2	-.0247	.0157	.0293	302.4
3	-.0214	.0142	.0257	303.5
4	-.0072	.0083	.0110	318.9
5	-.0070	.0047	.0084	303.7
6	-.0061	.0043	.0075	305.0
7	-.0071	.0037	.0080	297.8
8	-.0052	.0018	.0055	289.6
9	-.0054	.0050	.0073	312.8
10	-.0028	.0051	.0058	330.6

TABLE 9F - HARMONICS OF V_t/V

$r/R = 0.3$

n	$(A_t)_n/V$	$(B_t)_n/V$	$(V_t)_n/V$	$(\phi_t^*)_n$
0	.0089	0.0000	0.0000	0.0
1	-.0022	-.2094	.2094	180.6
2	.0080	-.0112	.0138	144.6
3	.0127	-.0195	.0233	146.9
4	.0056	-.0161	.0170	160.9
5	.0034	-.0114	.0119	163.2
6	.0035	-.0048	.0060	143.9
7	.0077	.0005	.0077	86.1
8	.0102	.0046	.0112	65.6
9	.0118	.0059	.0132	63.6
10	.0122	.0072	.0142	59.6

$r/R = 0.4$

n	$(A_t)_n/V$	$(B_t)_n/V$	$(V_t)_n/V$	$(\phi_t^*)_n$
0	-.0116	0.0000	0.0000	0.0
1	-.0178	-.1665	.1674	186.1
2	-.0015	-.0111	.0112	187.8
3	.0020	-.0112	.0114	170.0
4	-.0016	-.0086	.0088	190.7
5	-.0007	-.0062	.0062	186.9
6	.0001	-.0019	.0019	175.8
7	.0028	.0011	.0030	68.7
8	.0059	.0034	.0068	60.0
9	.0075	.0033	.0082	66.6
10	.0079	.0027	.0084	71.0

TABLE 9F (Continued)

r/R = 0.5

n	$(A_t)_n/V$	$(B_t)_n/V$	$(V_t)_n/V$	$(\phi_t^*)_n$
0	-.0236	0.0000	0.0000	0.0
1	-.0273	-.1367	.1394	191.3
2	-.0085	-.0104	.0134	219.3
3	-.0051	-.0052	.0073	224.3
4	-.0060	-.0036	.0070	239.4
5	-.0033	-.0026	.0042	231.0
6	-.0020	-.0002	.0020	265.6
7	-.0005	.0012	.0013	337.2
8	.0028	.0022	.0035	51.9
9	.0042	.0013	.0044	72.8
10	.0045	-.0004	.0045	95.0

r/R = 0.6

n	$(A_t)_n/V$	$(B_t)_n/V$	$(V_t)_n/V$	$(\phi_t^*)_n$
0	-.0241	0.0000	0.0000	0.0
1	-.0289	-.1242	.1275	193.1
2	-.0126	-.0089	.0154	234.8
3	-.0074	-.0022	.0077	253.3
4	-.0066	-.0015	.0068	257.3
5	-.0034	-.0011	.0036	252.8
6	-.0025	-.0002	.0025	264.9
7	-.0019	.0006	.0020	288.7
8	.0011	.0008	.0014	53.4
9	.0019	.0001	.0019	87.1
10	.0020	-.0019	.0027	133.7

TABLE 9F (Continued)

r/R = 0.7

n	$(A_t)_n/V$	$(B_t)_n/V$	$(V_t)_n/V$	$(\phi_t^*)_n$
0	-.0147	0.0000	0.0000	0.0
1	-.0241	-.1264	.1287	190.8
2	-.0140	-.0067	.0155	244.3
3	-.0055	-.0018	.0058	251.7
4	-.0041	-.0020	.0046	243.6
5	-.0018	-.0013	.0022	233.0
6	-.0015	-.0018	.0023	220.0
7	-.0015	-.0005	.0016	252.8
8	.0007	-.0005	.0009	126.8
9	.0007	-.0004	.0008	121.3
10	.0003	-.0019	.0019	170.3

r/R = 0.8

n	$(A_t)_n/V$	$(B_t)_n/V$	$(V_t)_n/V$	$(\phi_t^*)_n$
0	-.0112	0.0000	0.0000	0.0
1	-.0207	-.1261	.1278	189.3
2	-.0144	-.0056	.0154	248.8
3	-.0042	-.0016	.0045	249.7
4	-.0024	-.0023	.0033	226.6
5	-.0006	-.0018	.0019	197.7
6	-.0008	-.0025	.0026	198.9
7	-.0009	-.0010	.0014	221.8
8	.0002	-.0016	.0016	172.5
9	-.0001	-.0008	.0008	187.0
10	-.0009	-.0018	.0020	207.7

TABLE 9F (Continued)

r/R = 0.9

n	$(A_t)_n/V$	$(B_t)_n/V$	$(V_t)_n/V$	$(\phi_t^*)_n$
0	-.0135	0.0000	0.0000	0.0
1	-.0184	-.1234	.1248	188.5
2	-.0136	-.0054	.0146	248.4
3	-.0034	-.0014	.0037	247.5
4	-.0016	-.0022	.0027	215.3
5	.0001	-.0026	.0026	178.7
6	-.0006	-.0024	.0025	193.7
7	-.0001	-.0011	.0011	183.9
8	-.0005	-.0022	.0023	192.4
9	-.0004	-.0010	.0011	200.5
10	-.0017	-.0015	.0023	229.2

r/R = 1.0

n	$(A_t)_n/V$	$(B_t)_n/V$	$(V_t)_n/V$	$(\phi_t^*)_n$
0	-.0218	0.0000	0.0000	0.0
1	-.0179	-.1133	.1196	188.6
2	-.0117	-.0062	.0132	242.2
3	-.0032	-.0014	.0035	246.2
4	-.0015	-.0017	.0023	221.0
5	.0002	-.0035	.0035	177.4
6	-.0007	-.0016	.0017	204.0
7	.0011	-.0005	.0012	117.2
8	-.0013	-.0025	.0028	208.4
9	-.0002	-.0011	.0011	189.2
10	-.0022	-.0012	.0025	242.1

TABLE 9G - HARMONICS OF V_r/V

$r/R = 0.3$

n	$(A_r)_n/V$	$(B_r)_n/V$	$(V_r)_n/V$	$(\phi_r^*)_n$
0	-.0192	0.0000	0.0000	0.0
1	-.0062	-.0013	.0063	258.5
2	.0220	-.0054	.0226	103.7
3	.0158	-.0048	.0165	106.9
4	.0088	-.0013	.0089	98.7
5	.0018	.0026	.0032	34.5
6	-.0030	.0067	.0073	335.7
7	-.0053	.0086	.0101	328.5
8	-.0061	.0079	.0100	322.4
9	-.0058	.0056	.0081	314.2
10	-.0051	.0029	.0059	299.7

$r/R = 0.4$

n	$(A_r)_n/V$	$(B_r)_n/V$	$(V_r)_n/V$	$(\phi_r^*)_n$
0	.0015	0.0000	0.0000	0.0
1	-.0440	.0025	.0441	273.2
2	.0158	-.0062	.0170	111.5
3	.0127	-.0074	.0147	120.4
4	.0085	-.0052	.0100	121.5
5	.0042	-.0030	.0051	125.5
6	.0012	-.0001	.0012	94.2
7	-.0005	.0013	.0014	339.0
8	-.0012	.0010	.0016	309.5
9	-.0018	.0006	.0019	289.5
10	-.0019	-.0005	.0020	254.4

TABLE 9G (Continued)

r/R = 0.5

n	$(A_r)_n/V$	$(B_r)_n/V$	$(V_r)_n/V$	$(\phi_r^*)_n$
0	.0134	0.0000	0.0000	0.0
1	-.0741	.0057	.0743	274.4
2	.0107	-.0055	.0120	117.4
3	.0099	-.0083	.0129	130.0
4	.0077	-.0071	.0105	132.9
5	.0052	-.0062	.0081	140.1
6	.0038	-.0042	.0056	137.9
7	.0025	-.0033	.0041	143.2
8	.0018	-.0033	.0038	150.9
9	.0009	-.0027	.0028	161.4
10	.0001	-.0026	.0026	177.8

r/R = 0.6

n	$(A_r)_n/V$	$(B_r)_n/V$	$(V_r)_n/V$	$(\phi_r^*)_n$
0	.0128	0.0000	0.0000	0.0
1	-.0952	.0083	.0956	275.0
2	.0066	-.0024	.0070	110.2
3	.0073	-.0067	.0099	132.3
4	.0057	-.0063	.0085	137.7
5	.0044	-.0062	.0076	145.0
6	.0040	-.0046	.0061	138.8
7	.0030	-.0041	.0051	144.3
8	.0024	-.0039	.0046	148.3
9	.0015	-.0034	.0037	155.6
10	.0007	-.0025	.0026	163.8

TABLE 9G (Continued)

r/R = 0.7

n	$(A_r)_n/V$	$(B_r)_n/V$	$(V_r)_n/V$	$(\phi_r^*)_n$
0	.0020	0.0000	0.0000	0.0
1	-.1082	.0106	.1087	275.6
2	.0034	.0027	.0043	51.8
3	.0051	-.0030	.0059	120.5
4	.0029	-.0031	.0042	136.7
5	.0020	-.0036	.0041	150.2
6	.0024	-.0020	.0031	129.9
7	.0014	-.0019	.0024	143.0
8	.0009	-.0015	.0018	148.4
9	.0005	-.0021	.0022	165.7
10	.0001	-.0008	.0008	169.9

r/R = 0.8

n	$(A_r)_n/V$	$(B_r)_n/V$	$(V_r)_n/V$	$(\phi_r^*)_n$
0	-.0035	0.0000	0.0000	0.0
1	-.1165	.0129	.1172	276.3
2	.0009	.0061	.0062	8.8
3	.0034	-.0003	.0034	95.0
4	.0014	-.0011	.0018	128.2
5	.0010	-.0021	.0023	154.2
6	.0015	-.0008	.0017	118.1
7	.0006	-.0008	.0010	146.6
8	.0000	-.0003	.0003	177.4
9	-.0000	-.0015	.0015	180.0
10	-.0002	-.0000	.0002	268.1

TABLE 9G (Continued)

r/R = 0.9

n	$(A_r)_n/V$	$(B_r)_n/V$	$(V_r)_n/V$	$(\phi_r^*)_n$
0	-.0036	0.0000	0.0000	0.0
1	-.1201	.0150	.1210	277.1
2	-.0007	.0080	.0080	354.8
3	.0023	.0014	.0027	58.6
4	.0013	-.0004	.0014	107.0
5	.0013	-.0018	.0022	144.6
6	.0013	-.0010	.0016	127.0
7	.0003	-.0009	.0010	161.1
8	-.0004	-.0003	.0005	227.5
9	-.0001	-.0014	.0014	183.9
10	-.0003	-.0002	.0004	241.0

r/R = 1.0

n	$(A_r)_n/V$	$(B_r)_n/V$	$(V_r)_n/V$	$(\phi_r^*)_n$
0	.0017	0.0000	0.0000	0.0
1	-.1191	.0172	.1203	278.2
2	-.0017	.0082	.0084	348.6
3	.0016	.0021	.0028	40.3
4	.0025	-.0009	.0027	109.6
5	.0028	-.0026	.0038	133.0
6	.0019	-.0026	.0032	144.2
7	.0008	-.0023	.0024	161.1
8	-.0002	-.0015	.0015	186.4
9	.0003	-.0019	.0019	172.3
10	-.0002	-.0013	.0013	187.7

TABLE 10 - WAKE WITH DYNAMOMETER BOAT

TABLE 10A - MEASURED DATA

r/R = 0.370

θ_w	V_x/V	V_t/V	V_r/V	θ_w	V_x/V	V_t/V	V_r/V
-1.0	.772	.034	-.001	102.6	.979	-.166	-.014
1.0	.762	.036	-.000	122.6	.962	-.150	-.004
5.2	.750	.049	-.011	142.0	.950	-.103	.004
5.2	.755	.047	-.006	162.1	.930	-.057	.010
8.8	.740	.051	-.015	182.0	.932	-.011	.012
12.4	.726	.028	-.014	201.8	.934	.057	.009
12.4	.708	.040	-.014	221.0	.936	.102	.001
17.8	.682	-.051	-.005	241.0	.959	.129	-.006
19.0	.694	-.102	.007	260.0	.969	.154	-.020
21.5	.721	-.105	.008	280.8	.972	.147	-.031
23.3	.816	-.156	.015	300.0	.978	.128	-.044
23.3	.806	-.165	.021	318.7	.973	.122	-.033
25.1	.848	-.157	.009	320.4	.973	.122	-.032
25.1	.861	-.171	.011	322.1	.968	.128	-.028
28.6	.956	-.165	-.017	325.7	.967	.129	-.025
32.3	.995	-.140	-.051	331.1	.945	.133	-.025
35.8	.980	-.127	-.070	334.9	.822	.147	-.029
39.5	.970	-.124	-.074	339.0	.798	.045	-.015
41.3	.967	-.127	-.074	340.2	.761	.060	-.019
46.0	.964	-.132	-.071	343.8	.749	.024	-.010
52.1	.965	-.140	-.064	347.4	.761	.011	-.002
57.5	.971	-.146	-.058	351.1	.771	.007	.003
62.0	.963	-.160	-.051	356.0	.775	.024	.001
82.8	.980	-.171	-.031	359.0	.772	.034	-.001

TABLE 10A (Continued)

r/R = 0.574

θ_w	V_x/V	V_t/V	V_r/V	θ_w	V_x/V	V_t/V	V_r/V
.3	.876	-.025	-.029	180.3	.952	-.002	.046
1.0	.867	-.030	-.033	189.1	.957	.004	.044
3.0	.841	-.030	-.041	199.9	.950	.032	.040
5.7	.829	-.039	-.053	219.0	.956	.068	.027
9.0	.833	-.072	-.074	239.4	.956	.104	.006
11.1	.841	-.092	-.089	259.2	.960	.109	-.022
14.7	.891	-.098	-.103	269.0	.959	.113	-.042
14.7	.897	-.106	-.104	278.0	.962	.109	-.053
18.3	.902	-.104	-.119	289.8	.965	.101	-.065
19.0	.918	-.091	-.126	300.8	.952	.089	-.082
21.9	.923	-.108	-.128	309.7	.949	.079	-.085
27.3	.952	-.100	-.131	315.5	.940	.074	-.089
32.0	.952	-.106	-.127	320.5	.944	.080	-.092
37.0	.949	-.108	-.124	324.1	.922	.078	-.095
39.8	.944	-.109	-.122	327.8	.884	.064	-.097
59.0	.943	-.136	-.085	331.5	.865	.044	-.094
79.3	.960	-.141	-.055	334.0	.859	.025	-.092
98.9	.970	-.141	-.022	338.0	.846	.010	-.081
120.6	.954	-.118	.010	342.2	.855	.000	-.064
140.0	.957	-.091	.029	345.9	.872	-.009	-.052
149.6	.935	-.069	.037	351.3	.871	-.018	-.038
159.0	.940	-.057	.042	356.7	.882	-.022	-.028
169.0	.942	-.036	.045	360.3	.876	-.025	-.029

TABLE 10A (Continued)

r/R = 0.798

θ_w	V_x/V	V_t/V	V_r/V	θ_w	V_x/V	V_t/V	V_r/V
-.1	.831	-.040	-.116	199.9	.921	.032	.044
3.0	.825	-.042	-.120	219.6	.916	.068	.028
5.2	.842	-.048	-.117	239.0	.925	.101	.001
6.0	.843	-.050	-.118	259.1	.927	.112	-.032
8.8	.845	-.054	-.126	278.0	.934	.110	-.067
8.8	.850	-.057	-.124	300.0	.921	.094	-.107
10.6	.847	-.069	-.132	310.0	.929	.076	-.120
12.4	.891	-.085	-.140	315.0	.928	.067	-.122
14.2	.895	-.090	-.150	319.0	.902	.070	-.120
16.0	.917	-.086	-.149	321.0	.892	.052	-.120
17.0	.917	-.083	-.150	323.6	.885	.025	-.123
19.6	.920	-.075	-.147	325.2	.880	.016	-.130
21.2	.925	-.077	-.145	327.0	.898	.023	-.133
26.8	.927	-.081	-.142	328.8	.918	.019	-.136
30.4	.923	-.086	-.138	332.5	.903	.026	-.134
39.4	.920	-.091	-.130	336.2	.902	.039	-.130
59.3	.923	-.114	-.099	340.0	.893	.027	-.120
79.1	.916	-.124	-.066	341.0	.876	.025	-.123
99.0	.912	-.125	-.030	346.0	.846	.001	-.110
120.8	.921	-.102	.008	352.0	.806	-.012	-.110
140.0	.905	-.080	.031	358.0	.826	-.037	-.112
160.3	.910	-.050	.046	359.8	.821	-.046	-.117
180.1	.916	-.001	.050	359.9	.831	-.040	-.116

TABLE 10A (Continued)

r/R = 1.022

θ_w	V_x/V	V_t/V	V_r/V	θ_w	V_x/V	V_t/V	V_r/V
-1.2	.788	-.042	-.101	186.0	.960	-.007	.059
1.0	.817	-.056	-.109	188.0	.962	-.002	.058
5.6	.849	-.069	-.115	208.8	.968	.028	.047
9.0	.862	-.063	-.124	212.3	.969	.042	.043
12.9	.894	-.087	-.128	234.0	.970	.069	.016
16.4	.934	-.109	-.140	255.6	.980	.084	-.016
19.0	.970	-.093	-.141	277.2	.970	.091	-.062
23.6	.982	-.094	-.138	298.0	.955	.072	-.103
27.2	.958	-.099	-.139	310.0	.942	.057	-.115
30.8	.979	-.099	-.132	318.5	.936	.050	-.120
34.3	.995	-.105	-.125	320.5	.933	.047	-.124
40.0	.997	-.113	-.111	322.1	.869	.051	-.132
60.0	.998	-.125	-.087	324.1	.868	.024	-.132
77.4	.996	-.141	-.054	325.7	.915	0.000	-.134
77.7	.981	-.141	-.055	327.7	.910	.007	-.136
98.9	.995	-.133	-.018	329.5	.899	.011	-.135
109.9	.985	-.130	-.000	332.0	.902	.015	-.136
120.0	.975	-.120	.017	336.7	.882	.010	-.136
129.0	.965	-.112	.027	343.9	.849	.012	-.121
142.2	.959	-.091	.044	347.6	.829	.010	-.110
149.2	.957	-.082	.049	351.0	.821	-.005	-.099
169.0	.956	-.039	.060	354.8	.783	-.027	-.099
179.8	.959	-.016	.061	358.4	.788	-.042	-.101
183.3	.958	-.011	.060	361.0	.817	-.056	-.109

TABLE 10B - INTERPOLATED VALUES OF V_x/V

θ_w	r/R = 0.3	0.4	0.5	0.6	0.7	0.8	0.9	1.0
0.0	.689	.794	.861	.877	.850	.829	.815	.806
2.5	.705	.777	.825	.841	.829	.822	.822	.828
5.0	.711	.768	.810	.831	.835	.838	.842	.846
7.5	.702	.762	.806	.832	.840	.847	.852	.855
10.0	.677	.754	.808	.835	.838	.844	.853	.866
12.5	.642	.744	.820	.865	.882	.892	.896	.892
15.0	.585	.737	.845	.897	.899	.902	.908	.915
17.5	.565	.732	.850	.908	.912	.919	.931	.946
20.0	.566	.737	.858	.913	.913	.922	.941	.970
22.5	.686	.804	.887	.923	.920	.927	.946	.976
25.0	.801	.872	.920	.936	.926	.928	.941	.965
27.5	.906	.933	.948	.946	.930	.926	.934	.953
30.0	.986	.975	.962	.946	.927	.924	.936	.965
32.5	1.013	.988	.966	.943	.923	.922	.940	.977
35.0	.998	.979	.962	.942	.921	.921	.942	.984
37.5	.984	.971	.957	.939	.919	.920	.943	.986
40.0	.979	.965	.952	.935	.918	.920	.943	.985
42.5	.976	.962	.949	.933	.917	.920	.943	.986
45.0	.975	.960	.946	.931	.916	.920	.944	.986
47.5	.975	.959	.945	.930	.916	.921	.944	.987
50.0	.975	.959	.945	.930	.917	.921	.945	.987
52.5	.977	.960	.947	.931	.917	.922	.945	.987
55.0	.982	.964	.949	.933	.918	.923	.946	.987
57.5	.984	.966	.951	.935	.919	.923	.946	.987
60.0	.978	.964	.952	.936	.920	.923	.945	.986

TABLE 10B (Continued)

θ_w	r/R = 0.3	0.4	0.5	0.6	0.7	0.8	0.9	1.0
60.0	.978	.964	.952	.936	.920	.923	.945	.986
62.5	.968	.960	.952	.938	.920	.923	.944	.985
65.0	.964	.960	.953	.939	.921	.922	.943	.984
67.5	.962	.960	.955	.941	.921	.921	.941	.982
70.0	.962	.962	.958	.943	.921	.920	.940	.980
72.5	.964	.965	.960	.944	.921	.919	.938	.979
75.0	.967	.968	.963	.946	.921	.918	.937	.377
77.5	.971	.971	.966	.948	.921	.917	.935	.376
80.0	.975	.975	.969	.950	.921	.916	.934	.977
82.5	.979	.979	.972	.951	.921	.915	.934	.977
85.0	.980	.980	.974	.952	.921	.914	.933	.378
87.5	.979	.981	.975	.953	.920	.914	.933	.979
90.0	.978	.981	.976	.954	.920	.913	.933	.979
92.5	.977	.982	.977	.955	.920	.912	.932	.980
95.0	.976	.982	.978	.956	.920	.912	.932	.980
97.5	.975	.982	.978	.956	.920	.912	.932	.980
100.0	.974	.981	.978	.356	.920	.912	.932	.980
102.5	.974	.980	.976	.955	.921	.913	.933	.978
105.0	.973	.978	.974	.954	.922	.915	.933	.977
107.5	.972	.976	.972	.953	.922	.916	.933	.975
110.0	.970	.973	.970	.951	.923	.917	.934	.973
112.5	.969	.971	.967	.950	.923	.918	.934	.972
115.0	.967	.969	.965	.949	.924	.919	.935	.970
117.5	.965	.966	.962	.947	.924	.920	.935	.968
120.0	.963	.964	.960	.946	.924	.921	.934	.966

TABLE 10B (Continued)

θ_w	r/R = 0.3	0.4	0.5	0.6	0.7	0.8	0.9	1.0
120.0	.963	.964	.960	.946	.924	.921	.934	.966
122.5	.959	.963	.961	.947	.924	.919	.932	.963
125.0	.954	.962	.962	.948	.924	.918	.930	.960
127.5	.950	.961	.963	.949	.923	.916	.927	.957
130.0	.947	.960	.964	.949	.922	.913	.924	.955
132.5	.943	.959	.964	.950	.920	.911	.922	.953
135.0	.941	.958	.964	.949	.919	.909	.920	.951
137.5	.938	.957	.963	.948	.917	.907	.918	.950
140.0	.937	.955	.961	.946	.915	.905	.917	.949
142.5	.939	.952	.955	.940	.913	.905	.917	.949
145.0	.940	.948	.948	.935	.911	.905	.918	.948
147.5	.940	.944	.943	.930	.910	.906	.919	.948
150.0	.939	.941	.939	.927	.909	.906	.919	.948
152.5	.935	.939	.938	.927	.910	.907	.920	.948
155.0	.931	.938	.939	.929	.911	.908	.920	.948
157.5	.926	.936	.940	.931	.912	.909	.921	.948
160.0	.921	.935	.941	.932	.914	.910	.921	.948
162.5	.918	.934	.941	.933	.915	.911	.922	.948
165.0	.917	.934	.941	.934	.915	.911	.922	.948
167.5	.917	.934	.942	.935	.916	.912	.923	.948
170.0	.916	.934	.943	.936	.917	.913	.924	.949
172.5	.915	.935	.944	.938	.918	.914	.924	.950
175.0	.914	.936	.946	.940	.920	.915	.925	.951
177.5	.913	.937	.948	.942	.921	.915	.926	.951
180.0	.913	.938	.950	.944	.922	.916	.926	.951

TABLE 10B (Continued)

θ_w	r/R = 0.3	0.4	0.5	0.6	0.7	0.8	0.9	1.0
180.0	.913	.938	.950	.944	.922	.916	.926	.951
182.5	.913	.939	.952	.945	.924	.917	.926	.950
185.0	.912	.939	.953	.947	.925	.918	.927	.952
187.5	.912	.940	.954	.948	.925	.919	.928	.954
190.0	.912	.940	.954	.948	.926	.919	.930	.956
192.5	.914	.940	.953	.947	.926	.920	.931	.958
195.0	.915	.940	.952	.946	.925	.921	.932	.959
197.5	.917	.939	.951	.944	.925	.921	.932	.959
200.0	.919	.939	.949	.943	.925	.921	.933	.960
202.5	.919	.939	.949	.943	.924	.921	.932	.960
205.0	.919	.939	.950	.943	.924	.920	.932	.960
207.5	.918	.939	.950	.943	.923	.919	.931	.959
210.0	.917	.940	.951	.944	.923	.918	.931	.960
212.5	.916	.940	.952	.945	.922	.918	.930	.960
215.0	.916	.941	.953	.945	.922	.917	.930	.960
217.5	.916	.941	.954	.946	.922	.916	.929	.960
220.0	.916	.942	.955	.947	.922	.916	.929	.960
222.5	.919	.944	.955	.947	.923	.917	.930	.961
225.0	.924	.946	.956	.947	.924	.918	.931	.961
227.5	.928	.948	.956	.947	.925	.919	.931	.961
230.0	.933	.950	.957	.947	.926	.921	.932	.961
232.5	.938	.952	.957	.948	.926	.922	.933	.962
235.0	.944	.955	.958	.948	.927	.923	.935	.962
237.5	.949	.957	.959	.948	.928	.924	.936	.964
240.0	.953	.959	.959	.948	.929	.925	.937	.965

TABLE 10B (Continued)

θ_w	r/R = 0.3	0.4	0.5	0.6	0.7	0.8	0.9	1.0
240.0	.953	.959	.959	.948	.929	.925	.937	.955
242.5	.956	.961	.960	.949	.929	.926	.938	.966
245.0	.959	.963	.961	.949	.930	.926	.939	.967
247.5	.960	.964	.962	.950	.930	.926	.939	.968
250.0	.962	.965	.963	.950	.930	.927	.940	.969
252.5	.963	.966	.964	.951	.930	.927	.940	.970
255.0	.965	.967	.965	.951	.931	.927	.940	.971
257.5	.966	.968	.965	.952	.931	.927	.941	.971
260.0	.967	.969	.965	.952	.932	.928	.941	.970
262.5	.969	.969	.965	.952	.932	.929	.941	.970
265.0	.970	.969	.965	.952	.933	.930	.942	.969
267.5	.971	.969	.965	.952	.934	.931	.942	.968
270.0	.972	.970	.965	.952	.935	.932	.943	.967
272.5	.972	.970	.965	.953	.936	.933	.943	.966
275.0	.972	.971	.966	.954	.937	.934	.943	.965
277.5	.972	.971	.967	.955	.938	.934	.942	.964
280.0	.971	.972	.968	.956	.938	.933	.941	.962
282.5	.971	.973	.970	.957	.937	.931	.939	.960
285.0	.972	.974	.971	.957	.936	.929	.936	.959
287.5	.973	.975	.972	.957	.934	.927	.934	.957
290.0	.974	.976	.972	.956	.933	.925	.932	.955
292.5	.977	.976	.970	.954	.931	.923	.931	.953
295.0	.980	.976	.967	.951	.929	.922	.929	.951
297.5	.983	.975	.965	.948	.928	.921	.928	.949
300.0	.986	.975	.962	.946	.927	.921	.928	.947

TABLE 10B (Continued)

θ_w	r/R = 0.3	0.4	0.5	0.6	0.7	0.8	0.9	1.0
300.0	.986	.975	.962	.946	.927	.921	.928	.947
302.5	.986	.973	.961	.946	.929	.923	.929	.945
305.0	.984	.972	.960	.946	.931	.926	.930	.943
307.5	.983	.971	.959	.946	.933	.927	.930	.941
310.0	.983	.969	.957	.944	.933	.928	.931	.939
312.5	.986	.967	.952	.941	.934	.931	.933	.939
315.0	.987	.966	.950	.938	.930	.928	.930	.937
317.5	.982	.968	.954	.937	.918	.912	.916	.932
320.0	.980	.970	.957	.934	.906	.896	.905	.932
322.5	.977	.963	.947	.928	.905	.887	.874	.864
325.0	.990	.957	.930	.907	.889	.880	.881	.891
327.5	1.020	.951	.906	.889	.898	.904	.909	.911
330.0	1.019	.938	.888	.880	.905	.918	.917	.903
332.5	.931	.891	.868	.869	.890	.903	.907	.903
335.0	.810	.825	.842	.864	.889	.902	.904	.895
337.5	.769	.799	.828	.857	.884	.898	.898	.883
340.0	.742	.788	.826	.856	.877	.887	.885	.872
342.5	.701	.775	.829	.860	.869	.872	.868	.859
345.0	.682	.776	.840	.867	.859	.853	.848	.843
347.5	.691	.787	.849	.867	.847	.833	.827	.828
350.0	.698	.793	.852	.862	.832	.815	.811	.820
352.5	.702	.797	.855	.863	.828	.807	.798	.803
355.0	.703	.800	.860	.871	.840	.815	.797	.784
357.5	.702	.799	.861	.875	.848	.824	.804	.786
360.0	.689	.794	.861	.877	.850	.829	.815	.806

TABLE 10C - INTERPOLATED VALUES OF V_t/V

θ_w	r/R = 0.3	0.4	0.5	0.6	0.7	0.8	0.9	1.0
0.0	.066	.022	-.010	-.028	-.034	-.040	-.045	-.049
2.5	.076	.026	-.011	-.030	-.034	-.041	-.049	-.060
5.0	.092	.031	-.014	-.037	-.041	-.048	-.056	-.066
7.5	.113	.029	-.029	-.055	-.051	-.052	-.055	-.063
10.0	.125	.020	-.051	-.079	-.069	-.064	-.062	-.066
12.5	.109	.004	-.067	-.097	-.090	-.086	-.083	-.083
15.0	.041	-.031	-.081	-.099	-.091	-.089	-.092	-.101
17.5	-.036	-.070	-.091	-.094	-.084	-.081	-.086	-.100
20.0	-.070	-.090	-.100	-.096	-.082	-.075	-.077	-.087
22.5	-.150	-.134	-.119	-.102	-.086	-.078	-.079	-.088
25.0	-.193	-.153	-.122	-.099	-.086	-.080	-.082	-.093
27.5	-.200	-.154	-.119	-.096	-.086	-.082	-.086	-.096
30.0	-.183	-.146	-.118	-.099	-.089	-.085	-.087	-.096
32.5	-.153	-.133	-.116	-.102	-.091	-.087	-.090	-.098
35.0	-.137	-.126	-.115	-.103	-.093	-.089	-.092	-.103
37.5	-.130	-.122	-.114	-.104	-.094	-.090	-.095	-.106
40.0	-.130	-.122	-.115	-.105	-.095	-.092	-.097	-.109
42.5	-.135	-.126	-.117	-.107	-.097	-.094	-.099	-.112
45.0	-.138	-.128	-.120	-.110	-.100	-.097	-.102	-.114
47.5	-.141	-.132	-.123	-.113	-.103	-.100	-.104	-.116
50.0	-.143	-.135	-.127	-.117	-.106	-.103	-.107	-.117
52.5	-.145	-.138	-.131	-.121	-.110	-.106	-.109	-.119
55.0	-.146	-.141	-.135	-.125	-.114	-.109	-.111	-.120
57.5	-.148	-.144	-.139	-.129	-.117	-.112	-.113	-.121
60.0	-.157	-.151	-.143	-.133	-.120	-.114	-.115	-.122

TABLE 10C (Continued)

θ_w	r/R = 0.3	0.4	0.5	0.6	0.7	0.8	0.9	1.0
60.0	-.157	-.151	-.143	-.133	-.120	-.114	-.115	-.122
62.5	-.170	-.158	-.146	-.134	-.122	-.116	-.117	-.125
65.0	-.177	-.162	-.148	-.135	-.123	-.118	-.119	-.127
67.5	-.183	-.165	-.150	-.136	-.124	-.119	-.121	-.130
70.0	-.186	-.167	-.151	-.137	-.125	-.120	-.123	-.132
72.5	-.188	-.168	-.151	-.137	-.126	-.121	-.124	-.134
75.0	-.189	-.168	-.152	-.137	-.126	-.122	-.126	-.135
77.5	-.188	-.168	-.151	-.137	-.127	-.123	-.127	-.137
80.0	-.186	-.167	-.151	-.138	-.127	-.124	-.127	-.138
82.5	-.184	-.166	-.151	-.138	-.128	-.125	-.128	-.137
85.0	-.183	-.166	-.151	-.139	-.129	-.125	-.128	-.137
87.5	-.183	-.166	-.152	-.139	-.129	-.126	-.128	-.136
90.0	-.183	-.166	-.151	-.139	-.130	-.126	-.128	-.135
92.5	-.182	-.165	-.151	-.139	-.130	-.126	-.127	-.134
95.0	-.182	-.165	-.151	-.139	-.130	-.126	-.127	-.133
97.5	-.181	-.164	-.150	-.138	-.129	-.125	-.126	-.132
100.0	-.180	-.163	-.149	-.137	-.128	-.124	-.125	-.131
102.5	-.179	-.162	-.147	-.135	-.126	-.122	-.123	-.130
105.0	-.178	-.160	-.145	-.133	-.124	-.120	-.122	-.129
107.5	-.178	-.159	-.143	-.131	-.121	-.118	-.120	-.128
110.0	-.177	-.157	-.141	-.128	-.118	-.115	-.118	-.127
112.5	-.176	-.155	-.138	-.125	-.116	-.112	-.115	-.125
115.0	-.174	-.153	-.136	-.122	-.113	-.109	-.113	-.122
117.5	-.172	-.150	-.133	-.119	-.110	-.106	-.110	-.120
120.0	-.170	-.147	-.129	-.116	-.106	-.103	-.107	-.117

TABLE 10C (Continued)

θ_w	r/R = 0.3	0.4	0.5	0.6	0.7	0.8	0.9	1.0
120.0	-.170	-.147	-.129	-.116	-.106	-.103	-.107	-.117
122.5	-.166	-.144	-.126	-.113	-.103	-.101	-.104	-.115
125.0	-.160	-.139	-.123	-.110	-.101	-.098	-.102	-.112
127.5	-.153	-.134	-.119	-.107	-.098	-.095	-.099	-.110
130.0	-.146	-.129	-.115	-.104	-.095	-.092	-.096	-.107
132.5	-.138	-.123	-.111	-.100	-.092	-.089	-.093	-.103
135.0	-.130	-.118	-.107	-.097	-.088	-.086	-.090	-.100
137.5	-.123	-.111	-.102	-.093	-.085	-.083	-.087	-.096
140.0	-.115	-.105	-.097	-.089	-.082	-.080	-.083	-.092
142.5	-.109	-.099	-.090	-.083	-.078	-.077	-.080	-.088
145.0	-.104	-.093	-.084	-.078	-.074	-.074	-.078	-.085
147.5	-.099	-.087	-.078	-.072	-.070	-.070	-.075	-.082
150.0	-.093	-.081	-.073	-.068	-.066	-.067	-.071	-.079
152.5	-.086	-.076	-.069	-.064	-.062	-.063	-.067	-.074
155.0	-.079	-.071	-.065	-.061	-.059	-.059	-.063	-.069
157.5	-.072	-.066	-.061	-.058	-.055	-.055	-.058	-.064
160.0	-.065	-.061	-.057	-.054	-.051	-.051	-.053	-.058
162.5	-.058	-.055	-.052	-.049	-.046	-.045	-.047	-.053
165.0	-.053	-.050	-.047	-.044	-.040	-.039	-.041	-.047
167.5	-.048	-.045	-.042	-.038	-.034	-.033	-.035	-.041
170.0	-.043	-.039	-.036	-.031	-.027	-.027	-.029	-.035
172.5	-.039	-.033	-.028	-.024	-.020	-.020	-.023	-.029
175.0	-.035	-.027	-.020	-.016	-.013	-.014	-.017	-.023
177.5	-.030	-.020	-.013	-.009	-.007	-.008	-.012	-.018
180.0	-.024	-.014	-.007	-.002	0.000	-.002	-.006	-.014

TABLE 10C (Continued)

θ_w	r/R = 0.3	0.4	0.5	0.6	0.7	0.8	0.9	1.0
180.0	-.024	-.014	-.007	-.002	0.000	-.002	-.006	-.014
182.5	-.014	-.008	-.003	.001	.004	.003	-.002	-.010
185.0	-.001	-.001	0.000	.003	.008	.008	.003	-.006
187.5	.012	.006	.003	.005	.011	.012	.008	-.001
190.0	.024	.013	.007	.008	.015	.016	.013	.004
192.5	.035	.022	.014	.014	.019	.020	.016	.008
195.0	.044	.030	.021	.020	.024	.024	.019	.010
197.5	.054	.039	.029	.026	.029	.028	.022	.012
200.0	.062	.047	.037	.033	.035	.032	.025	.015
202.5	.072	.055	.043	.038	.040	.036	.029	.018
205.0	.079	.061	.049	.043	.044	.041	.033	.022
207.5	.087	.068	.054	.048	.049	.046	.038	.027
210.0	.094	.074	.059	.053	.053	.050	.044	.035
212.5	.101	.079	.064	.057	.057	.055	.051	.044
215.0	.107	.084	.069	.061	.061	.059	.056	.052
217.5	.113	.089	.073	.065	.065	.064	.061	.058
220.0	.116	.094	.078	.070	.070	.068	.066	.062
222.5	.121	.099	.083	.075	.075	.073	.070	.066
225.0	.125	.103	.087	.080	.080	.078	.074	.068
227.5	.127	.107	.092	.085	.085	.083	.078	.070
230.0	.130	.110	.096	.090	.090	.087	.081	.071
232.5	.133	.114	.100	.095	.095	.091	.084	.072
235.0	.135	.117	.104	.099	.099	.095	.087	.074
237.5	.138	.120	.108	.103	.103	.099	.090	.076
240.0	.141	.123	.111	.105	.106	.102	.093	.078

TABLE 10C (Continued)

θ_w	r/R = 0.3	0.4	0.5	0.6	0.7	0.8	0.9	1.0
240.0	.141	.123	.111	.105	.106	.102	.093	.078
242.5	.146	.126	.112	.107	.109	.105	.095	.080
245.0	.151	.129	.114	.108	.110	.107	.097	.082
247.5	.157	.132	.115	.109	.111	.108	.099	.084
250.0	.163	.135	.116	.109	.112	.109	.100	.085
252.5	.166	.138	.117	.110	.113	.110	.102	.086
255.0	.172	.140	.118	.110	.114	.111	.103	.088
257.5	.176	.143	.119	.111	.114	.112	.103	.089
260.0	.179	.144	.120	.111	.115	.112	.104	.090
262.5	.179	.145	.122	.112	.115	.112	.105	.091
265.0	.179	.146	.123	.113	.115	.113	.105	.092
267.5	.178	.146	.123	.114	.116	.113	.105	.093
270.0	.176	.145	.123	.114	.115	.112	.105	.094
272.5	.175	.144	.123	.113	.115	.112	.105	.094
275.0	.174	.143	.121	.112	.114	.111	.105	.094
277.5	.172	.141	.120	.111	.113	.110	.104	.094
280.0	.170	.139	.118	.109	.112	.110	.103	.092
282.5	.168	.137	.116	.108	.111	.109	.102	.091
285.0	.165	.135	.114	.106	.110	.108	.101	.089
287.5	.163	.132	.112	.104	.108	.106	.099	.087
290.0	.160	.130	.109	.102	.106	.105	.097	.084
292.5	.157	.127	.107	.100	.104	.103	.095	.082
295.0	.155	.125	.104	.097	.102	.100	.093	.079
297.5	.153	.122	.101	.095	.099	.098	.090	.076
300.0	.151	.120	.099	.092	.096	.094	.087	.073

TABLE 10C (Continued)

θ_w	r/R = 0.3	0.4	0.5	0.6	0.7	0.8	0.9	1.0
300.0	.151	.120	.099	.092	.096	.094	.087	.073
302.5	.149	.118	.096	.088	.092	.090	.082	.069
305.0	.149	.116	.094	.085	.087	.085	.078	.066
307.5	.148	.115	.092	.082	.083	.080	.073	.063
310.0	.148	.114	.090	.079	.079	.075	.069	.060
312.5	.148	.113	.088	.075	.073	.070	.065	.057
315.0	.148	.112	.086	.073	.071	.067	.062	.055
317.5	.146	.112	.088	.077	.076	.072	.065	.054
320.0	.141	.113	.092	.077	.069	.062	.055	.049
322.5	.147	.121	.096	.072	.048	.035	.034	.044
325.0	.149	.121	.095	.066	.036	.017	.007	.008
327.5	.157	.119	.086	.059	.038	.022	.012	.006
330.0	.169	.117	.076	.048	.031	.019	.013	.012
332.5	.200	.121	.064	.035	.031	.026	.021	.016
335.0	.219	.119	.050	.024	.034	.036	.030	.017
337.5	.152	.079	.031	.017	.032	.037	.032	.015
340.0	.077	.038	.014	.010	.023	.028	.025	.014
342.5	.050	.023	.005	.003	.012	.017	.017	.013
345.0	.035	.013	-.002	-.005	0.000	.005	.009	.011
347.5	.026	.005	-.008	-.012	-.007	-.003	.003	.008
350.0	.022	.002	-.012	-.016	-.011	-.007	-.004	-.001
352.5	.029	.004	-.012	-.018	-.015	-.014	-.013	-.013
355.0	.042	.011	-.010	-.021	-.023	-.024	-.026	-.027
357.5	.056	.019	-.008	-.024	-.030	-.035	-.037	-.038
360.0	.066	.022	-.010	-.028	-.034	-.040	-.045	-.049

TABLE 10D - INTERPOLATED VALUES OF V_r/V

θ_w	r/R = 0.3	0.4	0.5	0.6	0.7	0.8	0.9	1.0
0.0	-.002	-.001	-.012	-.043	-.090	-.117	-.124	-.111
2.5	.002	-.005	-.022	-.053	-.096	-.120	-.127	-.116
5.0	.002	-.013	-.032	-.061	-.097	-.118	-.125	-.118
7.5	.004	-.021	-.045	-.073	-.103	-.121	-.128	-.123
10.0	.012	-.027	-.060	-.090	-.115	-.130	-.134	-.128
12.5	.023	-.028	-.071	-.104	-.128	-.140	-.141	-.131
15.0	.037	-.026	-.076	-.114	-.138	-.151	-.151	-.140
17.5	.058	-.024	-.085	-.123	-.140	-.149	-.150	-.143
20.0	.071	-.022	-.091	-.129	-.141	-.147	-.147	-.142
22.5	.092	-.014	-.091	-.131	-.140	-.144	-.144	-.140
25.0	.088	-.018	-.094	-.133	-.140	-.143	-.143	-.140
27.5	.060	-.033	-.099	-.133	-.139	-.141	-.142	-.139
30.0	.023	-.050	-.103	-.131	-.136	-.139	-.138	-.135
32.5	-.013	-.067	-.107	-.129	-.134	-.136	-.135	-.130
35.0	-.036	-.078	-.109	-.127	-.132	-.134	-.132	-.125
37.5	-.046	-.083	-.110	-.125	-.131	-.132	-.128	-.120
40.0	-.049	-.083	-.109	-.124	-.129	-.129	-.124	-.114
42.5	-.050	-.083	-.107	-.121	-.126	-.126	-.120	-.109
45.0	-.049	-.081	-.103	-.117	-.122	-.122	-.117	-.106
47.5	-.048	-.078	-.099	-.113	-.118	-.119	-.113	-.102
50.0	-.047	-.074	-.095	-.108	-.114	-.115	-.110	-.099
52.5	-.045	-.071	-.090	-.103	-.109	-.111	-.107	-.097
55.0	-.045	-.067	-.085	-.097	-.105	-.107	-.103	-.094
57.5	-.043	-.063	-.079	-.091	-.100	-.102	-.100	-.092
60.0	-.041	-.059	-.075	-.086	-.095	-.098	-.096	-.089

TABLE 10D (Continued)

θ_w	r/R = 0.3	0.4	0.5	0.6	0.7	0.8	0.9	1.0
60.0	-.041	-.059	-.075	-.086	-.095	-.098	-.096	-.089
62.5	-.037	-.056	-.071	-.083	-.091	-.094	-.092	-.085
65.0	-.034	-.053	-.067	-.079	-.087	-.090	-.088	-.081
67.5	-.032	-.050	-.064	-.075	-.083	-.086	-.083	-.076
70.0	-.030	-.047	-.061	-.071	-.079	-.081	-.079	-.071
72.5	-.028	-.044	-.057	-.068	-.075	-.077	-.075	-.067
75.0	-.026	-.042	-.054	-.064	-.071	-.073	-.070	-.062
77.5	-.025	-.040	-.051	-.060	-.067	-.069	-.065	-.057
80.0	-.024	-.037	-.048	-.057	-.063	-.064	-.061	-.053
82.5	-.023	-.035	-.044	-.052	-.058	-.060	-.056	-.048
85.0	-.022	-.032	-.041	-.048	-.054	-.055	-.052	-.044
87.5	-.021	-.029	-.037	-.044	-.049	-.051	-.047	-.040
90.0	-.019	-.027	-.033	-.039	-.045	-.046	-.043	-.035
92.5	-.018	-.024	-.029	-.035	-.040	-.042	-.038	-.031
95.0	-.017	-.021	-.026	-.031	-.036	-.037	-.034	-.027
97.5	-.016	-.019	-.022	-.026	-.031	-.032	-.030	-.023
100.0	-.015	-.016	-.018	-.022	-.027	-.028	-.025	-.018
102.5	-.014	-.014	-.015	-.018	-.022	-.023	-.021	-.014
105.0	-.014	-.012	-.011	-.014	-.018	-.019	-.016	-.010
107.5	-.014	-.010	-.008	-.010	-.014	-.014	-.012	-.006
110.0	-.013	-.008	-.005	-.006	-.009	-.010	-.007	-.002
112.5	-.013	-.006	-.002	-.002	-.005	-.005	-.003	.003
115.0	-.013	-.005	.001	.002	-.001	-.001	.002	.007
117.5	-.013	-.003	.004	.005	.003	.003	.006	.011
120.0	-.013	-.002	.006	.009	.007	.007	.010	.015

TABLE 10D (Continued)

θ_w	r/R = 0.3	0.4	0.5	0.6	0.7	0.8	0.9	1.0
120.0	-.013	-.002	.006	.009	.007	.007	.010	.015
122.5	-.013	0.000	.009	.012	.010	.011	.013	.018
125.0	-.013	.001	.011	.015	.013	.014	.017	.021
127.5	-.012	.003	.013	.017	.016	.017	.020	.024
130.0	-.012	.004	.015	.020	.019	.020	.023	.027
132.5	-.011	.005	.017	.022	.022	.023	.026	.031
135.0	-.011	.007	.019	.025	.024	.026	.029	.034
137.5	-.010	.008	.021	.027	.027	.029	.032	.037
140.0	-.010	.009	.023	.029	.029	.031	.035	.040
142.5	-.010	.010	.024	.031	.031	.034	.037	.043
145.0	-.010	.011	.026	.033	.034	.036	.039	.045
147.5	-.009	.012	.028	.035	.036	.038	.041	.046
150.0	-.009	.013	.029	.037	.038	.040	.043	.048
152.5	-.009	.014	.030	.039	.039	.041	.045	.049
155.0	-.009	.015	.032	.040	.041	.043	.046	.051
157.5	-.009	.015	.033	.041	.042	.045	.048	.053
160.0	-.008	.016	.034	.042	.043	.046	.049	.054
162.5	-.008	.017	.034	.043	.044	.047	.051	.056
165.0	-.008	.017	.035	.044	.045	.048	.052	.057
167.5	-.007	.017	.035	.045	.046	.049	.053	.058
170.0	-.007	.018	.036	.045	.047	.049	.053	.059
172.5	-.007	.018	.036	.045	.047	.050	.054	.059
175.0	-.007	.018	.036	.046	.047	.050	.054	.059
177.5	-.007	.018	.036	.046	.047	.050	.054	.059
180.0	-.007	.018	.036	.046	.047	.050	.054	.059

TABLE 10D (Continued)

θ_w	r/R = 0.3	0.4	0.5	0.6	0.7	0.8	0.9	1.0
180.0	-.007	.018	.036	.046	.047	.050	.054	.059
182.5	-.006	.018	.036	.046	.047	.050	.054	.059
185.0	-.006	.018	.036	.045	.047	.050	.053	.058
187.5	-.006	.018	.036	.045	.046	.049	.053	.057
190.0	-.006	.018	.035	.044	.046	.048	.052	.057
192.5	-.007	.017	.034	.043	.045	.047	.051	.056
195.0	-.007	.017	.034	.042	.044	.046	.050	.055
197.5	-.007	.016	.033	.041	.042	.045	.049	.053
200.0	-.007	.016	.032	.040	.041	.044	.047	.052
202.5	-.008	.015	.031	.039	.040	.042	.046	.050
205.0	-.008	.014	.029	.037	.038	.040	.044	.049
207.5	-.009	.013	.028	.036	.037	.039	.042	.047
210.0	-.010	.011	.026	.034	.035	.037	.040	.044
212.5	-.010	.010	.025	.032	.033	.035	.038	.042
215.0	-.011	.009	.023	.030	.031	.033	.035	.039
217.5	-.011	.008	.021	.028	.028	.030	.033	.037
220.0	-.012	.006	.019	.026	.026	.027	.030	.034
222.5	-.012	.005	.018	.023	.023	.024	.027	.031
225.0	-.012	.004	.016	.021	.020	.021	.024	.028
227.5	-.012	.003	.014	.018	.017	.018	.020	.024
230.0	-.012	.002	.012	.016	.014	.015	.017	.021
232.5	-.012	.001	.010	.013	.011	.011	.013	.017
235.0	-.012	0.000	.008	.010	.007	.007	.009	.014
237.5	-.012	-.002	.005	.007	.004	.003	.006	.010
240.0	-.013	-.003	.003	.004	0.000	0.000	.002	.007

TABLE 10D (Continued)

θ_w	r/R = 0.3	0.4	0.5	0.6	0.7	0.8	0.9	1.0
240.0	-.013	-.003	.003	.004	0.000	0.000	.002	.007
242.5	-.013	-.005	.001	.001	-.003	-.004	-.002	.003
245.0	-.015	-.007	-.002	-.002	-.007	-.008	-.006	0.000
247.5	-.016	-.009	-.005	-.006	-.011	-.012	-.010	-.004
250.0	-.017	-.011	-.008	-.009	-.015	-.016	-.014	-.008
252.5	-.018	-.013	-.011	-.013	-.019	-.020	-.018	-.012
255.0	-.019	-.015	-.014	-.017	-.023	-.025	-.023	-.016
257.5	-.020	-.018	-.018	-.021	-.027	-.029	-.027	-.021
260.0	-.020	-.020	-.022	-.026	-.031	-.033	-.032	-.026
262.5	-.020	-.023	-.026	-.031	-.036	-.038	-.036	-.031
265.0	-.019	-.025	-.030	-.036	-.041	-.043	-.041	-.036
267.5	-.018	-.027	-.034	-.041	-.046	-.047	-.046	-.042
270.0	-.018	-.029	-.038	-.045	-.050	-.052	-.051	-.047
272.5	-.018	-.031	-.041	-.049	-.054	-.057	-.056	-.053
275.0	-.019	-.032	-.043	-.052	-.059	-.062	-.062	-.058
277.5	-.019	-.034	-.046	-.055	-.063	-.066	-.067	-.064
280.0	-.020	-.035	-.048	-.058	-.067	-.071	-.072	-.069
282.5	-.022	-.037	-.050	-.061	-.071	-.076	-.078	-.075
285.0	-.025	-.039	-.052	-.064	-.074	-.081	-.083	-.080
287.5	-.027	-.041	-.054	-.067	-.078	-.085	-.088	-.086
290.0	-.028	-.043	-.056	-.070	-.082	-.090	-.093	-.091
292.5	-.029	-.045	-.060	-.074	-.086	-.094	-.097	-.095
295.0	-.029	-.047	-.063	-.078	-.091	-.099	-.102	-.100
297.5	-.028	-.048	-.066	-.082	-.095	-.103	-.106	-.104
300.0	-.028	-.050	-.069	-.085	-.099	-.107	-.110	-.107

TABLE 10D (Continued)

θ_w	r/R = 0.3	0.4	0.5	0.6	0.7	0.8	0.9	1.0
300.0	-.028	-.050	-.069	-.085	-.099	-.107	-.110	-.107
302.5	-.027	-.050	-.070	-.087	-.102	-.111	-.114	-.110
305.0	-.025	-.049	-.070	-.089	-.106	-.115	-.118	-.113
307.5	-.023	-.048	-.070	-.090	-.108	-.118	-.121	-.115
310.0	-.021	-.047	-.070	-.091	-.110	-.121	-.123	-.117
312.5	-.017	-.046	-.071	-.093	-.111	-.121	-.124	-.118
315.0	-.013	-.045	-.072	-.095	-.112	-.122	-.124	-.119
317.5	-.009	-.044	-.073	-.095	-.111	-.121	-.124	-.120
320.0	-.005	-.043	-.074	-.096	-.111	-.120	-.124	-.123
322.5	.005	-.039	-.074	-.098	-.111	-.121	-.128	-.132
325.0	.008	-.038	-.074	-.101	-.118	-.129	-.135	-.134
327.5	.009	-.038	-.075	-.103	-.122	-.134	-.139	-.137
330.0	.006	-.037	-.073	-.102	-.123	-.136	-.141	-.137
332.5	.002	-.039	-.072	-.100	-.121	-.134	-.140	-.138
335.0	-.002	-.039	-.071	-.097	-.118	-.132	-.139	-.138
337.5	.002	-.033	-.063	-.090	-.113	-.128	-.136	-.136
340.0	.006	-.025	-.054	-.081	-.106	-.123	-.131	-.131
342.5	.005	-.020	-.045	-.072	-.099	-.117	-.126	-.126
345.0	.008	-.014	-.037	-.064	-.093	-.111	-.120	-.119
347.5	.011	-.008	-.030	-.058	-.089	-.109	-.117	-.113
350.0	.013	-.003	-.023	-.053	-.089	-.110	-.115	-.106
352.5	.010	0.000	-.018	-.048	-.088	-.110	-.115	-.103
355.0	.004	0.000	-.014	-.044	-.086	-.110	-.116	-.104
357.5	-.001	-.001	-.012	-.042	-.086	-.111	-.118	-.105
360.0	-.002	-.001	-.012	-.043	-.090	-.117	-.124	-.111

TABLE 10E - HARMONICS OF V_x/V

r/R = 0.3

n	$(A_x)_n/V$	$(B_x)_n/V$	$(V_x)_n/V$	$(\phi_x^*)_n$
0	.9175	0.0000	0.0000	0.0
1	-.0501	-.0003	.0501	269.6
2	-.0868	-.0105	.0874	263.1
3	-.0580	-.0053	.0582	264.8
4	-.0459	-.0072	.0465	261.1
5	-.0334	-.0070	.0341	258.2
6	-.0139	-.0065	.0153	244.9
7	.0033	-.0077	.0084	157.1
8	.0118	-.0028	.0121	103.5
9	.0205	-.0013	.0205	93.7
10	.0215	.0013	.0215	86.5

r/R = 0.4

n	$(A_x)_n/V$	$(B_x)_n/V$	$(V_x)_n/V$	$(\phi_x^*)_n$
0	.9330	0.0000	0.0000	0.0
1	-.0407	.0016	.0407	272.3
2	-.0596	-.0029	.0597	267.2
3	-.0359	-.0008	.0359	268.7
4	-.0263	.0021	.0264	274.5
5	-.0192	-.0010	.0192	266.9
6	-.0076	-.0026	.0080	251.0
7	.0013	-.0069	.0070	169.2
8	.0087	-.0044	.0098	117.0
9	.0114	-.0043	.0122	110.4
10	.0132	-.0043	.0139	107.9

TABLE 10E (Continued)

r/R = 0.5

n	$(A_x)_n/V$	$(B_x)_n/V$	$(V_x)_n/V$	$(\phi_x^*)_n$
0	.9399	0.0000	0.0000	0.0
1	-.0322	.0024	.0323	274.2
2	-.0392	.0025	.0393	273.7
3	-.0204	.0025	.0206	277.0
4	-.0130	.0080	.0153	301.7
5	-.0098	.0028	.0102	286.2
6	-.0037	.0003	.0037	274.9
7	-.0007	-.0054	.0054	187.3
8	.0055	-.0049	.0074	131.7
9	.0045	-.0055	.0071	141.1
10	.0064	-.0071	.0096	137.9

r/R = 0.6

n	$(A_x)_n/V$	$(B_x)_n/V$	$(V_x)_n/V$	$(\phi_x^*)_n$
0	.9326	0.0000	0.0000	0.0
1	-.0238	.0002	.0238	270.6
2	-.0258	.0046	.0262	280.2
3	-.0130	.0043	.0137	288.1
4	-.0073	.0094	.0119	322.0
5	-.0064	.0038	.0075	300.7
6	-.0028	.0022	.0035	308.2
7	-.0031	-.0026	.0040	230.0
8	.0014	-.0035	.0038	158.9
9	.0000	-.0045	.0045	179.9
10	.0012	-.0061	.0062	169.3

TABLE 10E (Continued)

$r/R = 0.7$

n	$(A_x)_n/V$	$(B_x)_n/V$	$(V_x)_n/V$	$(\phi_x^*)_n$
0	.9144	0.0000	0.0000	0.0
1	-.0160	-.0037	.0164	256.8
2	-.0192	.0041	.0196	282.1
3	-.0128	.0046	.0137	290.3
4	-.0085	.0070	.0110	309.3
5	-.0084	.0024	.0087	285.9
6	-.0045	.0031	.0054	304.4
7	-.0056	.0011	.0057	281.3
8	-.0033	-.0007	.0034	258.4
9	-.0022	-.0016	.0027	233.8
10	-.0026	-.0019	.0032	234.2

$r/R = 0.8$

n	$(A_x)_n/V$	$(B_x)_n/V$	$(V_x)_n/V$	$(\phi_x^*)_n$
0	.9107	0.0000	0.0000	0.0
1	-.0137	-.0030	.0140	257.7
2	-.0184	.0063	.0195	288.9
3	-.0140	.0058	.0152	292.6
4	-.0101	.0061	.0118	301.3
5	-.0103	.0020	.0105	280.8
6	-.0061	.0034	.0070	299.5
7	-.0068	.0031	.0075	294.5
8	-.0061	.0011	.0062	280.3
9	-.0038	.0003	.0038	274.5
10	-.0048	.0007	.0049	278.2

TABLE 10E (Continued)

r/R = 0.9

n	$(A_x)_n/V$	$(B_x)_n/V$	$(V_x)_n/V$	$(\phi_x^*)_n$
0	.9216	0.0000	0.0000	0.0
1	-.0171	.0026	.0173	278.5
2	-.0236	.0113	.0262	295.5
3	-.0166	.0075	.0182	294.4
4	-.0120	.0068	.0138	299.7
5	-.0120	.0025	.0123	281.8
6	-.0077	.0033	.0084	293.5
7	-.0069	.0035	.0077	296.7
8	-.0072	.0019	.0074	284.7
9	-.0049	.0012	.0050	283.5
10	-.0055	.0016	.0057	286.6

r/R = 1.0

n	$(A_x)_n/V$	$(B_x)_n/V$	$(V_x)_n/V$	$(\phi_x^*)_n$
0	.9470	0.0000	0.0000	0.0
1	-.0261	.0129	.0291	296.3
2	-.0348	.0190	.0396	298.6
3	-.0205	.0098	.0227	295.6
4	-.0142	.0091	.0169	302.7
5	-.0137	.0041	.0143	286.5
6	-.0092	.0027	.0096	286.6
7	-.0056	.0021	.0060	290.7
8	-.0063	.0016	.0065	284.1
9	-.0054	.0010	.0055	280.7
10	-.0046	.0009	.0047	281.6

TABLE 10F - HARMONICS OF V_t/V

r/R = 0.3

n	$(A_t)_n/V$	$(B_t)_n/V$	$(V_t)_n/V$	$(\phi_t^*)_n$
0	.0022	0.0000	0.0000	0.0
1	.0158	-.1880	.1887	175.2
2	.0133	-.0110	.0172	129.6
3	.0114	-.0119	.0165	136.2
4	.0066	-.0067	.0094	135.2
5	.0086	-.0016	.0087	100.4
6	.0019	.0068	.0071	15.6
7	.0100	.0128	.0163	38.0
8	.0054	.0172	.0180	17.5
9	.0026	.0191	.0193	7.6
10	.0006	.0174	.0174	2.0

r/R = 0.4

n	$(A_t)_n/V$	$(B_t)_n/V$	$(V_t)_n/V$	$(\phi_t^*)_n$
0	-.0091	0.0000	0.0000	0.0
1	.0014	-.1611	.1611	179.5
2	.0045	-.0085	.0096	151.8
3	.0047	-.0084	.0096	150.8
4	.0014	-.0057	.0059	165.9
5	.0032	-.0012	.0034	109.9
6	.0009	.0033	.0034	15.1
7	.0059	.0071	.0092	39.9
8	.0052	.0097	.0110	28.2
9	.0042	.0102	.0110	22.2
10	.0031	.0090	.0095	18.8

TABLE 10F (Continued)

r/R = 0.5

n	$(A_t)_n/V$	$(B_t)_n/V$	$(V_t)_n/V$	$(\phi_t^*)_n$
0	-.0162	0.0000	0.0000	0.0
1	-.0084	-.1408	.1410	183.4
2	-.0020	-.0062	.0065	198.0
3	-.0001	-.0055	.0055	180.9
4	-.0020	-.0047	.0051	202.8
5	-.0004	-.0010	.0011	201.7
6	.0004	.0006	.0007	33.9
7	.0026	.0026	.0038	46.8
8	.0045	.0039	.0060	49.0
9	.0046	.0036	.0059	51.8
10	.0042	.0030	.0051	54.6

r/R = 0.6

n	$(A_t)_n/V$	$(B_t)_n/V$	$(V_t)_n/V$	$(\phi_t^*)_n$
0	-.0168	0.0000	0.0000	0.0
1	-.0130	-.1282	.1289	185.8
2	-.0062	-.0039	.0073	238.1
3	-.0024	-.0029	.0038	219.8
4	-.0031	-.0034	.0046	222.4
5	-.0020	-.0014	.0024	234.4
6	.0007	-.0010	.0012	142.9
7	.0007	-.0006	.0009	132.3
8	.0031	.0004	.0031	83.4
9	.0035	.0002	.0035	87.4
10	.0033	.0001	.0033	88.9

TABLE 10F (Continued)

$r/R = 0.7$

n	$(A_t)_n/V$	$(B_t)_n/V$	$(V_t)_n/V$	$(\phi_t^*)_n$
0	-.0124	0.0000	0.0000	0.0
1	-.0127	-.1227	.1234	185.9
2	-.0081	-.0016	.0083	258.6
3	-.0027	-.0009	.0028	251.2
4	-.0023	-.0020	.0030	228.9
5	-.0016	-.0021	.0026	216.8
6	.0017	-.0014	.0022	130.7
7	-.0004	-.0025	.0025	188.5
8	.0011	-.0013	.0017	139.1
9	.0010	-.0007	.0012	123.3
10	.0008	-.0001	.0008	97.5

$r/R = 0.8$

n	$(A_t)_n/V$	$(B_t)_n/V$	$(V_t)_n/V$	$(\phi_t^*)_n$
0	-.0123	0.0000	0.0000	0.0
1	-.0123	-.1189	.1195	185.9
2	-.0086	-.0006	.0086	266.2
3	-.0027	-.0002	.0027	266.6
4	-.0015	-.0013	.0020	229.0
5	-.0010	-.0024	.0026	203.4
6	.0021	-.0022	.0030	135.8
7	-.0009	-.0033	.0034	195.9
8	.0001	-.0023	.0023	176.3
9	-.0007	-.0015	.0016	204.5
10	-.0006	-.0005	.0008	230.4

TABLE 10F (Continued)

r/R = 0.9

n	$(A_t)_n/V$	$(B_t)_n/V$	$(V_t)_n/V$	$(\phi_t^*)_n$
0	-.0166	0.0000	0.0000	0.0
1	-.0118	-.1164	.1170	185.8
2	-.0075	-.0006	.0075	265.1
3	-.0025	-.0007	.0026	254.6
4	-.0009	-.0015	.0017	211.0
5	-.0005	-.0026	.0026	190.5
6	.0020	-.0031	.0037	147.2
7	-.0010	-.0030	.0032	198.8
8	.0003	-.0028	.0028	174.8
9	-.0015	-.0021	.0026	216.3
10	-.0010	-.0011	.0015	223.3

r/R = 1.0

n	$(A_t)_n/V$	$(B_t)_n/V$	$(V_t)_n/V$	$(\phi_t^*)_n$
0	-.0254	0.0000	0.0000	0.0
1	-.0111	-.1154	.1159	185.5
2	-.0049	-.0019	.0052	249.1
3	-.0021	-.0025	.0033	219.9
4	-.0003	-.0023	.0023	187.2
5	.0002	-.0024	.0024	174.8
6	.0013	-.0042	.0044	162.3
7	-.0007	-.0018	.0019	201.1
8	.0014	-.0026	.0030	151.7
9	-.0017	-.0027	.0032	211.6
10	-.0005	-.0019	.0020	194.1

TABLE 10G - HARMONICS OF V_r/V

r/R = 0.3

n	$(A_r)_n/V$	$(B_r)_n/V$	$(V_r)_n/V$	$(\phi_r^*)_n$
0	-.0107	0.0000	0.0000	0.0
1	.0050	-.0013	.0052	105.0
2	.0159	-.0015	.0160	95.5
3	.0116	.0016	.0117	82.1
4	.0053	.0059	.0079	42.2
5	-.0023	.0073	.0077	342.6
6	-.0065	.0068	.0094	316.4
7	-.0079	.0045	.0091	299.5
8	-.0068	.0014	.0070	281.9
9	-.0050	-.0027	.0057	241.6
10	-.0036	-.0050	.0061	215.6

r/R = 0.4

n	$(A_r)_n/V$	$(B_r)_n/V$	$(V_r)_n/V$	$(\phi_r^*)_n$
0	-.0186	0.0000	0.0000	0.0
1	-.0292	-.0030	.0294	264.1
2	.0155	-.0057	.0165	110.1
3	.0139	-.0035	.0143	104.0
4	.0090	-.0001	.0090	90.9
5	.0042	.0020	.0047	64.4
6	.0016	.0023	.0028	35.3
7	-.0006	.0013	.0014	336.6
8	-.0016	.0000	.0016	271.7
9	-.0010	-.0020	.0022	207.0
10	-.0005	-.0032	.0032	189.4

TABLE 10G (Continued)

$r/R = 0.5$

n	$(A_r)_n/V$	$(B_r)_n/V$	$(V_r)_n/V$	$(\phi_r^*)_n$
0	-.0260	0.0000	0.0000	0.0
1	-.0564	-.0035	.0565	266.4
2	.0142	-.0078	.0162	118.8
3	.0145	-.0065	.0159	114.0
4	.0108	-.0040	.0115	110.5
5	.0080	-.0017	.0082	101.9
6	.0066	-.0008	.0066	96.9
7	.0041	-.0009	.0042	101.7
8	.0020	-.0009	.0022	115.1
9	.0017	-.0014	.0022	129.0
10	.0014	-.0018	.0023	141.1

$r/R = 0.6$

n	$(A_r)_n/V$	$(B_r)_n/V$	$(V_r)_n/V$	$(\phi_r^*)_n$
0	-.0342	0.0000	0.0000	0.0
1	-.0758	-.0024	.0758	268.2
2	.0116	-.0073	.0137	122.2
3	.0129	-.0067	.0145	117.5
4	.0096	-.0051	.0109	117.9
5	.0082	-.0033	.0088	112.1
6	.0072	-.0022	.0075	106.7
7	.0050	-.0016	.0053	107.8
8	.0030	-.0013	.0033	113.5
9	.0025	-.0011	.0027	113.9
10	.0020	-.0011	.0023	119.4

TABLE 10G (Continued)

r/R = 0.7

n	$(A_r)_n/V$	$(B_r)_n/V$	$(V_r)_n/V$	$(\phi_r^*)_n$
0	-.0426	0.0000	0.0000	0.0
1	-.0377	.0000	.0877	270.0
2	.0080	-.0046	.0092	119.7
3	.0092	-.0045	.0103	116.2
4	.0063	-.0039	.0074	121.7
5	.0052	-.0031	.0060	120.8
6	.0042	-.0020	.0047	115.3
7	.0030	-.0012	.0032	112.6
8	.0021	-.0012	.0024	120.9
9	.0017	-.0011	.0020	123.0
10	.0014	-.0010	.0017	127.2

r/R = 0.8

n	$(A_r)_n/V$	$(B_r)_n/V$	$(V_r)_n/V$	$(\phi_r^*)_n$
0	-.0463	0.0000	0.0000	0.0
1	-.0954	.0023	.0954	271.4
2	.0056	-.0022	.0060	112.0
3	.0070	-.0030	.0076	113.4
4	.0043	-.0031	.0053	126.4
5	.0033	-.0029	.0044	131.1
6	.0025	-.0018	.0031	125.4
7	.0020	-.0011	.0023	117.9
8	.0018	-.0013	.0022	125.1
9	.0013	-.0011	.0017	128.6
10	.0010	-.0010	.0014	133.9

TABLE 10G (Continued)

$r/R = 0.9$

n	$(A_r)_n/V$	$(B_r)_n/V$	$(V_r)_n/V$	$(\phi_r^*)_n$
0	-.0456	0.0000	0.0000	0.0
1	-.0990	.0043	.0991	272.5
2	.0043	-.0004	.0043	95.0
3	.0060	-.0020	.0063	108.9
4	.0037	-.0029	.0047	128.8
5	.0026	-.0028	.0038	136.7
6	.0022	-.0017	.0028	126.6
7	.0022	-.0011	.0025	116.7
8	.0021	-.0013	.0025	121.9
9	.0015	-.0010	.0018	125.2
10	.0009	-.0008	.0012	134.9

$r/R = 1.0$

n	$(A_r)_n/V$	$(B_r)_n/V$	$(V_r)_n/V$	$(\phi_r^*)_n$
0	-.0402	0.0000	0.0000	0.0
1	-.0984	.0060	.0986	273.5
2	.0043	.0010	.0044	76.5
3	.0062	-.0016	.0064	104.8
4	.0044	-.0032	.0054	126.2
5	.0030	-.0026	.0040	131.4
6	.0032	-.0015	.0035	114.6
7	.0037	-.0015	.0040	111.4
8	.0033	-.0015	.0036	115.4
9	.0021	-.0010	.0023	115.6
10	.0010	-.0008	.0013	127.9

TABLE 11 - EXPERIMENTAL LOADS FOR STEADY-AHEAD OPERATION AT V = 6.52 KNOTS, n = 14.08 REVOLUTIONS PER SECOND

TABLE 11A - VARIATION OF TOTAL LOADS WITH BLADE ANGULAR POSITION (UNFILTERED)

θ (deg)	$F_x/\bar{F}_x$	$M_y/\bar{M}_y$	$F_y/\bar{F}_y$	$M_x/\lvert\bar{M}_x\rvert$	$F_z/\bar{F}_z$	$M_z/\lvert\bar{M}_z\rvert$
0	.9856	.9649	1.0357	-1.0351	1.0084	-.8358
4	.9948	.9774	1.0586	-1.0756	1.0144	-.8774
8	1.0493	1.0281	1.0523	-1.0575	1.0100	-.8992
12	1.0795	1.0588	1.0200	-1.0145	1.0062	-.8607
16	1.0515	1.0302	1.0277	-1.0475	1.0125	-.9017
20	1.0347	1.0188	1.0220	-1.0425	1.0170	-.9034
24	1.0686	1.0503	1.0021	-1.0041	1.0090	-.9260
28	1.0785	1.0560	.9780	-.9769	1.0086	-.8786
32	1.0460	1.0192	1.0000	-1.0158	1.0100	-.9070
36	1.0513	1.0197	.9865	-.9976	1.0137	-.8985
40	1.0856	1.0510	.9756	-.9676	1.0115	-.8617
44	1.0883	1.0517	.9656	-.9634	1.0156	-.8289
48	1.0681	1.0341	.9784	-.9828	1.0210	-.7922
52	1.0834	1.0494	.9834	-.9875	1.0278	-.8187
56	1.1176	1.0861	.9701	-.9629	1.0268	-.7655
60	1.1307	1.0954	.9866	-.9903	1.0256	-.7933
64	1.1489	1.1116	1.0051	-1.0238	1.0325	-.7508
68	1.1870	1.1490	1.0166	-1.0387	1.0309	-.8060
72	1.2210	1.1822	1.0043	-1.0232	1.0416	-.7574
76	1.2344	1.1964	1.0162	-1.0404	1.0341	-.7681
80	1.2521	1.2152	1.0273	-1.0719	1.0425	-.7625
84	1.2772	1.2434	1.0519	-1.0996	1.0314	-.8110
88	1.2965	1.2679	1.0430	-1.0920	1.0351	-.8076
92	1.3123	1.2842	1.0585	-1.1115	1.0324	-.7859
96	1.3349	1.3070	1.0811	-1.1592	1.0365	-.8383
100	1.3540	1.3301	1.0935	-1.1761	1.0291	-.8659
104	1.3692	1.3704	1.0898	-1.1617	1.0318	-.9058
108	1.3874	1.3557	1.1004	-1.1802	1.0399	-.8589
112	1.3959	1.3739	1.1361	-1.2459	1.0331	-.9591
116	1.4066	1.3843	1.1375	-1.2501	1.0310	-.9646
120	1.4097	1.4010	1.1278	-1.2213	1.0215	-.9978

TABLE 11A (Continued)

θ (deg)	$F_x/\bar{F}_x$	$M_y/\bar{M}_y$	$F_y/\bar{F}_y$	$M_x/\lvert\bar{M}_x\rvert$	$F_z/\bar{F}_z$	$M_z/\lvert\bar{M}_z\rvert$
120	1.4097	1.4010	1.1278	-1.2213	1.0215	-.9978
124	1.4269	1.4108	1.1201	-1.2215	1.0266	-.9475
128	1.4112	1.3996	1.1573	-1.2821	1.0190	-1.0352
132	1.4012	1.3945	1.1499	-1.2756	1.0188	-1.0439
136	1.4095	1.4051	1.1335	-1.2314	1.0144	-1.0386
140	1.4019	1.4008	1.1322	-1.2431	1.0178	-1.0298
144	1.3742	1.3795	1.1529	-1.2827	1.0164	-1.0872
148	1.3658	1.3744	1.1429	-1.2644	1.0084	-1.1202
152	1.3737	1.3830	1.1202	-1.2124	1.0106	-1.0789
156	1.3495	1.3601	1.1313	-1.2482	1.0104	-1.1120
160	1.3126	1.3277	1.1380	-1.2729	1.0044	-1.1422
164	1.3037	1.3217	1.1325	-1.2343	.9992	-1.1668
168	1.3013	1.3214	1.0916	-1.1708	1.0031	-1.1084
172	1.2624	1.2810	1.1202	-1.2207	1.0024	-1.1527
176	1.2214	1.2452	1.1119	-1.2179	.9995	-1.1864
180	1.2161	1.2407	1.0970	-1.1679	.9929	-1.1814
184	1.2018	1.2278	1.0642	-1.1254	.9948	-1.1477
188	1.1529	1.1742	1.0785	-1.1468	.9971	-1.1596
192	1.1130	1.1449	1.0766	-1.1430	.9958	-1.2143
196	1.1050	1.1352	1.0532	-1.0853	.9999	-1.1661
200	1.0777	1.1091	1.0360	-1.0666	.9874	-1.1804
204	1.0267	1.0570	1.0395	-1.0787	.9968	-1.1657
208	.9940	1.0279	1.0403	-1.0651	.9924	-1.2195
212	.9814	1.0158	1.0001	-.9952	.9959	-1.1573
216	.9471	.9784	1.0052	-1.0024	.9930	-1.1689
220	.8985	.9306	.9900	-.9928	.9847	-1.1754
224	.8735	.9051	.9879	-.9699	.9787	-1.1889
228	.8589	.8924	.9511	-.9131	.9829	-1.1635
232	.8233	.8579	.9495	-.9102	.9782	-1.1331
236	.7857	.8167	.9502	-.9188	.9779	-1.1754
240	.7657	.8005	.9365	-.8810	.9758	-1.1365

TABLE 11A (Continued)

θ (deg)	$F_x/\bar{F}_x$	$M_y/\bar{M}_y$	$F_y/\bar{F}_y$	$M_x/\lvert\bar{M}_x\rvert$	$F_z/\bar{F}_z$	$M_z/\lvert\bar{M}_z\rvert$
240	.7657	.8005	.9365	-.8810	.9758	-1.1365
244	.7466	.7799	.9129	-.8467	.9674	-1.1631
248	.7134	.7477	.9076	-.8400	.9714	-1.0897
252	.6924	.7142	.9075	-.8364	.9614	-1.1520
256	.6702	.7014	.8948	-.8117	.9673	-1.1039
260	.6546	.6845	.8893	-.7978	.9634	-1.1370
264	.6350	.6615	.8729	-.7791	.9633	-1.0784
268	.6142	.6381	.8782	-.7747	.9589	-1.1087
272	.6007	.6249	.8610	-.7553	.9688	-1.0990
276	.5907	.6124	.8597	-.7472	.9645	-1.0884
280	.5759	.5976	.8498	-.7372	.9695	-1.0731
284	.5595	.5798	.8479	-.7285	.9699	-1.0553
288	.5479	.5710	.8427	-.7286	.9631	-1.1020
292	.5456	.5663	.8295	-.7046	.9685	-1.0405
296	.5379	.5552	.8276	-.6989	.9681	-1.0547
300	.5238	.5422	.8326	-.7123	.9685	-1.0286
304	.5222	.5392	.8475	-.7331	.9675	-1.0921
308	.5367	.5496	.8292	-.7013	.9690	-1.0184
312	.5371	.5478	.8284	-.6869	.9629	-1.0181
316	.5299	.5384	.8447	-.7283	.9724	-1.0160
320	.5396	.5456	.8656	-.7537	.9711	-1.0421
324	.5754	.5729	.8677	-.7468	.9735	-.9824
328	.6022	.5931	.8840	-.7698	.9813	-.9297
332	.6340	.6151	.9380	-.8671	.9861	-.9242
336	.7109	.6834	.9601	-.8951	.9951	-.9081
340	.7859	.7652	.9674	-.8906	.9940	-.8839
344	.8169	.7860	.9680	-.9095	.9989	-.8332
348	.8325	.8071	1.0133	-.9895	1.0011	-.8797
352	.8934	.8694	1.0140	-.9939	1.0107	-.8664
356	.9376	.9277	1.0359	-.9783	1.0054	-.8597
360	.9856	.9649	1.0357	-1.0351	1.0084	-.8358

TABLE 11B - VARIATION OF TOTAL LOADS WITH BLADE ANGULAR POSITION
(RECONSTRUCTED FROM FIRST TEN HARMONICS)

θ (deg)	$F_x/\bar{F}_x$	$M_y/\bar{M}_y$	$F_y/\bar{F}_y$	$M_x/\lvert\bar{M}_x\rvert$	$F_z/\bar{F}_z$	$M_z/\lvert\bar{M}_z\rvert$	$M_{0.3}/\bar{M}_{0.3}$	$M_{0.4}/\bar{M}_{0.4}$
0	.9798	.9609	1.0412	-1.0306	1.0097	-.8621	.9604	.9177
4	1.0100	.9921	1.0442	-1.0422	1.0106	-.8685	.9940	.9653
8	1.0335	1.0159	1.0426	-1.0477	1.0111	-.8765	1.0191	1.0023
12	1.0500	1.0323	1.0367	-1.0469	1.0112	-.8860	1.0350	1.0275
16	1.0599	1.0415	1.0276	-1.0404	1.0110	-.8958	1.0420	1.0406
20	1.0642	1.0446	1.0165	-1.0295	1.0108	-.9042	1.0409	1.0427
24	1.0646	1.0431	1.0049	-1.0162	1.0106	-.9089	1.0339	1.0361
28	1.0630	1.0390	.9942	-1.0026	1.0107	-.9075	1.0237	1.0240
32	1.0615	1.0345	.9854	-.9906	1.0112	-.8986	1.0131	1.0104
36	1.0616	1.0317	.9791	-.9816	1.0122	-.8824	1.0048	.9990
40	1.0646	1.0322	.9755	-.9760	1.0139	-.8606	1.0008	.9930
44	1.0711	1.0370	.9745	-.9740	1.0163	-.8364	1.0021	.9940
48	1.0813	1.0463	.9756	-.9753	1.0193	-.8133	1.0090	1.0027
52	1.0952	1.0600	.9786	-.9794	1.0229	-.7945	1.0211	1.0183
56	1.1126	1.0776	.9832	-.9862	1.0266	-.7816	1.0377	1.0399
60	1.1333	1.0981	.9891	-.9954	1.0301	-.7746	1.0579	1.0662
64	1.1567	1.1210	.9962	-1.0070	1.0330	-.7722	1.0811	1.0962
68	1.1821	1.1452	1.0041	-1.0206	1.0351	-.7726	1.1068	1.1293
72	1.2081	1.1703	1.0126	-1.0358	1.0362	-.7742	1.1343	1.1650
76	1.2336	1.1955	1.0216	-1.0522	1.0364	-.7763	1.1631	1.2029
80	1.2574	1.2203	1.0309	-1.0692	1.0360	-.7796	1.1927	1.2425
84	1.2791	1.2444	1.0406	-1.0866	1.0352	-.7856	1.2226	1.2830
88	1.2986	1.2675	1.0509	-1.1043	1.0345	-.7959	1.2523	1.3237
92	1.3164	1.2896	1.0620	-1.1226	1.0341	-.8116	1.2815	1.3635
96	1.3335	1.3105	1.0740	-1.1416	1.0340	-.8326	1.3098	1.4017
100	1.3505	1.3302	1.0865	-1.1614	1.0341	-.8576	1.3369	1.4376
104	1.3675	1.3485	1.0990	-1.1814	1.0339	-.8846	1.3625	1.4705
108	1.3837	1.3650	1.1109	-1.2007	1.0333	-.9114	1.3859	1.5002
112	1.3980	1.3791	1.1214	-1.2181	1.0320	-.9362	1.4065	1.5261
116	1.4090	1.3902	1.1297	-1.2325	1.0298	-.9582	1.4235	1.5479
120	1.4157	1.3980	1.1357	-1.2433	1.0271	-.9775	1.4366	1.5654

TABLE 11B (Continued)

θ (deg)	$F_x/\bar{F}_x$	$M_y/\bar{M}_y$	$F_y/\bar{F}_y$	$M_x/\lvert\bar{M}_x\rvert$	$F_z/\bar{F}_z$	$M_z/\lvert\bar{M}_z\rvert$	$M_{0.3}/\bar{M}_{0.3}$	$M_{0.4}/\bar{M}_{0.4}$
120	1.4157	1.3980	1.1357	-1.2433	1.0271	-.9775	1.4366	1.5654
124	1.4175	1.4024	1.1394	-1.2503	1.0240	-.9948	1.4456	1.5786
128	1.4151	1.4036	1.1412	-1.2540	1.0211	-1.0111	1.4511	1.5878
132	1.4094	1.4022	1.1417	-1.2556	1.0185	-1.0273	1.4536	1.5937
136	1.4016	1.3988	1.1414	-1.2559	1.0164	-1.0436	1.4540	1.5968
140	1.3929	1.3940	1.1407	-1.2558	1.0147	-1.0600	1.4528	1.5977
144	1.3834	1.3877	1.1397	-1.2553	1.0134	-1.0760	1.4503	1.5964
148	1.3730	1.3799	1.1382	-1.2541	1.0120	-1.0912	1.4459	1.5925
152	1.3607	1.3701	1.1359	-1.2516	1.0104	-1.1053	1.4390	1.5851
156	1.3459	1.3577	1.1327	-1.2470	1.0084	-1.1181	1.4289	1.5733
160	1.3282	1.3426	1.1284	-1.2398	1.0060	-1.1297	1.4148	1.5564
164	1.3077	1.3247	1.1230	-1.2301	1.0035	-1.1400	1.3969	1.5341
168	1.2851	1.3045	1.1167	-1.2180	1.0011	-1.1491	1.3754	1.5068
172	1.2612	1.2826	1.1095	-1.2040	.9990	-1.1568	1.3510	1.4755
176	1.2366	1.2595	1.1017	-1.1888	.9975	-1.1632	1.3247	1.4412
180	1.2116	1.2356	1.0933	-1.1726	.9965	-1.1682	1.2969	1.4049
184	1.1858	1.2108	1.0844	-1.1557	.9959	-1.1721	1.2682	1.3673
188	1.1588	1.1849	1.0751	-1.1382	.9958	-1.1752	1.2383	1.3284
192	1.1299	1.1576	1.0655	-1.1200	.9958	-1.1777	1.2072	1.2880
196	1.0991	1.1286	1.0557	-1.1014	.9957	-1.1798	1.1746	1.2457
200	1.0668	1.0981	1.0458	-1.0823	.9953	-1.1814	1.1405	1.2014
204	1.0339	1.0665	1.0357	-1.0630	.9946	-1.1823	1.1053	1.1552
208	1.0013	1.0346	1.0254	-1.0434	.9934	-1.1821	1.0693	1.1078
212	.9697	1.0030	1.0147	-1.0234	.9918	-1.1806	1.0331	1.0599
216	.9392	.9721	1.0032	-1.0028	.9896	-1.1778	.9972	1.0124
220	.9097	.9419	.9909	-.9816	.9872	-1.1739	.9617	.9657
224	.8806	.9125	.9780	-.9597	.9844	-1.1692	.9267	.9202
228	.8513	.8835	.9649	-.9376	.9815	-1.1641	.8922	.8757
232	.8218	.8547	.9521	-.9159	.9786	-1.1588	.8583	.8320
236	.7927	.8262	.9403	-.8954	.9758	-1.1530	.8251	.7891
240	.7646	.7983	.9296	-.8764	.9731	-1.1468	.7930	.7471

TABLE 11B (Continued)

θ (deg)	$F_x/\bar{F}_x$	$M_y/\bar{M}_y$	$F_y/\bar{F}_y$	$M_x/\lvert\bar{M}_x\rvert$	$F_z/\bar{F}_z$	$M_z/\lvert\bar{M}_z\rvert$	$M_{0.3}/\bar{M}_{0.3}$	$M_{0.4}/\bar{M}_{0.4}$
240	.7646	.7983	.9296	-.8764	.9731	-1.1468	.7930	.7471
244	.7383	.7716	.9202	-.8593	.9705	-1.1398	.7621	.7062
248	.7145	.7465	.9118	-.8436	.9682	-1.1323	.7328	.6666
252	.6930	.7231	.9039	-.8288	.9662	-1.1246	.7050	.6287
256	.6732	.7013	.8960	-.8141	.9646	-1.1172	.6784	.5924
260	.6545	.6808	.8878	-.7992	.9636	-1.1106	.6529	.5578
264	.6361	.6613	.8795	-.7841	.9631	-1.1049	.6284	.5251
268	.6180	.6427	.8712	-.7693	.9634	-1.0997	.6052	.4944
272	.6006	.6250	.8634	-.7559	.9643	-1.0944	.5838	.4664
276	.5847	.6087	.8566	-.7445	.9655	-1.0883	.5648	.4415
280	.5712	.5942	.8508	-.7355	.9669	-1.0810	.5487	.4203
284	.5603	.5820	.8458	-.7285	.9681	-1.0728	.5354	.4028
288	.5519	.5720	.8415	-.7229	.9687	-1.0646	.5247	.3885
292	.5450	.5638	.8375	-.7177	.9687	-1.0574	.5155	.3764
296	.5388	.5566	.8338	-.7125	.9682	-1.0522	.5071	.3653
300	.5328	.5500	.8309	-.7075	.9673	-1.0489	.4989	.3544
304	.5272	.5440	.8296	-.7039	.9666	-1.0465	.4914	.3437
308	.5236	.5393	.8310	-.7035	.9664	-1.0431	.4859	.3347
312	.5243	.5376	.8360	-.7085	.9672	-1.0362	.4845	.3296
316	.5317	.5408	.8455	-.7204	.9691	-1.0237	.4898	.3317
320	.5480	.5511	.8595	-.7400	.9722	-1.0048	.5038	.3439
324	.5742	.5701	.8775	-.7665	.9762	-.9802	.5280	.3685
328	.6100	.5984	.8985	-.7984	.9810	-.9521	.5622	.4065
332	.6536	.6355	.9213	-.8334	.9860	-.9238	.6054	.4569
336	.7026	.6798	.9444	-.8693	.9910	-.8985	.6555	.5175
340	.7542	.7289	.9669	-.9041	.9957	-.8785	.7097	.5852
344	.8058	.7803	.9878	-.9365	.9998	-.8651	.7654	.6566
348	.8555	.8311	1.0063	-.9658	1.0033	-.8580	.8202	.7281
352	.9017	.8793	1.0218	-.9916	1.0061	-.8560	.8720	.7971
356	.9434	.9230	1.0336	-1.0134	1.0082	-.8577	.9192	.8610
360	.9798	.9609	1.0412	-1.0306	1.0097	-.8621	.9604	.9177

TABLE 11C - VARIATION OF HYDRODYNAMIC LOADS WITH BLADE ANGULAR POSITION
(RECONSTRUCTED FROM FIRST TEN HARMONICS)

θ	$\frac{F_{x_H}}{\bar{F}_{x_H}}$	$\frac{M_{y_H}}{\bar{M}_{y_H}}$	$\frac{F_{y_H}}{\bar{F}_{y_H}}$	$\frac{M_{x_H}}{\lvert\bar{M}_{x_H}\rvert}$	$\frac{F_{z_H}}{\lvert\bar{F}_{z_H}\rvert}$	$\frac{M_{z_H}}{\lvert\bar{M}_{z_H}\rvert}$	$\frac{M_{0.3_H}}{\bar{M}_{0.3_H}}$	$\frac{M_{0.4_H}}{\bar{M}_{0.4_H}}$
0	.9793	.9591	1.0929	-1.0268	4.1503	-.7728	.9598	.9359
4	1.0103	.9917	1.1115	-1.0458	4.3625	-.7833	.9868	.9640
8	1.0344	1.0167	1.1217	-1.0588	4.4951	-.7967	1.0074	.9858
12	1.0513	1.0338	1.1243	-1.0654	4.5619	-.8122	1.0210	1.0007
16	1.0615	1.0435	1.1208	-1.0662	4.5792	-.8284	1.0279	1.0086
20	1.0659	1.0467	1.1134	-1.0625	4.5655	-.8423	1.0287	1.0101
24	1.0662	1.0451	1.1048	-1.0562	4.5403	-.8499	1.0250	1.0064
28	1.0646	1.0408	1.0973	-1.0495	4.5244	-.8476	1.0188	.9996
32	1.0630	1.0362	1.0926	-1.0442	4.5381	-.8330	1.0123	.9920
36	1.0632	1.0332	1.0918	-1.0415	4.6003	-.8063	1.0076	.9858
40	1.0663	1.0337	1.0952	-1.0420	4.7255	-.7704	1.0061	.9828
44	1.0729	1.0387	1.1023	-1.0457	4.9197	-.7305	1.0087	.9841
48	1.0834	1.0485	1.1126	-1.0523	5.1765	-.6926	1.0154	.9898
52	1.0976	1.0629	1.1254	-1.0615	5.4745	-.6615	1.0261	.9998
56	1.1155	1.0813	1.1402	-1.0728	5.7775	-.6402	1.0401	1.0134
60	1.1367	1.1028	1.1566	-1.0862	6.0400	-.6287	1.0568	1.0298
64	1.1608	1.1267	1.1741	-1.1014	6.2159	-.6248	1.0758	1.0484
68	1.1868	1.1521	1.1922	-1.1182	6.2699	-.6255	1.0965	1.0689
72	1.2135	1.1784	1.2106	-1.1362	6.1871	-.6280	1.1185	1.0909
76	1.2396	1.2048	1.2287	-1.1549	5.9778	-.6316	1.1415	1.1143
80	1.2641	1.2308	1.2466	-1.1736	5.6749	-.6371	1.1650	1.1387
84	1.2863	1.2560	1.2643	-1.1922	5.3245	-.6469	1.1886	1.1637
88	1.3063	1.2802	1.2821	-1.2106	4.9714	-.6639	1.2120	1.1888
92	1.3246	1.3033	1.3003	-1.2291	4.6452	-.6897	1.2348	1.2134
96	1.3422	1.3252	1.3191	-1.2478	4.3511	-.7242	1.2569	1.2371
100	1.3596	1.3459	1.3379	-1.2667	4.0693	-.7654	1.2780	1.2593
104	1.3769	1.3651	1.3560	-1.2853	3.7626	-.8099	1.2979	1.2799
108	1.3936	1.3823	1.3720	-1.3027	3.3913	-.8541	1.3159	1.2985
112	1.4083	1.3971	1.3846	-1.3178	2.9276	-.8950	1.3317	1.3149
116	1.4196	1.4087	1.3927	-1.3294	2.3672	-.9312	1.3447	1.3288
120	1.4264	1.4169	1.3957	-1.3368	1.7316	-.9630	1.3546	1.3401

TABLE 11C (Continued)

θ	$\frac{F_{x_H}}{\bar{F}_{x_H}}$	$\frac{M_{y_H}}{\bar{M}_{y_H}}$	$\frac{F_{y_H}}{\bar{F}_{y_H}}$	$\frac{M_{x_H}}{\lvert\bar{M}_{x_H}\rvert}$	$\frac{F_{z_H}}{\lvert\bar{F}_{z_H}\rvert}$	$\frac{M_{z_H}}{\lvert\bar{M}_{z_H}\rvert}$	$\frac{M_{0.3_H}}{\bar{M}_{0.3_H}}$	$\frac{M_{0.4_H}}{\bar{M}_{0.4_H}}$
120	1.4264	1.4169	1.3957	-1.3368	1.7316	-.9630	1.3546	1.3401
124	1.4283	1.4215	1.3940	-1.3400	1.0617	-.9915	1.3613	1.3489
128	1.4258	1.4227	1.3882	-1.3396	.4052	-1.0184	1.3652	1.3553
132	1.4199	1.4213	1.3794	-1.3365	-.1992	-1.0450	1.3667	1.3597
136	1.4120	1.4178	1.3687	-1.3319	-.7321	-1.0719	1.3665	1.3624
140	1.4030	1.4127	1.3565	-1.3263	-1.1981	-1.0988	1.3651	1.3638
144	1.3933	1.4061	1.3433	-1.3201	-1.6215	-1.1252	1.3624	1.3638
148	1.3826	1.3980	1.3288	-1.3129	-2.0350	-1.1503	1.3583	1.3622
152	1.3700	1.3877	1.3125	-1.3041	-2.4673	-1.1735	1.3522	1.3585
156	1.3549	1.3747	1.2942	-1.2929	-2.9324	-1.1946	1.3434	1.3521
160	1.3367	1.3589	1.2736	-1.2790	-3.4248	-1.2136	1.3317	1.3426
164	1.3156	1.3401	1.2510	-1.2622	-3.9223	-1.2306	1.3169	1.3299
168	1.2924	1.3190	1.2265	-1.2430	-4.3926	-1.2456	1.2994	1.3142
172	1.2679	1.2960	1.2004	-1.2218	-4.8045	-1.2583	1.2796	1.2960
176	1.2427	1.2718	1.1732	-1.1992	-5.1355	-1.2688	1.2582	1.2759
180	1.2170	1.2468	1.1450	-1.1757	-5.3777	-1.2771	1.2357	1.2547
184	1.1906	1.2208	1.1159	-1.1513	-5.5382	-1.2835	1.2124	1.2326
188	1.1628	1.1937	1.0863	-1.1264	-5.6354	-1.2885	1.1882	1.2096
192	1.1332	1.1650	1.0564	-1.1010	-5.6944	-1.2926	1.1630	1.1857
196	1.1016	1.1347	1.0264	-1.0751	-5.7413	-1.2961	1.1367	1.1606
200	1.0685	1.1027	.9966	-1.0489	-5.7986	-1.2988	1.1092	1.1342
204	1.0348	1.0697	.9670	-1.0226	-5.8835	-1.3003	1.0808	1.1066
208	1.0013	1.0363	.9374	-.9963	-6.0059	-1.2999	1.0519	1.0782
212	.9689	1.0031	.9075	-.9698	-6.1686	-1.2974	1.0228	1.0495
216	.9377	.9707	.8768	-.9430	-6.3677	-1.2928	.9939	1.0209
220	.9074	.9392	.8455	-.9158	-6.5936	-1.2864	.9654	.9928
224	.8775	.9083	.8137	-.8883	-6.8326	-1.2787	.9373	.9653
228	.8475	.8779	.7823	-.8609	-7.0697	-1.2704	.9095	.9383
232	.8173	.8478	.7522	-.8343	-7.2911	-1.2615	.8823	.9117
236	.7873	.8179	.7244	-.8092	-7.4861	-1.2521	.8557	.8856
240	.7585	.7888	.6997	-.7861	-7.6477	-1.2417	.8299	.8600

TABLE 11C (Continued)

θ	$\frac{F_{x_H}}{\bar{F}_{x_H}}$	$\frac{M_{y_H}}{\bar{M}_{y_H}}$	$\frac{F_{y_H}}{\bar{F}_{y_H}}$	$\frac{M_{x_H}}{\lvert\bar{M}_{x_H}\rvert}$	$\frac{F_{z_H}}{\lvert\bar{F}_{z_H}\rvert}$	$\frac{M_{z_H}}{\lvert\bar{M}_{z_H}\rvert}$	$\frac{M_{0.3_H}}{\bar{M}_{0.3_H}}$	$\frac{M_{0.4_H}}{\bar{M}_{0.4_H}}$
240	.7585	.7888	.6997	-.7861	-7.6477	-1.2417	.8299	.8600
244	.7316	.7608	.6780	-.7653	-7.7712	-1.2303	.8052	.8349
248	.7071	.7345	.6590	-.7465	-7.8516	-1.2179	.7817	.8106
252	.6851	.7099	.6417	-.7289	-7.8805	-1.2052	.7594	.7872
256	.6648	.6871	.6255	-.7120	-7.8456	-1.1931	.7381	.7647
260	.6456	.6657	.6096	-.6953	-7.7322	-1.1822	.7177	.7433
264	.6267	.6453	.5944	-.6789	-7.5279	-1.1728	.6982	.7229
268	.6082	.6257	.5802	-.6635	-7.2292	-1.1642	.6798	.7037
272	.5903	.6072	.5679	-.6498	-6.8465	-1.1555	.6628	.6861
276	.5740	.5901	.5581	-.6387	-6.4063	-1.1454	.6478	.6703
280	.5601	.5750	.5511	-.6305	-5.9476	-1.1335	.6350	.6567
284	.5490	.5622	.5465	-.6249	-5.5137	-1.1200	.6246	.6453
288	.5403	.5517	.5439	-.6211	-5.1402	-1.1064	.6161	.6357
292	.5333	.5430	.5427	-.6183	-4.8445	-1.0946	.6090	.6275
296	.5269	.5355	.5429	-.6159	-4.6192	-1.0859	.6025	.6199
300	.5207	.5287	.5453	-.6141	-4.4323	-1.0805	.5964	.6124
304	.5150	.5224	.5512	-.6143	-4.2345	-1.0766	.5908	.6052
308	.5114	.5175	.5626	-.6181	-3.9715	-1.0710	.5869	.5989
312	.5120	.5156	.5812	-.6277	-3.5980	-1.0596	.5863	.5950
316	.5196	.5190	.6083	-.6446	-3.0882	-1.0390	.5908	.5953
320	.5364	.5298	.6439	-.6694	-2.4415	-1.0079	.6020	.6017
324	.5633	.5497	.6871	-.7015	-1.6812	-.9674	.6211	.6155
328	.5999	.5793	.7361	-.7394	-.8473	-.9212	.6479	.6372
332	.6447	.6182	.7886	-.7806	.0126	-.8745	.6816	.6663
336	.6949	.6646	.8421	-.8229	.8531	-.8328	.7206	.7016
340	.7479	.7161	.8948	-.8644	1.6372	-.7999	.7629	.7411
344	.8008	.7698	.9448	-.9037	2.3393	-.7778	.8064	.7828
348	.8518	.8231	.9909	-.9401	2.9447	-.7660	.8492	.8246
352	.8992	.8736	1.0317	-.9732	3.4475	-.7628	.8899	.8651
356	.9420	.9194	1.0660	-1.0023	3.8479	-.7657	.9271	.9026
360	.9793	.9591	1.0929	-1.0268	4.1503	-.7728	.9598	.9359

TABLE 11D - HARMONIC CONTENT OF TOTAL LOADS

n	$\frac{(F_x)_n}{\bar{F}_x}$	$(\phi_{Fx})_n$ (deg)	$\frac{(M_y)_n}{\bar{M}_y}$	$(\phi_{My})_n$ (deg)	$\frac{(F_y)_n}{\bar{F}_y}$	$(\phi_{Fy})_n$ (deg)	$\frac{(M_x)_n}{\lvert\bar{M}_x\rvert}$	$(\phi_{Mx})_n$ (deg)
1	.4053	115.8	.3919	120.4	.1204	123.4	.2255	-55.7
2	.0637	1.7	.0654	2.1	.0504	-13.0	.0793	169.0
3	.0508	21.0	.0505	24.5	.0325	3.3	.0475	-168.6
4	.0311	23.0	.0322	28.8	.0156	3.8	.0227	-168.2
5	.0141	11.5	.0152	25.2	.0082	-26.4	.0099	169.9
6	.0063	4.7	.0071	14.7	.0037	-27.3	.0048	153.3
7	.0007	-101.1	.0018	-4.1	.0013	52.6	.0010	-110.9
8	.0028	-124.5	.0015	-129.4	.0012	-154.1	.0028	23.7
9	.0010	-114.5	.0012	-113.3	.0007	116.7	.0014	-55.7
10	.0025	123.0	.0013	152.8	.0010	72.3	.0019	-82.4
11	.0039	119.3	.0027	114.5	.0022	69.0	.0031	-104.9
12	.0042	115.7	.0031	116.2	.0022	51.1	.0034	-119.9
13	.0030	121.3	.0023	130.4	.0019	51.4	.0024	-116.9
14	.0017	79.5	.0018	56.4	.0006	30.8	.0009	-136.8
15	.0015	57.2	.0023	52.8	.0013	-70.5	.0016	87.6
16	.0014	49.2	.0009	63.2	.0011	-53.4	.0011	148.2
17	.0009	30.9	.0012	2.0	.0012	74.8	.0023	-79.3
18	.0004	60.9	.0014	42.4	.0011	-65.0	.0015	131.2
19	.0003	103.8	.0005	134.7	.0008	-72.9	.0005	73.3
20	.0004	178.9	.0011	-101.0	.0008	-117.2	.0008	7.9
21	.0019	-112.5	.0015	-90.6	.0016	-130.8	.0025	24.1
22	.0015	-115.2	.0013	-111.9	.0013	-79.8	.0016	97.3
23	.0101	-102.1	.0113	-109.4	.0100	95.8	.0212	-93.2
24	.0013	-100.3	.0018	-72.2	.0034	-161.1	.0073	5.8
25	.0071	-87.4	.0065	-85.1	.0039	88.0	.0109	-108.5

TABLE 11D (Continued)

n	$\frac{(F_z)_n}{\overline{F}_z}$	ϕ_{Fz} (deg)	$\frac{(M_z)_n}{\overline{M}_z}$	ϕ_{Mz} (deg)	$\frac{(M_{0.3})_n}{\overline{M}_{0.3}}$	$\phi_{M0.3}$ (deg)	$\frac{(M_{0.4})_n}{\overline{M}_{0.4}}$	$\phi_{M0.4}$ (deg)
1	.0324	88.9	.1857	41.4	.4288	124.2	.5642	126.1
2	.0029	65.6	.0354	164.0	.0931	-3.1	.1173	-1.6
3	.0050	-58.2	.0263	-82.3	.0625	24.2	.0785	28.7
4	.0023	7.1	.0268	-51.1	.0364	28.7	.0473	33.6
5	.0035	-17.9	.0150	-41.9	.0166	28.2	.0230	39.1
6	.0012	-60.1	.0068	-57.4	.0074	8.4	.0097	16.1
7	.0002	80.4	.0850	-71.0	.0021	10.1	.0036	6.7
8	.0012	167.7	.0015	69.4	.0025	-154.4	.0030	-162.3
9	.0002	-83.9	.0044	126.6	.0010	-170.5	.0014	-163.5
10	.0002	28.2	.0027	141.8	.0016	143.8	.0019	168.7
11	.0011	141.9	.0019	131.2	.0029	94.8	.0030	94.5
12	.0004	-89.2	.0011	142.3	.0033	91.3	.0036	94.5
13	.0008	-47.6	.0014	-33.7	.0022	113.9	.0026	129.9
14	.0004	.5	.0016	-6.8	.0020	45.6	.0028	40.5
15	.0006	-40.4	.0023	-5.6	.0013	47.3	.0023	58.6
16	.0005	166.1	.0008	60.3	.0007	47.4	.0010	76.5
17	.0009	41.9	.0010	-64.5	.0014	71.3	.0015	68.8
18	.0010	-109.1	.0018	178.7	.0020	18.9	.0034	27.1
19	.0005	-25.8	.0005	153.3	.0008	157.1	.0015	150.0
20	.0003	-55.4	.0014	87.1	.0011	-121.7	.0016	-114.2
21	.0010	93.9	.0024	98.0	.0017	-138.9	.0015	-145.2
22	.0003	175.6	.0024	66.6	.0014	-99.5	.0014	-103.3
23	.0008	57.5	.0197	-46.4	.0066	103.2	.0077	105.1
24	.0015	123.8	.0056	63.0	.0046	-162.2	.0056	-162.8
25	.0003	-175.9	.0071	-98.1	.0054	40.0	.0085	38.5

TABLE 11E - HARMONIC CONTENT OF HYDRODYNAMIC LOADS

n	$\frac{(F_{x_H})_n}{\bar{F}_{x_H}}$	$(\phi_{Fx_H})_n$ (deg)	$\frac{(M_{y_H})_n}{\bar{M}_{y_H}}$	$(\phi_{My_H})_n$ (deg)	$\frac{(F_{y_H})_n}{\bar{F}_{y_H}}$	$(\phi_{Fy_H})_n$ (deg)	$\frac{(M_{x_H})_n}{\lvert\bar{M}_{x_H}\rvert}$	$(\phi_{Mx_H})_n$ (deg)
1	.4158	115.8	.4105	120.4	.3818	104.8	.3202	-66.0
2	.0654	1.7	.0685	2.1	.0892	-13.0	.0730	169.0
3	.0521	21.0	.0530	24.5	.0575	3.3	.0473	-168.6
4	.0319	23.0	.0337	28.8	.0276	3.8	.0227	-168.2
5	.0145	11.5	.0159	25.2	.0145	-26.4	.0098	169.9
6	.0065	4.7	.0074	14.7	.0066	-27.2	.0048	153.3
7	.0007	-101.1	.0019	-4.1	.0023	52.6	.0010	-110.9
8	.0028	-124.5	.0016	-129.4	.0020	-154.2	.0027	23.7
9	.0010	-114.5	.0012	-113.3	.0012	116.6	.0014	-55.7
10	.0025	123.0	.0014	152.8	.0017	72.3	.0019	-82.4
11	.0040	119.3	.0029	114.5	.0040	69.0	.0031	-104.9
12	.0044	115.7	.0033	116.2	.0039	51.1	.0034	-119.9
13	.0031	121.3	.0025	130.4	.0033	51.4	.0024	-116.9
14	.0018	79.5	.0019	56.4	.0010	30.8	.0009	-136.8
15	.0015	57.2	.0024	52.8	.0024	-70.5	.0016	87.6
16	.0014	49.2	.0009	63.2	.0019	-53.4	.0011	148.3
17	.0010	30.9	.0013	2.0	.0021	74.7	.0023	-79.3
18	.0005	60.9	.0015	42.4	.0019	-65.0	.0015	131.2
19	.0003	103.8	.0005	134.7	.0013	-72.9	.0005	73.3
20	.0004	178.9	.0012	-101.0	.0014	-117.2	.0008	7.8
21	.0019	-112.5	.0016	-90.6	.0029	-130.8	.0025	24.1
22	.0015	-115.2	.0013	-111.9	.0024	-79.8	.0016	97.3
23	.0103	-102.1	.0118	-109.4	.0177	95.8	.0211	-93.2
24	.0013	-100.3	.0019	-72.2	.0061	-161.1	.0073	5.8
25	.0073	-87.4	.0069	-85.1	.0069	88.0	.0109	-108.5

TABLE 11E (Continued)

n	$\frac{(F_{z_H})_n}{\bar{F}_{z_H}}$	$(\phi_{Fz_H})_n$ (deg)	$\frac{(M_{z_H})_n}{\lvert\bar{M}_{z_H}\rvert}$	$(\phi_{Mz_H})_n$ (deg)	$\frac{(M_{0.3_H})_n}{\bar{M}_{0.3_H}}$	$(\phi_{0.3_H})_n$ (deg)	$\frac{(M_{0.4_H})_n}{\bar{M}_{0.4_H}}$	$(\phi_{0.4_H})_n$ (deg)
1	6.3652	54.3	.3059	41.4	.3485	123.7	.3412	128.4
2	.3644	65.6	.0583	164.0	.0708	-3.1	.0693	-1.6
3	.6294	-58.2	.0432	-82.3	.0475	24.2	.0464	28.7
4	.2870	7.1	.0442	-51.1	.0276	28.7	.0280	33.6
5	.4368	-17.9	.0243	-41.9	.0126	28.2	.0136	39.1
6	.1550	-60.1	.0112	-57.4	.0056	8.4	.0057	16.1
7	.0244	80.4	.0083	-71.0	.0016	10.1	.0021	6.7
8	.1560	167.7	.0025	69.4	.0019	-154.4	.0017	-162.3
9	.0230	-83.9	.0072	126.6	.0007	-170.5	.0008	-163.5
10	.0295	28.2	.0045	141.8	.0012	143.8	.0011	168.7
11	.1356	141.9	.0032	131.2	.0022	94.8	.0018	94.5
12	.0519	-89.2	.0017	142.3	.0025	91.3	.0021	94.5
13	.0985	-47.6	.0023	-33.7	.0017	113.9	.0015	129.9
14	.0492	.5	.0026	-6.8	.0015	45.6	.0017	40.5
15	.0804	-40.4	.0037	-5.6	.0010	47.3	.0014	58.6
16	.0629	166.0	.0014	60.3	.0006	47.4	.0006	76.5
17	.1114	41.9	.0017	-64.5	.0010	71.3	.0009	68.8
18	.1287	-109.1	.0030	178.7	.0015	18.9	.0020	27.1
19	.0570	-25.8	.0008	153.3	.0006	157.1	.0009	150.0
20	.0383	-55.4	.0022	87.1	.0008	-121.7	.0010	-114.2
21	.1257	93.9	.0039	98.0	.0013	-138.9	.0009	-145.2
22	.0414	175.6	.0040	66.6	.0011	-99.5	.0008	-103.3
23	.1052	57.5	.0324	-46.4	.0050	103.2	.0046	105.1
24	.1932	123.8	.0091	63.0	.0035	-162.2	.0033	-162.8
25	.0387	-175.9	.0117	-98.1	.0041	40.0	.0050	38.5

TABLE 12 - EXPERIMENTAL LOADS DURING QUASI-STEADY ACCELERATION
AT V = 2.65 KNOTS, n = 10.21 REVOLUTIONS PER SECOND

TABLE 12A - VARIATION OF HYDRODYNAMIC LOADS WITH BLADE ANGULAR POSITION

θ	$\frac{F_{x_H}}{\bar{F}_{x_{H,SP}}}$	$\frac{M_{y_H}}{\bar{M}_{y_{H,SP}}}$	$\frac{F_{y_H}}{\bar{F}_{y_{H,SP}}}$	$\frac{M_{x_H}}{\lvert\bar{M}_{x_{H,SP}}\rvert}$	$\frac{F_{z_H}}{\lvert\bar{F}_{z_{H,SP}}\rvert}$	$\frac{M_{z_H}}{\lvert\bar{M}_{z_{H,SP}}\rvert}$	$\frac{M_{0.3_H}}{\bar{M}_{0.3_{H,SP}}}$	$\frac{M_{0.4_H}}{\bar{M}_{0.4_{H,SP}}}$
0	1.0884	1.1794	.9396	-.8784	6.0667	-.4534	1.0515	1.0763
4	1.1110	1.1933	.9584	-.8953	6.7041	-.4489	1.0627	1.0841
8	1.1365	1.2103	.9765	-.9118	7.2907	-.4495	1.0756	1.0937
12	1.1635	1.2313	.9925	-.9266	7.6844	-.4569	1.0909	1.1070
16	1.1899	1.2553	1.0050	-.9384	7.7998	-.4714	1.1079	1.1234
20	1.2135	1.2796	1.0131	-.9462	7.6378	-.4911	1.1247	1.1408
24	1.2322	1.3007	1.0167	-.9498	7.2833	-.5124	1.1384	1.1557
28	1.2449	1.3151	1.0165	-.9497	6.8728	-.5306	1.1466	1.1650
32	1.2511	1.3209	1.0141	-.9469	6.5451	-.5414	1.1481	1.1665
36	1.2513	1.3182	1.0110	-.9428	6.3948	-.5421	1.1432	1.1605
40	1.2465	1.3086	1.0086	-.9387	6.4456	-.5324	1.1337	1.1488
44	1.2384	1.2951	1.0078	-.9355	6.6534	-.5138	1.1221	1.1346
48	1.2286	1.2809	1.0085	-.9335	6.9330	-.4898	1.1110	1.1211
52	1.2189	1.2686	1.0105	-.9327	7.1960	-.4641	1.1021	1.1103
56	1.2104	1.2594	1.0130	-.9326	7.3837	-.4396	1.0961	1.1032
60	1.2042	1.2537	1.0155	-.9330	7.4610	-.4184	1.0926	1.0992
64	1.2009	1.2507	1.0180	-.9336	7.5085	-.4009	1.0908	1.0969
68	1.2005	1.2497	1.0206	-.9346	7.5010	-.3865	1.0899	1.0954
72	1.2029	1.2501	1.0240	-.9365	7.4831	-.3746	1.0897	1.0942
76	1.2076	1.2519	1.0286	-.9398	7.4561	-.3647	1.0907	1.0938
80	1.2140	1.2555	1.0346	-.9447	7.4013	-.3571	1.0934	1.0953
84	1.2215	1.2611	1.0420	-.9514	7.2960	-.3524	1.0986	1.0998
88	1.2295	1.2690	1.0502	-.9595	7.1339	-.3516	1.1065	1.1076
92	1.2377	1.2790	1.0584	-.9683	6.9364	-.3551	1.1168	1.1186
96	1.2462	1.2903	1.0662	-.9772	6.7478	-.3627	1.1285	1.1316
100	1.2548	1.3021	1.0730	-.9856	6.6170	-.3736	1.1405	1.1451
104	1.2638	1.3138	1.0788	-.9932	6.5717	-.3866	1.1520	1.1581
108	1.2729	1.3250	1.0840	-1.0001	6.6006	-.4004	1.1625	1.1698
112	1.2821	1.3358	1.0887	-1.0062	6.6523	-.4143	1.1722	1.1804
116	1.2911	1.3461	1.0932	-1.0120	6.6528	-.4283	1.1814	1.1905
120	1.2996	1.3562	1.0974	-1.0175	6.5362	-.4427	1.1904	1.2004

TABLE 12A (Continued)

θ	$\frac{F_{x_H}}{\bar{F}_{x_{H,SP}}}$	$\frac{M_{y_H}}{\bar{M}_{y_{H,SP}}}$	$\frac{F_{y_H}}{\bar{F}_{y_{H,SP}}}$	$\frac{M_{x_H}}{\lvert\bar{M}_{x_{H,SP}}\rvert}$	$\frac{F_{z_H}}{\lvert\bar{F}_{z_{H,SP}}\rvert}$	$\frac{M_{z_H}}{\lvert\bar{M}_{z_{H,SP}}\rvert}$	$\frac{M_{0.3_H}}{\bar{M}_{0.3_{H,SP}}}$	$\frac{M_{0.4_H}}{\bar{M}_{0.4_{H,SP}}}$
120	1.2996	1.3562	1.0974	-1.0175	6.5362	-.4427	1.1904	1.2004
124	1.3072	1.3659	1.1008	-1.0225	6.2736	-.4582	1.1993	1.2106
128	1.3138	1.3751	1.1031	-1.0269	5.8885	-.4751	1.2079	1.2207
132	1.3196	1.3832	1.1038	-1.0302	5.4493	-.4934	1.2157	1.2300
136	1.3245	1.3901	1.1028	-1.0323	5.0425	-.5125	1.2222	1.2380
140	1.3286	1.3956	1.1001	-1.0329	4.7378	-.5315	1.2270	1.2442
144	1.3322	1.3999	1.0962	-1.0321	4.5596	-.5495	1.2303	1.2486
148	1.3349	1.4032	1.0914	-1.0303	4.4788	-.5660	1.2325	1.2518
152	1.3365	1.4057	1.0861	-1.0277	4.4275	-.5807	1.2339	1.2543
156	1.3367	1.4076	1.0805	-1.0246	4.3307	-.5939	1.2349	1.2566
160	1.3355	1.4084	1.0745	-1.0212	4.1407	-.6057	1.2354	1.2585
164	1.3327	1.4078	1.0680	-1.0173	3.8589	-.6166	1.2351	1.2596
168	1.3286	1.4054	1.0607	-1.0130	3.5347	-.6266	1.2335	1.2593
172	1.3234	1.4011	1.0527	-1.0079	3.2438	-.6354	1.2302	1.2570
176	1.3174	1.3952	1.0440	-1.0019	3.0535	-.6431	1.2253	1.2528
180	1.3109	1.3883	1.0347	-.9951	2.9933	-.6494	1.2191	1.2469
184	1.3039	1.3808	1.0250	-.9874	3.0417	-.6545	1.2120	1.2402
188	1.2961	1.3732	1.0151	-.9791	3.1367	-.6587	1.2047	1.2333
192	1.2875	1.3655	1.0051	-.9704	3.2037	-.6623	1.1974	1.2267
196	1.2778	1.3575	.9947	-.9614	3.1891	-.6654	1.1901	1.2202
200	1.2671	1.3486	.9840	-.9522	3.0825	-.6680	1.1823	1.2134
204	1.2557	1.3384	.9729	-.9430	2.9203	-.6698	1.1737	1.2056
208	1.2438	1.3268	.9616	-.9338	2.7666	-.6705	1.1640	1.1964
212	1.2319	1.3141	.9502	-.9245	2.6824	-.6701	1.1534	1.1859
216	1.2200	1.3009	.9391	-.9152	2.6968	-.6687	1.1422	1.1746
220	1.2081	1.2879	.9284	-.9058	2.7924	-.6667	1.1309	1.1632
224	1.1961	1.2755	.9182	-.8965	2.9122	-.6645	1.1201	1.1524
228	1.1837	1.2636	.9085	-.8874	2.9843	-.6626	1.1099	1.1423
232	1.1709	1.2518	.8992	-.8784	2.9526	-.6610	1.1000	1.1327
236	1.1577	1.2397	.8902	-.8696	2.8005	-.6594	1.0900	1.1231
240	1.1444	1.2270	.8813	-.8612	2.5565	-.6572	1.0797	1.1130

TABLE 12A (Continued)

θ	$\frac{F_{x_H}}{\bar{F}_{x_{H,SP}}}$	$\frac{M_{y_H}}{\bar{M}_{y_{H,SP}}}$	$\frac{F_{y_H}}{\bar{F}_{y_{H,SP}}}$	$\frac{M_{x_H}}{\lvert\bar{M}_{x_{H,SP}}\rvert}$	$\frac{F_{z_H}}{\lvert\bar{F}_{z_{H,SP}}\rvert}$	$\frac{M_{z_H}}{\lvert\bar{M}_{z_{H,SP}}\rvert}$	$\frac{M_{0.3_H}}{\bar{M}_{0.3_{H,SP}}}$	$\frac{M_{0.4_H}}{\bar{M}_{0.4_{H,SP}}}$
240	1.1444	1.2270	.8813	-.8612	2.5565	-.6572	1.0797	1.1130
244	1.1313	1.2137	.8725	-.8531	2.2810	-.6541	1.0690	1.1023
248	1.1188	1.2003	.8640	-.8454	2.0412	-.6497	1.0582	1.0912
252	1.1070	1.1874	.8557	-.8379	1.8842	-.6443	1.0477	1.0803
256	1.0957	1.1756	.8479	-.8305	1.8226	-.6386	1.0379	1.0703
260	1.0848	1.1648	.8404	-.8231	1.8357	-.6333	1.0289	1.0613
264	1.0738	1.1546	.8332	-.8157	1.8855	-.6287	1.0203	1.0528
268	1.0626	1.1442	.8262	-.8083	1.9376	-.6250	1.0113	1.0439
272	1.0514	1.1326	.8195	-.8009	1.9779	-.6217	1.0013	1.0335
276	1.0403	1.1196	.8131	-.7936	2.0156	-.6179	.9900	1.0212
280	1.0300	1.1056	.8073	-.7868	2.0742	-.6129	.9776	1.0072
284	1.0206	1.0918	.8023	-.7806	2.1756	-.6062	.9652	.9928
288	1.0123	1.0795	.7983	-.7753	2.3265	-.5982	.9541	.9798
292	1.0050	1.0697	.7953	-.7708	2.5146	-.5894	.9454	.9698
296	.9983	1.0628	.7933	-.7672	2.7177	-.5808	.9394	.9633
300	.9917	1.0581	.7922	-.7645	2.9185	-.5730	.9359	.9600
304	.9854	1.0544	.7919	-.7629	3.1175	-.5659	.9336	.9582
308	.9795	1.0502	.7927	-.7624	3.3355	-.5590	.9314	.9562
312	.9747	1.0448	.7947	-.7634	3.6026	-.5513	.9284	.9526
316	.9721	1.0389	.7985	-.7660	3.9379	-.5422	.9248	.9474
320	.9724	1.0341	.8043	-.7703	4.3311	-.5315	.9219	.9421
324	.9760	1.0329	.8123	-.7763	4.7353	-.5196	.9215	.9395
328	.9829	1.0375	.8223	-.7838	5.0794	-.5078	.9257	.9423
332	.9922	1.0490	.8339	-.7925	5.2955	-.4973	.9356	.9523
336	1.0032	1.0668	.8466	-.8020	5.3513	-.4890	.9510	.9695
340	1.0149	1.0888	.8600	-.8121	5.2724	-.4828	.9703	.9918
344	1.0269	1.1120	.8740	-.8229	5.1426	-.4780	.9909	1.0158
348	1.0394	1.1335	.8886	-.8346	5.0791	-.4731	1.0103	1.0378
352	1.0531	1.1516	.9043	-.8477	5.1892	-.4672	1.0268	1.0553
356	1.0692	1.1664	.9214	-.8624	5.5272	-.4603	1.0402	1.0676
360	1.0884	1.1794	.9396	-.8784	6.0667	-.4534	1.0515	1.0763

TABLE 12B - VARIATION OF TOTAL LOADS WITH BLADE ANGULAR POSITION

θ	$\frac{F_x}{\bar{F}_{x_{SP}}}$	$\frac{M_y}{\bar{M}_{y_{SP}}}$	$\frac{F_y}{\bar{F}_{y_{SP}}}$	$\frac{M_x}{\lvert\bar{M}_{x_{SP}}\rvert}$	$\frac{F_z}{\bar{F}_{z_{SP}}}$	$\frac{M_z}{\lvert\bar{M}_{z_{SP}}\rvert}$	$\frac{M_{0.3}}{\bar{M}_{0.3_{SP}}}$	$\frac{M_{0.4}}{\bar{M}_{0.4_{SP}}}$
0	1.0726	1.1517	.7640	-.8834	.5445	-.4809	1.2216	1.4631
4	1.0947	1.1650	.7671	-.8928	.5488	-.4782	1.2344	1.4764
8	1.1195	1.1813	.7700	-.9019	.5529	-.4786	1.2493	1.4928
12	1.1458	1.2013	.7717	-.9094	.5556	-.4831	1.2675	1.5150
16	1.1716	1.2242	.7716	-.9139	.5562	-.4919	1.2878	1.5427
20	1.1945	1.2474	.7692	-.9145	.5548	-.5039	1.3078	1.5718
24	1.2128	1.2675	.7646	-.9111	.5520	-.5168	1.3237	1.5966
28	1.2252	1.2812	.7580	-.9042	.5490	-.5278	1.3324	1.6116
32	1.2313	1.2868	.7505	-.8947	.5467	-.5344	1.3323	1.6135
36	1.2314	1.2842	.7429	-.8843	.5460	-.5348	1.3238	1.6025
40	1.2267	1.2750	.7361	-.8741	.5471	-.5289	1.3092	1.5817
44	1.2188	1.2621	.7305	-.8651	.5496	-.5176	1.2920	1.5567
48	1.2093	1.2486	.7263	-.8578	.5528	-.5031	1.2754	1.5326
52	1.1998	1.2368	.7231	-.8519	.5561	-.4874	1.2617	1.5132
56	1.1916	1.2281	.7207	-.8473	.5589	-.4726	1.2519	1.4998
60	1.1855	1.2226	.7189	-.8434	.5611	-.4597	1.2455	1.4915
64	1.1823	1.2197	.7174	-.8403	.5628	-.4491	1.2414	1.4862
68	1.1819	1.2188	.7165	-.8380	.5644	-.4404	1.2387	1.4821
72	1.1843	1.2192	.7166	-.8371	.5661	-.4331	1.2369	1.4784
76	1.1889	1.2209	.7179	-.8381	.5677	-.4271	1.2367	1.4760
80	1.1951	1.2243	.7205	-.8413	.5693	-.4225	1.2390	1.4768
84	1.2023	1.2297	.7244	-.8467	.5705	-.4196	1.2447	1.4825
88	1.2101	1.2373	.7293	-.8540	.5713	-.4191	1.2540	1.4941
92	1.2182	1.2468	.7348	-.8626	.5719	-.4212	1.2666	1.5108
96	1.2264	1.2575	.7404	-.8718	.5727	-.4259	1.2812	1.5309
100	1.2349	1.2688	.7461	-.8810	.5739	-.4325	1.2964	1.5520
104	1.2436	1.2800	.7518	-.8900	.5759	-.4404	1.3110	1.5721
108	1.2525	1.2907	.7575	-.8986	.5784	-.4488	1.3245	1.5902
112	1.2615	1.3010	.7636	-.9072	.5812	-.4572	1.3370	1.6063
116	1.2702	1.3108	.7699	-.9158	.5836	-.4657	1.3490	1.6216
120	1.2785	1.3205	.7765	-.9245	.5850	-.4744	1.3609	1.6367

TABLE 12B (Continued)

θ	$\frac{F_x}{\overline{F}_{x_{SP}}}$	$\frac{M_y}{\overline{M}_{y_{SP}}}$	$\frac{F_y}{\overline{F}_{y_{SP}}}$	$\frac{M_x}{\lvert\overline{M}_{x_{SP}}\rvert}$	$\frac{F_z}{\overline{F}_{z_{SP}}}$	$\frac{M_z}{\lvert\overline{M}_{z_{SP}}\rvert}$	$\frac{M_{0.3}}{\overline{M}_{0.3_{SP}}}$	$\frac{M_{0.4}}{\overline{M}_{0.4_{SP}}}$
120	1.2785	1.3205	.7765	-.9245	.5850	-.4744	1.3609	1.6367
124	1.2859	1.3298	.7831	-.9333	.5852	-.4839	1.3729	1.6523
128	1.2924	1.3385	.7895	-.9419	.5844	-.4941	1.3846	1.6677
132	1.2980	1.3463	.7953	-.9499	.5831	-.5053	1.3953	1.6820
136	1.3027	1.3529	.8006	-.9570	.5820	-.5168	1.4045	1.6940
140	1.3068	1.3581	.8052	-.9630	.5816	-.5284	1.4117	1.7031
144	1.3102	1.3622	.8095	-.9680	.5822	-.5393	1.4170	1.7093
148	1.3129	1.3654	.8135	-.9722	.5835	-.5493	1.4209	1.7135
152	1.3144	1.3678	.8174	-.9760	.5849	-.5583	1.4239	1.7167
156	1.3147	1.3695	.8214	-.9795	.5859	-.5662	1.4265	1.7194
160	1.3135	1.3703	.8253	-.9829	.5860	-.5734	1.4286	1.7218
164	1.3108	1.3697	.8290	-.9860	.5852	-.5801	1.4297	1.7229
168	1.3067	1.3675	.8325	-.9889	.5840	-.5861	1.4292	1.7217
172	1.3017	1.3634	.8355	-.9911	.5829	-.5915	1.4266	1.7173
176	1.2959	1.3578	.8382	-.9925	.5824	-.5961	1.4219	1.7097
180	1.2896	1.3511	.8405	-.9931	.5828	-.6000	1.4156	1.6995
184	1.2827	1.3439	.8426	-.9929	.5840	-.6031	1.4082	1.6880
188	1.2751	1.3367	.8444	-.9921	.5854	-.6056	1.4006	1.6763
192	1.2667	1.3294	.8460	-.9907	.5863	-.6078	1.3930	1.6652
196	1.2572	1.3217	.8473	-.9890	.5865	-.6097	1.3854	1.6545
200	1.2468	1.3132	.8482	-.9870	.5858	-.6112	1.3772	1.6433
204	1.2357	1.3035	.8486	-.9848	.5845	-.6123	1.3680	1.6305
208	1.2241	1.2924	.8487	-.9824	.5830	-.6128	1.3574	1.6156
212	1.2125	1.2803	.8484	-.9797	.5820	-.6125	1.3455	1.5985
216	1.2009	1.2677	.8479	-.9767	.5816	-.6117	1.3328	1.5802
220	1.1893	1.2553	.8473	-.9734	.5816	-.6104	1.3201	1.5619
224	1.1776	1.2434	.8467	-.9698	.5818	-.6091	1.3079	1.5447
228	1.1655	1.2321	.8459	-.9660	.5813	-.6079	1.2964	1.5288
232	1.1530	1.2208	.8449	-.9619	.5800	-.6070	1.2853	1.5138
236	1.1402	1.2093	.8435	-.9578	.5775	-.6060	1.2741	1.4989
240	1.1272	1.1972	.8418	-.9535	.5741	-.6047	1.2623	1.4833

TABLE 12B (Continued)

θ	$\frac{F_x}{\bar{F}_{x_{SP}}}$	$\frac{M_y}{\bar{M}_{y_{SP}}}$	$\frac{F_y}{\bar{F}_{y_{SP}}}$	$\frac{M_x}{\lvert\bar{M}_{x_{SP}}\rvert}$	$\frac{F_z}{\bar{F}_{z_{SP}}}$	$\frac{M_z}{\lvert\bar{M}_{z_{SP}}\rvert}$	$\frac{M_{0.3}}{\bar{M}_{0.3_{SP}}}$	$\frac{M_{0.4}}{\bar{M}_{0.4_{SP}}}$
240	1.1272	1.1972	.8418	-.9535	.5741	-.6047	1.2623	1.4833
244	1.1145	1.1845	.8397	-.9492	.5704	-.6028	1.2499	1.4666
248	1.1023	1.1717	.8373	-.9446	.5668	-.6001	1.2373	1.4493
252	1.0907	1.1594	.8344	-.9399	.5637	-.5969	1.2250	1.4326
256	1.0798	1.1481	.8313	-.9348	.5614	-.5934	1.2135	1.4174
260	1.0691	1.1378	.8279	-.9293	.5595	-.5901	1.2030	1.4039
264	1.0584	1.1281	.8241	-.9231	.5579	-.5874	1.1928	1.3913
268	1.0475	1.1181	.8199	-.9164	.5561	-.5852	1.1821	1.3780
272	1.0365	1.1070	.8153	-.9092	.5543	-.5831	1.1698	1.3622
276	1.0257	1.0946	.8104	-.9017	.5523	-.5808	1.1557	1.3432
280	1.0156	1.0813	.8052	-.8941	.5505	-.5778	1.1401	1.3214
284	1.0065	1.0681	.8001	-.8866	.5490	-.5737	1.1243	1.2989
288	.9984	1.0563	.7950	-.8794	.5479	-.5688	1.1100	1.2787
292	.9913	1.0470	.7899	-.8725	.5470	-.5635	1.0987	1.2634
296	.9847	1.0404	.7850	-.8661	.5463	-.5583	1.0910	1.2543
300	.9784	1.0359	.7801	-.8602	.5455	-.5535	1.0862	1.2503
304	.9722	1.0323	.7753	-.8548	.5448	-.5492	1.0831	1.2491
308	.9664	1.0283	.7706	-.8501	.5443	-.5450	1.0798	1.2472
312	.9618	1.0232	.7663	-.8465	.5442	-.5404	1.0754	1.2427
316	.9592	1.0176	.7626	-.8440	.5447	-.5349	1.0700	1.2353
320	.9595	1.0130	.7598	-.8430	.5458	-.5283	1.0653	1.2278
324	.9631	1.0119	.7579	-.8433	.5470	-.5211	1.0639	1.2246
328	.9697	1.0163	.7568	-.8448	.5478	-.5140	1.0683	1.2305
332	.9789	1.0272	.7564	-.8471	.5477	-.5076	1.0802	1.2486
336	.9896	1.0442	.7565	-.8500	.5464	-.5025	1.0992	1.2787
340	1.0010	1.0653	.7568	-.8533	.5442	-.4988	1.1232	1.3173
344	1.0127	1.0874	.7572	-.8571	.5417	-.4959	1.1488	1.3587
348	1.0248	1.1079	.7580	-.8617	.5398	-.4929	1.1728	1.3966
352	1.0382	1.1252	.7593	-.8675	.5395	-.4893	1.1928	1.4268
356	1.0539	1.1392	.7613	-.8748	.5411	-.4851	1.2085	1.4481
360	1.0726	1.1517	.7640	-.8834	.5445	-.4809	1.2216	1.4631

TABLE 12C - HARMONIC CONTENT OF HYDRODYNAMIC LOADS

n	$\frac{(F_{x_H})_n}{\bar{F}_{x_{H,SP}}}$	$(\phi_{Fx_H})_n$ (deg)	$\frac{(M_{y_H})_n}{\bar{M}_{y_{H,SP}}}$	$(\phi_{My_H})_n$ (deg)	$\frac{(F_{y_H})_n}{\bar{F}_{y_{H,SP}}}$	$(\phi_{Fy_H})_n$ (deg)	$\frac{(M_{x_H})_n}{\lvert\bar{M}_{x_{H,SP}}\rvert}$	$(\phi_{Mx_H})_n$ (deg)
1	.1549	133.4	.1482	137.9	.1417	114.7	.1161	-55.0
2	.0462	44.1	.0547	39.0	.0271	18.4	.0297	-159.9
3	.0300	80.4	.0348	73.0	.0208	47.5	.0211	-125.6
4	.0143	107.9	.0135	95.8	.0085	66.2	.0081	-104.1
5	.0075	146.5	.0047	152.8	.0029	91.2	.0030	-60.8
6	.0052	-170.0	.0038	-143.6	.0024	99.3	.0022	-58.7
7	.0036	-141.9	.0037	-101.7	.0014	133.1	.0017	-48.8
8	.0023	-129.5	.0049	-92.3	.0014	138.9	.0013	-44.3
9	.0012	-130.5	.0043	-86.8	.0015	159.0	.0015	-10.5
10	.0010	164.0	.0030	-102.2	.0011	-157.9	.0006	35.1

n	$\frac{(F_{z_H})_n}{\bar{F}_{z_{H,SP}}}$	$(\phi_{Fz_H})_n$ (deg)	$\frac{(M_{z_H})_n}{\lvert\bar{M}_{z_{H,SP}}\rvert}$	$(\phi_{Mz_H})_n$ (deg)	$\frac{(M_{0.3_H})_n}{\bar{M}_{0.3_{H,SP}}}$	$(\phi_{0.3_H})_n$ (deg)	$\frac{(M_{0.4_H})_n}{\bar{M}_{0.4_{H,SP}}}$	$(\phi_{0.4_H})_n$ (deg)
1	2.6859	61.0	.1257	55.5	.1233	139.2	.1191	144.9
2	.2230	57.8	.0434	-143.5	.0469	31.5	.0513	30.9
3	.3734	-42.6	.0357	-61.8	.0304	65.6	.0329	65.1
4	.0912	143.4	.0194	-20.6	.0108	86.5	.0109	84.0
5	.1312	66.4	.0113	10.6	.0030	150.0	.0025	161.6
6	.1671	75.8	.0081	47.4	.0019	-147.5	.0020	-123.5
7	.2640	115.6	.0052	78.5	.0018	-94.3	.0024	-77.1
8	.2188	126.6	.0035	92.1	.0034	-89.6	.0046	-83.7
9	.0593	70.9	.0040	124.9	.0036	-93.5	.0049	-88.3
10	.2018	135.4	.0029	140.4	.0029	-94.8	.0040	-90.4

TABLE 12D - HARMONIC CONTENT OF TOTAL LOADS

n	$\frac{(F_x)_n}{\bar{F}_{x_{SP}}}$	$(\phi_{Fx})_n$ (deg)	$\frac{(M_y)_n}{\bar{M}_{y_{SP}}}$	$(\phi_{My})_n$ (deg)	$\frac{(F_y)_n}{\bar{F}_{y_{SP}}}$	$(\phi_{Fy})_n$ (deg)	$\frac{(M_x)_n}{\lvert\bar{M}_{x_{SP}}\rvert}$	$(\phi_{Mx})_n$ (deg)
1	.1510	133.4	.1415	137.9	.0571	-141.6	.0642	10.6
2	.0450	44.1	.0522	39.0	.0153	18.4	.0298	-159.9
3	.0292	80.4	.0332	73.0	.0118	47.5	.0212	-125.6
4	.0139	107.9	.0129	96.8	.0048	66.2	.0081	-104.1
5	.0073	146.5	.0045	152.8	.0016	91.2	.0030	-60.8
6	.0050	-170.0	.0036	-143.6	.0014	99.4	.0022	-58.7
7	.0035	-141.9	.0035	-101.7	.0008	133.2	.0017	-48.7
8	.0022	-129.5	.0046	-92.3	.0008	139.0	.0013	-44.3
9	.0012	-130.5	.0041	-86.8	.0009	159.1	.0015	-10.4
10	.0009	164.0	.0029	-102.2	.0006	-157.9	.0006	35.1

n	$\frac{(F_z)_n}{\bar{F}_{z_{SP}}}$	$(\phi_{Fz})_n$ (deg)	$\frac{(M_z)_n}{\lvert\bar{M}_{z_{SP}}\rvert}$	$(\phi_{Mz})_n$ (deg)	$\frac{(M_{0.3})_n}{\bar{M}_{0.3_{SP}}}$	$(\phi_{0.3})_n$ (deg)	$\frac{(M_{0.4})_n}{\bar{M}_{0.4_{SP}}}$	$(\phi_{0.4})_n$ (deg)
1	.0221	162.4	.0763	55.5	.1350	144.3	.1830	139.3
2	.0018	57.8	.0264	-143.5	.0617	31.5	.0868	30.9
3	.0030	-42.6	.0217	-61.8	.0401	65.6	.0556	65.1
4	.0007	143.4	.0118	-20.6	.0142	86.5	.0185	84.0
5	.0010	66.4	.0069	10.6	.0040	150.0	.0042	161.6
6	.0013	75.8	.0049	47.4	.0025	-147.5	.0034	-123.5
7	.0021	115.6	.0032	78.5	.0024	-94.3	.0041	-77.1
8	.0017	126.6	.0021	92.1	.0044	-89.6	.0078	-83.7
9	.0005	70.9	.0024	124.9	.0047	-93.5	.0083	-88.3
10	.0016	135.4	.0017	140.4	.0039	-94.8	.0068	-90.4

TABLE 13 - EXPERIMENTAL LOADS DURING QUASI-STEADY ACCELERATION AT V = 3.55 KNOTS, n = 10.96 REVOLUTIONS PER SECOND

TABLE 13A - VARIATION OF HYDRODYNAMIC LOADS WITH BLADE ANGULAR POSITION

θ	$\frac{F_{x_H}}{\bar{F}_{x_{H,SP}}}$	$\frac{M_{y_H}}{\bar{M}_{y_{H,SP}}}$	$\frac{F_{y_H}}{\bar{F}_{y_{H,SP}}}$	$\frac{M_{x_H}}{\lvert\bar{M}_{x_{H,SP}}\rvert}$	$\frac{F_{z_H}}{\lvert\bar{F}_{z_{H,SP}}\rvert}$	$\frac{M_{z_H}}{\lvert\bar{M}_{z_{H,SP}}\rvert}$	$\frac{M_{0.3_H}}{\bar{M}_{0.3_{H,SP}}}$	$\frac{M_{0.4_H}}{\bar{M}_{0.4_{H,SP}}}$
0	1.0798	1.1546	.9946	-.9280	4.1584	-.5061	1.0535	1.0696
4	1.1098	1.1763	1.0178	-.9482	4.8382	-.5051	1.0702	1.0828
8	1.1408	1.1982	1.0380	-.9660	5.4556	-.5083	1.0857	1.0949
12	1.1713	1.2211	1.0540	-.9800	5.8530	-.5167	1.1007	1.1071
16	1.1989	1.2440	1.0646	-.9891	5.9388	-.5297	1.1148	1.1197
20	1.2212	1.2645	1.0696	-.9929	5.7176	-.5451	1.1262	1.1307
24	1.2364	1.2794	1.0693	-.9917	5.2847	-.5594	1.1331	1.1378
28	1.2433	1.2861	1.0651	-.9865	4.7885	-.5687	1.1338	1.1385
32	1.2423	1.2836	1.0585	-.9788	4.3772	-.5699	1.1278	1.1319
36	1.2347	1.2728	1.0516	-.9704	4.1514	-.5615	1.1164	1.1190
40	1.2227	1.2563	1.0461	-.9630	4.1399	-.5440	1.1018	1.1023
44	1.2088	1.2380	1.0428	-.9577	4.3057	-.5201	1.0871	1.0852
48	1.1953	1.2212	1.0424	-.9550	4.5735	-.4931	1.0748	1.0709
52	1.1842	1.2084	1.0446	-.9547	4.8664	-.4668	1.0665	1.0612
56	1.1764	1.2006	1.0487	-.9566	5.1329	-.4437	1.0624	1.0562
60	1.1725	1.1972	1.0540	-.9598	5.3553	-.4249	1.0616	1.0549
64	1.1721	1.1969	1.0598	-.9637	5.5396	-.4101	1.0627	1.0555
68	1.1747	1.1984	1.0658	-.9680	5.6953	-.3982	1.0645	1.0565
72	1.1794	1.2010	1.0716	-.9723	5.8188	-.3880	1.0666	1.0575
76	1.1854	1.2045	1.0773	-.9768	5.8896	-.3787	1.0691	1.0588
80	1.1921	1.2094	1.0830	-.9814	5.8807	-.3707	1.0728	1.0616
84	1.1991	1.2160	1.0887	-.9865	5.7774	-.3650	1.0783	1.0669
88	1.2062	1.2245	1.0944	-.9921	5.5927	-.3627	1.0859	1.0750
92	1.2135	1.2346	1.1003	-.9983	5.3693	-.3650	1.0954	1.0856
96	1.2212	1.2455	1.1061	-1.0050	5.1648	-.3723	1.1060	1.0976
100	1.2294	1.2566	1.1121	-1.8123	5.0268	-.3841	1.1169	1.1099
104	1.2382	1.2674	1.1180	-1.0201	4.9687	-.3993	1.1276	1.1218
108	1.2477	1.2778	1.1239	-1.0281	4.9597	-.4169	1.1380	1.1331
112	1.2574	1.2882	1.1296	-1.0362	4.9344	-.4356	1.1484	1.1443
116	1.2671	1.2988	1.1349	-1.0442	4.8201	-.4549	1.1591	1.1561
120	1.2762	1.3097	1.1396	-1.0518	4.5690	-.4744	1.1702	1.1685

TABLE 13A (Continued)

θ	$\frac{F_{x_H}}{\bar{F}_{x_{H,SP}}}$	$\frac{M_{y_H}}{\bar{M}_{y_{H,SP}}}$	$\frac{F_{y_H}}{\bar{F}_{y_{H,SP}}}$	$\frac{M_{x_H}}{\lvert\bar{M}_{x_{H,SP}}\rvert}$	$\frac{F_{z_H}}{\lvert\bar{F}_{z_{H,SP}}\rvert}$	$\frac{M_{z_H}}{\lvert\bar{M}_{z_{H,SP}}\rvert}$	$\frac{M_{0.3_H}}{\bar{M}_{0.3_{H,SP}}}$	$\frac{M_{0.4_H}}{\bar{M}_{0.4_{H,SP}}}$
120	1.2762	1.3097	1.1396	-1.0518	4.5690	-.4744	1.1702	1.1685
124	1.2842	1.3205	1.1432	-1.0585	4.1821	-.4942	1.1812	1.1812
128	1.2909	1.3304	1.1456	-1.0639	3.7116	-.5142	1.1913	1.1933
132	1.2962	1.3385	1.1465	-1.0678	3.2413	-.5343	1.1997	1.2034
136	1.3000	1.3443	1.1457	-1.0700	2.8514	-.5541	1.2055	1.2106
140	1.3025	1.3477	1.1432	-1.0703	2.5849	-.5732	1.2088	1.2149
144	1.3038	1.3492	1.1390	-1.0688	2.4300	-.5912	1.2098	1.2168
148	1.3040	1.3495	1.1332	-1.0656	2.3261	-.6080	1.2096	1.2173
152	1.3029	1.3494	1.1259	-1.0612	2.1932	-.6235	1.2088	1.2176
156	1.3005	1.3490	1.1174	-1.0557	1.9686	-.6379	1.2079	1.2182
160	1.2968	1.3479	1.1077	-1.0495	1.6378	-.6512	1.2065	1.2186
164	1.2918	1.3453	1.0972	-1.0427	1.2428	-.6635	1.2042	1.2181
168	1.2857	1.3406	1.0862	-1.0354	.8652	-.6746	1.2002	1.2155
172	1.2786	1.3334	1.0750	-1.0277	.5917	-.6843	1.1940	1.2101
176	1.2708	1.3243	1.0636	-1.0195	.4766	-.6925	1.1858	1.2022
180	1.2622	1.3140	1.0522	-1.0106	.5186	-.6994	1.1764	1.1927
184	1.2529	1.3037	1.0407	-1.0009	.6614	-.7055	1.1667	1.1831
188	1.2426	1.2941	1.0289	-.9906	.8181	-.7110	1.1576	1.1746
192	1.2311	1.2852	1.0164	-.9797	.9077	-.7162	1.1493	1.1676
196	1.2184	1.2762	1.0033	-.9684	.8877	-.7212	1.1414	1.1614
200	1.2045	1.2661	.9896	-.9571	.7674	-.7255	1.1329	1.1547
204	1.1898	1.2538	.9755	-.9458	.5989	-.7285	1.1231	1.1463
208	1.1746	1.2389	.9613	-.9348	.4489	-.7298	1.1113	1.1353
212	1.1591	1.2219	.9474	-.9242	.3658	-.7293	1.0979	1.1219
216	1.1437	1.2041	.9341	-.9137	.3580	-.7272	1.0836	1.1073
220	1.1284	1.1868	.9216	-.9034	.3914	-.7244	1.0696	1.0930
224	1.1129	1.1711	.9098	-.8931	.4085	-.7216	1.0569	1.0803
228	1.0973	1.1571	.8987	-.8828	.3571	-.7196	1.0455	1.0696
232	1.0815	1.1441	.8879	-.8723	.2157	-.7184	1.0349	1.0599
236	1.0656	1.1308	.8772	-.8618	.0039	-.7176	1.0240	1.0498
240	1.0501	1.1160	.8666	-.8513	-.2274	-.7165	1.0116	1.0375

TABLE 13A (Continued)

θ	$\frac{F_{x_H}}{\bar{F}_{x_{H,SP}}}$	$\frac{M_{y_H}}{\bar{M}_{y_{H,SP}}}$	$\frac{F_{y_H}}{\bar{F}_{y_{H,SP}}}$	$\frac{M_{x_H}}{\lvert\bar{M}_{x_{H,SP}}\rvert}$	$\frac{F_{z_H}}{\lvert\bar{F}_{z_{H,SP}}\rvert}$	$\frac{M_{z_H}}{\lvert\bar{M}_{z_{H,SP}}\rvert}$	$\frac{M_{0.3_H}}{\bar{M}_{0.3_{H,SP}}}$	$\frac{M_{0.4_H}}{\bar{M}_{0.4_{H,SP}}}$
240	1.0501	1.1160	.8666	-.8513	-.2274	-.7165	1.0116	1.0375
244	1.0352	1.0992	.8560	-.8410	-.4204	-.7142	.9972	1.0224
248	1.0212	1.0809	.8454	-.8308	-.5361	-.7101	.9811	1.0047
252	1.0083	1.0624	.8349	-.8206	-.5703	-.7045	.9645	.9861
256	.9962	1.0453	.8246	-.8105	-.5502	-.6979	.9488	.9686
260	.9845	1.0309	.8147	-.8005	-.5165	-.6913	.9353	.9541
264	.9727	1.0192	.8053	-.7908	-.4978	-.6856	.9246	.9433
268	.9605	1.0096	.7965	-.7816	-.4939	-.6811	.9161	.9355
272	.9480	1.0006	.7886	-.7734	-.4745	-.6775	.9087	.9292
276	.9355	.9907	.7819	-.7664	-.3958	-.6741	.9010	.9221
280	.9236	.9790	.7764	-.7606	-.2268	-.6700	.8921	.9131
284	.9127	.9657	.7722	-.7560	.0289	-.6644	.8819	.9018
288	.9031	.9521	.7690	-.7524	.3277	-.6572	.8712	.8894
292	.8947	.9396	.7666	-.7492	.6020	-.6487	.8612	.8776
296	.8871	.9295	.7648	-.7462	.7905	-.6394	.8531	.8681
300	.8801	.9223	.7636	-.7434	.8701	-.6301	.8473	.8618
304	.8736	.9174	.7631	-.7411	.8727	-.6208	.8437	.8582
308	.8679	.9140	.7640	-.7400	.8768	-.6114	.8415	.8563
312	.8641	.9113	.7668	-.7407	.9762	-.6014	.8401	.8547
316	.8634	.9095	.7724	-.7442	1.2375	-.5904	.8396	.8532
320	.8669	.9098	.7813	-.7508	1.6663	-.5782	.8408	.8526
324	.8755	.9144	.7937	-.7608	2.1971	-.5654	.8455	.8553
328	.8893	.9256	.8095	-.7737	2.7156	-.5530	.8556	.8638
332	.9074	.9448	.8281	-.7892	3.1039	-.5421	.8723	.8802
336	.9288	.9716	.8489	-.8064	3.2907	-.5335	.8954	.9046
340	.9520	1.0042	.8714	-.8249	3.2857	-.5270	.9237	.9355
344	.9760	1.0394	.8950	-.8443	3.1810	-.5222	.9543	.9692
348	1.0005	1.0737	.9195	-.8644	3.1170	-.5181	.9843	1.0020
352	1.0255	1.1046	.9445	-.8854	3.2275	-.5139	1.0113	1.0303
356	1.0517	1.1313	.9698	-.9068	3.5829	-.5096	1.0343	1.0527
360	1.0798	1.1546	.9946	-.9280	4.1584	-.5061	1.0535	1.0696

TABLE 13B - VARIATION OF TOTAL LOADS WITH BLADE ANGULAR POSITION

θ	$\frac{F_x}{\bar{F}_{x_{SP}}}$	$\frac{M_y}{\bar{M}_{y_{SP}}}$	$\frac{F_y}{\bar{F}_{y_{SP}}}$	$\frac{M_x}{\lvert\bar{M}_{x_{SP}}\rvert}$	$\frac{F_z}{\bar{F}_{z_{SP}}}$	$\frac{M_z}{\lvert\bar{M}_{z_{SP}}\rvert}$	$\frac{M_{0.3}}{\bar{M}_{0.3_{SP}}}$	$\frac{M_{0.4}}{\bar{M}_{0.4_{SP}}}$
0	1.0695	1.1323	.8282	-.9329	.6093	-.5445	1.1994	1.3966
4	1.0987	1.1530	.8338	-.9457	.6140	-.5439	1.2195	1.4192
8	1.1289	1.1739	.8378	-.9560	.6183	-.5459	1.2379	1.4396
12	1.1586	1.1957	.8395	-.9626	.6211	-.5510	1.2556	1.4603
16	1.1856	1.2176	.8384	-.9645	.6215	-.5588	1.2720	1.4813
20	1.2073	1.2372	.8343	-.9611	.6196	-.5682	1.2851	1.4996
24	1.2221	1.2514	.8274	-.9528	.6161	-.5769	1.2920	1.5111
28	1.2289	1.2579	.8185	-.9407	.6124	-.5826	1.2908	1.5117
32	1.2279	1.2555	.8087	-.9264	.6095	-.5833	1.2808	1.4998
36	1.2205	1.2451	.7990	-.9117	.6082	-.5782	1.2637	1.4771
40	1.2088	1.2294	.7903	-.8982	.6088	-.5676	1.2425	1.4479
44	1.1952	1.2119	.7834	-.8871	.6109	-.5530	1.2211	1.4180
48	1.1821	1.1958	.7785	-.8790	.6141	-.5367	1.2029	1.3926
52	1.1712	1.1837	.7755	-.8737	.6176	-.5207	1.1901	1.3749
56	1.1636	1.1762	.7740	-.8710	.6210	-.5067	1.1828	1.3651
60	1.1598	1.1729	.7737	-.8700	.6242	-.4952	1.1799	1.3615
64	1.1594	1.1727	.7741	-.8702	.6272	-.4863	1.1797	1.3609
68	1.1619	1.1741	.7751	-.8712	.6301	-.4790	1.1805	1.3611
72	1.1665	1.1766	.7766	-.8728	.6328	-.4728	1.1816	1.3611
76	1.1724	1.1800	.7785	-.8749	.6353	-.4672	1.1835	1.3617
80	1.1789	1.1846	.7809	-.8778	.6372	-.4623	1.1871	1.3647
84	1.1858	1.1909	.7839	-.8816	.6384	-.4588	1.1931	1.3719
88	1.1927	1.1990	.7874	-.8864	.6391	-.4575	1.2021	1.3838
92	1.1998	1.2086	.7915	-.8924	.6395	-.4589	1.2136	1.3999
96	1.2073	1.2191	.7961	-.8994	.6401	-.4633	1.2268	1.4184
100	1.2153	1.2297	.8013	-.9075	.6413	-.4704	1.2405	1.4374
104	1.2239	1.2400	.8070	-.9166	.6431	-.4797	1.2541	1.4557
108	1.2331	1.2499	.8132	-.9265	.6454	-.4904	1.2674	1.4730
112	1.2426	1.2598	.8197	-.9370	.6476	-.5018	1.2809	1.4902
116	1.2521	1.2700	.8265	-.9478	.6490	-.5135	1.2949	1.5083
120	1.2609	1.2804	.8334	-.9586	.6493	-.5253	1.3095	1.5276

TABLE 13B (Continued)

θ	$\frac{F_x}{\overline{F}_{x_{SP}}}$	$\frac{M_y}{\overline{M}_{y_{SP}}}$	$\frac{F_y}{\overline{F}_{y_{SP}}}$	$\frac{M_x}{\lvert\overline{M}_{x_{SP}}\rvert}$	$\frac{F_z}{\overline{F}_{z_{SP}}}$	$\frac{M_z}{\lvert\overline{M}_{z_{SP}}\rvert}$	$\frac{M_{0.3}}{\overline{M}_{0.3_{SP}}}$	$\frac{M_{0.4}}{\overline{M}_{0.4_{SP}}}$
120	1.2609	1.2804	.8334	-.9586	.6493	-.5253	1.3095	1.5276
124	1.2687	1.2907	.8402	-.9691	.6485	-.5373	1.3243	1.5475
128	1.2753	1.3001	.8466	-.9788	.6470	-.5494	1.3380	1.5662
132	1.2804	1.3079	.8526	-.9873	.6455	-.5616	1.3494	1.5818
136	1.2841	1.3134	.8579	-.9945	.6446	-.5737	1.3578	1.5926
140	1.2866	1.3166	.8627	-1.0002	.6445	-.5853	1.3628	1.5985
144	1.2878	1.3180	.8667	-1.0044	.6453	-.5962	1.3652	1.6003
148	1.2880	1.3184	.8702	-1.0073	.6464	-.6064	1.3659	1.6000
152	1.2869	1.3183	.8730	-1.0092	.6472	-.6158	1.3661	1.5995
156	1.2846	1.3179	.8753	-1.0103	.6471	-.6245	1.3661	1.5994
160	1.2810	1.3168	.8771	-1.0109	.6461	-.6326	1.3658	1.5993
164	1.2761	1.3143	.8786	-1.0112	.6444	-.6401	1.3642	1.5976
168	1.2701	1.3098	.8799	-1.0111	.6427	-.6468	1.3605	1.5925
172	1.2632	1.3030	.8812	-1.0107	.6417	-.6527	1.3541	1.5828
176	1.2556	1.2943	.8823	-1.0098	.6419	-.6577	1.3451	1.5690
180	1.2473	1.2845	.8835	-1.0083	.6431	-.6619	1.3346	1.5527
184	1.2382	1.2747	.8845	-1.0062	.6451	-.6656	1.3238	1.5364
188	1.2281	1.2655	.8852	-1.0033	.6469	-.6689	1.3138	1.5219
192	1.2169	1.2570	.8855	-.9998	.6481	-.6721	1.3048	1.5101
196	1.2046	1.2484	.8852	-.9958	.6482	-.6751	1.2965	1.4998
200	1.1910	1.2387	.8844	-.9916	.6474	-.6777	1.2875	1.4890
204	1.1767	1.2270	.8831	-.9873	.6460	-.6796	1.2766	1.4752
208	1.1618	1.2128	.8815	-.9831	.6446	-.6804	1.2632	1.4571
212	1.1468	1.1966	.8798	-.9791	.6436	-.6800	1.2476	1.4352
216	1.1317	1.1796	.8782	-.9749	.6430	-.6788	1.2309	1.4113
220	1.1168	1.1631	.8765	-.9707	.6425	-.6771	1.2146	1.3881
224	1.1017	1.1481	.8750	-.9661	.6418	-.6754	1.1999	1.3677
228	1.0865	1.1347	.8733	-.9610	.6404	-.6741	1.1869	1.3506
232	1.0711	1.1223	.8715	-.9555	.6382	-.6734	1.1748	1.3355
236	1.0556	1.1096	.8693	-.9496	.6352	-.6729	1.1623	1.3197
240	1.0405	1.0954	.8666	-.9433	.6319	-.6723	1.1478	1.3004

TABLE 13 (Continued)

θ	$\frac{F_x}{\bar{F}_{x_{SP}}}$	$\frac{M_y}{\bar{M}_{y_{SP}}}$	$\frac{F_y}{\bar{F}_{y_{SP}}}$	$\frac{M_x}{\lvert\bar{M}_{x_{SP}}\rvert}$	$\frac{F_z}{\bar{F}_{z_{SP}}}$	$\frac{M_z}{\lvert\bar{M}_{z_{SP}}\rvert}$	$\frac{M_{0.3}}{\bar{M}_{0.3_{SP}}}$	$\frac{M_{0.4}}{\bar{M}_{0.4_{SP}}}$
240	1.0405	1.0954	.8666	-.9433	.6319	-.6723	1.1478	1.3004
244	1.0259	1.0794	.8635	-.9367	.6289	-.6708	1.1306	1.2763
248	1.0124	1.0619	.8598	-.9297	.6263	-.6684	1.1110	1.2479
252	.9998	1.0443	.8557	-.9223	.6242	-.6650	1.0906	1.2180
256	.9880	1.0280	.8512	-.9144	.6225	-.6610	1.0714	1.1901
260	.9765	1.0142	.8464	-.9062	.6208	-.6570	1.0550	1.1673
264	.9650	1.0031	.8413	-.8978	.6189	-.6535	1.0420	1.1508
268	.9531	.9939	.8361	-.8894	.6168	-.6508	1.0319	1.1395
272	.9409	.9853	.8309	-.8814	.6148	-.6486	1.0231	1.1305
276	.9288	.9758	.8258	-.8740	.6131	-.6465	1.0137	1.1205
280	.9172	.9646	.8208	-.8675	.6122	-.6440	1.0027	1.1070
284	.9066	.9520	.8161	-.8616	.6119	-.6406	.9898	1.0897
288	.8972	.9390	.8114	-.8561	.6120	-.6363	.9761	1.0705
292	.8890	.9270	.8067	-.8506	.6118	-.6311	.9632	1.0523
296	.8816	.9174	.8019	-.8448	.6110	-.6255	.9525	1.0381
300	.8748	.9105	.7970	-.8387	.6093	-.6198	.9449	1.0291
304	.8684	.9058	.7921	-.8326	.6070	-.6142	.9399	1.0247
308	.8629	.9026	.7875	-.8273	.6047	-.6085	.9366	1.0230
312	.8592	.9000	.7836	-.8234	.6033	-.6024	.9343	1.0219
316	.8584	.8983	.7809	-.8218	.6032	-.5957	.9330	1.0208
320	.8619	.8986	.7798	-.8231	.6046	-.5883	.9338	1.0212
324	.8703	.9030	.7804	-.8274	.6068	-.5805	.9391	1.0271
328	.8837	.9137	.7826	-.8343	.6090	-.5730	.9513	1.0427
332	.9014	.9319	.7862	-.8435	.6103	-.5664	.9720	1.0715
336	.9222	.9576	.7909	-.8542	.6101	-.5611	1.0013	1.1139
340	.9449	.9887	.7963	-.8658	.6084	-.5572	1.0370	1.1669
344	.9683	1.0223	.8022	-.8783	.6061	-.5543	1.0758	1.2249
348	.9921	1.0551	.8085	-.8913	.6042	-.5518	1.1136	1.2809
352	1.0165	1.0846	.8151	-.9050	.6039	-.5493	1.1475	1.3295
356	1.0421	1.1101	.8218	-.9190	.6057	-.5467	1.1760	1.3678
360	1.0695	1.1323	.8282	-.9329	.6093	-.5445	1.1994	1.3966

TABLE 13C - HARMONIC CONTENT OF HYDRODYNAMIC LOADS

n	$\frac{(F_{x_H})_n}{\overline{F}_{x_{H,SP}}}$	$(\phi_{Fx_H})_n$ (deg)	$\frac{(M_{Y_H})_n}{\overline{M}_{Y_{H,SP}}}$	$(\phi_{MY_H})_n$ (deg)	$\frac{(F_{Y_H})_n}{\overline{F}_{Y_{H,SP}}}$	$(\phi_{FY_H})_n$ (deg)	$\frac{(M_{x_H})_n}{\lvert\overline{M}_{x_{H,SP}}\rvert}$	$(\phi_{Mx_H})_n$ (deg)
1	.1871	122.6	.1779	125.8	.1758	108.1	.1397	-63.0
2	.0639	38.5	.0733	34.1	.0405	18.0	.0424	-163.2
3	.0399	65.8	.0443	58.6	.0298	40.0	.0289	-136.4
4	.0186	78.6	.0194	71.5	.0119	42.5	.0101	-129.2
5	.0065	106.8	.0060	70.9	.0072	44.2	.0066	-132.5
6	.0050	158.4	.0018	-171.8	.0046	72.9	.0040	-108.8
7	.0043	-155.3	.0039	-122.1	.0013	150.9	.0020	-23.2
8	.0031	-128.1	.0036	-107.5	.0019	155.7	.0015	-14.5
9	.0018	-127.2	.0035	-67.2	.0010	173.6	.0014	-10.0
10	.0009	177.9	.0043	-96.3	.0006	167.0	.0004	-33.7

n	$\frac{(F_{z_H})_n}{\overline{F}_{z_{H,SP}}}$	$(\phi_{Fz_H})_n$ (deg)	$\frac{(M_{z_H})_n}{\lvert\overline{M}_{z_{H,SP}}\rvert}$	$(\phi_{Mz_H})_n$ (deg)	$\frac{(M_{0.3_H})_n}{\overline{M}_{0.3_{H,SP}}}$	$(\phi_{0.3_H})_n$ (deg)	$\frac{(M_{0.4_H})_n}{\overline{M}_{0.4_{H,SP}}}$	$(\phi_{0.4_H})_n$ (deg)
1	3.0057	60.9	.1463	58.5	.1453	127.9	.1376	132.9
2	.1342	84.9	.0492	-151.8	.0627	26.4	.0674	25.6
3	.4916	-46.1	.0370	-71.7	.0386	51.4	.0407	50.4
4	.1987	59.5	.0192	-32.9	.0149	64.6	.0153	64.2
5	.2210	33.8	.0078	-4.5	.0067	48.7	.0072	41.5
6	.1777	87.6	.0048	19.6	.0010	38.3	.0016	-12.5
7	.2111	123.8	.0047	52.3	.0025	-128.1	.0028	-113.4
8	.2696	143.4	.0044	67.5	.0024	-112.0	.0028	-101.4
9	.0748	130.2	.0032	130.6	.0024	-68.1	.0034	-59.5
10	.2346	114.8	.0027	136.5	.0038	-91.7	.0054	-88.9

TABLE 13D - HARMONIC CONTENT OF TOTAL LOADS

n	$\frac{(F_x)_n}{\bar{F}_{x_{SP}}}$	$(\phi_{Fx})_n$ (deg)	$\frac{(M_y)_n}{\bar{M}_{y_{SP}}}$	$(\phi_{My})_n$ (deg)	$\frac{(F_y)_n}{\bar{F}_{y_{SP}}}$	$(\phi_{Fy})_n$ (deg)	$\frac{(M_x)_n}{\lvert\bar{M}_{x_{SP}}\rvert}$	$(\phi_{Mx})_n$ (deg)
1	.1824	122.6	.1698	125.8	.0445	-161.9	.0625	-16.3
2	.0623	38.5	.0700	34.1	.0229	17.9	.0425	-163.2
3	.0389	65.8	.0423	58.6	.0168	40.0	.0290	-136.4
4	.0181	78.6	.0186	71.5	.0068	42.5	.0101	-129.2
5	.0063	106.8	.0057	70.9	.0041	44.2	.0067	-132.5
6	.0048	158.4	.0017	-171.8	.0026	72.9	.0040	-108.8
7	.0042	-155.3	.0038	-122.1	.0007	151.0	.0020	-23.2
8	.0030	-128.1	.0035	-107.5	.0011	155.8	.0015	-14.5
9	.0018	-127.2	.0034	-67.2	.0006	173.8	.0014	-9.9
10	.0009	177.9	.0041	-95.3	.0003	167.2	.0004	-33.6

n	$\frac{(F_z)_n}{\bar{F}_{z_{SP}}}$	$(\phi_{Fz})_n$ (deg)	$\frac{(M_z)_n}{\lvert\bar{M}_{z_{SP}}\rvert}$	$(\phi_{Mz})_n$ (deg)	$\frac{(M_{0.3})_n}{\bar{M}_{0.3_{SP}}}$	$(\phi_{0.3})_n$ (deg)	$\frac{(M_{0.4})_n}{\bar{M}_{0.4_{SP}}}$	$(\phi_{0.4})_n$ (deg)
1	.0217	155.8	.0888	58.5	.1618	130.1	.2185	127.3
2	.0011	85.0	.0299	-151.8	.0825	26.4	.1140	25.6
3	.0039	-46.1	.0225	-71.7	.0509	51.4	.0690	50.4
4	.0016	59.5	.0116	-32.9	.0196	64.6	.0259	64.2
5	.0018	33.8	.0047	-4.5	.0088	48.7	.0123	41.5
6	.0014	87.6	.0029	19.6	.0013	38.3	.0028	-12.5
7	.0017	123.8	.0028	52.3	.0032	-128.1	.0047	-113.4
8	.0022	143.4	.0027	67.5	.0031	-112.0	.0047	-101.4
9	.0006	130.2	.0019	130.6	.0032	-68.1	.0058	-59.5
10	.0019	114.8	.0016	136.5	.0051	-91.7	.0091	-88.9

TABLE 14 - EXPERIMENTAL LOADS DURING QUASI-STEADY ACCELERATION
AT V = 5.36 KNOTS, n = 12.70 REVOLUTIONS PER SECOND

TABLE 14A - VARIATION OF HYDRODYNAMIC LOADS WITH BLADE ANGULAR POSITION

θ	$\frac{F_{x_H}}{\bar{F}_{x_{H,SP}}}$	$\frac{M_{y_H}}{\bar{M}_{y_{H,SP}}}$	$\frac{F_{y_H}}{\bar{F}_{y_{H,SP}}}$	$\frac{M_{x_H}}{\lvert\bar{M}_{x_{H,SP}}\rvert}$	$\frac{F_{z_H}}{\lvert\bar{F}_{z_{H,SP}}\rvert}$	$\frac{M_{z_H}}{\lvert\bar{M}_{z_{H,SP}}\rvert}$	$\frac{M_{0.3_H}}{\bar{M}_{0.3_{H,SP}}}$	$\frac{M_{0.4_H}}{\bar{M}_{0.4_{H,SP}}}$
0	1.0130	1.0539	1.0619	-1.0040	7.4278	-.6839	1.0260	1.0278
4	1.0504	1.0776	1.0824	-1.0226	8.1402	-.6873	1.0413	1.0381
8	1.0853	1.0952	1.0974	-1.0360	8.9631	-.6901	1.0496	1.0404
12	1.1165	1.1098	1.1066	-1.0437	9.6833	-.6927	1.0538	1.0389
16	1.1422	1.1227	1.1102	-1.0456	10.1350	-.6955	1.0559	1.0368
20	1.1603	1.1336	1.1085	-1.0422	10.2579	-.6981	1.0566	1.0351
24	1.1694	1.1406	1.1023	-1.0345	10.1100	-.6987	1.0553	1.0331
28	1.1693	1.1414	1.0935	-1.0244	9.8345	-.6952	1.0509	1.0290
32	1.1614	1.1350	1.0838	-1.0136	9.5963	-.6853	1.0427	1.0212
36	1.1483	1.1222	1.0752	-1.0042	9.5157	-.6681	1.0312	1.0095
40	1.1336	1.1056	1.0695	-.9973	9.6280	-.6438	1.0181	.9952
44	1.1208	1.0891	1.0674	-.9939	9.8822	-.6148	1.0059	.9811
48	1.1125	1.0769	1.0691	-.9938	10.1749	-.5843	.9972	.9704
52	1.1101	1.0717	1.0742	-.9968	10.4032	-.5558	.9940	.9655
56	1.1137	1.0742	1.0815	-1.0020	10.5102	-.5321	.9966	.9672
60	1.1224	1.0833	1.0903	-1.0089	10.5035	-.5144	1.0042	.9745
64	1.1345	1.0966	1.0996	-1.0168	10.4432	-.5024	1.0149	.9855
68	1.1485	1.1114	1.1091	-1.0253	10.4045	-.4944	1.0267	.9976
72	1.1630	1.1257	1.1184	-1.0345	10.4381	-.4888	1.0384	1.0092
76	1.1773	1.1386	1.1277	-1.0440	10.5439	-.4843	1.0493	1.0198
80	1.1907	1.1506	1.1371	-1.0539	10.6720	-.4810	1.0599	1.0302
84	1.2033	1.1626	1.1465	-1.0642	10.7476	-.4803	1.0712	1.0415
88	1.2149	1.1757	1.1563	-1.0749	10.7067	-.4841	1.0840	1.0551
92	1.2258	1.1900	1.1665	-1.0862	10.5245	-.4943	1.0987	1.0712
96	1.2360	1.2053	1.1772	-1.0981	10.2245	-.5120	1.1148	1.0894
100	1.2461	1.2208	1.1883	-1.1106	9.8631	-.5369	1.1315	1.1083
104	1.2564	1.2355	1.1998	-1.1237	9.5011	-.5671	1.1477	1.1264
108	1.2671	1.2489	1.2111	-1.1367	9.1735	-.6001	1.1626	1.1426
112	1.2783	1.2609	1.2215	-1.1491	8.8764	-.6328	1.1758	1.1565
116	1.2897	1.2721	1.2302	-1.1599	8.5732	-.6630	1.1874	1.1686
120	1.3005	1.2827	1.2363	-1.1683	8.2185	-.6895	1.1977	1.1793

TABLE 14A (Continued)

θ	$\frac{F_{x_H}}{\bar{F}_{x_{H,SP}}}$	$\frac{M_{Y_H}}{\bar{M}_{Y_{H,SP}}}$	$\frac{F_{Y_H}}{\bar{F}_{Y_{H,SP}}}$	$\frac{M_{x_H}}{\lvert\bar{M}_{x_{H,SP}}\rvert}$	$\frac{F_{z_H}}{\lvert\bar{F}_{z_{H,SP}}\rvert}$	$\frac{M_{z_H}}{\lvert\bar{M}_{z_{H,SP}}\rvert}$	$\frac{M_{0.3_H}}{\bar{M}_{0.3_{H,SP}}}$	$\frac{M_{0.4_H}}{\bar{M}_{0.4_{H,SP}}}$
120	1.3005	1.2827	1.2363	-1.1683	8.2185	-.6895	1.1977	1.1793
124	1.3100	1.2929	1.2392	-1.1737	7.7858	-.7122	1.2068	1.1894
128	1.3173	1.3022	1.2388	-1.1762	7.2847	-.7320	1.2147	1.1989
132	1.3219	1.3099	1.2352	-1.1759	6.7593	-.7505	1.2211	1.2073
136	1.3236	1.3152	1.2291	-1.1736	6.2679	-.7688	1.2256	1.2140
140	1.3229	1.3175	1.2211	-1.1700	5.8546	-.7880	1.2278	1.2185
144	1.3202	1.3170	1.2119	-1.1655	5.5281	-.8083	1.2279	1.2205
148	1.3161	1.3141	1.2019	-1.1606	5.2575	-.8294	1.2263	1.2204
152	1.3109	1.3096	1.1911	-1.1550	4.9898	-.8506	1.2234	1.2190
156	1.3047	1.3042	1.1795	-1.1485	4.6779	-.8710	1.2196	1.2168
160	1.2972	1.2981	1.1669	-1.1409	4.3089	-.8897	1.2151	1.2139
164	1.2878	1.2909	1.1534	-1.1319	3.9146	-.9063	1.2096	1.2102
168	1.2765	1.2820	1.1389	-1.1216	3.5608	-.9206	1.2024	1.2048
172	1.2632	1.2707	1.1238	-1.1102	3.3180	-.9325	1.1931	1.1970
176	1.2482	1.2568	1.1082	-1.0979	3.2280	-.9426	1.1815	1.1865
180	1.2320	1.2406	1.0922	-1.0848	3.2815	-.9512	1.1678	1.1733
184	1.2151	1.2229	1.0757	-1.0710	3.4191	-.9591	1.1526	1.1584
188	1.1976	1.2046	1.0583	-1.0563	3.5548	-.9663	1.1367	1.1429
192	1.1794	1.1864	1.0398	-1.0408	3.6129	-.9730	1.1207	1.1274
196	1.1605	1.1683	1.0202	-1.0243	3.5601	-.9787	1.1048	1.1125
200	1.1405	1.1500	.9998	-1.0072	3.4187	-.9828	1.0889	1.0978
204	1.1193	1.1308	.9792	-.9897	3.2540	-.9849	1.0725	1.0828
208	1.0972	1.1104	.9591	-.9726	3.1409	-.9844	1.0553	1.0667
212	1.0745	1.0885	.9400	-.9560	3.1268	-.9816	1.0371	1.0492
216	1.0517	1.0657	.9220	-.9402	3.2063	-.9770	1.0184	1.0308
220	1.0292	1.0426	.9049	-.9251	3.3212	-.9717	.9995	1.0119
224	1.0071	1.0200	.8880	-.9102	3.3855	-.9665	.9811	.9936
228	.9851	.9983	.8709	-.8952	3.3239	-.9621	.9633	.9762
232	.9632	.9773	.8532	-.8798	3.1065	-.9587	.9462	.9598
236	.9411	.9567	.8351	-.8640	2.7636	-.9558	.9293	.9438
240	.9189	.9359	.8174	-.8483	2.3732	-.9525	.9121	.9273

TABLE 14A (Continued)

θ	$\frac{F_{x_H}}{\bar{F}_{x_{H,SP}}}$	$\frac{M_{y_H}}{\bar{M}_{y_{H,SP}}}$	$\frac{F_{y_H}}{\bar{F}_{y_{H,SP}}}$	$\frac{M_{x_H}}{\lvert\bar{M}_{x_{H,SP}}\rvert}$	$\frac{F_{z_H}}{\lvert\bar{F}_{z_{H,SP}}\rvert}$	$\frac{M_{z_H}}{\lvert\bar{M}_{z_{H,SP}}\rvert}$	$\frac{M_{0.3_H}}{\bar{M}_{0.3_{H,SP}}}$	$\frac{M_{0.4_H}}{\bar{M}_{0.4_{H,SP}}}$
240	.9189	.9359	.8174	-.8483	2.3732	-.9525	.9121	.9273
244	.8971	.9148	.8007	-.8329	2.0283	-.9481	.8944	.9100
248	.8762	.8937	.7860	-.8184	1.7991	-.9420	.8764	.8919
252	.8566	.8732	.7734	-.8050	1.7072	-.9344	.8587	.8735
256	.8385	.8542	.7627	-.7926	1.7243	-.9259	.8418	.8557
260	.8218	.8370	.7532	-.7810	1.7941	-.9174	.8263	.8394
264	.8059	.8212	.7437	-.7698	1.8660	-.9098	.8121	.8247
268	.7903	.8060	.7337	-.7588	1.9233	-.9031	.7987	.8110
272	.7749	.7905	.7229	-.7480	1.9910	-.8970	.7854	.7976
276	.7599	.7740	.7118	-.7378	2.1185	-.8907	.7716	.7833
280	.7457	.7566	.7013	-.7286	2.3476	-.8834	.7573	.7681
284	.7331	.7395	.6921	-.7206	2.6805	-.8746	.7431	.7524
288	.7224	.7240	.6850	-.7140	3.0681	-.8644	.7301	.7376
292	.7136	.7117	.6801	-.7084	3.4250	-.8538	.7193	.7253
296	.7060	.7030	.6771	-.7035	3.6688	-.8437	.7114	.7165
300	.6984	.6972	.6754	-.6992	3.7643	-.8348	.7060	.7110
304	.6903	.6925	.6748	-.6957	3.7517	-.8269	.7023	.7077
308	.6814	.6872	.6760	-.6939	3.7417	-.8190	.6989	.7047
312	.6729	.6802	.6800	-.6950	3.8760	-.8094	.6953	.7008
316	.6670	.6725	.6888	-.7007	4.2669	-.7964	.6921	.6959
320	.6664	.6669	.7040	-.7122	4.9416	-.7792	.6914	.6921
324	.6740	.6681	.7271	-.7304	5.8174	-.7581	.6963	.6934
328	.6913	.6806	.7581	-.7550	6.7211	-.7349	.7104	.7040
332	.7187	.7076	.7959	-.7849	7.4486	-.7124	.7358	.7274
336	.7548	.7494	.8385	-.8186	7.8426	-.6934	.7729	.7646
340	.7970	.8033	.8831	-.8539	7.8565	-.6802	.8194	.8133
344	.8422	.8636	.9270	-.8891	7.5780	-.6735	.8707	.8684
348	.8877	.9237	.9680	-.9226	7.2001	-.6724	.9213	.9229
352	.9317	.9774	1.0045	-.9534	6.9503	-.6752	.9661	.9702
356	.9734	1.0211	1.0359	-.9807	7.0059	-.6796	1.0013	1.0057
360	1.0130	1.0539	1.0619	-1.0040	7.4278	-.6839	1.0260	1.0278

TABLE 14B - VARIATION OF TOTAL LOADS WITH BLADE ANGULAR POSITION

θ	$\frac{F_x}{\bar{F}_{x_{SP}}}$	$\frac{M_y}{\bar{M}_{y_{SP}}}$	$\frac{F_y}{\bar{F}_{y_{SP}}}$	$\frac{M_x}{\lvert\bar{M}_{x_{SP}}\rvert}$	$\frac{F_z}{\bar{F}_{z_{SP}}}$	$\frac{M_z}{\lvert\bar{M}_{z_{SP}}\rvert}$	$\frac{M_{0.3}}{\bar{M}_{0.3_{SP}}}$	$\frac{M_{0.4}}{\bar{M}_{0.4_{SP}}}$
0	1.0088	1.0444	.9496	-1.0089	.8371	-.7310	1.1027	1.1931
4	1.0453	1.0670	.9537	-1.0201	.8420	-.7331	1.1208	1.2108
8	1.0793	1.0838	.9547	-1.0261	.8480	-.7348	1.1297	1.2148
12	1.1097	1.0977	.9527	-1.0264	.8533	-.7364	1.1333	1.2121
16	1.1348	1.1101	.9476	-1.0210	.8566	-.7381	1.1340	1.2082
20	1.1524	1.1205	.9396	-1.0103	.8574	-.7396	1.1328	1.2050
24	1.1613	1.1271	.9294	-.9956	.8563	-.7400	1.1290	1.2011
28	1.1612	1.1279	.9180	-.9785	.8543	-.7379	1.1211	1.1936
32	1.1535	1.1218	.9063	-.9612	.8528	-.7319	1.1082	1.1798
36	1.1407	1.1096	.8957	-.9453	.8527	-.7215	1.0910	1.1591
40	1.1264	1.0937	.8870	-.9324	.8542	-.7067	1.0716	1.1339
44	1.1139	1.0780	.8807	-.9232	.8571	-.6891	1.0535	1.1090
48	1.1058	1.0664	.8770	-.9178	.8604	-.6706	1.0402	1.0897
52	1.1035	1.0613	.8756	-.9157	.8634	-.6533	1.0340	1.0802
56	1.1070	1.0637	.8760	-.9164	.8655	-.6389	1.0355	1.0817
60	1.1154	1.0724	.8776	-.9190	.8669	-.6282	1.0437	1.0927
64	1.1272	1.0851	.8800	-.9232	.8680	-.6208	1.0561	1.1097
68	1.1409	1.0993	.8830	-.9286	.8693	-.6160	1.0701	1.1286
72	1.1551	1.1129	.8865	-.9349	.8714	-.6126	1.0839	1.1466
76	1.1689	1.1253	.8904	-.9421	.8741	-.6099	1.0969	1.1629
80	1.1821	1.1367	.8949	-.9503	.8771	-.6079	1.1096	1.1787
84	1.1943	1.1482	.9000	-.9593	.8797	-.6074	1.1232	1.1962
88	1.2057	1.1606	.9058	-.9693	.8815	-.6097	1.1391	1.2173
92	1.2162	1.1743	.9123	-.9804	.8823	-.6159	1.1574	1.2428
96	1.2262	1.1889	.9197	-.9926	.8821	-.6267	1.1778	1.2718
100	1.2361	1.2037	.9278	-1.0060	.8815	-.6418	1.1991	1.3019
104	1.2461	1.2177	.9366	-1.0204	.8810	-.6602	1.2199	1.3307
108	1.2565	1.2305	.9459	-1.0353	.8807	-.6802	1.2392	1.3563
112	1.2675	1.2420	.9551	-1.0500	.8807	-.7000	1.2564	1.3781
116	1.2785	1.2527	.9638	-1.0636	.8806	-.7184	1.2716	1.3967
120	1.2891	1.2628	.9715	-1.0753	.8801	-.7344	1.2852	1.4132

TABLE 14B (Continued)

θ	$\frac{F_x}{\bar{F}_{x_{SP}}}$	$\frac{M_y}{\bar{M}_{y_{SP}}}$	$\frac{F_y}{\bar{F}_{y_{SP}}}$	$\frac{M_x}{\lvert\bar{M}_{x_{SP}}\rvert}$	$\frac{F_z}{\bar{F}_{z_{SP}}}$	$\frac{M_z}{\lvert\bar{M}_{z_{SP}}\rvert}$	$\frac{M_{0.3}}{\bar{M}_{0.3_{SP}}}$	$\frac{M_{0.4}}{\bar{M}_{0.4_{SP}}}$
120	1.2891	1.2628	.9715	-1.0753	.8801	-.7344	1.2852	1.4132
124	1.2984	1.2725	.9779	-1.0846	.8789	-.7482	1.2974	1.4286
128	1.3055	1.2814	.9827	-1.0912	.8772	-.7603	1.3082	1.4430
132	1.3099	1.2888	.9861	-1.0956	.8752	-.7715	1.3171	1.4558
136	1.3116	1.2938	.9885	-1.0983	.8735	-.7826	1.3236	1.4657
140	1.3109	1.2961	.9901	-1.1000	.8723	-.7942	1.3273	1.4718
144	1.3083	1.2955	.9913	-1.1013	.8717	-.8066	1.3284	1.4739
148	1.3043	1.2927	.9924	-1.1024	.8714	-.8194	1.3273	1.4726
152	1.2993	1.2885	.9932	-1.1031	.8711	-.8323	1.3246	1.4690
156	1.2932	1.2834	.9938	-1.1033	.8703	-.8446	1.3210	1.4642
160	1.2858	1.2775	.9940	-1.1025	.8690	-.8560	1.3165	1.4586
164	1.2768	1.2707	.9938	-1.1005	.8673	-.8661	1.3107	1.4515
168	1.2657	1.2621	.9931	-1.0974	.8659	-.8747	1.3029	1.4417
172	1.2527	1.2513	.9922	-1.0933	.8651	-.8820	1.2923	1.4280
176	1.2381	1.2380	.9909	-1.0883	.8655	-.8881	1.2788	1.4097
180	1.2223	1.2226	.9895	-1.0826	.8668	-.8934	1.2626	1.3872
184	1.2058	1.2057	.9876	-1.0763	.8687	-.8981	1.2446	1.3618
188	1.1887	1.1883	.9852	-1.0690	.8704	-.9025	1.2257	1.3354
192	1.1711	1.1708	.9821	-1.0608	.8713	-.9066	1.2067	1.3094
196	1.1526	1.1536	.9781	-1.0516	.8712	-.9100	1.1878	1.2843
200	1.1331	1.1361	.9736	-1.0416	.8702	-.9125	1.1689	1.2599
204	1.1124	1.1178	.9686	-1.0312	.8688	-.9138	1.1494	1.2349
208	1.0909	1.0983	.9637	-1.0208	.8677	-.9135	1.1288	1.2082
212	1.0688	1.0774	.9590	-1.0108	.8672	-.9118	1.1071	1.1794
216	1.0466	1.0556	.9547	-1.0013	.8673	-.9090	1.0845	1.1490
220	1.0246	1.0336	.9505	-.9922	.8676	-.9058	1.0617	1.1181
224	1.0030	1.0120	.9460	-.9830	.8672	-.9026	1.0395	1.0881
228	.9817	.9913	.9410	-.9733	.8657	-.9000	1.0181	1.0599
232	.9602	.9713	.9353	-.9628	.8629	-.8979	.9975	1.0333
236	.9387	.9516	.9289	-.9516	.8589	-.8961	.9771	1.0075
240	.9171	.9317	.9221	-.9400	.8543	-.8942	.9562	.9811

TABLE 14B (Continued)

θ	$\frac{F_x}{\bar{F}_{x_{SP}}}$	$\frac{M_y}{\bar{M}_{y_{SP}}}$	$\frac{F_y}{\bar{F}_{y_{SP}}}$	$\frac{M_x}{\lvert\bar{M}_{x_{SP}}\rvert}$	$\frac{F_z}{\bar{F}_{z_{SP}}}$	$\frac{M_z}{\lvert\bar{M}_{z_{SP}}\rvert}$	$\frac{M_{0.3}}{\bar{M}_{0.3_{SP}}}$	$\frac{M_{0.4}}{\bar{M}_{0.4_{SP}}}$
240	.9171	.9317	.9221	-.9400	.8543	-.8942	.9562	.9811
244	.8958	.9116	.9156	-.9283	.8500	-.8915	.9347	.9533
248	.8754	.8914	.9096	-.9171	.8465	-.8878	.9127	.9242
252	.8563	.8719	.9043	-.9064	.8440	-.8831	.8908	.8947
256	.8387	.8537	.8996	-.8963	.8423	-.8780	.8701	.8663
260	.8224	.8373	.8950	-.8864	.8409	-.8728	.8509	.8404
264	.8069	.8222	.8899	-.8765	.8394	-.8682	.8334	.8173
268	.7918	.8077	.8840	-.8662	.8377	-.8641	.8168	.7960
272	.7767	.7929	.8771	-.8556	.8361	-.8604	.8003	.7751
276	.7620	.7772	.8695	-.8452	.8348	-.8566	.7829	.7528
280	.7482	.7606	.8617	-.8351	.8344	-.8522	.7648	.7288
284	.7359	.7442	.8542	-.8258	.8347	-.8468	.7466	.7041
288	.7255	.7294	.8473	-.8173	.8355	-.8407	.7298	.6809
292	.7169	.7177	.8412	-.8094	.8360	-.8342	.7159	.6619
296	.7095	.7094	.8357	-.8017	.8356	-.8281	.7055	.6487
300	.7022	.7038	.8305	-.7941	.8340	-.8226	.6983	.6412
304	.6942	.6994	.8255	-.7868	.8316	-.8179	.6932	.6372
308	.6856	.6943	.8211	-.7808	.8292	-.8131	.6884	.6338
312	.6773	.6876	.8179	-.7773	.8281	-.8072	.6831	.6286
316	.6715	.6802	.8170	-.7780	.8290	-.7994	.6783	.6218
320	.6710	.6749	.8195	-.7842	.8323	-.7889	.6765	.6169
324	.6783	.6761	.8261	-.7966	.8373	-.7761	.6822	.6203
328	.6952	.6880	.8369	-.8153	.8426	-.7620	.6996	.6394
332	.7219	.7137	.8514	-.8390	.8466	-.7483	.7319	.6801
336	.7571	.7537	.8684	-.8662	.8480	-.7368	.7794	.7441
340	.7982	.8051	.8863	-.8948	.8465	-.7288	.8392	.8275
344	.8423	.8627	.9037	-.9231	.8428	-.7247	.9052	.9215
348	.8866	.9201	.9193	-.9495	.8385	-.7241	.9702	1.0144
352	.9295	.9714	.9324	-.9731	.8352	-.7258	1.0274	1.0950
356	.9702	1.0131	.9425	-.9931	.8346	-.7284	1.0720	1.1555
360	1.0088	1.0444	.9496	-1.0089	.8371	-.7310	1.1027	1.1931

TABLE 14C - HARMONIC CONTENT OF HYDRODYNAMIC LOADS

n	$\frac{(F_{x_H})_n}{\bar{F}_{x_{H,SP}}}$	$(\phi_{Fx_H})_n$ (deg)	$\frac{(M_{Y_H})_n}{\bar{M}_{Y_{H,SP}}}$	$(\phi_{MY_H})_n$ (deg)	$\frac{(F_{Y_H})_n}{\bar{F}_{Y_{H,SP}}}$	$(\phi_{FY_H})_n$ (deg)	$\frac{(M_{x_H})_n}{\lvert\bar{M}_{x_{H,SP}}\rvert}$	$(\phi_{Mx_H})_n$ (deg)
1	.2868	120.6	.2710	124.0	.2491	106.2	.2022	-64.4
2	.0723	32.3	.0799	25.1	.0624	8.5	.0596	-173.1
3	.0504	51.7	.0569	44.5	.0483	23.9	.0432	-153.9
4	.0292	54.2	.0319	42.8	.0236	21.3	.0206	-154.8
5	.0156	53.7	.0168	37.6	.0121	-4.7	.0098	-172.5
6	.0053	78.5	.0064	25.4	.0061	8.6	.0058	-170.6
7	.0030	-147.0	.0041	-46.3	.0008	130.7	.0010	-44.6
8	.0044	-110.8	.0070	-69.9	.0015	-109.9	.0014	33.5
9	.0028	-118.0	.0061	-77.2	.0020	-129.3	.0009	24.6
10	.0021	-140.6	.0045	-79.8	.0017	168.0	.0013	-24.7

n	$\frac{(F_{z_H})_n}{\bar{F}_{z_{H,SP}}}$	$(\phi_{Fz_H})_n$ (deg)	$\frac{(M_{z_H})_n}{\lvert\bar{M}_{z_{H,SP}}\rvert}$	$(\phi_{Mz_H})_n$ (deg)	$\frac{(M_{0.3_H})_n}{\bar{M}_{0.3_{H,SP}}}$	$(\phi_{0.3_H})_n$ (deg)	$\frac{(M_{0.4_H})_n}{\bar{M}_{0.4_{H,SP}}}$	$(\phi_{0.4_H})_n$ (deg)
1	4.2760	58.5	.2108	52.6	.2186	126.3	.2084	131.1
2	.4528	104.1	.0597	-173.4	.0719	16.0	.0749	14.7
3	.6204	-65.8	.0374	-88.6	.0511	35.8	.0530	35.1
4	.1598	116.6	.0254	-56.1	.0269	33.5	.0280	31.4
5	.0488	69.3	.0098	-24.7	.0138	25.5	.0146	23.9
6	.1776	-167.9	.0039	-90.3	.0076	7.3	.0091	1.4
7	.2594	172.7	.0033	-72.1	.0036	-28.1	.0055	-23.8
8	.2798	137.6	.0034	72.5	.0050	-65.9	.0063	-58.5
9	.2103	146.6	.0056	159.0	.0046	-70.5	.0060	-64.4
10	.2932	129.2	.0025	159.7	.0034	-73.1	.0048	-65.7

TABLE 14D - HARMONIC CONTENT OF TOTAL LOADS

n	$\frac{(F_x)_n}{\overline{F}_{x_{SP}}}$	$(\phi_{Fx})_n$ (deg)	$\frac{(M_y)_n}{\overline{M}_{y_{SP}}}$	$(\phi_{My})_n$ (deg)	$\frac{(F_y)_n}{\overline{F}_{y_{SP}}}$	$(\phi_{Fy})_n$ (deg)	$\frac{(M_x)_n}{\lvert\overline{M}_{x_{SP}}\rvert}$	$(\phi_{Mx})_n$ (deg)
1	.2796	120.6	.2587	124.0	.0575	152.0	.1131	-42.0
2	.0704	32.3	.0763	26.1	.0353	8.4	.0598	-173.1
3	.0492	51.7	.0543	44.5	.0273	23.8	.0433	-153.9
4	.0285	54.2	.0304	42.8	.0133	21.3	.0207	-154.8
5	.0152	53.7	.0161	37.6	.0068	-4.7	.0098	-172.5
6	.0051	78.5	.0061	25.4	.0035	8.6	.0059	-170.6
7	.0029	-147.0	.0039	-46.3	.0004	130.8	.0010	-44.5
8	.0043	-110.8	.0066	-69.9	.0008	-109.9	.0014	33.6
9	.0027	-118.0	.0059	-77.2	.0011	-129.3	.0009	24.7
10	.0021	-140.6	.0043	-79.8	.0010	168.1	.0013	-24.7

n	$\frac{(F_z)_n}{\overline{F}_{z_{SP}}}$	$(\phi_{Fz})_n$ (deg)	$\frac{(M_z)_n}{\lvert\overline{M}_{z_{SP}}\rvert}$	$(\phi_{Mz})_n$ (deg)	$\frac{(M_{0.3})_n}{\overline{M}_{0.3_{SP}}}$	$(\phi_{0.3})_n$ (deg)	$\frac{(M_{0.4})_n}{\overline{M}_{0.4_{SP}}}$	$(\phi_{0.4})_n$ (deg)
1	.0218	128.6	.1280	52.6	.2580	127.5	.3386	127.4
2	.0036	104.1	.0362	-173.4	.0946	16.0	.1268	14.7
3	.0050	-65.8	.0227	-88.6	.0673	35.0	.0897	35.1
4	.0013	116.6	.0154	-56.1	.0355	3[illegible].5	.0475	31.4
5	.0004	69.3	.0060	-24.7	.0181	25.5	.0247	23.9
6	.0014	-167.9	.0024	-90.3	.0100	7.3	.0153	1.4
7	.0021	172.7	.0020	-72.1	.0047	-28.1	.0092	-23.8
8	.0022	137.6	.0021	72.5	.0066	-65.9	.0107	-58.5
9	.0017	146.6	.0034	159.0	.0060	-70.5	.0101	-64.4
10	.0023	129.3	.0015	159.7	.0044	-73.1	.0081	-65.7

TABLE 15 - EXPERIMENTAL LOADS DURING QUASI-STEADY ACCELERATION
AT V = 6.26 KNOTS, n = 13.78 REVOLUTIONS PER SECOND

TABLE 15A - VARIATION OF HYDRODYNAMIC LOADS WITH BLADE ANGULAR POSITION

θ	$\frac{F_{x_H}}{\bar{F}_{x_{H,SP}}}$	$\frac{M_{y_H}}{\bar{M}_{y_{H,SP}}}$	$\frac{F_{y_H}}{\bar{F}_{y_{H,SP}}}$	$\frac{M_{x_H}}{\lvert\bar{M}_{x_{H,SP}}\rvert}$	$\frac{F_{z_H}}{\lvert\bar{F}_{z_{H,SP}}\rvert}$	$\frac{M_{z_H}}{\lvert\bar{M}_{z_{H,SP}}\rvert}$	$\frac{M_{0.3_H}}{\bar{M}_{0.3_{H,SP}}}$	$\frac{M_{0.4_H}}{\bar{M}_{0.4_{H,SP}}}$
0	.9498	.9231	1.0833	-1.0187	4.3504	-.6973	.9349	.9084
4	.9899	.9685	1.1043	-1.0385	5.0560	-.7076	.9699	.9457
8	1.0262	1.0097	1.1179	-1.0527	5.8371	-.7222	1.0006	.9789
12	1.0573	1.0441	1.1243	-1.0610	6.5027	-.7398	1.0246	1.0051
16	1.0818	1.0691	1.1244	-1.0636	6.9013	-.7581	1.0401	1.0221
20	1.0985	1.0836	1.1198	-1.0616	6.9796	-.7741	1.0469	1.0291
24	1.1071	1.0880	1.1128	-1.0566	6.8001	-.7841	1.0459	1.0275
28	1.1082	1.0845	1.1055	-1.0504	6.5127	-.7848	1.0396	1.0200
32	1.1039	1.0765	1.1000	-1.0448	6.2942	-.7745	1.0313	1.0104
36	1.0969	1.0680	1.0976	-1.0411	6.2811	-.7533	1.0241	1.0022
40	1.0903	1.0622	1.0991	-1.0404	6.5235	-.7236	1.0202	.9979
44	1.0870	1.0610	1.1043	-1.0428	6.9758	-.6896	1.0206	.9983
48	1.0888	1.0652	1.1128	-1.0483	7.5247	-.6560	1.0252	1.0030
52	1.0965	1.0741	1.1241	-1.0564	8.0396	-.6271	1.0331	1.0106
56	1.1098	1.0865	1.1372	-1.0667	8.4219	-.6053	1.0432	1.0197
60	1.1276	1.1015	1.1518	-1.0787	8.6327	-.5909	1.0547	1.0299
64	1.1483	1.1184	1.1671	-1.0921	8.6920	-.5825	1.0678	1.0413
68	1.1704	1.1373	1.1830	-1.1065	8.6524	-.5785	1.0828	1.0551
72	1.1924	1.1582	1.1989	-1.1218	8.5642	-.5767	1.1004	1.0722
76	1.2133	1.1810	1.2149	-1.1375	8.4492	-.5769	1.1206	1.0932
80	1.2326	1.2051	1.2306	-1.1536	8.2950	-.5800	1.1429	1.1174
84	1.2501	1.2291	1.2464	-1.1700	8.0695	-.5880	1.1660	1.1431
88	1.2663	1.2516	1.2624	-1.1866	7.7467	-.6032	1.1884	1.1679
92	1.2816	1.2712	1.2786	-1.2035	7.3281	-.6267	1.2087	1.1898
96	1.2970	1.2874	1.2952	-1.2208	6.8474	-.6584	1.2260	1.2076
100	1.3130	1.3007	1.3117	-1.2383	6.3579	-.6966	1.2406	1.2214
104	1.3299	1.3125	1.3275	-1.2555	5.9067	-.7381	1.2534	1.2326
108	1.3473	1.3241	1.3416	-1.2716	5.5111	-.7798	1.2655	1.2432
112	1.3644	1.3370	1.3531	-1.2857	5.1489	-.8187	1.2783	1.2551
116	1.3798	1.3514	1.3612	-1.2970	4.7692	-.8533	1.2920	1.2693
120	1.3924	1.3669	1.3655	-1.3050	4.3179	-.8833	1.3063	1.2857

AD-A048 385 DAVID W TAYLOR NAVAL SHIP RESEARCH AND DEVELOPMENT CE--ETC F/G 13/10
EXPERIMENTAL UNSTEADY AND TIME AVERAGE LOADS ON THE BLADES OF T--ETC(U)
DEC 77 S D JESSUP, R J BOSWELL, J J NELKA
UNCLASSIFIED DTNSRDC-77-0110 NL

4 OF 4
AD
A048385

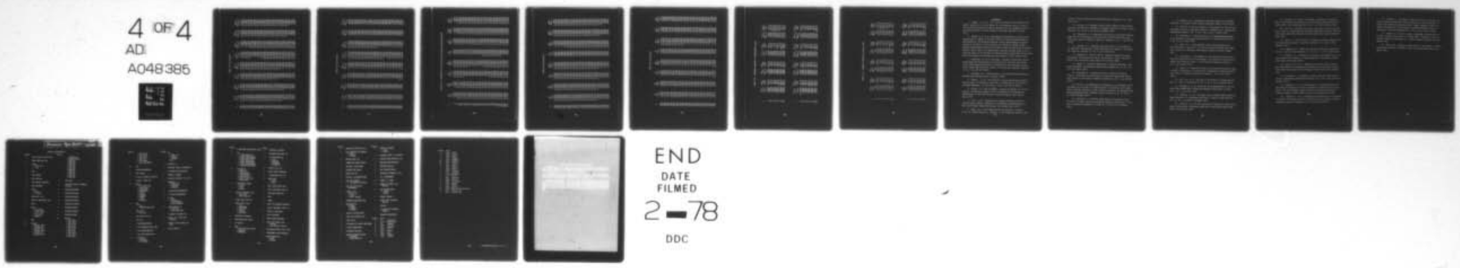

END
DATE
FILMED
2-78
DDC

TABLE 15A (Continued)

θ	$\frac{F_{x_H}}{\bar{F}_{x_{H,SP}}}$	$\frac{M_{y_H}}{\bar{M}_{y_{H,SP}}}$	$\frac{F_{y_H}}{\bar{F}_{y_{H,SP}}}$	$\frac{M_{x_H}}{\lvert\bar{M}_{x_{H,SP}}\rvert}$	$\frac{F_{z_H}}{\lvert\bar{F}_{z_{H,SP}}\rvert}$	$\frac{M_{z_H}}{\lvert\bar{M}_{z_{H,SP}}\rvert}$	$\frac{M_{0.3_H}}{\bar{M}_{0.3_{H,SP}}}$	$\frac{M_{0.4_H}}{\bar{M}_{0.4_{H,SP}}}$
120	1.3924	1.3669	1.3655	-1.3050	4.3179	-.8833	1.3063	1.2857
124	1.4011	1.3819	1.3660	-1.3094	3.7663	-.9096	1.3202	1.3029
128	1.4055	1.3947	1.3632	-1.3106	3.1290	-.9338	1.3323	1.3190
132	1.4060	1.4040	1.3576	-1.3090	2.4610	-.9572	1.3412	1.3321
136	1.4035	1.4088	1.3497	-1.3054	1.8352	-.9810	1.3464	1.3409
140	1.3989	1.4092	1.3399	-1.3003	1.3107	-1.0055	1.3478	1.3452
144	1.3931	1.4058	1.3283	-1.2940	.9066	-1.0306	1.3460	1.3455
148	1.3861	1.3996	1.3148	-1.2866	.5938	-1.0558	1.3416	1.3428
152	1.3777	1.3912	1.2994	-1.2780	.3087	-1.0803	1.3355	1.3382
156	1.3672	1.3809	1.2821	-1.2678	-.0166	-1.1034	1.3279	1.3324
160	1.3537	1.3688	1.2631	-1.2558	-.4220	-1.1243	1.3188	1.3254
164	1.3369	1.3546	1.2427	-1.2418	-.9011	-1.1425	1.3080	1.3170
168	1.3169	1.3381	1.2212	-1.2258	-1.4031	-1.1574	1.2951	1.3064
172	1.2946	1.3193	1.1986	-1.2080	-1.8564	-1.1691	1.2798	1.2933
176	1.2708	1.2985	1.1750	-1.1884	-2.2008	-1.1777	1.2621	1.2775
180	1.2463	1.2760	1.1501	-1.1672	-2.4146	-1.1839	1.2423	1.2593
184	1.2216	1.2523	1.1238	-1.1448	-2.5231	-1.1887	1.2210	1.2391
188	1.1965	1.2275	1.0963	-1.1214	-2.5854	-1.1930	1.1984	1.2175
192	1.1704	1.2017	1.0679	-1.0974	-2.6668	-1.1972	1.1751	1.1953
196	1.1427	1.1746	1.0391	-1.0732	-2.8089	-1.2014	1.1512	1.1726
200	1.1132	1.1463	1.0105	-1.0490	-3.0133	-1.2051	1.1270	1.1496
204	1.0820	1.1169	.9826	-1.0253	-3.2447	-1.2073	1.1024	1.1265
208	1.0500	1.0869	.9554	-1.0018	-3.4527	-1.2074	1.0776	1.1031
212	1.0180	1.0568	.9289	-.9786	-3.5997	-1.2048	1.0527	1.0793
216	.9870	1.0271	.9025	-.9553	-3.6819	-1.1998	1.0275	1.0551
220	.9573	.9979	.8760	-.9318	-3.7316	-1.1933	1.0023	1.0305
224	.9289	.9692	.8495	-.9083	-3.8007	-1.1861	.9770	1.0057
228	.9013	.9407	.8231	-.8850	-3.9327	-1.1792	.9517	.9807
232	.8739	.9124	.7977	-.8625	-4.1379	-1.1730	.9268	.9560
236	.8465	.8843	.7739	-.8413	-4.3847	-1.1670	.9026	.9319
240	.8192	.8568	.7522	-.8217	-4.6113	-1.1606	.8794	.9089

TABLE 15A (Continued)

θ	$\frac{F_{x_H}}{\bar{F}_{x_{H,SP}}}$	$\frac{M_{y_H}}{\bar{M}_{y_{H,SP}}}$	$\frac{F_{y_H}}{\bar{F}_{y_{H,SP}}}$	$\frac{-M_{x_H}}{\lvert\bar{M}_{x_{H,SP}}\rvert}$	$\frac{F_{z_H}}{\lvert\bar{F}_{z_{H,SP}}\rvert}$	$\frac{M_{z_H}}{\lvert\bar{M}_{z_{H,SP}}\rvert}$	$\frac{M_{0.3_H}}{\bar{M}_{0.3_{H,SP}}}$	$\frac{M_{0.4_H}}{\bar{M}_{0.4_{H,SP}}}$
240	.8192	.8568	.7522	-.8217	-4.6113	-1.1606	.8794	.9089
244	.7926	.8305	.7328	-.8036	-4.7534	-1.1529	.8576	.8873
248	.7675	.8060	.7152	-.7869	-4.7739	-1.1435	.8373	.8672
252	.7445	.7836	.6988	-.7707	-4.6798	-1.1326	.8182	.8482
256	.7236	.7630	.6828	-.7548	-4.5180	-1.1209	.7999	.8298
260	.7044	.7434	.6671	-.7388	-4.3502	-1.1094	.7817	.8113
264	.6861	.7239	.6519	-.7230	-4.2204	-1.0988	.7634	.7924
268	.6681	.7041	.6379	-.7081	-4.1304	-1.0893	.7448	.7729
272	.6500	.6838	.6262	-.6949	-4.0370	-1.0803	.7265	.7533
276	.6323	.6637	.6175	-.6843	-3.8736	-1.0709	.7093	.7346
280	.6157	.6450	.6119	-.6764	-3.5868	-1.0602	.6940	.7177
284	.6013	.6287	.6091	-.6710	-3.1704	-1.0481	.6812	.7034
288	.5896	.6156	.6080	-.6673	-2.6785	-1.0351	.6710	.6919
292	.5806	.6055	.6075	-.6643	-2.2087	-1.0226	.6630	.6827
296	.5736	.5976	.6070	-.6614	-1.8605	-1.0116	.6563	.6750
300	.5675	.5907	.6068	-.6587	-1.6858	-1.0028	.6502	.6679
304	.5615	.5840	.6082	-.6570	-1.6558	-.9955	.6444	.6611
308	.5555	.5773	.6133	-.6578	-1.6597	-.9877	.6395	.6547
312	.5507	.5715	.6243	-.6630	-1.5425	-.9765	.6365	.6497
316	.5493	.5686	.6431	-.6743	-1.1657	-.9592	.6371	.6478
320	.5539	.5710	.6704	-.6926	-.4690	-.9339	.6429	.6502
324	.5671	.5805	.7060	-.7177	.4966	-.9008	.6547	.6580
328	.5902	.5984	.7483	-.7488	1.5781	-.8618	.6728	.6713
332	.6232	.6245	.7951	-.7841	2.5734	-.8205	.6964	.6897
336	.6645	.6576	.8439	-.8217	3.3058	-.7809	.7245	.7124
340	.7116	.6961	.8925	-.8598	3.6921	-.7467	.7557	.7383
344	.7615	.7382	.9392	-.8970	3.7751	-.7204	.7891	.7671
348	.8116	.7828	.9825	-.9322	3.7057	-.7029	.8242	.7988
352	.8602	.8289	1.0216	-.9647	3.6830	-.6939	.8607	.8333
356	.9064	.8760	1.0555	-.9938	3.8747	-.6924	.8979	.8702
360	.9498	.9231	1.0833	-1.0187	4.3504	-.6973	.9349	.9084

TABLE 15B - VARIATION OF TOTAL LOADS WITH BLADE ANGULAR POSITION

θ	$\frac{F_x}{\bar{F}_{x_{SP}}}$	$\frac{M_y}{\bar{M}_{y_{SP}}}$	$\frac{F_y}{\bar{F}_{y_{SP}}}$	$\frac{M_x}{\lvert\bar{M}_{x_{SP}}\rvert}$	$\frac{F_z}{\bar{F}_{z_{SP}}}$	$\frac{M_z}{\lvert\bar{M}_{z_{SP}}\rvert}$	$\frac{M_{0.3}}{\bar{M}_{0.3_{SP}}}$	$\frac{M_{0.4}}{\bar{M}_{0.4_{SP}}}$
0	.9502	.9250	1.0190	-1.0226	.9602	-.7970	.9400	.8982
4	.9894	.9683	1.0233	-1.0350	.9651	-.8032	.9842	.9614
8	1.0247	1.0077	1.0235	-1.0418	.9707	-.8121	1.0226	1.0177
12	1.0550	1.0405	1.0198	-1.0426	.9756	-.8228	1.0521	1.0620
16	1.0789	1.0644	1.0128	-1.0379	.9785	-.8339	1.0705	1.0905
20	1.0952	1.0782	1.0032	-1.0287	.9790	-.8436	1.0773	1.1020
24	1.1036	1.0824	.9925	-1.0167	.9776	-.8496	1.0739	1.0987
28	1.1047	1.0790	.9820	-1.0036	.9755	-.8501	1.0635	1.0855
32	1.1004	1.0715	.9727	-.9913	.9741	-.8438	1.0505	1.0685
36	1.0936	1.0633	.9656	-.9814	.9746	-.8310	1.0389	1.0539
40	1.0872	1.0577	.9609	-.9746	.9772	-.8129	1.0317	1.0456
44	1.0840	1.0567	.9588	-.9713	.9816	-.7923	1.0302	1.0453
48	1.0857	1.0607	.9589	-.9714	.9870	-.7719	1.0343	1.0520
52	1.0932	1.0691	.9610	-.9745	.9923	-.7544	1.0427	1.0635
56	1.1062	1.0810	.9647	-.9802	.9966	-.7411	1.0541	1.0777
60	1.1235	1.0953	.9695	-.9880	.9997	-.7324	1.0675	1.0934
64	1.1438	1.1114	.9754	-.9978	1.0017	-.7273	1.0830	1.1113
68	1.1653	1.1294	.9820	-1.0090	1.0031	-.7248	1.1012	1.1330
72	1.1867	1.1494	.9892	-1.0215	1.0041	-.7238	1.1228	1.1604
76	1.2071	1.1712	.9969	-1.0350	1.0051	-.7239	1.1479	1.1943
80	1.2259	1.1942	1.0050	-1.0493	1.0058	-.7258	1.1760	1.2335
84	1.2430	1.2171	1.0137	-1.0644	1.0061	-.7306	1.2053	1.2751
88	1.2587	1.2386	1.0229	-1.0803	1.0056	-.7398	1.2337	1.3154
92	1.2737	1.2573	1.0329	-1.0971	1.0045	-.7541	1.2594	1.3506
96	1.2887	1.2728	1.0436	-1.1147	1.0029	-.7734	1.2815	1.3789
100	1.3043	1.2855	1.0548	-1.1330	1.0013	-.7965	1.3000	1.4004
104	1.3207	1.2967	1.0661	-1.1516	1.0000	-.8218	1.3163	1.4175
108	1.3377	1.3078	1.0769	-1.1695	.9992	-.8470	1.3320	1.4336
112	1.3544	1.3201	1.0867	-1.1860	.9986	-.8707	1.3485	1.4519
116	1.3694	1.3339	1.0951	-1.2002	.9979	-.8916	1.3665	1.4742
120	1.3817	1.3486	1.1018	-1.2115	.9967	-.9099	1.3854	1.5002

TABLE 15B (Continued)

θ	$\frac{F_x}{\bar{F}_{x_{SP}}}$	$\frac{M_y}{\bar{M}_{y_{SP}}}$	$\frac{F_y}{\bar{F}_{y_{SP}}}$	$\frac{M_x}{\lvert\bar{M}_{x_{SP}}\rvert}$	$\frac{F_z}{\bar{F}_{z_{SP}}}$	$\frac{M_z}{\lvert\bar{M}_{z_{SP}}\rvert}$	$\frac{M_{0.3}}{\bar{M}_{0.3_{SP}}}$	$\frac{M_{0.4}}{\bar{M}_{0.4_{SP}}}$
120	1.3817	1.3486	1.1018	-1.2115	.9967	-.9099	1.3854	1.5002
124	1.3901	1.3630	1.1068	-1.2197	.9946	-.9259	1.4039	1.5277
128	1.3945	1.3752	1.1102	-1.2251	.9917	-.9405	1.4201	1.5533
132	1.3950	1.3841	1.1125	-1.2281	.9886	-.9548	1.4325	1.5740
136	1.3925	1.3886	1.1139	-1.2295	.9858	-.9692	1.4400	1.5875
140	1.3881	1.3890	1.1145	-1.2298	.9837	-.9841	1.4426	1.5934
144	1.3823	1.3858	1.1144	-1.2292	.9825	-.9993	1.4411	1.5926
148	1.3756	1.3799	1.1134	-1.2279	.9819	-1.0146	1.4364	1.5868
152	1.3674	1.3718	1.1117	-1.2255	.9815	-1.0295	1.4295	1.5779
156	1.3571	1.3621	1.1090	-1.2219	.9806	-1.0435	1.4208	1.5670
160	1.3439	1.3505	1.1056	-1.2167	.9789	-1.0562	1.4103	1.5544
164	1.3275	1.3370	1.1015	-1.2097	.9766	-1.0673	1.3976	1.5392
168	1.3081	1.3212	1.0968	-1.2009	.9739	-1.0763	1.3821	1.5207
172	1.2863	1.3032	1.0917	-1.1903	.9715	-1.0834	1.3637	1.4980
176	1.2631	1.2833	1.0859	-1.1781	.9698	-1.0886	1.3422	1.4709
180	1.2393	1.2619	1.0794	-1.1643	.9690	-1.0924	1.3181	1.4397
184	1.2152	1.2392	1.0721	-1.1493	.9689	-1.0953	1.2919	1.4053
188	1.1907	1.2156	1.0640	-1.1333	.9691	-1.0979	1.2642	1.3689
192	1.1653	1.1909	1.0552	-1.1166	.9689	-1.1005	1.2355	1.3313
196	1.1383	1.1651	1.0460	-1.0996	.9680	-1.1030	1.2061	1.2931
200	1.1095	1.1381	1.0368	-1.0826	.9665	-1.1052	1.1763	1.2546
204	1.0791	1.1100	1.0277	-1.0658	.9646	-1.1066	1.1461	1.2159
208	1.0479	1.0814	1.0188	-1.0491	.9628	-1.1066	1.1156	1.1769
212	1.0167	1.0527	1.0099	-1.0324	.9612	-1.1051	1.0848	1.1373
216	.9864	1.0243	1.0008	-1.0153	.9600	-1.1021	1.0538	1.0973
220	.9575	.9964	.9913	-.9979	.9589	-1.0981	1.0227	1.0566
224	.9299	.9690	.9814	-.9800	.9575	-1.0937	.9914	1.0156
228	.9029	.9418	.9712	-.9620	.9555	-1.0896	.9601	.9745
232	.8762	.9148	.9610	-.9444	.9527	-1.0858	.9293	.9339
236	.8495	.8879	.9514	-.9277	.9495	-1.0821	.8992	.8945
240	.8229	.8616	.9425	-.9122	.9462	-1.0782	.8705	.8570

TABLE 15B (Continued)

θ	$\frac{F_x}{\bar{F}_{x_{SP}}}$	$\frac{M_y}{\bar{M}_{y_{SP}}}$	$\frac{F_y}{\bar{F}_{y_{SP}}}$	$\frac{M_x}{\lvert\bar{M}_{x_{SP}}\rvert}$	$\frac{F_z}{\bar{F}_{z_{SP}}}$	$\frac{M_z}{\lvert\bar{M}_{z_{SP}}\rvert}$	$\frac{M_{0.3}}{\bar{M}_{0.3_{SP}}}$	$\frac{M_{0.4}}{\bar{M}_{0.4_{SP}}}$
240	.8229	.8616	.9425	-.9122	.9462	-1.0782	.8705	.8570
244	.7970	.8366	.9344	-.8979	.9436	-1.0736	.8436	.8220
248	.7725	.8132	.9268	-.8843	.9417	-1.0679	.8185	.7895
252	.7501	.7918	.9193	-.8709	.9407	-1.0612	.7949	.7590
256	.7297	.7721	.9116	-.8572	.9401	-1.0541	.7721	.7295
260	.7110	.7534	.9035	-.8430	.9395	-1.0472	.7495	.7000
264	.6932	.7349	.8951	-.8284	.9385	-1.0407	.7265	.6697
268	.6756	.7159	.8870	-.8142	.9371	-1.0350	.7032	.6385
272	.6580	.6965	.8796	-.8013	.9356	-1.0295	.6800	.6072
276	.6407	.6774	.8733	-.7903	.9347	-1.0238	.6582	.5773
280	.6246	.6595	.8684	-.7817	.9347	-1.0173	.6387	.5506
284	.6105	.6439	.8644	-.7749	.9357	-1.0099	.6224	.5282
288	.5991	.6314	.8609	-.7694	.9373	-1.0021	.6093	.5105
292	.5903	.6217	.8573	-.7641	.9387	-.9944	.5990	.4968
296	.5835	.6142	.8532	-.7584	.9391	-.9878	.5902	.4855
300	.5776	.6077	.8489	-.7523	.9382	-.9825	.5821	.4753
304	.5717	.6012	.8450	-.7469	.9361	-.9780	.5743	.4653
308	.5658	.5948	.8428	-.7435	.9338	-.9733	.5674	.4561
312	.5612	.5893	.8436	-.7441	.9325	-.9665	.5630	.4493
316	.5598	.5866	.8484	-.7505	.9334	-.9560	.5632	.4475
320	.5643	.5888	.8577	-.7634	.9368	-.9406	.5700	.4529
324	.5771	.5979	.8714	-.7829	.9425	-.9205	.5846	.4674
328	.5997	.6150	.8886	-.8080	.9493	-.8968	.6073	.4912
332	.6318	.6399	.9081	-.8371	.9554	-.8717	.6373	.5235
336	.6721	.6715	.9286	-.8682	.9595	-.8477	.6729	.5628
340	.7180	.7082	.9488	-.8996	.9610	-.8270	.7126	.6076
344	.7666	.7485	.9677	-.9299	.9602	-.8110	.7551	.6572
348	.8155	.7910	.9847	-.9580	.9583	-.8004	.7997	.7114
352	.8629	.8351	.9993	-.9833	.9569	-.7949	.8459	.7703
356	.9079	.8800	1.0108	-1.0051	.9573	-.7940	.8931	.8332
360	.9502	.9250	1.0190	-1.0226	.9602	-.7970	.9400	.8982

TABLE 15C - HARMONIC CONTENT OF HYDRODYNAMIC LOADS

n	$\frac{(F_{x_H})_n}{\bar{F}_{x_{H,SP}}}$	$(\phi_{Fx_H})_n$ (deg)	$\frac{(M_{y_H})_n}{\bar{M}_{y_{H,SP}}}$	$(\phi_{My_H})_n$ (deg)	$\frac{(F_{y_H})_n}{\bar{F}_{y_{H,SP}}}$	$(\phi_{Fy_H})_n$ (deg)	$\frac{(M_{x_H})_n}{\lvert\bar{M}_{x_{H,SP}}\rvert}$	$(\phi_{Mx_H})_n$ (deg)
1	.3887	119.9	.3758	124.9	.3451	106.0	.2883	-64.6
2	.0676	17.1	.0670	18.0	.0767	-9.9	.0676	171.9
3	.0519	44.7	.0502	49.3	.0514	11.8	.0437	-161.0
4	.0291	44.2	.0284	47.2	.0250	9.9	.0208	-162.2
5	.0148	42.2	.0171	55.3	.0130	-11.7	.0089	-177.9
6	.0067	59.0	.0085	89.8	.0072	-12.3	.0057	173.6
7	.0019	171.6	.0010	144.0	.0005	6.9	.0006	-110.1
8	.0043	-121.3	.0004	-36.6	.0021	-162.8	.0023	31.3
9	.0025	-95.7	.0030	174.2	.0018	150.9	.0015	-37.3
10	.0023	-173.2	.0030	-169.0	.0016	80.3	.0012	-83.1

n	$\frac{(F_{z_H})_n}{\bar{F}_{z_{H,SP}}}$	$(\phi_{Fz_H})_n$ (deg)	$\frac{(M_{z_H})_n}{\lvert\bar{M}_{z_{H,SP}}\rvert}$	$(\phi_{Mz_H})_n$ (deg)	$\frac{(M_{0.3_H})_n}{\bar{M}_{0.3_{H,SP}}}$	$(\phi_{0.3_H})_n$ (deg)	$\frac{(M_{0.4_H})_n}{\bar{M}_{0.4_{H,SP}}}$	$(\phi_{0.4_H})_n$ (deg)
1	6.3873	57.8	.2883	42.4	.3135	127.3	.3050	132.5
2	.4729	111.0	.0503	168.2	.0624	7.4	.0603	9.5
3	.4632	-76.3	.0436	-77.1	.0430	41.9	.0418	47.3
4	.1896	-20.8	.0402	-45.7	.0228	41.0	.0223	45.8
5	.2327	-13.1	.0242	-29.3	.0127	53.7	.0141	63.8
6	.0239	-161.2	.0088	-43.6	.0056	81.4	.0069	96.5
7	.1914	149.7	.0081	-65.3	.0009	90.7	.0012	78.1
8	.2967	162.3	.0037	32.2	.0005	61.1	.0019	51.8
9	.2192	149.7	.0047	140.7	.0035	151.1	.0048	146.5
10	.2734	133.6	.0035	143.0	.0020	179.9	.0024	-174.4

TABLE 15D - HARMONIC CONTENT OF TOTAL LOADS

n	$\frac{(F_x)_n}{\bar{F}_{x_{SP}}}$	$(\phi_{Fx})_n$ (deg)	$\frac{(M_y)_n}{\bar{M}_{y_{SP}}}$	$(\phi_{My})_n$ (deg)	$\frac{(F_y)_n}{\bar{F}_{y_{SP}}}$	$(\phi_{Fy})_n$ (deg)	$\frac{(M_x)_n}{\lvert\bar{M}_{x_{SP}}\rvert}$	$(\phi_{Mx})_n$ (deg)
1	.3790	119.9	.3588	124.9	.1027	129.4	.1955	-52.0
2	.0659	17.1	.0640	18.0	.0434	-9.9	.0679	171.9
3	.0506	44.7	.0479	49.3	.0291	11.8	.0439	-161.0
4	.0284	44.2	.0271	47.2	.0141	9.9	.0209	-162.2
5	.0144	42.2	.0163	55.3	.0073	-11.7	.0089	-177.9
6	.0066	59.0	.0081	89.8	.0041	-12.3	.0057	173.5
7	.0018	171.6	.0010	144.0	.0003	6.6	.0006	-110.2
8	.0042	-121.3	.0004	-36.6	.0012	-162.8	.0023	31.3
9	.0024	-95.7	.0029	174.2	.0010	150.9	.0016	-37.3
10	.0022	-173.2	.0028	-169.0	.0009	80.3	.0012	-83.1

n	$\frac{(F_z)_n}{\bar{F}_{z_{SP}}}$	$(\phi_{Fz})_n$ (deg)	$\frac{(M_z)_n}{\lvert\bar{M}_{z_{SP}}\rvert}$	$(\phi_{Mz})_n$ (deg)	$\frac{(M_{0.3})_n}{\bar{M}_{0.3_{SP}}}$	$(\phi_{0.3})_n$ (deg)	$\frac{(M_{0.4})_n}{\bar{M}_{0.4_{SP}}}$	$(\phi_{0.4})_n$ (deg)
1	.0314	97.8	.1750	42.4	.3831	128.2	.5014	130.1
2	.0038	111.0	.0305	168.2	.0821	7.4	.1021	9.5
3	.0037	-76.3	.0265	-77.1	.0566	41.9	.0707	47.3
4	.0015	-20.8	.0244	-45.7	.0300	41.0	.0378	45.8
5	.0019	-13.1	.0147	-29.3	.0167	53.7	.0239	63.8
6	.0002	-161.1	.0054	-43.6	.0074	81.4	.0117	96.5
7	.0015	149.7	.0049	-65.3	.0012	90.7	.0020	78.1
8	.0024	162.3	.0023	32.2	.0007	61.1	.0032	51.8
9	.0018	149.7	.0028	140.7	.0047	151.1	.0081	146.5
10	.0022	133.6	.0021	143.0	.0026	179.9	.0041	-174.4

REFERENCES

1. Angelo, J.J. et al. "U.S. Navy Controllable Pitch Propeller Programs," presented at a Joint Session of the Chesapeake Section of the Society of Naval Architects and Marine Engineers and the Flagship Section of the American Society of Naval Engineers, Bethesda, Maryland (19 April 1977).

2. Boswell, R.J. et al, "Experimental Determination of Mean and Unsteady Loads on a Model CP Propeller Blade for Various Simulated Modes of Ship Operation," The Eleventh Symposium on Naval Hydrodynamics sponsored Jointly by the Office of Naval Research and University College London, Mechanical Engineering Publications Limited, London and New York, pp 789-823, 832-834, (April 1976); also "Experimental Unsteady and Mean Loads on a CP Propeller Blade of the FF-1088 for Simulated Modes of Operation," David Taylor Naval Ship Research and Development Center Report 76-0125, October 1976.

3. Schwanecke, H. and R. Wereldsma, "Strength of Propellers Considering Steady and Unsteady Shaft and Blade Forces, Stationary and Nonstationary Environmental Conditions," Proceedings of the Thirteenth International Towing Tank Conference, Report of the Propeller Committee, Appendix 2b, Vol. 2, pp 495-526 (1972).

4. Rusetskiy, A.A., "Hydrodynamics of Controllable Pitch Propellers," Shipbuilding Publishing House, Leningrad (1968).

5. Hawdon, L. et al, "The Analysis of Controllable-Pitch Propeller Characteristics at Off-Design Conditions," Transactions of the Institute of Marine Engineers, Vol. 88, Series A, Part 4, pp 162-184 (1976).

6. Kerwin, J.E., "The Development of Numerical Methods for the Computation of Unsteady Propeller Forces," Presented to the Symposium on Hydrodynamics of Ship and Off-Shore Propulsion Systems, Oslo, Norway (March 1977).

7. Ito, T. et al, "Calculation of Unsteady Propeller Forces by Lifting Surface Theory," Presented to the Symposium on Hydrodynamics of Ship and Off-Shore Propulsion Systems, Oslo, Norway (March 1977).

8. Roddy, R.F., "A New Method for the Calculation of Unsteady Forces on a Marine Propeller," Presented to the Chesapeake Section of the

Society of Naval Architects and Marine Engineers, Washington, D.C. (February 1977).

9. van Gent, W., "Unsteady Lifting Surface Theory for Ship Screws: Derivation and Numerical Treatment of Integral Equations," Journal of Ship Research, Vol. 19, No. 4, pp 243-253 (December 1975).

10. Schwanecke, H., "Comparative Calculations on Unsteady Propeller Blade Forces," Proceedings of the Fourteenth International Towing Tank Conference, Report of Propeller Committee, Appendix 4, Vol. 3, pp 357-397 (1975).

11. Breslin, J.P., "Propeller Excitation Theory," Proceedings of the Thirteenth International Towing Tank Conference, Report of the Propeller Committee, Appendix 2c, Vol. 2, pp 527-540 (1972).

12. Boswell, R.J. and M.L. Miller, "Unsteady Propeller Loading - Measurement, Correlation with Theory, and Parametric Study," Naval Ship Research and Development Center Report 2625 (October 1968).

13. Meyne, K., "Propeller Manufacture - Propeller Materials - Propeller Strength," International Shipbuilding Progress, Vol. 22, No. 247, pp 77-102 (March 1975).

14. Wereldsma, R., "Comparative Tests on Vibratory Propeller Forces," Proceedings of the Thirteenth International Towing Tank Conference, Report of the Propeller Committee, Appendix 2a, Vol. 2, pp 482-494 (1972).

15. Huse, E., "An Experimental Investigation of the Dynamic Forces and Moments on One Blade of a Ship Propeller," Proceedings of the Symposium on Testing Techniques in Ship Cavitation Research, the Norwegian Ship Model Experimental Tank, Trondheim, Norway, Publication No. 99, Vol II, pp 19-188 (December 1967).

16. Blaurock, J., "Propeller Blade Loading in Nonuniform Flow," The Society of Naval Architects and Marine Engineers, Propellers 75 Technical and Research Symposium S-4, Paper No. 4, pp 4/1-4/17 (February 1976).

17. Raestad, A.E., "Hydrodynamic Propeller Loading in the Behind Condition," det Norske Veritas Research Department Report 74-31-M (1974).

18. Albrecht, K. and K.R. Suhrbier, "Investigation of the Fluctuating Blade Forces of a Cavitating Propeller in Oblique Flow," International Shipbuilding Progress, Vol. 22, No. 248, pp 132-147 (April 1975).

19. Bednarzik, R., "Untersuchung uber die Belastungsschwankungen am Einzelflugel schrag angestromter Propeller," Schiffbauforschung, Vol. 8, No. 1/2, pp 57-80 (1969).

20. Dobay, G.F., "Time-Dependent Blade-Load Measurements on a Screw-Propeller," Presented to the Sixteenth American Towing Tank Conference, Instituto De Pesquisas Technologicas, Marinha Do Brasil (August 1971).

21. Wereldsma, R., "Last Remarks on the Comparative Model Tests on Vibratory Propeller Forces," Proceedings of the Fourteenth International Towing Tank Conference, Report of the Propeller Committee, Appendix 7, Vol. 3, pp 421-426 (1975).

22. Tasaki, R., "Propulsion Factors and Fluctuating Propeller Loads in Waves," Proceedings of the Fourteenth International Towing Tank Conference, Report of Seakeeping Committee, Appendix 7, Vol. 4, pp 224-236 (1975).

23. Keil, H.G. et al, "Stresses in the Blades of a Cargo Ship Propeller," Journal of Hydronautics, Vol. 6, No. 1, pp 2-7 (January 1972).

24. Watanabe, K. et al, "Propeller Stress Measurements on the Container Ship HAKONE MARU," Shipbuilding Research Association of Japan, Vol. 3, No. 3, pp 41-51 (1973).

25. Tsakonas, S. et al, "An Exact Linear Lifting Surface Theory for Marine Propeller in a Nonuniform Flow Field," Journal of Ship Research, Vol. 17, No. 4, pp 196-207 (December 1974).

26. McCarthy, J.H., "On the Calculation of Thrust and Torque Fluctuations of Propellers in Nonuniform Wake Flow," David Taylor Model Basin Report 1533 (October 1961).

27. Brandau, J.H., "Static and Dynamic Calibration of Propeller Model Fluctuating Force Balances," David Taylor Model Basin Report 2350 (March 1967); also Technologia Naval, Vol. 1, pp 48-74 (January 1968).

28. Day, W.G., "The Effect of Speed on the Wake in Way of the Propeller Plane for the DD-963 Class Destroyer Represented by Model 5265-1B," David Taylor Naval Ship Research and Development Center Report SPD-311-37 (July 1975).

29. Rubis, C.J. and T.R. Harper, "Propulsion Dynamics Simulation of the DD-963 Class Destroyer," Propulsion Dynamics, Inc., Report 74R1B (January 1975).

30. Cummings, D.E., "Numerical Prediction of Propeller Characteristics," Journal of Ship Research, Vol. 17, No. 1, pp 12-18 (March 1973).

31. Boswell, R.J., "A Method of Calculating the Spindle Torque of a Controllable-Pitch Propeller at Design Conditions," David Taylor Model Basin Report 1529 (August 1961).

32. Boswell, R.J. et al, "Experimental Spindle Torque and Open-Water Performance of Two Skewed Controllable-Pitch Propellers," David W. Taylor Naval Ship Research and Development Center Report 4753 (December 1975).

33. Wereldsma, R., "Tendencies of Marine Propeller Shaft Excitations," International Shipbuilding Progress, Vol. 19, No. 218, pp 328-332 (October 1972).

34. Tsakonas, S. et al, "Documentation of a Computer Program for the Pressure Distribution, Forces and Moments on Ship Propellers in Hull Wakes," (In Four Volumes), Stevens Institute of Technology, Davidson Laboratory Report SIT-DL-76-1863 (January 1976) Revised April 1977.

35. Tsakonas, S. et al, "Correlation and Application of an Unsteady Flow Theory for Propeller Forces," Transactions of the Society of Naval Architects and Marine Engineers, Vol. 75, pp 158-193 (1967).

36. Gutsche, F., "The Study of Ships' Propellers in Oblique Flow," Defence Research Information Centre Translation No. 4306, Copyright Controller: Her Majesties Stationary Office, London, England, October 1975; English Translation of "Untersuchung von Schiffsschrauben in schrager Anstromung," Schiffbauforschung, Vol. 3, No. 3/4, pp 97-102 (1964).

37. Boswell, R.J. and S.D. Jessup, "Experimental Determination of Periodic Propeller Blade Loads in a Towing Tank," Presented to the 18th American Towing Tank Conference, U.S. Naval Academy, Annapolis, Maryland (August 1977).

38. Cheng, H.M., "Analysis of Wake Survey of Ship Models - Computer Program AML Problem No. 840-219F," David Taylor Model Basin Report 1804 (March 1964).

Preceding Page Blank - NOT FILMED

INITIAL DISTRIBUTION

Copies		Copies	
1	ARMY CHIEF OF RES & DEV		1 NAVSEA 08
			2 NAVSEA 09G32
1	ARMY ENGR R&D LAB		1 PMS-378
			1 PMS-380
2	CHONR		1 PMS-381
	1 Code 438		1 PMS-383
	1 LIB		1 PMS-389
			1 PMS-391
1	NRL		1 PMS-392
			1 PMS-393
4	ONR BOSTON		1 PMS-397
			1 PMS-399
4	ONR CHICAGO		
		1	FAC 032C
4	ONR LONDON, ENGLAND		
		1	MILITARY SEALIFT COMMAND (M-4EX)
4	ONR PASADENA		
2	USNA	1	NAVSHIPYD/PTSMH
	1 LIB		
	1 JOHNSON	1	NAVSHIPYD/PHILA
1	NAVPGSCOL LIB	1	NAVSHIPYD/NORVA
1	NROTC & NAVADMINU, MIT	1	NAVSHIPYD/CHASN
1	NADC	1	NAVSHIPYD/LBEACH
5	NOSC	1	NAVSHIPYD/MARE
	1 1311 LIB		
	1 6005/FABULA	1	NAVSHIPYD/PUGET
	1 13111 LIB		
	1 2501/HOYT	1	NAVSHIPD/PEARL
	1 NELSON		
		19	NAVSEC
1	NWC		1 SEC 6100
			1 SEC 6101A
23	NAVSEA		1 SEC 6101D
	1 NAVSEA 0311G		1 SEC 6110
	5 NAVSEA 033		1 SEC 6114H
	1 NAVSEA 034		1 SEC 6120
	1 NAVSEA 03412		1 SEC 6136
	1 NAVSEA 037		1 SEC 6140
	1 NAVSEA 037Z		1 SEC 6140B
			2 SEC 6144

Copies	
	1 SEC 6144G
	1 SEC 6145B
	2 SEC 6148
	1 SEC 6152
	2 SEC 6334B
	1 SEC 6600 NORVA
12	DDC
1	BUSTAND/KLEBANOFF
2	HQS COGARD
1	US COAST GUARD (G-ENE-4A)
1	LC/SCI & TECH DIV
9	MARAD
	1 DIV SHIP DES
	1 COORD RES
	1 NACHTSHEIM
	1 SCHUBERT
	1 FALLS
	1 DASHNAW
	1 HAMMER
	1 LASKY
	1 SIEBOLD
2	MMA
	1 LIB
	1 MARITIME RES CEN
2	NASA STIF
	1 DIR RES
1	NSF ENGR DIV LIB
1	DOT LIB
1	U BRIDGEPORT/URAM
1	U CAL BERKELEY/DEPT NAME
1	U CAL NAME/WEHAUSEN
1	U CAL SAN DIEGO/ELLIS
2	UC SCRIPPS
	1 POLLACK
	1 SILVERMAN

Copies	
4	CIT
	1 AERO LIB
	1 ACOSTA
	1 PLESSET
	1 WU
1	CATHOLIC U
1	COLORADO STATE U/ALBERTSON
1	U CONNECTICUT/SCOTTRON
1	CORNELL U/SEARS
1	FLORIDA ATLANTIC U OE LIB
3	HARVARD U
	1 MCKAY LIB
	1 BIRKHOFF
	1 CARRIER
2	U HAWAII/BRETSCHNEIDER
1	U ILLINOIS/ROBERTSON
3	U IOWA
	1 ROUSE
	1 IHR/KENNEDY
	1 IHR/LANDWEBER
2	JOHNS HOPKINS U
	1 PHILLIPS
	1 INST COOP RES
1	U KANSAS CIV ENGR LIB
1	KANSAS ST U ENGR EXP/ NESMITH
1	LEHIGH U FRITZ ENGR LAB LIB
1	LONG ISLAND U

Copies		Copies	
1	U MARYLAND/GLEN MARTIN INST	1	STANFORD U/ASHLEY
7	MIT 1 OCEAN ENGR/LIB 1 OCEAN ENGR/KERWIN 1 OCEAN ENGR/LEEHEY 1 OCEAN ENGR/LYON 1 OCEAN ENGR/MANDEL 1 OCEAN ENGR/NEWMAN 1 PARSONS LAB/IPPEN	1	STANFORD RES INST LIB
		4	SIT DAVIDSON LAB 1 LIB 1 BRESLIN 1 TSAKONAS 1 VALENTINE
		1	TEXAS U ARL LIB
6	U MICHIGAN 1 NAME LIB 1 NAME/COUCH 1 DEPT/HAMMITT 1 NAME/OGILVIE 1 WILLOW RUN LABS 1 NAME/VORUS	1	UTAH STATE U/JEPPSON
		1	U WASHINGTON APL LIB
		2	WEBB INST 1 LEWIS 1 WARD
3	U MINNESOTA SAFHL 1 KILLEN 1 SONG 1 WETZEL	1	WHOI OCEAN ENGR DEPT
		1	WPI ALDEN HYDR LAB LIB
2	STATE U MARITIME COLL 1 ENGR DEPT 1 INST MATH SCI	1	ASME/RES COMM INFO
		1	ASNE
1	NOTRE DAME ENGR LIB	1	SNAME
5	PENN STATE U ARL 1 LIB 1 HENDERSON 1 TSUCHIMA 1 PARKIN 1 THOMPSON	1	AERO JET-GENERAL/BECKWITH
		1	ALLIS CHALMERS, YORK, PA
		5	ARCTEC, INC/NELKA
		1	AVCO LYCOMING
1	PRINCETON U/MELLOR	1	BAKER MANUFACTURING
1	RENSSELAER/DEPT MATH	2	BATH IRON WORKS CORP 1 HANSEN 1 FFG PROJECT OFFICE
1	ST JOHNS U		
3	SWRI 1 APPLIED MECH REVIEW 1 ABRAMSON 1 BURNSIDE	1	BETHLEHEM STEEL NY/DE LUCE
		1	BETHLEHEM STEEL SPARROWS
		2	BIRD-JOHNSON CO 1 CASE 1 RIDLEY

Copies		Copies	
1	BOEING ADV MAR SYS DIV	2	DOUGLAS AIRCRAFT 1 HESS 1 SMITH
2	BOLT BERANEK AND NEWMAN 1 BROWN 1 JACKSON	1	NATIONAL STEEL & SHIPBLDG
1	BREWER ENGR LAB	1	NEWPORT NEWS SHIPBLDG LIB
1	CAMBRIDGE ACOUS/JUNGER	1	NIELSEN ENGR/SPANGLER
1	CALSPAN, INC/RITTER	1	OCEANICS/KAPLAN
1	EASTERN RES GROUP	1	NAR SPACE/UJIHARA
1	EXXON DES DIV	1	PROPULSION DYNAMICS, INC
1	FRIEDE & GOLDMAN/MICHEL	1	K.E. SCHOENHERR
1	GEN DYN CONVAIR 1 ASW-MARINE SCIENCES	1	GEORGE G. SHARP
1	GEN DYN ELEC BOAT/ BOATWRIGHT	1	SPERRY SYS MGMT LIB/ SHAPIRO
3	GIBBS & COX 1 TECH LIB 1 OLSON 1 CAPT. NELSON	2	SUN SHIPBUILDING 1 PAVLIK 1 SINGH
		1	ROBERT TAGGART
1	GRUMMAN AEROSPACE/CARL	1	TETRA TECH PASADENA/ CHAPKIS
3	HYDRONAUTICS 1 DUNNE 1 SCHERER 1 LIBRARY	1	TRACOR
		1	UA HAMILTON STANDARD/ CORNELL
1	INGALLS SHIPBUILDING		
1	INST FOR DEFENSE ANAL		
1	ITEK VIDYA		
1	LITTLETON R & ENGR CORP/REED		
1	LITTON INDUSTRIES		
1	LOCKHEED M&S/WAID		
2	MARINE VIBRATION ASSOC 1 BRADSHOW 1 VASSILOPOULIS		

CENTER DISTRIBUTION

Copies	Code	
1	11	Ellsworth
1	1102.1	Nakonechny
1	15	Cummins
1	1509	Pollard
1	152	Wermter
1	1524	Lin
1	1524	Hecker
1	1524	Day
1	1524	Remmers
1	1524	Gordon

Copies	Code	
1	1524	Roddy
1	1532	Dobay
1	1532L	Denny
1	154	Morgan
1	1544	Cumming
30	1544	Boswell
10	1544	Jessup
1	156	Hagen
1	1556	Santore
1	1556	Wisler
1	1556	Jeffers
1	172	Krenzke
1	1720.6	Rockwell
1	19	Sevik
1	1962	Zaloumis
1	1962	Noonan
1	1962	Antonides
1	2723	Spargo
1	2731	Moken
1	2814	Czyryca
30	5214.1	Reports Distribution
1	5221	Library (C)
1	5222	Library (A)

☆U.S. GOVERNMENT PRINTING OFFICE:1977 261-250/269 1-3